



Universiteit  
Leiden  
The Netherlands

## **Liposomes as delivery system for allergen-specific immunotherapy**

Leboux, R.J.T.

### **Citation**

Leboux, R. J. T. (2021, November 16). *Liposomes as delivery system for allergen-specific immunotherapy*. Retrieved from <https://hdl.handle.net/1887/3240101>

Version: Publisher's Version

License: [Licence agreement concerning inclusion of doctoral thesis in the Institutional Repository of the University of Leiden](#)

Downloaded from: <https://hdl.handle.net/1887/3240101>

**Note:** To cite this publication please use the final published version (if applicable).

# **Liposomes as delivery system for allergen-specific immunotherapy**

About the cover: Dendritic cells after short exposure to liposomes (red) with antigen (green) attached via coiled coil

Design and layout: R.B. van Duijvenvoorde

Printing: IPSKamp

ISBN: 978-94-6421-546-5

© R. J. T. Leboux, 2021. All rights reserved. No part of this book may be reproduced in any form or by any means without permission of the author.







# **Liposomes as delivery system for allergen-specific immunotherapy**

## **Proefschrift**

ter verkrijging van de graad van doctor aan de Universiteit Leiden,  
op gezag van rector magnificus prof. dr. ir. H. Bijl,  
volgens besluit van het college voor promoties  
te verdedigen op 16 november 2021  
klokke 16.15 uur

door

**Romanus Johannes Theodorus Leboux**

Geboren te Utrecht op 13 april 1990

**Promotoren:** Prof. dr. W. Jiskoot†, Prof. dr. A. Kros, Prof. dr. H. Irth  
**Co-promotor:** dr. B.A. Slütter

**Promotiecommissie:**

Prof. dr. H. Irth (chair)

Prof. dr. J. Bouwstra (secretary)

Prof. dr. C. Foged (University of Copenhagen, Denmark)

Prof. dr. G.F.A. Kersten

Dr. S.I. van Kasteren

Prof. dr. E. Mastrobattista (Utrecht University)

Prof. dr. Y. Perrie (University of Strathclyde, United Kingdom)

The research described in this thesis was performed at the Division of BioTherapeutics at the Leiden Academic Centre for Drug Research (LACDR), part of Leiden University.

# Table of contents

Chapter 1	General introduction	p9
Chapter 2	Enhanced immunogenicity of recombinant Bet v 1 through combined encapsulation in and adsorption to cationic liposomes	p23
Chapter 3	Atomic force microscopy measurements of anionic liposomes reveal the effect of liposomal rigidity on antigen-specific regulatory T cell responses	p43
Chapter 4	Antigen uptake after intradermal microinjection depends on antigen nature and formulation, but not on injection depth	p71
Chapter 5	High-affinity antigen association to cationic liposomes via coiled coil-forming peptides induces a strong antigen-specific CD4+ T-cell response	p99
Chapter 6	Bet v 1 attached to cationic liposomes through coiled coil-forming peptides induces stronger antibody responses than aluminum-adsorbed Bet v 1	p131
Chapter 7	Summary, discussion, conclusion	p153
Chapter 8	Nederlandse samenvatting	p163
Chapter 9	Curriculum Vitae	p169



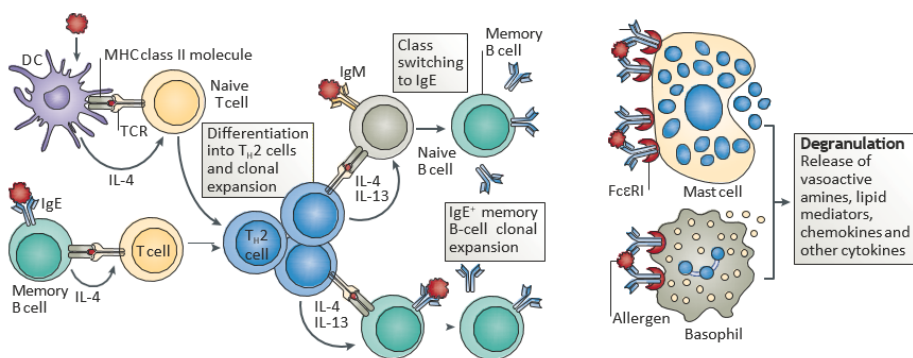
# **Chapter 1**

## **General introduction**

## Allergy

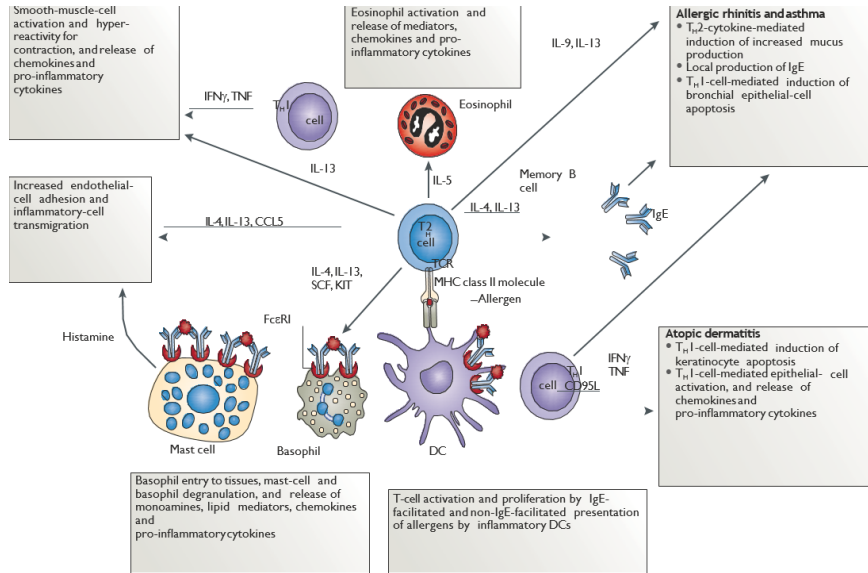
We are constantly exposed to airborne allergens. Not everyone is allergic or develops an allergy over time, but the incidence of allergic rhinitis, conjunctivitis and asthma is increasing rapidly. Estimates indicate that allergies affect approximately 30% of the population in the developed countries [1-5]. Sensitization to airborne allergens, such as pollen, is an overreaction to an otherwise harmless substance. Pollen from birch and other Fagales family members are the most dominant tree pollen in Northern and Central Europe. Birch pollen allergy often comes with allergies to other types of pollen (e.g. hazelnut, oak, chestnut) [6] and even food allergies [7, 8] as a result of protein homology. Based on samples in populations throughout Europe, it is estimated that between 10 and 20% of all citizens are sensitized to the main allergen of birch pollen: Bet v 1 [2-4, 9]. Among pollen-allergic patients, between 50 and 99% have Bet v 1-specific immunoglobulin (Ig) E.

An allergy is developed in two phases: the sensitization phase (Figure 1) and the effector phase (Figure 2). During sensitization, the immune response to an allergen is skewed towards a T-helper (Th) 2-type response. Allergen-specific Th2 cells secrete cytokines, including interleukin (IL)-4, IL-5 and IL-13, which ultimately results in antibody isotype switching towards IgE. In the effector phase, mast cells (MCs) and basophils are loaded with allergen-specific IgE. Upon binding of allergen to these specific IgE molecules, the MCs and basophils degranulate and thereby release a storm of molecules, such as histamines, prostaglandins and leukotrienes [10-15]. These are responsible for the most common symptoms of allergy, including sneezing, rhinitis and conjunctivitis.



*Figure 1. Proposed mechanism of the sensitization phase of developing an allergy. Dendritic cells are exposed to allergens and, in the presence of IL-4, induce the differentiation of naive CD4<sup>+</sup> T-cells into Th<sub>2</sub> CD4<sup>+</sup> T-cells. These cells produce IL-4, IL-5 and IL-13 and subsequently induce antibody isotype switching towards IgE on B-cells. This allergen-specific IgE can then bind FcεRI receptors on basophils and mast cells. Image was adapted from Larché et al. [15].*

Even though allergic reactions most often are not lethal, the economic burden of allergies is severe. It was estimated to be 2-5 billion dollar in the United States in 2003 (approximately 20 dollar per citizen) [16], and more than 1 billion euro in Sweden in 2015 (approximately 960 euro per citizen) [17].



*Figure 2. Proposed mechanism of the effector phase of an allergy. Upon subsequent exposure to the allergen, DCs take up allergen and IgE-bound allergen and activate Th2 CD4+ T-cells, which produce various cytokines and chemokines, resulting in activation of eosinophils, smooth muscle cells, mucus production and basophils. Image was adapted from Larché et al. [15].*

## Allergy therapies

The most effective allergy treatment is avoiding the allergen source. Unfortunately this is very difficult if not impossible for airborne allergens. First line therapy includes the administration of drugs, such as anti-histamines or corticosteroids [18]. These treat the symptoms, but not the underlying cause. The only curative treatment is allergen-specific immunotherapy (AIT) using allergy vaccines [18]. AIT is available as sublingual immunotherapy (SLIT) or subcutaneous immunotherapy (SCIT). In SLIT, atopic patients must administer themselves allergen sublingually daily for at least a year. SCIT consists of weekly subcutaneous injections by a general practitioner during the scale-up phase (first 3-6 months) of therapy, and monthly or bi-monthly injections during the maintenance phase (3-5 years) [19-21].

Allergy vaccines for SCIT are usually composed of an allergen extract, containing water-soluble proteins, adsorbed to aluminum hydroxide. The latter is a commonly used colloidal adjuvant in childhood vaccines, known to induce



strong Th2 mediated responses [22]. A recent advance in the field of AIT is the use of (well-defined) recombinant proteins instead of (poorly defined) allergen extracts [23-26]. As allergen extract content varies between allergen-source and even between batches of the same supplier [23, 27-29], this is the first step towards well characterized and reproducible vaccine formulations.

While proven effective, SCIT requires at least 3 years before sufficient effect is achieved. IgE levels first increase, before decreasing in the course of SCIT [12]. This may be explained by the Th2-type of immune response that aluminum hydroxide initially induces, resulting in IgE induction, before inducing IgG4 and IL-10 production. If the vaccine could directly induce either a regulatory response or a Th1 type response, the increase of allergy-related biomarkers probably would not happen. Thus, by replacing the adjuvant, the therapy might require less injections and work more quickly [10, 26, 30, 31].

Some issues about the safety of aluminum salts have been raised [21, 32-34]. Although the toxicity is debatable, development of new allergies has been reported as a result of AIT [35-37], which may be attributed to the induction of antigen-specific IgE as a result of the aluminum adjuvant. Moreover, there is a regulatory wish to replace aluminum salts in allergy vaccines [10, 26, 31]. Nanoparticles are an interesting alternative adjuvant for immunotherapy. A broad range of nanoparticles has been prepared and described as alternatives. Liposomes are among the most studied and several liposomal formulations are for purposes other than allergy vaccination are on the market [38].

### **Liposomes**

Liposomes are nanoparticles composed of one or more (phospho-)lipid bilayers. Liposomes are a biocompatible, bio-degradable and highly versatile and tunable delivery system [39]. Molecules can be physically associated to liposomes in three ways (Figure 3): water-soluble molecules can be encapsulated in the aqueous core or adsorbed to the surface, while lipid-soluble molecules can be incorporated in the lipid bilayer [40]. Incorporation of molecules in liposomes typically alters the bio-distribution after administration. This formulation strategy has successfully been used to alter the pharmacokinetics of cytostatic drug molecules, such as doxorubicin [41]. Liposomes are also investigated and used as adjuvant for vaccination, to carry antigenic peptides or proteins as cargo.

Liposomes can serve as vaccine adjuvant in two ways. Firstly, they can act as a delivery system to enhance the delivery of antigenic cargo towards and into antigen presenting cells (APCs) [42, 43]. Secondly, they can induce, enhance or direct the subsequent immune response via various immunostimulatory mechanisms [43-45]. In order for an adjuvant to induce its effect, both antigen

and adjuvant need to be taken up by the same APC [46, 47]. The *in vivo* behavior of liposomes strongly depends on the physico-chemical properties, which in turn is determined by the content and lipid composition. The hydrodynamic diameter and zeta potential of liposomes and their impact on immunogenicity have been widely studied [42, 48-53].

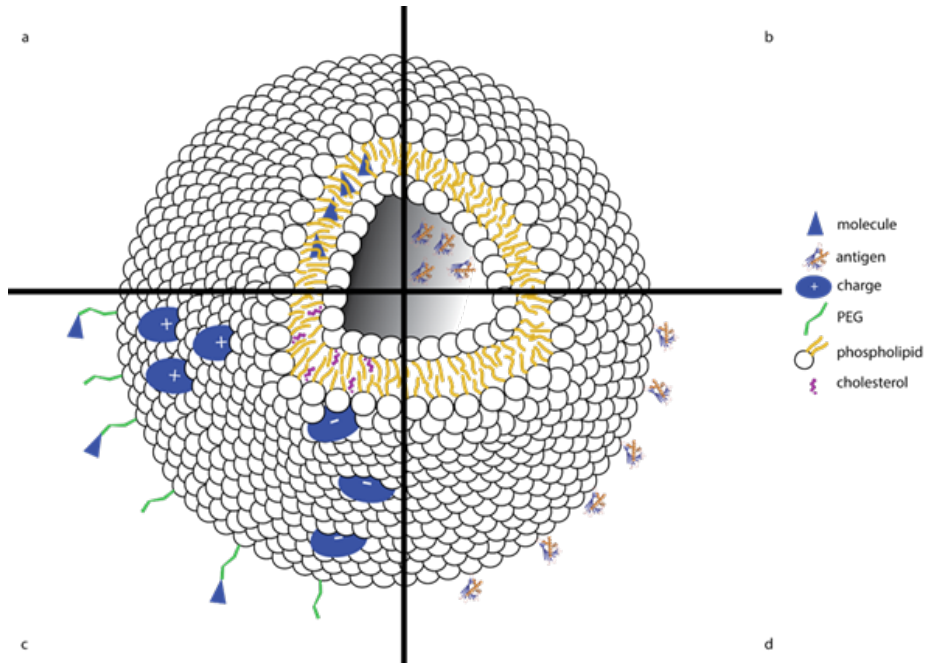


Figure 3. Schematic overview of structure and composition of a unilamellar liposome. Liposomes consist of one or more lipid bilayers, in which hydrophobic molecules can be incorporated (A). The aqueous core can be used to encapsulate hydrophilic molecules (B). The surface of liposomes can contain charged lipids, PEG-conjugated lipids and lipids conjugated to targeting molecules (C). Molecules can also be adsorbed to the surface via e.g. electrostatic interactions (D).

Small particles (<500 nm) are thought to migrate towards the lymph node and then be taken up by lymph node resident APCs, whereas larger particles (>500 nm) are primarily taken up at the injection site [54, 55]. Consequently, small liposomes were shown to disappear more quickly from the injection site than large ones [56]. While smaller solid nanoparticles are often associated with a Th1-skewed immune response and stronger CD8 T-cell responses, this does not seem to be the case for liposomes [48]. Large neutral liposomes induced a strong Th1 response, whereas small liposomes induced a Th2 response [53, 57]. Small cationic liposomes containing pDNA were more effective at inducing both a humoral [56] and especially CD8+ T-cell response [51, 56]. This illustrates that not only size, but also other parameters, such as zeta potential and surface chemistry, are to be considered.

Liposomes can be either neutral, anionic or cationic. Neutral liposomes are typically composed of phosphatidylcholines (PC), phosphoethanolamines (PE) and cholesterol. Neutral liposomes are not stabilized by electrostatic repulsion, which can result in rapid aggregation or sedimentation [58]. Despite this challenge, neutral liposomes are the basis of AS01 (in combination with MPL-A and Saponin), GSK's adjuvant used in malaria and recombinant Zoster vaccine [46]. Cationic liposomes generally form a depot at the site of injection, where they accumulate and need to be taken up by APCs to remove them from the injection site. Cationic liposomes are efficiently taken up by APCs and generally induce a strong T-helper cell type (Th) 1 response and are able to induce antigen specific CD8+ T-cell responses [44, 59-62]. The uptake mechanism for cationic liposomes seems to be based on electrostatic interaction between liposomes and cell surface [45, 68]. Anionic liposomes are taken up via scavenger receptors present on macrophages and liver sinusoidal endothelial cells [66, 67]. Studies with anionic liposomes have shown that liposomes containing lipids with either a phospho-glycerol or a phospho-serine headgroup can induce a regulatory immune response rather than an inflammatory Th1 or Th2 response [45, 63-65].

Besides improving the delivery of the antigen, another advantage of using liposomes, or nanoparticles in general, is their ability to co-encapsulate molecular immune modulators [66-72]. This will ensure the delivery of both antigen and immune modulator into the same APC. This co-delivery is necessary for an optimal effect of the immune modulator on antigen specific immune responses. Additionally, targeting moieties could be coupled to the surface to enhance uptake by specific subsets of cells (e.g. dendritic cells, Langerhans Cells or foam cells) [73-77]. In this thesis we use liposomes as antigen delivery systems for two different antigens: model antigen ovalbumin (OVA) and Bet v 1, the major allergen in birch pollen allergy.

## Aim and outline of this thesis

In this thesis we investigate liposomes as a delivery system for SCIT. We set out to gain fundamental knowledge on the effect of antigen association method on the subsequent induced immune responses *in vitro* and *in vivo*. Moreover, we developed a new method of antigen association that can both reduce antigen loss during preparation and improve the immunogenicity of the antigen. We have prepared cationic and anionic liposomes and focused on the delivery of antigens in different animal models and in *ex vivo* human skin biopsies.

**Chapter 2** compares different methods of Bet v 1 association to cationic liposomes. Bet v 1 was adsorbed to the surface, encapsulated in the aqueous core and resulting association efficiencies were determined. Aggregation was observed after exceeding a 0.15 protein/lipid ratio (w/w) in all cases. Liposomes with Bet v 1 encapsulated, adsorbed, and unbound induced the strongest IgG1 response.

In **chapter 3** atomic force microscopy was used to accurately measure the rigidity (Young's modulus,  $Y_m$ ) of anionic liposomes as function of lipid composition. The  $Y_m$  was correlated to liposome uptake *in vitro* and induction of regulatory T-cells *in vivo*. A linear correlation was observed between liposome rigidity and the uptake of liposomes by cultured dendritic cells. Moreover, the linear correlation was also observed between liposome rigidity and induction of antigen-specific regulatory T-cells (Tregs) *in vivo*: the more rigid the liposome membrane, the more Tregs.

We evaluated the fate of two liposome formulations (cationic and anionic) after intradermal injection in human skin biopsies in **chapter 4**. Fluorescent OVA or Bet v 1 was encapsulated in fluorescent anionic and cationic liposomes. Subsequently, we analyzed which subsets of dendritic cells had taken up antigen and liposomes. Antigen uptake in different subsets was not affected by injection depth. We found that most CD14<sup>+</sup> dDCs take up antigen, while Langerhans cells showed the smallest fraction of antigen-positive cells. Moreover, encapsulation of Bet v 1 in liposomes greatly enhanced uptake by APCs.

In order to reduce the loss of precious antigen during the preparation of liposomal antigen formulations, we developed a novel antigen association platform, which is described in **chapter 5**. This association method is based on the interaction between two complementary peptides (pepE and pepK, figure 4) that form a coiled coil. PepE was covalently linked to an antigenic peptide sequence (yielding a pepE-antigen conjugate), while pepK was covalently linked to cholesterol (yielding CPK). CPK was subsequently incorporated in the lipid

bilayers of cationic liposomes. This coiled coil-based association of pepE-antigen conjugates to liposomes was compared to association to non-functionalized cationic liposomes and showed superior *in vivo* co-localization, as well as *in vitro* and *in vivo* antigen specific CD4+ T-cell responses.

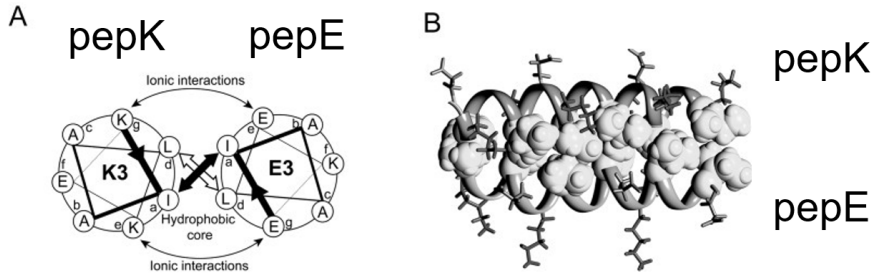


Figure 4. Schematic overview of the intermolecular interactions that happen when pepE and pepK form a coiled coil (A) and a representative image of what the coiled coil looks like on a molecular scale (B). Image was adapted from Fernandez-Rodriguez et al. [78]

Mice were immunized with Bet v 1 associated to liposomes or aluminum hydroxide in **chapter 6**. We compared the coiled coil-based association to the gold standard in SCIT: adsorption to aluminum hydroxide. Coiled coil associated Bet v 1 resulted in a superior immune response compared to plain adsorbed Bet v 1 to either cationic liposomes or aluminum hydroxide, with high levels of Bet v 1-specific IgG1 and IgG2a. Moreover, cells derived from lung draining lymph nodes produced high levels of IL-4, IL-5, IL-10 and IL-13.

Finally, in **chapter 7** the results of this thesis are summarized and the possible application of liposomes as adjuvant in (allergen specific) immunotherapy is discussed.

## References

1. Biedermann, T., et al., *Birch pollen allergy in Europe*. Allergy, 2019. **74**(7): p. 1237-1248.
2. Stemeseder, T., et al., *Cross-sectional study on allergic sensitization of Austrian adolescents using molecule-based IgE profiling*. Allergy, 2017. **72**(5): p. 754-763.
3. Blomme, K., et al., *Prevalence of Allergic Sensitization versus Allergic Rhinitis Symptoms in an Unselected Population*. International Archives of Allergy and Immunology, 2013. **160**(2): p. 200-207.
4. Linneberg, A., et al., *Increasing prevalence of specific IgE to aeroallergens in an adult population: Two cross-sectional surveys 8 years apart: The Copenhagen Allergy Study*. Journal of Allergy and Clinical Immunology, 2000. **106**(2): p. 247-252.
5. Platts-Mills, T.A., *The allergy epidemics: 1870-2010*. J Allergy Clin Immunol, 2015. **136**(1): p. 3-13.
6. Asam, C., et al., *Tree pollen allergens-an update from a molecular perspective*. Allergy, 2015. **70**(10): p. 1201-11.
7. Roulias, A., et al., *Differences in the intrinsic immunogenicity and allergenicity of Bet v 1 and related food allergens revealed by site-directed mutagenesis*. Allergy, 2013. **69**(2): p. 208-215.
8. Geroldinger-Simic, M., et al., *Birch pollen-related food allergy: clinical aspects and the role of allergen-specific IgE and IgG4 antibodies*. J Allergy Clin Immunol, 2011. **127**(3): p. 616-622.
9. Schmitz, R., et al., *Patterns of Sensitization to Inhalant and Food Allergens - Findings from the German Health Interview and Examination Survey for Children and Adolescents*. International Archives of Allergy and Immunology, 2013. **162**(3): p. 263-270.
10. Gunawardana, N.C. and S.R. Durham, *New approaches to allergen immunotherapy*. Annals of Allergy, Asthma & Immunology, 2018: p. 293-305.
11. Shamji, M.H. and S.R. Durham, *Mechanisms of allergen immunotherapy for inhaled allergens and predictive biomarkers*. J Allergy Clin Immunol, 2017. **140**(6): p. 1485-1498.
12. Akdis, M. and C.A. Akdis, *Mechanisms of allergen-specific immunotherapy: Multiple suppressor factors at work in immune tolerance to allergens*. Journal of Allergy and Clinical Immunology, 2014. **133**(3): p. 621-631.
13. Akdis, M., *Immune tolerance in allergy*. Current Opinion in Immunology, 2009. **21**(6): p. 700-707.
14. Akdis, M. and C.A. Akdis, *Mechanisms of allergen-specific immunotherapy*. Journal of Allergy and Clinical Immunology, 2007. **119**(4): p. 780-789.
15. Larche, M., C.A. Akdis, and R. Valenta, *Immunological mechanisms of allergen-specific immunotherapy*. Nat Rev Immunol, 2006. **6**(10): p. 761-771.
16. Reed, S.D., T.A. Lee, and D.C. McCrory, *The Economic Burden of Allergic Rhinitis*. Pharmacoeconomics, 2004. **22**(6): p. 345-361.
17. Cardell, L.-O., et al., *TOTAL: high cost of allergic rhinitis—a national Swedish population-based questionnaire study*. npj Primary Care Respiratory Medicine, 2016. **26**(1): p. 15082.
18. A.P.E. Sachs, et al., *NHG-Standaard Allergische en niet-allergische rhinitis*. Huisarts Wet, 2006.
19. Dretzke, J., et al., *Subcutaneous and sublingual immunotherapy for seasonal allergic rhinitis: A systematic review and indirect comparison*. Journal of Allergy and Clinical

- Immunology, 2013. **131**(5): p. 1361-1366.
20. Meadows, A., et al., *A systematic review and economic evaluation of subcutaneous and sublingual allergen immunotherapy in adults and children with seasonal allergic rhinitis*. Health Technol Assess, 2013. **17**(27): p. vi, xi-xiv, 1-322.
21. Exley, C., *Aluminium adjuvants and adverse events in sub-cutaneous allergy immunotherapy*. Allergy, asthma, and clinical immunology : official journal of the Canadian Society of Allergy and Clinical Immunology, 2014. **10**(1): p. 4-4.
22. Jensen-Jarolim, E., *Aluminium in Allergies and Allergen immunotherapy*. The World Allergy Organization Journal, 2015. **8**(1): p. 7.
23. Valenta, R., et al., *Allergen Extracts for In Vivo Diagnosis and Treatment of Allergy: Is There a Future?* The Journal of Allergy and Clinical Immunology: In Practice, 2018.
24. Valenta, R., et al., *Recombinant allergens for allergen-specific immunotherapy: 10 years anniversary of immunotherapy with recombinant allergens*. Allergy, 2011. **66**(6): p. 775-783.
25. Valenta, R., et al., *Vaccine development for allergen-specific immunotherapy based on recombinant allergens and synthetic allergen peptides: Lessons from the past and novel mechanisms of action for the future*. The Journal of allergy and clinical immunology, 2016. **137**(2): p. 351-357.
26. Klimek, L., et al., *Development of subcutaneous allergen immunotherapy (part 2): preventive aspects and innovations*. Allergo Journal International, 2019. **28**(4): p. 107-119.
27. Esch, R.E., *Allergen Source Materials and Quality Control of Allergenic Extracts*. Methods, 1997. **13**(1): p. 2-13.
28. Carnés, J., et al., *Mite allergen extracts and clinical practice*. Annals of Allergy, Asthma & Immunology, 2017. **118**(3): p. 249-256.
29. Cox, L., *Standardized allergen extracts: past, present and future*. Expert Review of Clinical Immunology, 2005. **1**(4): p. 579-588.
30. Klimek, L., et al., *Evolution of subcutaneous allergen immunotherapy (part 1): from first developments to mechanism-driven therapy concepts*. Allergo Journal International, 2019: p. 78-95.
31. Pfaar, O., et al., *Perspectives in allergen immunotherapy: 2019 and beyond*. Allergy, 2019. **74 Suppl 108**: p. 3-25.
32. Jensen-Jarolim, E., et al., *State-of-the-art in marketed adjuvants and formulations in Allergen Immunotherapy: a position paper of the European Academy of Allergy and Clinical Immunology (EAACI)*. Allergy, 2019: p. 746-760.
33. Kawahara, M. and M. Kato-Negishi, *Link between Aluminum and the Pathogenesis of Alzheimer's Disease: The Integration of the Aluminum and Amyloid Cascade Hypotheses*. International Journal of Alzheimer's Disease, 2011. **2011**: p. 276393.
34. Harrington, C.R., et al., *Alzheimer's-disease-like changes in tau protein processing: association with aluminium accumulation in brains of renal dialysis patients*. The Lancet, 1994. **343**(8904): p. 993-997.
35. Gellrich, D., et al., *De novo sensitization during subcutaneous allergen specific immunotherapy - an analysis of 51 cases of SCIT and 33 symptomatically treated controls*. Sci Rep, 2020. **10**(1): p. 6048.
36. Asero, R., *Injection Immunotherapy with Different Airborne Allergens Did Not Prevent de novo Sensitization to Ragweed and Birch Pollen North of Milan*. International Archives of Allergy and Immunology, 2004. **133**(1): p. 49-54.
37. Harmanci, K., et al., *Evaluation of new sensitizations in asthmatic children*



- monosensitized to house dust mite by specific immunotherapy.* Asian Pac J Allergy Immunol, 2010. **28**(1): p. 7-13.
38. Bobo, D., et al., *Nanoparticle-Based Medicines: A Review of FDA-Approved Materials and Clinical Trials to Date.* Pharmaceutical Research, 2016. **33**(10): p. 2373-2387.
  39. Li, J., et al., *A review on phospholipids and their main applications in drug delivery systems.* Asian Journal of Pharmaceutical Sciences, 2015. **10**(2): p. 81-98.
  40. Watson, D.S., A.N. Endsley, and L. Huang, *Design considerations for liposomal vaccines: Influence of formulation parameters on antibody and cell-mediated immune responses to liposome associated antigens.* Vaccine, 2012. **30**(13): p. 2256-2272.
  41. Vaage, J., et al., *Tumour uptake of doxorubicin in polyethylene glycol-coated liposomes and therapeutic effect against a xenografted human pancreatic carcinoma.* British journal of cancer, 1997. **75**(4): p. 482-486.
  42. Schwendener, R.A., *Liposomes as vaccine delivery systems: a review of the recent advances.* Therapeutic Advances in Vaccines, 2014. **2**(6): p. 159-182.
  43. Perrie, Y., et al., *Designing liposomal adjuvants for the next generation of vaccines.* Adv Drug Deliv Rev, 2016. **99**(Pt A): p. 85-96.
  44. Christensen, D., et al., *Cationic liposomes as vaccine adjuvants.* Expert Review of Vaccines, 2007. **6**(5): p. 785-796.
  45. Benne, N., et al., *Anionic 1,2-distearoyl-sn-glycero-3-phosphoglycerol (DSPG) liposomes induce antigen-specific regulatory T cells and prevent atherosclerosis in mice.* J Control Release, 2018. **291**: p. 135-146.
  46. Didierlaurent, A.M., et al., *Adjuvant system AS01: helping to overcome the challenges of modern vaccines.* Expert Review of Vaccines, 2017. **16**(1): p. 55-63.
  47. Calabro, S., et al., *Vaccine adjuvants alum and MF59 induce rapid recruitment of neutrophils and monocytes that participate in antigen transport to draining lymph nodes.* Vaccine, 2011. **29**(9): p. 1812-23.
  48. Benne, N., et al., *Orchestrating immune responses: How size, shape and rigidity affect the immunogenicity of particulate vaccines.* Journal of Controlled Release, 2016. **234**: p. 124-134.
  49. Zolnik, B.S., et al., *Minireview: Nanoparticles and the Immune System.* Endocrinology, 2010. **151**(2): p. 458-465.
  50. Ibaraki, H., et al., *Effects of surface charge and flexibility of liposomes on dermal drug delivery.* Journal of Drug Delivery Science and Technology, 2019. **50**: p. 155-162.
  51. Henriksen-Lacey, M., A. Devitt, and Y. Perrie, *The vesicle size of DDA:TDB liposomal adjuvants plays a role in the cell-mediated immune response but has no significant effect on antibody production.* Journal of Controlled Release, 2011. **154**(2): p. 131-137.
  52. Bachmann, M.F. and G.T. Jennings, *Vaccine delivery: a matter of size, geometry, kinetics and molecular patterns.* Nature Reviews Immunology, 2010. **10**: p. 787-796.
  53. Brewer, J.M., et al., *Lipid Vesicle Size Determines the Th1 or Th2 Response to Entrapped Antigen.* The Journal of Immunology, 1998. **161**(8): p. 4000-4007.
  54. Manolova, V., et al., *Nanoparticles target distinct dendritic cell populations according to their size.* European Journal of Immunology, 2008. **38**(5): p. 1404-1413.
  55. Oussoren, C. and G. Storm, *Liposomes to target the lymphatics by subcutaneous administration.* Advanced Drug Delivery Reviews, 2001. **50**(1): p. 143-156.
  56. Carstens, M.G., et al., *Effect of vesicle size on tissue localization and immunogenicity*



- of liposomal DNA vaccines. *Vaccine*, 2011. **29**(29): p. 4761-4770.
57. Badiie, A., et al., *The role of liposome size on the type of immune response induced in BALB/c mice against leishmaniasis: rgp63 as a model antigen*. *Experimental Parasitology*, 2012. **132**(4): p. 403-409.
  58. Trefalt, G. and M. Borkovec, *Overview of DLVO theory*. Laboratory of Colloid and Surface Chemistry, University of Geneva, Switzerland, 2014: p. 1-10.
  59. Heuts, J., et al., *Cationic Liposomes: A Flexible Vaccine Delivery System for Physicochemically Diverse Antigenic Peptides*. *Pharmaceutical Research*, 2018. **35**(11).
  60. Varypataki, E.M., et al., *Cationic DOTAP-based liposomes: a vaccine formulation platform for synthetic long peptides with widely different physicochemical properties*, in *Leiden Academic Center for Drug Research*. 2016, Leiden University: Leiden.
  61. Hussain, M.J., et al., *Th1 immune responses can be modulated by varying dimethyldioctadecylammonium and distearoyl-sn-glycero-3-phosphocholine content in liposomal adjuvants*. *J Pharm Pharmacol*, 2014. **66**(3): p. 358-366.
  62. Foged, C., et al., *Interaction of dendritic cells with antigen-containing liposomes: effect of bilayer composition*. *Vaccine*, 2004. **22**(15-16): p. 1903-13.
  63. Pujol-Autonell, I., et al., *Use of Autoantigen-Loaded Phosphatidylserine-Liposomes to Arrest Autoimmunity in Type 1 Diabetes*. *PLOS ONE*, 2015. **10**(6).
  64. Nagata, S., R. Hanayama, and K. Kawane, *Autoimmunity and the clearance of dead cells*. *Cell*, 2010. **140**(5): p. 619-30.
  65. Ramos, G.C., et al., *Apoptotic mimicry: phosphatidylserine liposomes reduce inflammation through activation of peroxisome proliferator-activated receptors (PPARs) in vivo*. *British Journal of Pharmacology*, 2007. **151**(6): p. 844-850.
  66. Short, K.K., et al., *Co-encapsulation of synthetic lipidated TLR4 and TLR7/8 agonists in the liposomal bilayer results in a rapid, synergistic enhancement of vaccine-mediated humoral immunity*. *Journal of Controlled Release*, 2019.
  67. Du, G., et al., *Intradermal vaccination with hollow microneedles: A comparative study of various protein antigen and adjuvant encapsulated nanoparticles*. *Journal of Controlled Release*, 2017. **266**: p. 109-118.
  68. Bal, S.M., et al., *Co-encapsulation of antigen and Toll-like receptor ligand in cationic liposomes affects the quality of the immune response in mice after intradermal vaccination*. *Vaccine*, 2011. **29**(5): p. 1045-1052.
  69. Varypataki, E.M., et al., *Cationic Liposomes Loaded with a Synthetic Long Peptide and Poly(I:C): a Defined Adjuvanted Vaccine for Induction of Antigen-Specific T Cell Cytotoxicity*. *The AAPS Journal*, 2015. **17**(1): p. 216-226.
  70. Wilkinson, A., et al., *Lipid conjugation of TLR7 agonist Resiquimod ensures co-delivery with the liposomal Cationic Adjuvant Formulation 01 (CAF01) but does not enhance immunopotential compared to non-conjugated Resiquimod+CAF01*. *Journal of Controlled Release*, 2018. **291**: p. 1-10.
  71. Cheng, N., et al., *A nanoparticle-incorporated STING activator enhances antitumor immunity in PD-L1-insensitive models of triple-negative breast cancer*. *JCI Insight*, 2018. **3**(22).
  72. Schmidt, S.T., et al., *The administration route is decisive for the ability of the vaccine adjuvant CAF09 to induce antigen-specific CD8+ T-cell responses: The immunological consequences of the biodistribution profile*. *Journal of Controlled Release*, 2016. **239**: p. 107-117.

73. Schulze, J., et al., *A Liposomal Platform for Delivery of a Protein Antigen to Langerin-Expressing Cells*. *Biochemistry*, 2019. **58**(21): p. 2576-2580.
74. Joshi, M.D., et al., *Targeting tumor antigens to dendritic cells using particulate carriers*. *J Control Release*, 2012. **161**(1): p. 25-37.
75. Tacken, P.J., et al., *Targeting DC-SIGN via its neck region leads to prolonged antigen residence in early endosomes, delayed lysosomal degradation, and cross-presentation*. *Blood*, 2011. **118**(15): p. 4111.
76. Benne, N., et al., *Complement Receptor Targeted Liposomes Encapsulating the Liver X Receptor Agonist GW3965 Accumulate in and Stabilize Atherosclerotic Plaques*. *Adv Healthc Mater*, 2020. **9**(10): p. e2000043.
77. Rosalia, R.A., et al., *CD40-targeted dendritic cell delivery of PLGA-nanoparticle vaccines induce potent anti-tumor responses*. *Biomaterials*, 2015. **40**: p. 88-97.
78. Fernandez-Rodriguez, J. and T.C. Marlovits, *Induced heterodimerization and purification of two target proteins by a synthetic coiled-coil tag*. *Protein Science : A Publication of the Protein Society*, 2012. **21**(4): p. 511-519.



# Chapter 2

## Enhanced immunogenicity of recombinant Bet v 1 through combined encapsulation in and adsorption to cationic liposomes

R.J.T. Leboux<sup>a</sup>, P. Català<sup>a#</sup>, H.J.M. Warmenhoven<sup>b,c</sup>, A. Logiantara<sup>b</sup>, A. Kros<sup>d</sup>, L. van Rijt<sup>b</sup>, B. Slütter<sup>a</sup>, R. van Ree<sup>b,e</sup>, W. Jiskoot<sup>a@</sup>

<sup>a</sup> Division of BioTherapeutics, Leiden Academic Centre for Drug Research, Leiden University, Leiden, The Netherlands

<sup>b</sup> Department of Experimental Immunology, Amsterdam University Medical Centers, location AMC, Meibergdreef 9, Amsterdam, The Netherlands

<sup>c</sup> HAL Allergy BV, J.H. Oortweg, Leiden, The Netherlands

<sup>d</sup> Division of Supramolecular & Biomaterials Chemistry, Leiden Institute of Chemistry, Leiden University, Leiden, The Netherlands

<sup>e</sup> Department of Otorhinolaryngology, Amsterdam University Medical Centers, location AMC, Meibergdreef 9, Amsterdam, The Netherlands

<sup>#</sup> current address: University Eye Clinic Maastricht, Maastricht University Medical Center and Department of Cell Biology-Inspired Tissue Engineering, MERLN Institute for Technology-Inspired Regenerative Medicine, Maastricht, The Netherlands

<sup>@</sup> **Correspondence:** w.jiskoot@lacdr.leidenuniv.nl

## **Abstract**

Liposomes are a commonly used vaccine adjuvant and an interesting candidate to replace aluminum hydroxide (alum) in allergy vaccines. Antigens are often either encapsulated in the aqueous core of liposomes, or adsorbed to the lipid surface. We have evaluated the effect of association method on the availability of antigen for IgE binding and the ability to induce an immune response.

Increasing amounts of Bet v 1, a recombinant version of the major allergen in birch pollen allergy, were formulated with cationic liposomes, either adsorbed or encapsulated, or a combination of both. Upon increasing the Bet v 1/lipid ratio, liposome size increased slightly, and signs of aggregation were visible starting at a protein/lipid mass ratio of 0.15. With increasing Bet v 1 concentration, the association efficiency decreased. Encapsulated allergen was approximately 8-fold less effective at binding IgE than Bet v 1 in buffer, as determined by ImmunoCAP inhibition. Bet v 1 adsorbed to or encapsulated in cationic liposomes was able to induce an antigen-specific IgG1 response, but liposomes with both encapsulated and adsorbed Bet v 1 resulted in a stronger IgG1 and response as well as a stronger cytokine production upon stimulation.

In conclusion, encapsulation of Bet v 1 resulted in the most hypo-allergenic formulation. The combination of adsorption and encapsulation resulted in the most efficient antigen association to cationic liposomes, as well as the strongest immune response.

## Introduction

Subcutaneous allergen immunotherapy (SCIT) has been used to treat allergies for more than 100 years [1]. During immunotherapy, the ongoing immune response is redirected from a T helper (Th)2 response towards a response that suppresses Th2-driven allergy symptoms by induction of Th1 or regulatory Th cells (Treg). The treatment usually consists of weekly subcutaneous injections of allergen extracts in the build-up phase and monthly injections in the maintenance phase and requires 3-5 years to achieve sustained therapeutic effect [2]. The long duration of the therapy and frequent (local) side effects are associated with low therapy adherence [3].

In mice, the desired protective immune response has been reported to be characterized by IL-10 and IgG2a, a mixed Treg/Th1 response [4, 5]. Apart from being an adjuvant, adsorption to aluminium hydroxide (alum) also decreases the access of IgE to allergen, which results in less side-effects [6]. An alternative adjuvant should ideally also contribute to achieving a similar or preferably higher degree of hypo-allergenicity, in order to prevent allergic adverse events. Many innovative ideas are explored to improve the efficacy and safety of SCIT, among which recombinant hypoallergenic allergens and new adjuvants [7]. Nanoparticles such as liposomes are an example of a new adjuvant that could replace alum [8].

Liposomes consist of at least one lipid bilayer and an aqueous core and are a versatile delivery system and adjuvant for vaccines [9-11]. The versatility is related to the large variety of synthetic and natural (phospho)lipids that are available and can be incorporated in the lipid bilayer [10, 12, 13]. Cationic liposomes are considered to be taken up more efficiently by antigen-presenting cells (APCs) than neutral or anionic counterparts, which is ascribed to the ability to interact with anionic cell surfaces [14, 15]. As uptake in APCs is a crucial first step to induce an immune response, cationic, rather than anionic, liposomes are often used in combination with an antigen for vaccination against a wide variety of diseases [11, 16, 17].

For vaccination purposes, antigens (= allergens in case of allergy vaccines) are commonly associated with liposomes in either of the following two ways: via adsorption to the surface of the liposome or by encapsulation in the aqueous core of the vesicle [18]. Association to the liposome surface is an easy method, in which antigen and pre-formed liposomes are mixed. The efficiency of adsorption, however, depends on the physicochemical properties of the antigen and the liposomes and often relies on electrostatic interactions [19, 20]. Upon *in vivo* administration, however competition with endogenous compounds, such as salts and proteins, may lead to rapid antigen desorption from the liposome

[21, 22]. Encapsulation in the aqueous core ensures that antigen and liposomes stay associated for a longer time *in vivo*. However, the manufacturing is often a laborious and inefficient process, in which both precious antigen and liposomes can be lost [16].

In order to assess the effect of association method on the induced immune response, we formulated Bet v 1, the main allergen in birch pollen allergy [23], with cationic liposomes via adsorption onto the surface of the lipid bilayer, encapsulation in the aqueous core, or a combination with Bet v 1 both encapsulated and adsorbed. We assessed the effect of allergen concentration in the initial formulation on particle size, zeta potential and final allergen association. Subsequently, we immunized mice with 10 µg bet v 1 in the different liposomal Bet v 1 formulations and compared the immune response to that of Bet v 1 adsorbed to alum (Bet v 1-alum). We observed that liposomal Bet v 1 formulations induced stronger antibody responses than Bet v 1-alum. The cationic liposome formulation with Bet v 1 both adsorbed on the surface and encapsulated in the core induced the strongest humoral immune response.

## Materials & Methods

### Chemicals and reagents

Cholesterol (CHOL), 1,2-distearoyl-*sn*-glycero-3-phosphocoline (DSPC) and 1,2-dioleoyl-3-trimethylammonium-propane (DOTAP) were purchased from Avanti Lipids. Sucrose, HEPES and sodium azide were obtained from Sigma Aldrich, and aluminum hydroxide (Imject<sup>®</sup> Alum) from Thermo Scientific. Recombinant Bet v 1 (isoform Bet v 1.0101) was purchased from the Department of Molecular Biology of the University of Salzburg (Salzburg, Austria).

### Preparation of liposome formulations

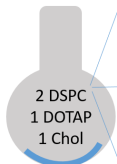


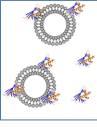

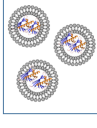



The liposomes consisted of DSPC, DOTAP and cholesterol in a 2:1:1 molar ratio. These lipids were dissolved in chloroform and mixed in the desired ratio. Subsequently, the organic solvent was evaporated in a rotary evaporator at 37 ° C and 180 mbar, leaving a lipid film. This film was hydrated at 37 ° C in the presence of glass beads with 1 mL of 10 mM HEPES (pH 7.4), 280 mM sucrose buffer (H/S buffer). After hydration, the suspension was snap-frozen and lyophilized resulting in a fluffy cake. The lipid cake was rehydrated at 37 ° C with filtered Milli-Q water to a final volume of 2 mL and homogenized by using a LIPEX extruder (Evonik, Canada) over a stacked 400-nm and 200-nm Nucleopore Track-Etch membrane (Whatman, the Netherlands).

For adsorbed Bet v 1, liposomes were prepared as described above. To adsorb Bet v 1, liposomes were mixed with varying amounts of Bet v 1 and incubated at

ambient temperature for at least 15 minutes prior to sample analysis or injection.

Encapsulated Bet v 1 liposomes were prepared as described above, but varying amounts of Bet v 1 were dissolved in the H/S buffer in the hydration step. After preparation, any free and bound Bet v 1 was removed with centrifuge membrane concentrators. Three repeated wash-steps were performed, in which the liposomes were concentrated approximately 5-fold, reconstituted with H/S to the original volume, and unbound fractions were collected.

For a combination of adsorbed and encapsulated Bet v 1, liposomes were prepared as for encapsulated Bet v 1, with varying amounts of Bet v 1 in the H/S buffer in the hydration step. Here, however, no purification step was performed to remove free and bound Bet v 1. The differences between these formulations are schematically depicted in Figure 1.

	Lipid film hydration	After extrusion	DLS	Association efficiency
1. Mix lipids in desired ratio 2. Evaporate solvents in rotary evaporator 1. 150 mbar 2. 37 °C 	<b>adsorbed</b>  Hydrate with buffer	 Store at 2-8 °C until measurements		Separate unbound Measure unbound $\frac{(CONC_{initial} - CONC_{unbound})}{CONC_{initial}} * 100\%$
	<b>encapsulated</b>  Hydrate with Bet v 1 in buffer	Purification: Remove unbound Bet v 1		Break open liposome Measure protein $\frac{(CONC_{liposomes})}{CONC_{initial}} * 100\%$
	<b>adsorbed &amp; encapsulated</b>  Hydrate with Bet v 1 in buffer	 Store at 2-8 °C until measurements		Separate unbound Measure unbound $\frac{(CONC_{initial} - CONC_{unbound})}{CONC_{initial}} * 100\%$

*Figure 1. Overview of the different formulations. The differences in the preparation process and schematically what is measured in the characterization. For adsorbed Bet v 1, no antigen is added in the liposome preparation. Only liposomes with encapsulated Bet v 1 were purified directly after they were formed in the extrusion process. For adsorbed and adsorbed and encapsulated formulation, there is also a fraction of unbound protein present.*

### Liposome characterization

Hydrodynamic diameter (Z-average diameter) and polydispersity index were measured by dynamic light scattering (DLS) using a Zetasizer Nano ZS (Malvern Instruments Ltd., Worcestershire, UK). The zeta potential was measured using laser Doppler electrophoresis (IDe) on the same machine with a Zeta Dip Cell (Malvern Instruments Ltd.). Each sample was diluted 100-fold in 10 mM HEPES buffer (pH 7.4, 0.2-µm filtered) before measurement.



### Determination of association efficiency

To determine the association efficiency of the different formulations, unbound protein was separated from liposomes with centrifuge membrane concentrators (Vivaspin2, 300.000 MWCO, Sartorius) by spinning down at 500 x g at 5 °C until concentrated approximately 5-fold. The flow through, which contained unbound Bet v 1 was collected, while the concentrate was diluted to the original volume with H/S buffer.

For liposomes with Bet v 1 adsorbed, the unbound fraction was removed as described above. The unbound fraction was collected and used to determine the percentage of unbound protein. Adsorption efficiency was calculated as:

$$\text{Adsorption efficiency} = \frac{(\text{CONC initial} - \text{CONC unbound})}{\text{CONC initial}} * 100\%$$

For encapsulated Bet v 1, the liposomes were purified directly after the extrusion step. The unbound protein was separated as described above. This process was repeated 3 times, to ensure that > 99% of unbound protein was removed. Subsequently, the liposomes were dissolved in methanol and the protein content was determined as described below. Encapsulation efficiency is calculated as:

$$\text{Encapsulation efficiency} = \frac{\text{CONC in liposomes}}{\text{CONC initial}} * 100\%$$

For the combination of encapsulated and adsorbed Bet v 1, the association efficiency was determined as for adsorbed Bet v 1. The unbound fraction was removed as described above and the protein content of this fraction was determined. Subsequently, the association efficiency was calculated:

$$\text{Association efficiency} = \frac{(\text{CONC initial} - \text{CONC unbound})}{\text{CONC initial}} * 100\%$$

### Protein concentration determination

Protein concentration was determined with a Micro BCA assay kit (Boster Biological Technology, Pleasanton, CA, USA) according to the manufacturer's protocol. This kit was chosen as it is compatible with methanol. Flow through fractions after separation with Vivaspin2 columns were measured without sample preparation. For encapsulated fraction, a modified Bligh-Dyer extraction was performed as described previously [24]. In short, 100 µL of liposome suspension were mixed with 250 µL of methanol and 125 µL of chloroform. The mixture was vigorously vortexed for 10 seconds before 125 µL of chloroform and 250 µL of 0.1 M HCl were added to the mixture. The mixture was vigorously vortexed for 20 seconds and centrifuged during 5 minutes at 2100 rpm and room temperature. After centrifugation, the upper phase (methanol-water), containing the Bet v 1, was collected and its protein content was determined.

### ImmunoCAP inhibition assay

The IgE binding potency of various liposome formulations was determined by ImmunoCAP IgE inhibition assay [25]. To that end, liposomes were serially diluted (dilution factor 10) in 10 mM HEPES, 280 mM sucrose, pH 7.4. A pool of 36 sera from birch pollen allergic patients (from a reference serum bank at AMC [26, 27]) was diluted to 12 kU/mL of specific IgE against Bet v 1 and added 1:1 (v/v) to all serial dilutions, followed by incubation at room temperature for one hour. Uncomplexed IgE in the samples was measured on a Phadia-250 machine (ThermoFisher Scientific, Uppsala, Sweden) loaded with rBet v 1 ImmunoCAPs (catalogue code t215, ThermoFisher Scientific). The percentage inhibition was calculated on a scale from 100% inhibition (no serum) to an 0% inhibition (PBS + serum). The concentration at which 50% inhibition occurred (IC<sub>50</sub>) was determined by non-linear regression fit with variable slope (4 parameters: no restriction for top, bottom was set to 0, Hill coefficient was set to “shared for all data sets”, and IC<sub>50</sub> must be greater than 0).

### *In vivo* immunogenicity

Mice were immunized subcutaneously at day 0, 7 and 14 with 10 µg Bet v 1, as determined by BCA, in various formulations containing liposomes or alum (1 mg per injection). Serum for antibody detection was collected at days -1, 6, 13 and 20. At day 27, 28 and 29 the animals received an intranasal challenge under 3% (v/v) isoflurane anesthesia with 100 µg/mL birch pollen extract (BPE, HAL Allergy, Netherlands) in PBS to induce lung inflammation. On day 31, the mice were sacrificed, and blood was collected to analyze Bet v 1 specific levels of IgG1 and IgG2a in serum. Moreover, lung draining lymph nodes were collected to determine the production of IL-4, IL-5, IL-13, IL-10 and IFN-γ cytokines after stimulation with Bet v 1.

### Determination of Bet v 1 specific antibodies

Serum was analyzed by ELISA for the level of Bet v 1-specific IgG1 and IgG2a (IgG1: Opteia, BD, San Diego, CA, USA, IgG2a: eBioscience) as previously described [4]. In short, Maxisorp plates were coated with recombinant Bet v 1 overnight and subsequently washed. After blocking with 10% fetal calf serum, serum samples were diluted 100-fold, prior to addition to the microtiter plate and incubated for 2 hours at room temperature. Subsequently, detecting biotin-conjugated antibodies specific for IgG1 or IgG2a, respectively, were added, followed by an streptavidin-HRP and TMB substrate detection step. Coloring reaction was stopped by addition of H<sub>2</sub>SO<sub>4</sub>, according to the manufacturer's instructions.

### *Ex vivo* re-stimulation of lung draining lymph node cells

Lung draining lymph node cell suspensions were plated in a 96-well round bottom plate at a density of 2 x 10<sup>5</sup> cells per well in RPMI supplemented with gentamicin,

fetal calf serum and  $\beta$ -mercaptoethanol. The cells were re-stimulated for 4 days with 10  $\mu\text{g}/\text{mL}$  recombinant Bet v 1. Expression levels of cytokines IL-4, IL-5, IL-10, IL-13 and IFN- $\gamma$  were determined in the supernatant by ELISA (eBioscience).

## Statistics

Data was processed and analyzed in GraphPad v8 (Prism) for Windows. Statistical analysis was performed with the same program and the method of analysis is indicated in the figure legends.

## Results

Increasing amounts of Bet v 1 adsorbed to cationic liposomes ultimately results in aggregation

The association method of Bet v 1 with liposomes may affect the colloidal stability of the liposomes. Therefore, we evaluated how Bet v 1 loading of liposomes via adsorption or encapsulation affected the size and charge of liposomes. Empty liposomes consisting of DSPC, DOTAP and cholesterol had a hydrodynamic diameter of circa 200 nm and a zeta potential of > 35 mV. Mixing of increasing

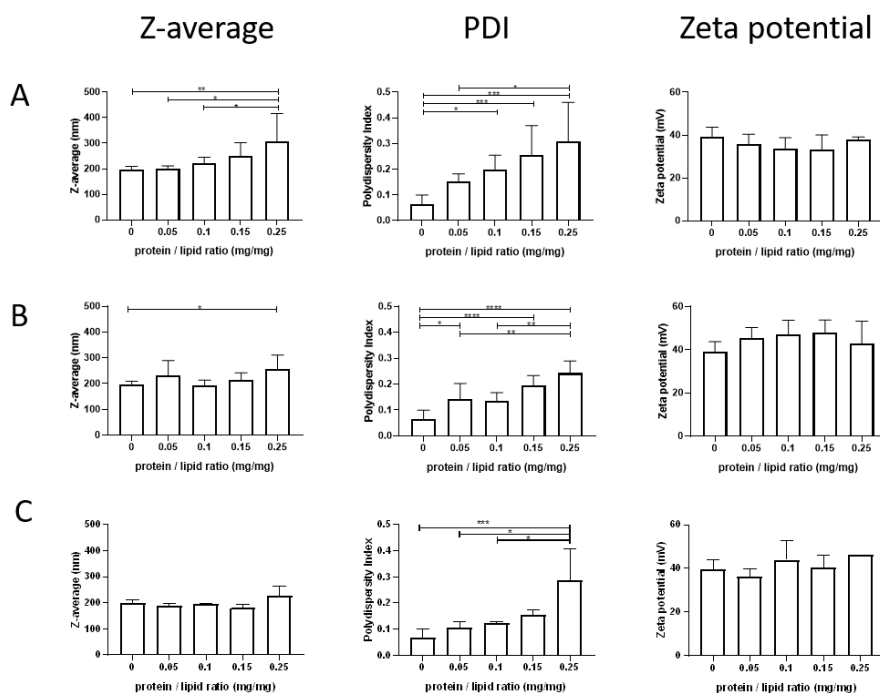


Figure 2. Liposome properties: Z-average diameter (left column), polydispersity index (middle column) and zeta potential (right column) of liposomes with increasing amounts of Bet v 1 adsorbed (A) or encapsulated (B) or both adsorbed and encapsulated (C). Mean values with standard deviations are plotted (n=2-6). Means were compared with a 1-way ANOVA and Tukey's multiple comparison post-test. \* =  $p < 0.05$ , \*\*  $p < 0.01$ , \*\*\* =  $p < 0.001$ , \*\*\*\* =  $p < 0.0001$ .

amounts of Bet v 1 (resulting in final Bet v 1 concentrations of 65 – 325 µg/mL) with empty liposomes (final concentration 1.25 mg lipid/mL) resulted in a slightly increased size and polydispersity index, while the zeta potential was not significantly changed (Figure 2A). While the size and zeta potential did not vary with increasing amounts of Bet v 1 encapsulated, the polydispersity index increased in a similar manner as for adsorption (Figure 2B). For a combination of adsorbed and encapsulated Bet v 1, the only changes observed were in the polydispersity index (Figure 2C). Although the effect on size seems low, from a protein/lipid ratio between 0.10 and 0.15 a second peak is visible in the size-intensity plot after adsorption, encapsulation and the combination of both (Supplementary Figure 1, 2 and 3 respectively), suggesting that some aggregation had occurred.

**Increasing amounts of Bet v 1 results in decreased association efficiency, but increased amount of associated antigen**

Next, we set out to investigate how increasing Bet v 1/lipid ratios affects the allergen association efficiency with liposomes for all formulations. Regardless of association method, more Bet v 1 was associated to liposomes with increasing amounts of initial Bet v 1 (Figure 2). The association efficiency, however, was decreased as more Bet v 1 was added for adsorption (Figure 2A) and encapsulation (Figure 2B), while the association efficiency was constant for the combination of encapsulation and association (Figure 2C). To have the highest possible allergen-association, without any visible aggregation, subsequent formulations for immunoCAP and the animal study were prepared with a protein/lipid ratio of 0.1 (w/w).

**Bet v 1 encapsulation in cationic liposomes decreases IgE binding**

In allergic patients, binding of IgE to Bet v 1 can cause potentially severe side effects. An ImmunoCAP assay was performed to evaluate whether the different association methods had effect on the IgE binding potency of Bet v 1. Adsorbed Bet v 1 should be accessible for IgE binding, while encapsulated Bet v 1 theoretically should not, unless liposomes break open or allergen can leak out. As shown in Figure 3, Bet v 1 adsorbed to liposomes bound IgE in a similar, dose-dependent manner as free Bet v 1. Bet v 1 which was encapsulated in liposomes showed an 8-fold reduction in IgE binding. This suggests that not all Bet v 1 has been removed from the outside of the liposomes. Based on figure 3, the liposomes with both encapsulated and adsorbed Bet v 1, should have approximately 50% of the Bet v 1 encapsulated, and 50% available for binding IgE. The IgE inhibition of liposomes with adsorbed and encapsulated Bet v 1 showed an inhibition curve in between that of adsorbed and encapsulated Bet v 1 (Figure 4).

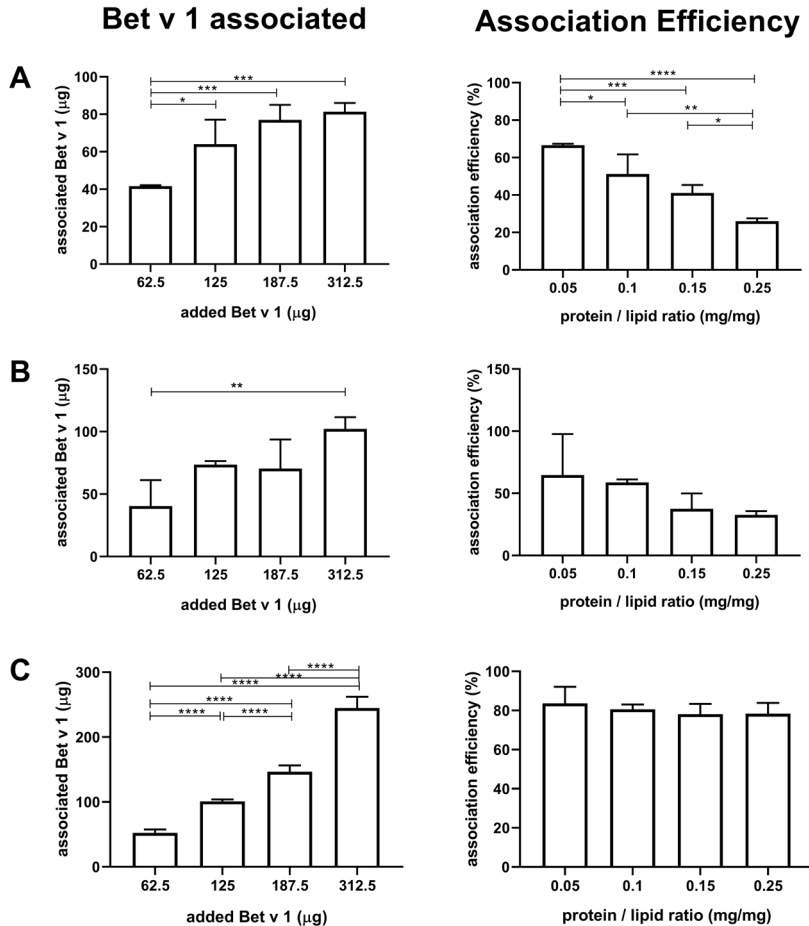


Figure 3. Total amount of antigen associated to liposomes (left panel) and association efficiency (right panel) after increasing amounts of Bet v 1 were adsorbed to (A), encapsulated in (B), or adsorbed to and encapsulated in (C) liposomes. Mean values with standard deviations are plotted (n=2-6). Means were compared with a 1-way ANOVA and Tukey's multiple comparison post-test. \* =  $p < 0.05$ , \*\*  $p < 0.01$ , \*\*\* =  $p < 0.001$ , \*\*\*\* =  $p < 0.0001$ .

### Cationic liposomes with Bet v 1 on surface and in core induced strongest IgG1 response in mice

To assess the impact of the method of allergen association to liposomes on immunogenicity, mice were immunized with 10 μg of Bet v 1 in the different liposome formulations. The liposomal Bet v 1 formulations were compared to a formulation of Bet v 1 adsorbed to alum. Bet v 1-specific IgG1, IgG2a and IgE were measured in the mouse sera at the end of the experiment. At the (100-fold) dilution used for IgG detection, liposomes without allergen and alum-adsorbed Bet v 1 did not induce detectable antigen-specific antibodies (Figure 5A). In contrast, all liposomal Bet v 1 formulations induced antigen-specific IgG1.

The liposomal formulation in which Bet v 1 was both encapsulated and adsorbed induced the strongest IgG1 response (4 out of 5 responders). None of the tested formulations induced detectable amounts of Bet v 1-specific IgG2a or IgE.

	Bet v 1	Adsorbed	Encapsulated	Adsorbed + encapsulated
IC50	0.001700	0.002247	0.01225	0.006104

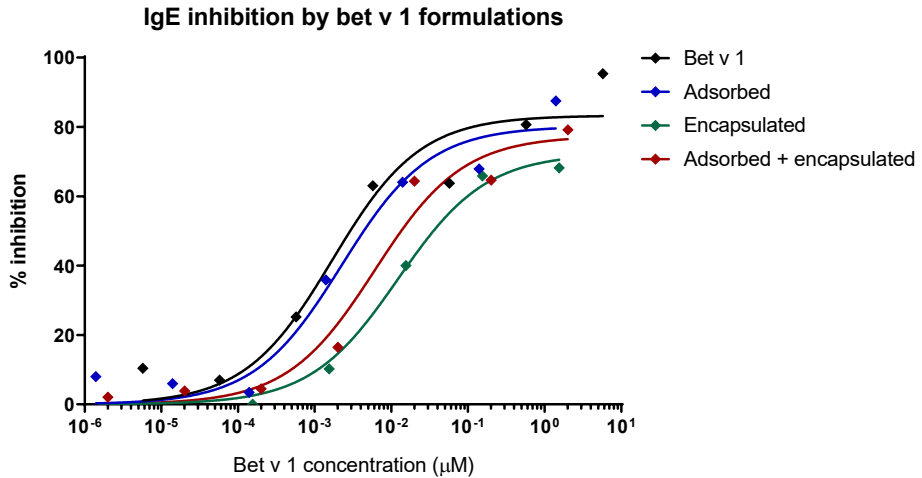


Figure 4. The ability of free Bet v 1 (black), or Bet v 1 adsorbed to (blue), encapsulated in (green), both adsorbed to and encapsulated in (red) liposomes to bind patient-derived Bet v 1 specific IgE.

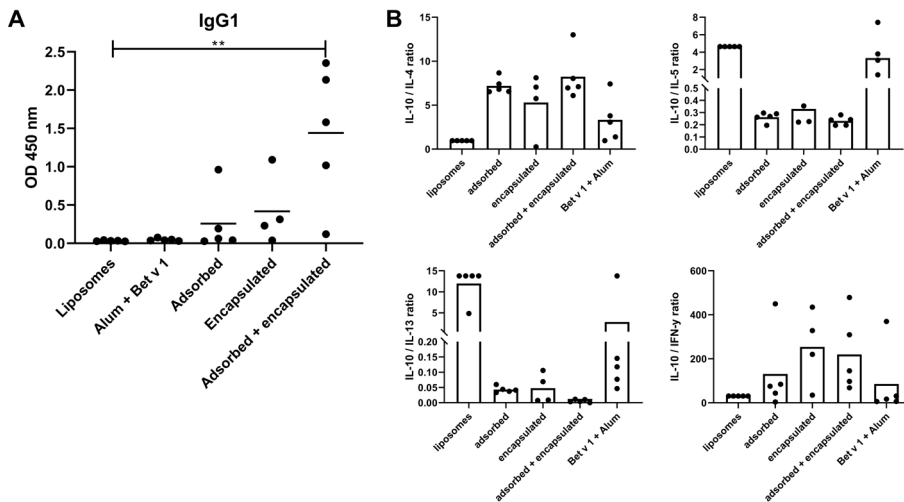


Figure 5. A. Bet v 1-specific IgG1 in serum after immunization of mice with Bet v 1 associated to liposomes in different ways. Group mean and standard deviation are plotted ( $n = 4-5$  mice/group). B. Production of IL-4, IL-5, IL-10, IL-13 and IFN- $\gamma$  by lung draining lymph node cells from immunized mice after exposure to Bet v 1. Group mean and standard deviation are plotted ( $n = 4-5$  mice/group). Groups were compared with a Kruskal-Wallis test followed by Dunn's correction for multiple comparisons. \* =  $p < 0.05$ , \*\* =  $p < 0.01$ , \*\*\* =  $p < 0.001$ .

After sacrifice, lung draining lymph nodes were isolated and the production of cytokines by lymph node cells was measured after exposure to Bet v 1. The cytokine production trend followed that of the antibody responses. No cytokines were detected for the groups immunized with liposomes alone, or alum-adsorbed Bet v 1. The highest IL-5, IL-10 and IL-13 levels were observed after immunization with a combination of adsorbed and encapsulated Bet v 1, while encapsulated Bet v 1 resulted in higher cytokine levels than adsorbed Bet v 1 (Supplementary Figure 4), except for IFN- $\gamma$ , which had low levels in all groups. In cytokine ratios (IL-10 / IL-4, IL-5, IL-13 and IFN- $\gamma$ ) all liposome formulations induce the same pattern compared to liposomes without antigen or alum-adsorbed Bet v 1 (Figure 5B). The IL-10/IL-4 ratio is increased compared to empty liposomes or alum-adsorbed Bet v 1, while the IL-10/IL-5 and IL-10/IL-13 ratio is decreased. The IL-10/IFN- $\gamma$  ratio is very high in all groups, as very little IFN- $\gamma$  was detected.

## Discussion

In this study we set out to explore the effect of allergen association method on liposome properties and immunogenicity of the allergen (Bet v 1). Allergen adsorption to liposomes is most efficient with opposite charges, which happens in the case of cationic liposomes with negatively charged Bet v 1 (isoelectric point = 5.4 [28]). The adsorption of anionic model antigens ( $\alpha$ -lactalbumin, ovalbumin and bovine serum albumin) to cationic liposomes has been reported to result in up to almost 100% adsorption efficiencies. There is a maximum antigen adsorption capacity of liposomes and a threshold above which aggregation starts occurring, which depends on properties of both protein and formulation. The aggregation which was detected for Bet v 1/lipid ratios larger than 0.1-0.15 (w/w) is in line with previous studies [19, 20]. The association efficiency increased with decreasing antigen / lipid ratio, which is in line with other studies [29].

Successful removal of unbound Bet v 1 in encapsulated Bet v 1 was confirmed by the results of the ImmunoCAP assay. While adsorbed Bet v 1 resulted in practically the same IgE binding as Bet v 1 in buffer, encapsulated Bet v 1 resulted in an 8-fold lower IgE binding. This suggests that approximately 12% of all Bet v 1 was present on the surface of the liposomes or had leaked out under the assay conditions. The presence of adsorbed Bet v 1 on the liposome surface might be an inevitable consequence of the formulation process because of incomplete removal of adsorbed Bet v 1 despite multiple washing steps. In the formulation where the washing steps were omitted (adsorbed + encapsulated, figure 4), the IC<sub>50</sub> of IgE binding was in between the IC<sub>50</sub> of liposomes with adsorbed and encapsulated Bet v 1, respectively. This is in line with the Bet v 1 encapsulation efficiency of approximately 50% that was found for a 0.1 antigen / lipid ratio. With regard to safety, encapsulated antigen would be the preferred option over

adsorption, or a combination, as approximately 8-fold more Bet v 1 was required to achieve a similar IgE binding.

Formulations with adsorbed allergen also had a fraction of unbound, free allergen. Based on the ImmunoCAP assay, even the formulation which was washed repeatedly to remove any bound and free Bet v 1, was able to bind Bet v 1-specific IgE, albeit to a lesser extent than adsorbed Bet v 1. This unbound fraction is not likely to interfere in DLS measurements, as proteins are much smaller than liposomes and therefore will hardly contribute to the light scattering signal [30]. The unbound fraction is definitely found in the ImmunoCAP assay, where also surface-adsorbed Bet v 1 seems to be detected as free Bet v 1. This unbound fraction may be problematic when applying these formulations for immunotherapy, where free allergen is associated with side effects [5, 31]. The unbound Bet v 1 is however not expected to contribute significantly to the induced immune response, as free Bet v 1 has previously shown to not induce an immune response in naïve mice [data not shown, Lebourg et al., Chapter 6]. The immune responses that were reported in this manuscript were unexpected, both for the cationic liposomes as for aluminium hydroxide. Cationic liposomes reportedly induce a strong Th1 skewed immune response, of which antigen-specific IgG2a and IFN- $\gamma$  are hallmarks [10, 11, 32]. Surprisingly, no IgG2a induction in mice by any of the liposome formulations was observed. Moreover, barely any IFN- $\gamma$  was detected after stimulation of lung draining lymph node cells *ex vivo*. This poor IFN- $\gamma$  production is not in line with previous observations [33, 34]. However, it is important to note that others used spleen-derived cells while in this study lung draining lymph node cells were used, because a strong response in these cells was expected after the intranasal boost that was administered at the end of the experiment. These cells produced large quantities of IL-5, IL-10, IL-13, and to a lesser extent IL-4, which are signature cytokines for a Th2-skewed response [35].

The weak response in mice that received alum-adsorbed Bet v 1 was also unexpected. In several reports, alum-adsorbed Bet v 1 has been described to induce a strong, allergy-like pathology in mice [4, 36-38]. For this purpose however, the formulation is typically administered intraperitoneally (i.p.). It has been reported that subcutaneous administration of alum-adsorbed Bet v 1 is less efficient at inducing antigen-specific antibodies than i.p. administration [38, 39]. Perhaps another dosing regimen, or increased allergen dose per injection would have increased the immune response. Altogether, the formulations used in this manuscript did not induce an immune response which is associated with relief of allergy symptoms in mice [4], but give insight into the effect of antigen association method on the induced immune response.



Similarly to the results presented in this manuscript, no significant differences were found between either adsorption or encapsulation of influenza antigens with cationic liposomes in a previous study [40], but a combination of both methods was not explored. Tetanus toxoid either mixed or encapsulated (but not purified) in liposomes in both cases induced similar IgG1, IgG2a and IgG2b levels. The antibody response lasted longer in mice injected with liposomes that contained encapsulated antigen. The combination of adsorption and encapsulation, as tested in our study, may induce the strongest response because there is more and potentially longer antigen exposure. First, surface antigen is (partially) desorbed from the liposomes and can quickly migrate away from the injection site [19, 21]. Subsequently, cationic liposomes containing antigen remain at the injection site and are removed by APCs that process and present antigen fragments as well. This may be beneficial, because a humoral response requires intact antigen (quickly desorbed antigen), which is enhanced by helper T-cell stimulation with antigen derived peptides (from processed encapsulated antigen) [41]. The same mechanism is assumed for colloidal aluminum salt-based adjuvants, which slowly release antigen from the injection site [42].

In conclusion, we have shown that preparing cationic liposomes with increasing amounts of Bet v 1 results in more association to liposomes, but a lower association efficiency. Bet v 1 causes aggregation between an antigen/lipid ratio of 0.10 and 0.15 (w/w) regardless of association method. Encapsulation of Bet v 1 in liposomes seems to result in a hypo-allergenic product, as the ability of Bet v 1 to bind IgE was reduced 8-fold. Unpurified liposomes in which Bet v 1 was both adsorbed and encapsulated (and partly unbound) were more allergenic than the ones with only encapsulated Bet v 1, but induced a stronger IgG1 response as well as a stronger cellular response to *ex vivo* stimulation, than otherwise associated Bet v 1. This demonstrates that the association method not only affects the association efficiency, but also the subsequent (hypo)allergenicity and immunogenicity. The most hypo-allergenic formulation is the one with encapsulated Bet v 1, while liposomes with both encapsulated and adsorbed Bet v 1 showed the highest immunogenicity.

## **Funding**

This work was supported by the Nederlandse Organisatie voor Wetenschappelijk Onderzoek (TKI-NCI, grant 731.014.207).

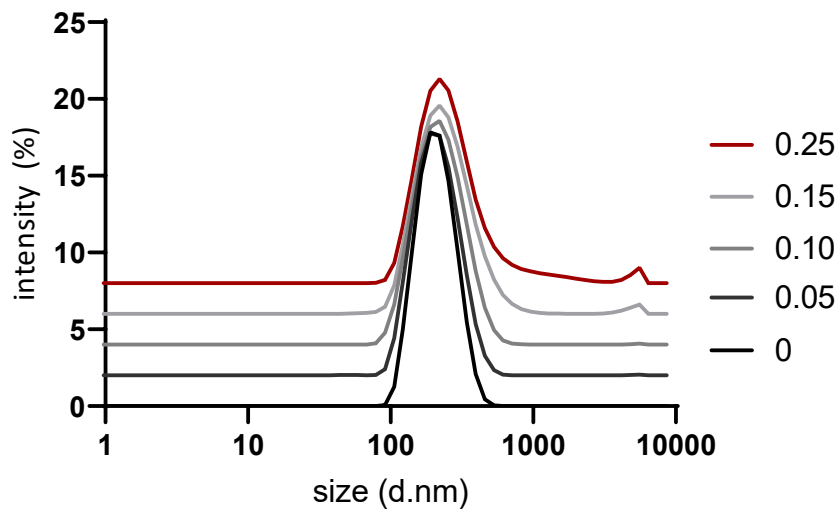
## References

1. Finegold, I., et al., *Immunotherapy throughout the decades: from Noon to now*. Annals of Allergy, Asthma & Immunology, 2010. **105**(5): p. 328-336.
2. Alvaro-Lozano, M., et al., *EAACI Allergen Immunotherapy User's Guide*. Pediatric allergy and immunology : official publication of the European Society of Pediatric Allergy and Immunology, 2020. **31 Suppl 25**(Suppl 25): p. 1-101.
3. Allam, J.P., et al., *Comparison of allergy immunotherapy medication persistence with a sublingual immunotherapy tablet versus subcutaneous immunotherapy in Germany*. J Allergy Clin Immunol, 2018. **141**(5): p. 1898-1901.
4. van Rijt, L.S., et al., *Birch Pollen Immunotherapy in Mice: Inhibition of Th2 Inflammation Is Not Sufficient to Decrease Airway Hyper-Responsivity*. International Archives of Allergy and Immunology, 2014. **165**(2): p. 128-139.
5. Pfaar, O., et al., *Perspectives in allergen immunotherapy: 2019 and beyond*. Allergy, 2019. **74 Suppl 108**: p. 3-25.
6. van der Kleij, H.P.M., et al., *Chemically modified peanut extract shows increased safety while maintaining immunogenicity*. Allergy, 2019. **74**(5): p. 986-995.
7. Jongejan, L. and R. van Ree, *Modified allergens and their potential to treat allergic disease*. Curr Allergy Asthma Rep, 2014. **14**(12): p. 478.
8. Schijns, V., et al., *Modulation of immune responses using adjuvants to facilitate therapeutic vaccination*. Immunological Reviews, 2020. **296**(1): p. 169-190.
9. Christensen, D., et al., *Cationic liposomes as vaccine adjuvants*. Expert Rev Vaccines, 2007. **6**(5): p. 785-96.
10. Schwendener, R.A., *Liposomes as vaccine delivery systems: a review of the recent advances*. Therapeutic Advances in Vaccines, 2014. **2**(6): p. 159-182.
11. Christensen, D., et al., *Cationic liposomes as vaccine adjuvants*. Expert Review of Vaccines, 2007. **6**(5): p. 785-796.
12. Perrie, Y., et al., *Designing liposomal adjuvants for the next generation of vaccines*. Adv Drug Deliv Rev, 2016. **99**(Pt A): p. 85-96.
13. Li, J., et al., *A review on phospholipids and their main applications in drug delivery systems*. Asian Journal of Pharmaceutical Sciences, 2015. **10**(2): p. 81-98.
14. Ibaraki, H., et al., *Effects of surface charge and flexibility of liposomes on dermal drug delivery*. Journal of Drug Delivery Science and Technology, 2019. **50**: p. 155-162.
15. Foged, C., et al., *Interaction of dendritic cells with antigen-containing liposomes: effect of bilayer composition*. Vaccine, 2004. **22**(15): p. 1903-1913.
16. Heuts, J., et al., *Cationic Liposomes: A Flexible Vaccine Delivery System for Physicochemically Diverse Antigenic Peptides*. Pharmaceutical Research, 2018. **35**(11).
17. Loney, C., M. Vandenbranden, and J.-M. Ruysschaert, *Cationic lipids activate intracellular signaling pathways*. Advanced Drug Delivery Reviews, 2012. **64**(15): p. 1749-1758.
18. Watson, D.S., A.N. Endsley, and L. Huang, *Design considerations for liposomal vaccines: Influence of formulation parameters on antibody and cell-mediated immune responses to liposome associated antigens*. Vaccine, 2012. **30**(13): p. 2256-2272.
19. Hamborg, M., et al., *Elucidating the mechanisms of protein antigen adsorption to the CAF/NAF liposomal vaccine adjuvant systems: Effect of charge, fluidity and antigen-to-lipid ratio*. Biochimica et Biophysica Acta (BBA) - Biomembranes, 2014.

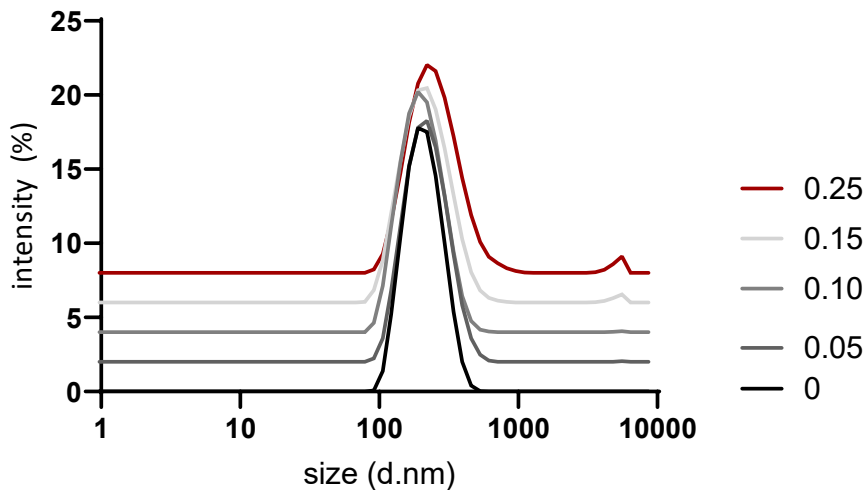
- 1838**(8): p. 2001-2010.
20. Hamborg, M., et al., *Protein Antigen Adsorption to the DDA/TDB Liposomal Adjuvant: Effect on Protein Structure, Stability, and Liposome Physicochemical Characteristics*. Pharmaceutical Research, 2013. **30**(1): p. 140-155.
  21. Schmidt, S.T., et al., *The administration route is decisive for the ability of the vaccine adjuvant CAF09 to induce antigen-specific CD8+ T-cell responses: The immunological consequences of the biodistribution profile*. Journal of Controlled Release, 2016. **239**: p. 107-117.
  22. Kaur, R., et al., *Pegylation of DDA:TDB liposomal adjuvants reduces the vaccine depot effect and alters the Th1/Th2 immune responses*. J Control Release, 2012. **158**(1): p. 72-7.
  23. Biedermann, T., et al., *Birch pollen allergy in Europe*. Allergy, 2019. **74**(7): p. 1237-1248.
  24. Varypataki, E.M., et al., *Cationic liposomes loaded with a synthetic long peptide and poly(I:C): a defined adjuvanted vaccine for induction of antigen-specific T cell cytotoxicity*. The AAPS journal, 2014. **17**(1): p. 216-226.
  25. AB, P., *Directions for use. ImmunoCAP specific IgE*. 2014: <https://dfu.phadia.com/Data/Pdf/56cb2b6389c23251d0d2b2ff.pdf>. p. 4.
  26. van Ree, R., et al., *The CREATE Project: Development of Certified Reference Materials for Allergenic Products and Validation of Methods for Their Quantification*, in *Multidisciplinary Approaches to Allergies*, Z.-S. Gao, et al., Editors. 2012, Springer Berlin Heidelberg: Berlin, Heidelberg. p. 149-179.
  27. Chapman, M.D., et al., *The European Union CREATE Project: A model for international standardization of allergy diagnostics and vaccines*. Journal of Allergy and Clinical Immunology, 2008. **122**(5): p. 882-889.e2.
  28. Breitenbach, M., et al., *Biological and immunological importance of Bet v 1 isoforms*. Adv Exp Med Biol, 1996. **409**: p. 117-26.
  29. Colletier, J.-P., et al., *Protein encapsulation in liposomes: efficiency depends on interactions between protein and phospholipid bilayer*. BMC Biotechnology, 2002. **2**(1): p. 2-9.
  30. Bhattacharjee, S., *DLS and zeta potential – What they are and what they are not?* Journal of Controlled Release, 2016. **235**: p. 337-351.
  31. Patil, S.U. and W.G. Shreffler, *Novel vaccines: Technology and development*. J Allergy Clin Immunol, 2019. **143**(3): p. 844-851.
  32. Benne, N., et al., *Anionic 1,2-distearoyl-sn-glycero-3-phosphoglycerol (DSPG) liposomes induce antigen-specific regulatory T cells and prevent atherosclerosis in mice*. J Control Release, 2018. **291**: p. 135-146.
  33. Guan, H.H., et al., *Liposomal Formulations of Synthetic MUC1 Peptides: Effects of Encapsulation versus Surface Display of Peptides on Immune Responses*. Bioconjugate Chemistry, 1998. **9**(4): p. 451-458.
  34. Liu, L., et al., *Immune responses to vaccines delivered by encapsulation into and/or adsorption onto cationic lipid-PLGA hybrid nanoparticles*. Journal of Controlled Release, 2016. **225**: p. 230-239.
  35. Okano, M., et al., *Interleukin-4-independent production of Th2 cytokines by nasal lymphocytes and nasal eosinophilia in murine allergic rhinitis*. Allergy, 2000. **55**(8): p. 723-731.
  36. van Rijt, L.S., et al., *Birch pollen-specific subcutaneous immunotherapy reduces ILC2 frequency but does not suppress IL-33 in mice*. Clinical & Experimental Allergy, 2018.

- 48(11):** p. 1402-1411.
37. Kitzmuller, C., et al., *Fusion proteins of flagellin and the major birch pollen allergen Bet v 1 show enhanced immunogenicity, reduced allergenicity, and intrinsic adjuvanticity*. J Allergy Clin Immunol, 2018. **141(1):** p. 293-299
  38. Repa, A., et al., *Influence of the route of sensitization on local and systemic immune responses in a murine model of type I allergy*. Clinical & Experimental Immunology, 2004. **137(1):** p. 12-18.
  39. Wallner, M., et al., *Reshaping the Bet v 1 fold modulates T(H) polarization*. J Allergy Clin Immunol, 2011. **127(6):** p. 1571-8 e9.
  40. Barnier-Quer, C., et al., *Adjuvant effect of cationic liposomes for subunit influenza vaccine: influence of antigen loading method, cholesterol and immune modulators*. Pharmaceuticals, 2013. **5(3):** p. 392-410.
  41. Parham, P., *Chapter 9: Immunity Mediated by B cells and antibodies*, in *The immune system*. 2009, Garland Science. p. 249-288.
  42. Heydenreich, B., et al., *Adjuvant effects of aluminium hydroxide-adsorbed allergens and allergoids - differences in vivo and in vitro*. Clin Exp Immunol, 2014. **176(3):** p. 310-319.

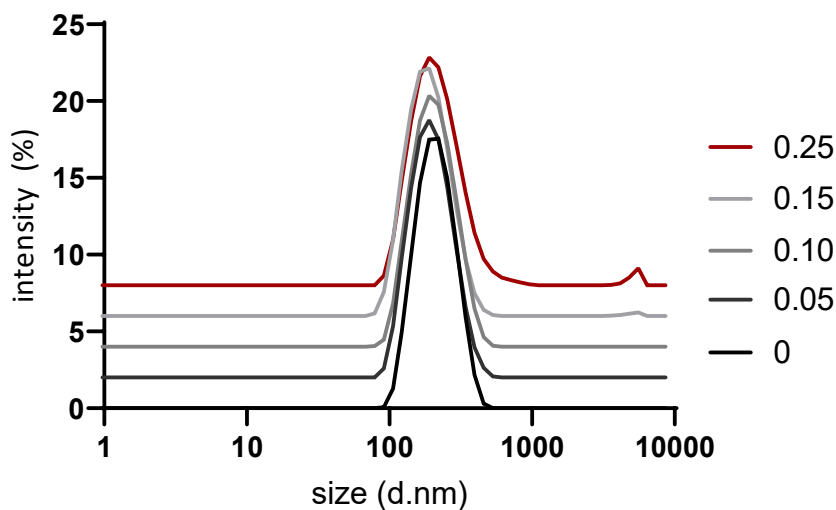
Supplementary Figures



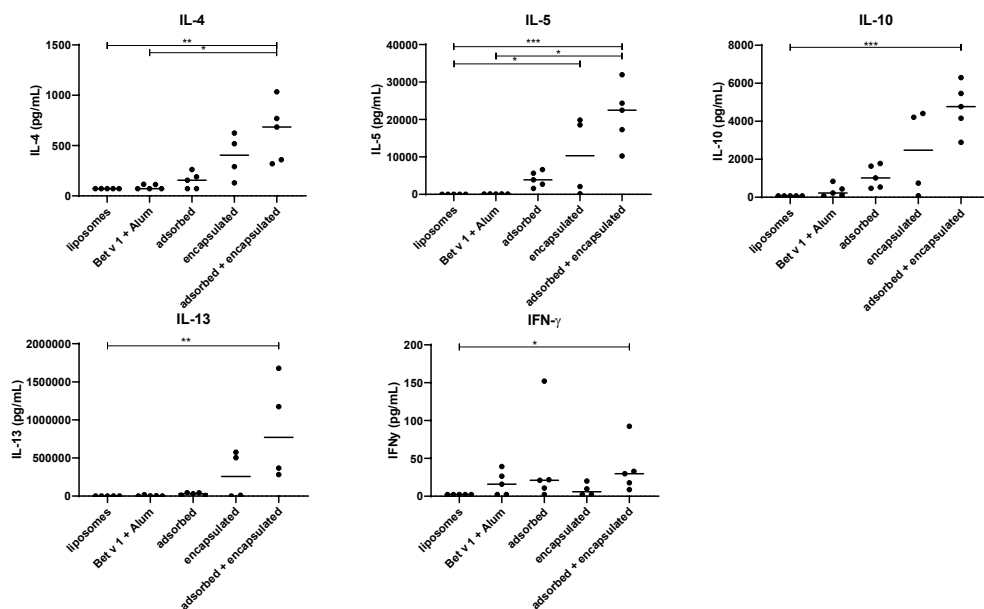
Supplementary Figure 1. Effect of protein/lipid ratio on particle size distribution of pre-formed cationic liposomes mixed with Bet v 1. The graphs shown are the average of 4-5 separate experiments, in which 3 repeated measurements were made. The graphs were artificially nudged by 2 y-axis values for sake of clarity.



Supplementary Figure 2. Effect of protein/lipid ratio on particle size distribution of cationic liposomes with encapsulated Bet v 1. The graphs shown are the average of 4-6 separate experiments, in which 3 repeated measures were made. The graphs were artificially nudged by 2 y-axis values for sake of clarity.



Supplementary Figure 3. Effect of protein/lipid ratio on particle size distribution of cationic liposomes with both adsorbed and encapsulated Bet v 1. The graphs shown are the average of 2 separate experiments, in which 3 repeated measures were mad. The graphs were artificially nudged by 2 y-axis values for sake of clarity.



Supplementary Figure 4. Production of IL-4, IL-5, IL-10, IL-13 and IFN- $\gamma$  by lung draining lymph node cells from immunized mice after exposure to Bet v 1. Group mean and standard deviation are plotted ( $n = 4-5$  mice/group). Groups were compared with a Kruskal-Wallis test followed by Dunn's correction for multiple comparisons. \* =  $p < 0.05$ , \*\* =  $p < 0.01$ , \*\*\* =  $p < 0.001$ .



# Chapter 3

## Atomic Force Microscopy

### Measurements of Anionic Liposomes Reveal the Effect of Liposomal Rigidity on Antigen-Specific Regulatory T Cell Responses

Naomi Benne<sup>a</sup>, Romain J. T. Leboux<sup>a</sup>, Marco Glandrup<sup>a</sup>, Janine van Duijn<sup>a</sup>, Fernando Lozano Vigario<sup>a</sup>, Malene Aaby Neustrup<sup>a</sup>, Stefan Romeijn<sup>a</sup>, Federica Galli<sup>b</sup>, Johan Kuiper<sup>a</sup>, Wim Jiskoot<sup>a</sup>, Bram Slütter<sup>a\*</sup>

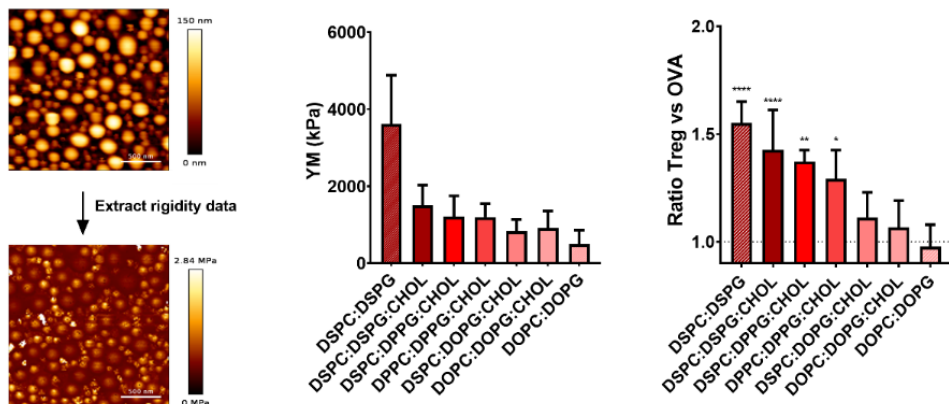
<sup>a</sup>Division of BioTherapeutics, Leiden Academic Centre for Drug Research, Leiden, the Netherlands

<sup>b</sup>Leiden Institute of Physics, Leiden, the Netherlands

**Correspondence:** Bram Slütter: [b.a.slutter@lacdr.leidenuniv.nl](mailto:b.a.slutter@lacdr.leidenuniv.nl)



## Graphical Abstract



## Abstract

Regulatory T cells (Tregs) are vital for maintaining a balanced immune response and their dysfunction is often associated with auto-immune disorders. We have previously shown that antigen-loaded anionic liposomes composed of phosphatidylcholine (PC) and phosphatidylglycerol (PG) and cholesterol can induce strong antigen-specific Treg responses. We hypothesized that altering the rigidity of these liposomes while maintaining their size and surface charge would affect their capability of inducing Treg responses. The rigidity of liposomes is affected in part by the length and saturation of carbon chains of the phospholipids in the bilayer, and in part by the presence of cholesterol.

We used atomic force microscopy (AFM) to measure the rigidity of anionic OVA<sub>323</sub>-containing liposomes composed of different types of PC and PG, with or without cholesterol, in a molar ratio of 4:1(:2) distearoyl (DS)PC:DSPG (Young's modulus (YM) 3611 ± 1271 kPa), DSPC:DSPG:CHOL (1498 ± 531 kPa), DSPC:dipalmitoyl (DP)PG:CHOL (1208 ± 538), DPPC:DPPG:CHOL (1195 ± 348 kPa), DSPC:dioleoyl (DO)PG:CHOL (825 ± 307 kPa), DOPC:DOPG:CHOL (911 ± 447 kPa), and DOPC:DOPG (494 ± 365 kPa). Next, we assessed if rigidity affects the association of liposomes to bone marrow-derived dendritic cells (BMDCs) *in vitro*. Aside from DOPC:DOPG liposomes, we observed a positive correlation between liposomal rigidity and cellular association. Finally, we show that rigidity positively correlates with Treg responses *in vitro* in murine DCs and *in vivo* in mice. Our findings underline the suitability of AFM to measure liposome rigidity and the importance of this parameter when designing liposomes as a vaccine delivery system.

## Introduction

Regulatory T cells (Tregs) are important for the resolution of inflammation after infection, immune suppression, and immune homeostasis<sup>1</sup>. They do so by producing anti-inflammatory cytokines<sup>2</sup>, consuming pro-inflammatory interleukin 2 (IL-2) and interrupting effector T cell metabolism<sup>3</sup>. A reduction in the number or the dysfunction of Tregs has been implicated in many diseases, including type 1 diabetes, rheumatoid arthritis, and multiple sclerosis<sup>4</sup>. Due to their immunosuppressive capacity, inducing Tregs is an attractive approach for immunotherapy in inflammatory and auto-immune diseases. Approaches to induce tolerance include oral administration of disease-specific antigens<sup>5</sup>, as well as the use of tolerogenic nanoparticles (reviewed by Kishimoto and Maldonado<sup>6</sup>).

Many of these tolerogenic nanoparticles co-encapsulate antigens with ligands to enhance tolerance or inhibit effector responses, such as CD22<sup>7</sup> or rapamycin<sup>8,9</sup>, respectively. However, it is possible to use “bare” particles that exploit natural tolerogenic processes, generally by targeting scavenger receptors<sup>10</sup>. When using such nanoparticles, their physicochemical properties determine their efficiency to induce antigen-specific Treg responses. For instance, cationic particles are superior to anionic particles when comparing the efficiency of their association to APCs, as well as induction of pro-inflammatory responses<sup>11</sup>, whereas we and other groups have shown that anionic nanoparticles like PG-containing liposomes are more efficient at inducing tolerance<sup>12,13</sup>. Besides the surface charge, particle size has also been shown to affect liposome-APC interactions and subsequent induction of antigen-specific Tregs. For example, nano-sized particles are taken up more efficiently by APCs than micron-sized particles, leading to stronger APC activation and subsequent immune responses<sup>14</sup>.

Finally, the rigidity of nanoparticles is another important parameter for the induction of T cell responses<sup>15,16</sup>, however, to our knowledge, it is unknown whether Treg responses are similarly affected by this parameter. The rigidity of a particle, expressed here as YM, describes the deformation of an entire particle and is not the same as the intrinsic deformation property of the material(s) that the particle is made of. Rigid particles were previously shown to be more efficiently taken up by macrophages compared to soft particles<sup>17</sup>, and rigid liposomes were able to induce stronger DC activation *in vivo*<sup>18</sup>. Furthermore, rigid liposomes led to higher levels of antigen presentation on MHC-II in DCs<sup>19</sup>. Finally, increasing liposomal rigidity has been shown to result in increased humoral and cellular immune responses<sup>20-22</sup>.

Here, we aimed to study the relationship between liposomal rigidity and

induced antigen-specific Treg responses. Liposomal rigidity is related to, but not the same as, the rigidity of the lipid bilayer. Bilayer rigidity is strongly dependent on the transition temperature ( $T_m$ ) of the constituent phospholipids. Below the  $T_m$ , phospholipid bilayers are in a relatively rigid gel state, whereas above the  $T_m$  they are in a (much less rigid) liquid disordered state<sup>23</sup>. Analytical techniques such as differential scanning calorimetry (DSC)<sup>24</sup> are commonly used to determine the average  $T_m$  of liposomal bilayers. However, these techniques do not measure the absolute rigidity of bilayers, let alone of liposomal particles. Moreover, bilayers containing substantial amounts of cholesterol (CHOL) lack a clear  $T_m$ <sup>25</sup>, making the use of these analytical techniques less useful. In the present study, we employed atomic force microscopy (AFM), as this technique allows for simultaneous imaging and rigidity measurement of individual liposomes, whether or not they contain CHOL<sup>26</sup>. Here we present an AFM-based method to measure the YM of a range of anionic liposomes, by immobilizing them on (3-aminopropyl)triethoxysilane (APTES)-modified silicon plates. Moreover, we show that liposomal rigidity is positively correlated with Treg responses against a loaded antigen *in vitro* and *in vivo*.

## Materials and Methods

### Materials

The phospholipids 1,2-distearoyl-sn-glycero-3-phosphocholine (DSPC), 1,2-dipalmitoyl-sn-glycero-3-phosphocholine (DPPC), 1,2-dioleoyl-sn-glycero-3-phosphocholine (DOPC), 1,2-distearoyl-sn-glycero-3-phosphoglycerol (DSPG), 1,2-dipalmitoyl-sn-glycero-3-phosphoglycerol (DPPG), 1,2-dioleoyl-sn-glycero-3-phosphoglycerol (DOPG), and 1,2-dipalmitoyl-sn-glycero-3-phosphoethanolamine-N-(lissamine rhodamine B sulfonyl) (DPPE-Rho) were purchased from Avanti Polar Lipids (Alabaster, AL, USA). Cholesterol (CHOL), APTES, acetic acid, N,N'-diisopropyl carbodiimide (DIC), and triisopropyl silane were purchased from Sigma-Aldrich (Zwijndrecht, the Netherlands). The ovalbumin-derived peptide OVA<sub>323</sub> (ISQAVHAAHAEINEAGR) was purchased from Invivogen (San Diego, California, USA). Tentagel R-RAM resin was purchased from Rapp Polymere (Tübingen, Germany). Amino acids were supplied by Novabiochem (Merck, Darmstadt, Germany). Dimethylformamide (DMF), trifluoroacetic acid (TFA), piperidine, pyridine, and acetonitrile were purchased from Biosolve (Valkenswaard, the Netherlands). Oxyma was supplied by Carl Roth (Karlsruhe, Germany). DCM was purchased from Honeywell (Fisher, Landsmeer, the Netherlands). Diethyl ether was acquired from VWR (Amsterdam, the Netherlands). Polycarbonate track-etched membranes with a pore size of 400 nm and 200 nm were obtained from Millipore (Kent, UK).

For cell culture, Ca<sup>2+</sup>- and Mg<sup>2+</sup>-free phosphate-buffered saline (PBS), Iscove's Modified Dulbecco's Medium (IMDM), Roswell Park Memorial Institute Medium

(RPMI 1640), L-glutamine, and penicillin/streptomycin were purchased from Lonza (Basel, Switzerland). Fetal calf serum (FCS) was purchased from PAA Laboratories (Ontario, Canada).  $\beta$ -mercaptoethanol was purchased from Sigma-Aldrich (Zwijndrecht, the Netherlands). Granulocyte-macrophage colony-stimulating factor (GM-CSF) was purchased from PeptroTech (London, UK).

The antibodies CD45.1-PE-Dazzle594 (A20), Thy1.2-PE-Cy7 (53-2.1), Gata-3-PE (16E10A23), T-bet-APC (4B10), IL-17A-AF488 (TC11-18H10.1), and CD11c-PerCP-Cy5.5 (N418) were purchased from Biolegend (CA, USA). FOXP3-eFluor450 (FJK-16S), CD25-AF488 (PC61.5), Ki-67-FITC (SolA15), fixable viability dye-APC-eFluor780, IL-10-PerCP-Cy5.5 (JES5-16E3), IFN $\gamma$ -APC (XMG1.2), and FOXP3/transcription factor staining kit were purchased from eBioscience (ThermoFisher Scientific, MA, USA). CD4-V500 (RM4-5) was purchased from BD Biosciences (CA, USA).

#### Preparation of OVA<sub>323</sub>-AF488

The OVA<sub>323</sub> peptide with the sequence ISQAVHAAHAEINEAGRGC was synthesized using a Liberty Blue microwave-assisted peptide synthesizer. Synthesis was performed on a 0.1 mmol scale with a low-loading (0.18 mmol/g) Tentagel® R-RAM resin. Amino acid activation was performed using DIC as the activator and oxyma as a base, and Fmoc-deprotection was performed with 20% piperidine in DMF. The resin was washed five times with DMF and five times with dichloromethane. To protect the N-terminal amine, the peptide was reacted with 5% v/v acetic anhydride and 6% pyridine v/v in DMF for 1 hour at room temperature. Subsequently, cleavage from the resin was performed using a mixture of TFA:triisopropyl silane:water, 38/1/1 v/v/v. The peptide was precipitated using ice-cold diethyl ether. The precipitate was collected by centrifugation before resuspension in water:acetonitrile 4/1 v/v, after which the acetonitrile was evaporated and the remaining aqueous solution was lyophilized overnight. Purification was performed by RP-HPLC on a Kinetik Evo C18 column with a Shimadzu system comprising two LC-8A pumps and an SPD-10AVP UV-Vis detector. The collected fractions were analyzed using LC-MS and pure fractions were pooled, the organic solvent was evaporated and the peptide solution was lyophilized overnight. To obtain fluorescently labeled OVA<sub>323</sub>, the peptide was incubated for 48 hours at 4°C with AlexaFluor 488 C<sub>5</sub> maleimide (ThermoFisher Scientific, Landsmeer, Netherlands) at pH 7.4 (100 mM HEPES buffer). The purified fluorescent peptide was obtained by RP-HPLC and mass was confirmed by LC-MS.

#### Liposome preparation

Liposomes were prepared using the thin film dehydration-rehydration method, as described previously<sup>27</sup>. Briefly, phospholipids with or without CHOL (10 mg/

mL, 1 mL) were dissolved in chloroform and mixed in a 50 mL round-bottom flask at a molar ratio of 4:1(:2) PC:PG(:CHOL). The chloroform was evaporated under vacuum in a rotary evaporator (Rotavapor R-210, Büchi, Switzerland) for 1 hour at 40°C. The resulting lipid film was rehydrated with 250 µg OVA<sub>323</sub> dissolved in 1 mL Milli-Q water and homogenized using glass beads. The liposome dispersion was snap-frozen in liquid nitrogen, followed by freeze-drying overnight (Christ alpha 1–2 freeze-dryer, Osterode, Germany). The freeze-dried lipid cake was slowly rehydrated using 10 mM sodium phosphate buffer (PB), pH 7.4. Two volumes of 500 µL and one volume of 1,000 µL PB were successively added, with intervals of 30 min between each addition. The mixture was vortexed well between each hydration step, and the resulting dispersion was left to rehydrate for at least 1 hour. The multilamellar vesicles were sized by high-pressure extrusion (LIPEX Extruder, Northern Lipids Inc., Canada) by passing the dispersion four times through stacked 400-nm and 200-nm pore size membranes (Whatman® Nuclepore™, GE Healthcare, Little Chalfont, UK). The resulting liposomes were assumed to be unilamellar. Homogenization, rehydration, and extrusion were performed at a temperature above the  $T_m$  of the phospholipids. To separate non-encapsulated OVA<sub>323</sub> from the liposomes, liposomes were washed in a Vivaspin 2 centrifuge membrane concentrator (MWCO 300 kDa, Sartorius, Göttingen, Germany) by centrifugation at 524 g and 4°C. To prepare fluorescently labeled liposomes, 0.1 mol% of PC was replaced with DPPE-Rho. To prepare liposomes with fluorescently labeled OVA<sub>323</sub>, 10% of the OVA<sub>323</sub> was replaced with OVA<sub>323</sub>-AF488. Liposomes were stored at 4°C and used for further experiments within 2 weeks.

### Liposome characterization

The Z-average diameter and polydispersity index (PDI) of the liposomes were measured by dynamic light scattering (DLS) using a NanoZS Zetasizer (Malvern Ltd., Malvern, UK). The same instrument was used to measure  $\zeta$ -potential by laser Doppler electrophoresis. The liposomes were diluted 100-fold in PB to a total volume of 1 mL for these measurements. Particle concentration was measured using nanoparticle tracking analysis (NTA), as described previously<sup>28</sup>, for optimal AFM measurements. Liposomes were diluted in PB to a particle concentration between  $10^7$  and  $10^9$  particles/mL based on the DLS attenuation. NTA measurements were performed using a NanoSight LM20 (NanoSight, Amesbury, UK). Capture time was 60 seconds, the camera shutter was set to 1500 ms, and gain to 680. To determine the concentration of loaded OVA<sub>323</sub>, the peptide was extracted from liposomes using a modified Bligh-Dyer method, as described previously<sup>29</sup>. Briefly, 100 µL of aqueous liposomal dispersion or a known concentration of free peptide as control was mixed with 250 µL methanol and 125 µL chloroform and vortexed. Then, 250 µL of 0.1 M HCl and 125 µL chloroform were added and the mixture was vortexed and subsequently

centrifuged for 5 min at 524 g to separate the two phases. The upper phase was collected and analyzed by RP- UPLC. Sample injections were 10  $\mu$ L and the column used was a 1.7  $\mu$ m BEH C18 column (2.1 x 50 mm, Waters ACQUITY UPLC, Waters, MA, USA). Column and sample temperatures were 40°C and 4°C, respectively. The mobile phases were Milli-Q water with 0.1% TFA (solvent A) and acetonitrile with 0.1% TFA (solvent B). For separation, the mobile phases were applied in a linear gradient from 5% to 95% solvent B over 5 minutes at a flow rate of 0.370 mL/min. Peptides were detected by absorbance at 214 nm using an ACQUITY UPLC TUV detector (Waters ACQUITY UPLC, Waters, MA, USA).

### Preparation of APTES-modified silicon plates

To allow for imaging of anionic liposomes, (negatively charged) silicon plates were modified with APTES, to obtain a positively charged surface, as described previously<sup>30</sup>. Briefly, the plates were washed with acetone and methanol and dried in a vacuum oven (Binder, Germany) for 30 minutes at 50°C. The plates were incubated in a solution of 3/7 v/v  $\text{H}_2\text{O}_2/\text{H}_2\text{SO}_4$  at 120°C to remove any organic contaminants and to hydroxylize the silicon surface. The plates were then washed with water and dried for 30 minutes in a vacuum oven. The plates were incubated overnight in 2% v/v APTES in toluene, washed thoroughly with toluene to remove any excess APTES, and subsequently washed with methanol, and dried in a vacuum oven at 175°C. Lastly, a curing step for the hydrolysis of residual ethoxy groups was performed at 120°C for 30 minutes followed by incubation in Milli-Q water at 40°C for 2 hours after which the plates were washed with methanol and stored in a vacuum oven at 175°C until use. The smoothness of the APTES-modified plates was confirmed using AFM in QI mode. A sharp cantilever (Oltespa, Opus, Bulgaria) with a nominal spring constant of 2 N/m, a nominal resonance frequency of 70 kHz and a tip radius of <7 nm was used to image the surface of the plates. The sample tilt was corrected using the JPK Data Processing software v6.1.79 flattening function. Images were extracted using Gwyddion v2.50 and the heights of structures on the plates were determined. The roughness of the plates was expressed as root mean square (RMS)<sup>31</sup>, and plates used had RMS values between 0.6 and 3 nm, which was deemed to have minimal interference and to favor adsorption of liposomes<sup>32</sup>.

### Sample preparation for AFM measurements

APTES-modified plates were attached to glass microscope slides using Reprorubber® (Thin Pour Kit, Flexbar Machine Corporation, USA). A small glass ring with a diameter of 15 mm and a height of 3 mm was attached on the plate to form a small basin. Next, 200  $\mu$ L of liposomal formulation (particle concentrations of about  $10^{12}$  –  $10^{13}$  particles/mL, as measured by NTA) was applied to the plate and incubated at room temperature for 5 min. The plate was gently washed with PB without exposure of the plate to air to remove free liposomes.

## Scanning electron microscopy (SEM) of cantilevers

The cantilever tip radius of the HSC-20 cantilever (Team Nanotec, Germany) was assessed by SEM using an FEI Nova nanoSEM 200. Imaging was performed in high vacuum mode at 15 kV and a spot of 4.0 at a tilt of 45°. Images were captured at 200,000-fold magnification and the radius of the cantilever tip was determined using the SEM software.

## AFM measurements

To image the liposomes a JPK Nanowizard 3 (JPK Instruments AG, Berlin, Germany) was used. Measurements were performed at  $25 \pm 1^\circ\text{C}$  in QI mode. The AFM probe used was a Team Nanotec (Germany) HSC-20 hemispherical cone-shaped tip cantilever with gold-reflective coating and metal carbide coating on the tip side, with a nominal spring constant of 0.2 N/m, a nominal resonance frequency of 15 kHz and a tip radius of 35 nm, as determined by SEM. The cantilever was calibrated using contact-based calibration and thermal tuning. For calibration, the setpoint was 0.1 V on approach with a dynamic baseline. Imaging of the liposomes was performed with a z-length 200 nm and a set point between 0.5 – 0.85 nN. The area of the image was  $2 \times 2 \mu\text{m}$  at a resolution of  $128 \times 128$  pixels with a pixel rate of 20 msec/pixel. Scan line artifacts were removed, line fitting was applied to the images, and sample tilt was corrected. Liposomes with a height below 40 nm were excluded from the analysis to prevent interference from the substrate. Force vs. height curves were measured for each pixel of the AFM image. After subtracting the cantilever deflection, the force vs. tip-sample separation (or distance) curves were fitted using the Hertz/Sneddon model<sup>33</sup> for a hemispherical cantilever tip according to the following equation:

$$F = \frac{4\sqrt{R}}{3} \frac{E}{1-\nu^2} \delta^{\frac{3}{2}} \quad (\text{equation 1})^{34}$$

where F is the force as measured by AFM, R is the tip radius as measured by SEM, E is the YM,  $\nu$  is Poisson's ratio, set to 0.5 for soft materials such as liposomes<sup>35</sup>, and  $\delta$  is the indentation of the sample, also measured by AFM. The YM was determined for the center of the liposomes.

Raw data images and force vs. height curves were processed using JPK Data Processing software v6.1.70. Data from the images were extracted using Gwyddion v2.50. Between 31 and 450 liposomes were analyzed per formulation (Figure 1A).

## BMDC culture

Bone marrow was isolated from the tibias and femurs of wild-type (WT) C57BL/6 mice. A single-cell suspension of bone marrow cells was obtained by straining over a  $70 \mu\text{m}$  cell strainer (Greiner Bio-One B.V., Alphen aan den Rijn, NL).



Cells were cultured for 10 days in complete IMDM (cIMDM) which contains IMDM supplemented with 2 mM L-glutamine, 8% v/v FCS, 100 U/mL penicillin/streptomycin, and 50  $\mu$ M  $\beta$ -mercaptoethanol at 37°C and 5% CO<sub>2</sub> in 95-mm Petri dishes (Greiner Bio-One B.V., Alphen aan den Rijn, NL) and 20 ng/mL GM-CSF. The medium was refreshed every other day.

#### Liposome or antigen association to BMDCs

BMDCs were cultured as described above. After 10 days of culture, BMDCs were plated in F-bottom 96-well plates (Greiner Bio-One B.V., Alphen aan den Rijn, Netherlands) at 50,000 cells/well. To measure association (either by uptake or adsorption) of liposomes to BMDCs, liposomes prepared with 0.1 mol% Rho-DPPE or controls (non-fluorescent liposomes or medium) were added at a concentration of 20  $\mu$ g/mL lipids in supplemented IMDM. To measure OVA<sub>323</sub> association to DCs, liposomes encapsulating fluorescently labeled OVA<sub>323</sub> were added to a concentration of 0.1  $\mu$ g/mL OVA<sub>323</sub>. Cells were incubated for 4 hours at 37°C and 5% CO<sub>2</sub>. Subsequently, excess liposomes were removed by washing the cells several times with cIMDM, and cells were incubated overnight. Cells were stained with a fluorescent antibody against CD11c-PerCP-Cy5.5 (N418) and fixable viability dye-APC-eFluor780 and subsequently analyzed by flow cytometry (CytoFLEX S, Beckman Coulter, CA, USA). The presence of the fluorescent label in DCs indicated the association of either liposomes or peptide by BMDCs. Data were analyzed with FlowJo software V10 (Treestar, OR, USA).

#### *In vitro* Treg induction by liposome-pulsed BMDCs

BMDCs were cultured as described above, plated to 50,000 cell/well in a 96-well F-bottom plate, and pulsed for 4 hours with liposomes or controls in cIMDM. Spleens from OT-II mice were strained through a 70  $\mu$ m cell strainer to obtain a single-cell suspension. Erythrocytes were lysed using ammonium-chloride-potassium (ACK) lysis buffer (0.15 M NH<sub>4</sub>Cl, 1 mM KHCO<sub>3</sub>, 0.1 mM Na<sub>2</sub>EDTA; pH 7.3). CD4<sup>+</sup> T cells were isolated using a CD4<sup>+</sup> T cell isolation kit (Miltenyi Biotec B.V., Leiden, Netherlands) according to the manufacturer's protocol. After exposure, BMDCs were washed with cIMDM to remove free liposomes, and 100,000 CD4<sup>+</sup> T cells/well were added to the BMDCs. Co-cultures were incubated for 72 hours in RPMI 1640 medium supplemented with 2 mM L-glutamine, 10% v/v FCS, 100 U/mL penicillin/streptomycin, and 50  $\mu$ M  $\beta$ -mercaptoethanol. Cells were stained for Thy1.2-PE-Cy7, CD4-V500, viability-APC-eFluor780, FOXP3-eFluor450, and Ki-67-FITC, and analyzed by flow cytometry (CytoFLEX S, Beckman Coulter, CA, USA). Data were analyzed using FlowJo software V10 (Treestar, OR, USA).

#### Animals

C57BL/6 and OT-II transgenic mice on a C57BL/6 background were purchased from Jackson Laboratory (CA, USA), bred in-house under standard laboratory



conditions, and provided with food and water *ad libitum*. All animal work was performed in compliance with the Dutch government guidelines and the Directive 2010/63/EU of the European Parliament. Experiments were approved by the Ethics Committee for Animal Experiments of Leiden University.

### Adoptive transfer

Eleven-week-old female C57BL/6 mice were randomized into 4 groups based on weight. On day 0, all mice received 500,000 CD45.1<sup>+</sup>CD4<sup>+</sup> T cells splenocytes isolated from a female OT-II transgenic mouse *via* the tail vein. On day 1, mice were immunized intravenously (i.v.) with a single injection of DSPC:DSPG, DSPC:DSPG:CHOL, DOPC:DOPG or DOPC:DOPG:CHOL liposomes containing 1 nmol OVA<sub>323</sub> in PBS, in a total volume of 200  $\mu$ L *via* the tail vein. On day nine, mice were sacrificed by cervical dislocation and spleens were immediately removed. Spleens were processed as mentioned above and stained for CD4-V500, CD45.1-PE-Dazzle594, Thy1.2-PE-Cy7, viability-APC-eFluor780, CD25-AF488, Gata-3-PE, T-bet-APC, and FOXP3-eFluor450 and measured by flow cytometry (CytoFLEX S, Beckman Coulter, CA, USA). To measure cytokine production, splenocytes were stimulated *ex vivo* with OVA<sub>323</sub> (10  $\mu$ g/mL). After 1 hour brefeldin A (3  $\mu$ g/mL) was added and cells were incubated for a further 5 hours. Cells were subsequently stained for CD4-V500, CD45.1-PE-Dazzle594, Thy1.2-PE-Cy7, viability-APC-eFluor780, IFN $\gamma$ -APC, IL-17A-AF 488, and IL-10-PerCP-Cy5.5, and analyzed by flow cytometry. Data were analyzed using FlowJo software V10 (Treestar, OR, USA).

### Statistical analysis

Results were analyzed using one-way or two-way ANOVA, followed by Bonferroni's multiple comparisons test and was performed using GraphPad Prism version 8.1.1 for Windows (GraphPad Software, CA, USA).

## Results

### Preparation of liposomes

Tregs are vital for maintaining immune homeostasis and are an attractive target for immunotherapy. We have previously demonstrated that liposomes prepared with DSPC, DSPG and CHOL in a molar ratio of 4:1:2 and loaded with an initial OVA<sub>323</sub> concentration of 250  $\mu$ g/ml induce strong antigen-specific Treg responses. In order to assess how the rigidity of these liposomes affects the Treg responses, we altered the rigidity of the liposomes by using phospholipids with different carbon chain-lengths (*e.g.* DSPC, di-18:0 PC vs. DPPC, di-16:0 PC), unsaturation in the lipid chain (*e.g.* DSPC, di-18:0 PC vs. DOPC, di-18:1 ( $\Delta$ 9-Cis) PC) or exclusion of CHOL (Table S1). The resulting liposomes were between 138 and 177 nm in size (Table 1). Exclusion of CHOL slightly, but significantly, reduced the size of the liposomes ( $p < 0.05$ ). All formulations were monodisperse, indicated by a

PDI of about 0.1. As expected, because of the incorporation of an anionic PG phospholipid, all liposomes had a negative  $\zeta$ -potential. The loading efficiency (LE) of the OVA<sub>323</sub> was between 11.4 and 24.6%.

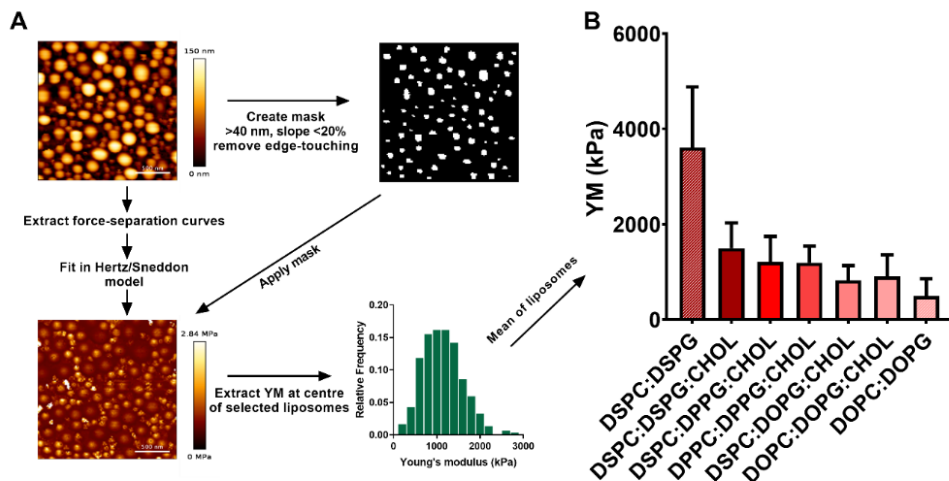
*Table 1. Physicochemical characteristics of liposomal formulations.*

Lipid composition (molar ratio)	Z-average $\pm$ SD (nm)	PDI $\pm$ SD	$\zeta$ -potential $\pm$ SD (mV)	LE (%) <sup>a</sup>	Phase state at room temperature
DSPC:DSPG:CHOL (4:1:2)	166.1 $\pm$ 8.5	0.09 $\pm$ 0.05	-48.0 $\pm$ 6.0	16.0 $\pm$ 8.5	Lo
DSPC:DPPG:CHOL (4:1:2)	177.3 $\pm$ 6.6	0.08 $\pm$ 0.03	-46.4 $\pm$ 9.5	15.8 $\pm$ 5.5	Lo
DPPC:DPPG:CHOL (4:1:2)	173.5 $\pm$ 10.6	0.08 $\pm$ 0.04	-46.2 $\pm$ 11.7	24.7 $\pm$ 10.2	Lo
DSPC:DOPG:CHOL (4:1:2)	168.1 $\pm$ 17.0	0.10 $\pm$ 0.05	-45.8 $\pm$ 4.9	13.9 $\pm$ 3.9	Lo
DOPC:DOPG:CHOL (4:1:2)	158.7 $\pm$ 14.7	0.12 $\pm$ 0.03	-43.4 $\pm$ 5.1	24.8 $\pm$ 12.8	Lo
DSPC:DSPG (4:1)	138.4 $\pm$ 13.2	0.10 $\pm$ 0.03	-39.7 $\pm$ 5.7	11.4 $\pm$ 6.2	Gel
DOPC:DOPG (4:1)	140.1 $\pm$ 4.9	0.13 $\pm$ 0.03	-44.9 $\pm$ 5.9	24.6 $\pm$ 12.9	Ld

<sup>a</sup> Percentage of OVA<sub>323</sub> amount remaining in liposomes after purification compared to the initial amount. Lo= Liquid ordered, Ld= liquid disordered

### Effect of lipid composition on liposome rigidity

To study the effect of lipid composition on the rigidity of the liposomes, we measured the YM of the anionic liposomes by AFM. Liposomes were successfully immobilized on APTES-modified silicon plates and were imaged in quantitative imaging (QI) mode (Figure 1 and Table S2). AFM confirmed the size and monodispersity measured by dynamic light scattering and allowed extraction of force-separation curves and determination of the YM of single liposomes (Figure 1A). The most rigid liposomes were DSPC:DSPG liposomes, while the least rigid liposomes were DOPC:DOPG liposomes (Figure 1B). This was expected, since DSPC:DSPG bilayers are in a gel state, and DOPC:DOPG bilayers are in a liquid disordered state at 25°C (Table 1). For DSPC:DSPG liposomes, the addition of CHOL significantly reduced the YM (from 3611  $\pm$  1271 kPa to 1498  $\pm$  530 kPa,  $p < 0.001$ ), while this was reversed for DOPC:DOPG liposomes (from 493  $\pm$  365 kPa to 911  $\pm$  447 kPa,  $p = 0.0153$ ). Interestingly, we observed that replacing a small amount of a high- $T_m$  phospholipid with a lower- $T_m$  phospholipid has the same effect as replacing all phospholipids by a lower- $T_m$  one. For instance, both DSPC:DPPG:CHOL (YM = 1159  $\pm$  525 kPa), where DSPC has a higher  $T_m$  than DPPC, and DPPC:DPPG:CHOL liposomes (YM = 1211  $\pm$  399 kPa) were significantly less rigid than DSPC:DSPG:CHOL liposomes (YM = 1498  $\pm$  531  $p < 0.005$ ), while not being significantly different from each other ( $p > 0.99$ ). A similar effect was observed for DSPC:DOPG:CHOL and DOPC:DOPG:CHOL liposomes. Finally, we found that the  $T_m$  values and the molar ratio of the constituent lipids do not significantly correlate with the rigidity of the liposomes (Figure S1).



**Figure 1.** AFM measurements of liposomes. (A) Schematic overview of the AFM method used to determine the rigidity of liposomes. Liposomes were immobilized on APTES-modified silicon plates. The rigidity of the liposomes was measured using AFM in QI mode. AFM images were processed in JPK data processing software v6.1.70. Scan line artifacts were removed and images were corrected for baseline tilt. YM data per pixel was extracted by fitting each force-separation curve with the Hertz/Sneddon model resulting in a YM map. To remove the interference of the silicon substrate, a mask was created in Gwyddion 2.50, selecting a threshold of 40 nm with a slope of less than 20%. Liposomes touching the edges of the image were not included in the analysis. This mask was applied to the YM map, and YM data was extracted for each liposome. Only the center of each liposome was used to calculate the mean YM per formulation. Representative AFM images of DSPC:DPPG:CHOL liposomes. (B) Rigidity, expressed as YM, of the different liposomes. Data shown is mean values  $\pm$  SD,  $n = 31 - 450$ . Significant differences as measured by one-way ANOVA are displayed in Table S3.

## Effect of liposomal composition on liposome association to BMDCs and Treg responses *in vitro*

Next, we assessed how the rigidity of liposomes affects the uptake by APCs and the induction of Tregs by the APCs. To this end, we incorporated a fluorescently labeled phospholipid, Rho-DPPE, into the lipid bilayer and exposed BMDCs for 4 hours to these formulations (Figure 2A). For almost all formulations, we observed a positive trend between liposomal rigidity and association. Interestingly, the highest association was observed for the least rigid, DOPC:DOPG liposomes. It should be noted, however, that the DOPC:DOPG liposomes showed primarily passive association, indicated by high cell association at 4°C (Figure 2B), while all other liposomes showed negligible association at 4°C (Figure S2). Furthermore, DOPC:DOPG liposomes did not appear to effectively deliver their cargo; while the association of DSPC:DSPG liposomes led to a significant 7.5-fold increase in OVA<sub>323</sub> association compared to free OVA<sub>323</sub> (control), both DOPC:DOPG:CHOL and DOPC:DOPG liposomes did not increase OVA<sub>323</sub> association compared to the control (Figure 2C).

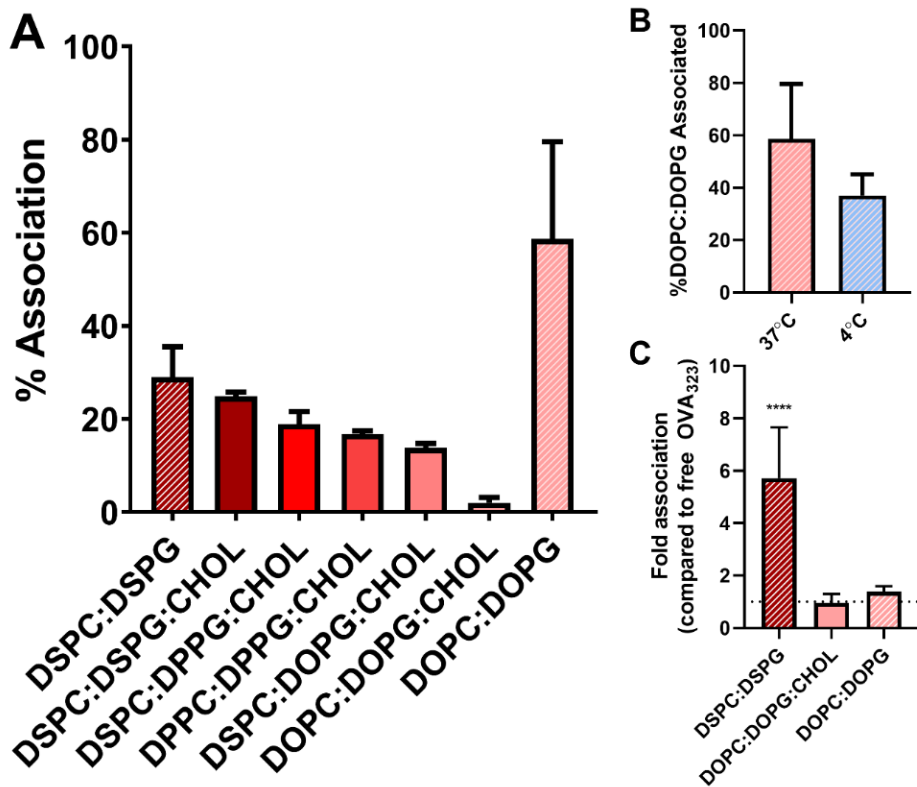
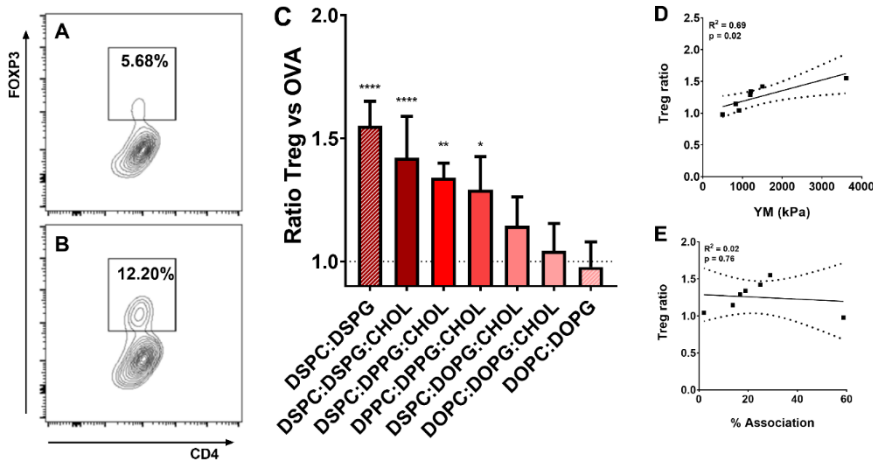


Figure 2. Liposomal association (uptake and/or adsorption) by BMDCs in vitro. (A) OVA<sub>323</sub>-containing fluorescently labeled liposomes were incubated for 4 hours with BMDCs at 37°C. Liposomes were subsequently washed away and cells were incubated overnight before being analyzed via flow cytometry. % Association indicates the percentage of live BMDCs that are positive for the fluorescent label in the liposomes. (B) Association of OVA<sub>323</sub>-containing fluorescently labeled DOPC:DOPG liposomes at 37°C vs. 4°C. (C) Association of encapsulated OVA<sub>323</sub> to BMDCs. Fluorescently labeled OVA<sub>323</sub> was encapsulated in liposomes and incubated for 4 hours with BMDCs at 37°C. Liposomes were subsequently washed away and cells were incubated overnight before being analyzed by flow cytometry. Association was normalized to % of BMDCs positive for fluorescently labeled OVA<sub>323</sub> in the free OVA<sub>323</sub> control. Graphs show mean  $\pm$  SD, (A)  $n = 3$ , (B)  $n = 9$ , (C)  $n = 6$ . \*\*\*\* $p < 0.0001$ , compared to free OVA<sub>323</sub> determined by one-way ANOVA and Bonferroni's multiple comparisons test.

To determine whether the liposomal composition affected Treg responses, BMDCs were pulsed with liposomes for 4 hours, and subsequently co-cultured with OT-II CD4<sup>+</sup> T cells. After three days of incubation, induced Tregs were identified using flow cytometry (Figure 3A, B, and C). Among all tested OVA<sub>323</sub>-containing liposomes, the DSPC:DSPG liposomes induced the strongest Treg responses, with a 1.6-fold increase in % FOXP3<sup>+</sup> population in live CD4<sup>+</sup>Ki-67<sup>+</sup> T cell population compared to free OVA<sub>323</sub>. Also DSPC:DSPG, DSPC:DSPG:CHOL,

DSPC:DPPG:CHOL, and DPPC:DPPG:CHOL liposomes showed significantly higher Treg responses compared to free OVA<sub>323</sub>. Furthermore, we observed a significant correlation between the liposomal rigidity (determined by AFM) and Treg responses (Figure 3D). Interestingly, there was no clear relationship between the association of liposomes with BMDCs and subsequent Treg responses (Figure 3E).



**Figure 3: Induction of Tregs by OVA<sub>323</sub>-loaded liposomes *in vitro*.** BMDCs were pulsed for 4 hours with liposomes or controls and subsequently co-cultured for 72 hours with CD4<sup>+</sup> T cells isolated from OT-II splenocytes. Flow cytometry was used to measure FOXP3<sup>+</sup>Ki-67<sup>+</sup>CD4<sup>+</sup> T cells. Representative flow cytometry plots of FOXP3<sup>+</sup>CD4<sup>+</sup> T cells in the live Ki-67<sup>+</sup>CD4<sup>+</sup> T cell population of OT-II T cells cultured with (A) free OVA<sub>323</sub> (0.1 µg/mL) and (B) OVA<sub>323</sub>-loaded DSPC:DSPG liposomes (0.1 µg/mL OVA<sub>323</sub>). (C) Summary Treg data of all liposomal formulations tested. Results were normalized to % FOXP3<sup>+</sup>Ki-67<sup>+</sup>CD4<sup>+</sup> T cells in the free OVA<sub>323</sub> control. The dashed line at Y = 1 represents the free OVA<sub>323</sub> control. The graph shows mean ± SD, n = 4. Linear correlations (95% CI) between (D) YM and Treg response ratio, and (E) % association and Treg response ratio. \*\*\*\*p < 0.0001, \*\*p < 0.01. \*p < 0.05, compared to free OVA<sub>323</sub> determined by one-way ANOVA and Bonferroni's multiple comparisons test.

### Effect of liposomal composition on Treg response *in vivo*

Next, we aimed to assess whether liposome rigidity affects Treg induction *in vivo*. An adoptive transfer mouse model using ovalbumin-specific OT-II T cells was used to study the induction of antigen-specific Treg responses by the liposomes *in vivo*. We selected the highest rigidity (DSPC:DSPG) and lowest rigidity liposomes (DOPC:DOPG) and their CHOL-containing counterparts. Both DSPC:DSPG and DSPC:DSPG:CHOL liposomes showed a significantly higher expansion of antigen-specific CD4<sup>+</sup> T cells than the formulations containing DOPC and DOPG (DSPC:DSPG 7.3 ± 0.9%, DSPC:DSPG:CHOL 7.3 ± 2.6%, DOPC:DOPG:CHOL 4.1 ± 0.3%, and DOPC:DOPG 4.1 ± 0.7%, Figure 4A, B, C, D, and E). Moreover, in line

with the *in vitro* results, the total percentage of antigen-specific Tregs within the CD4<sup>+</sup> T cell population was highest for DSPC:DSPG liposomes, and decreased with decreasing liposome rigidity (Figure 4F). We observed no differences in Th1 and Th2 responses between liposomal formulations (Figure S3). Furthermore, there were no differences in the production of IFN $\gamma$ , IL-10 and IL-17A by splenocytes between liposomal formulations upon restimulation with OVA<sub>323</sub> for 6 hours (Figure 4G, H and I), although we did find a significant increase in production of IL-10 in all groups comparing antigen-specific CD4<sup>+</sup> T cells to CD45.1<sup>+</sup>CD4<sup>+</sup> T cells, suggesting liposomal vaccination induces functional Tregs.

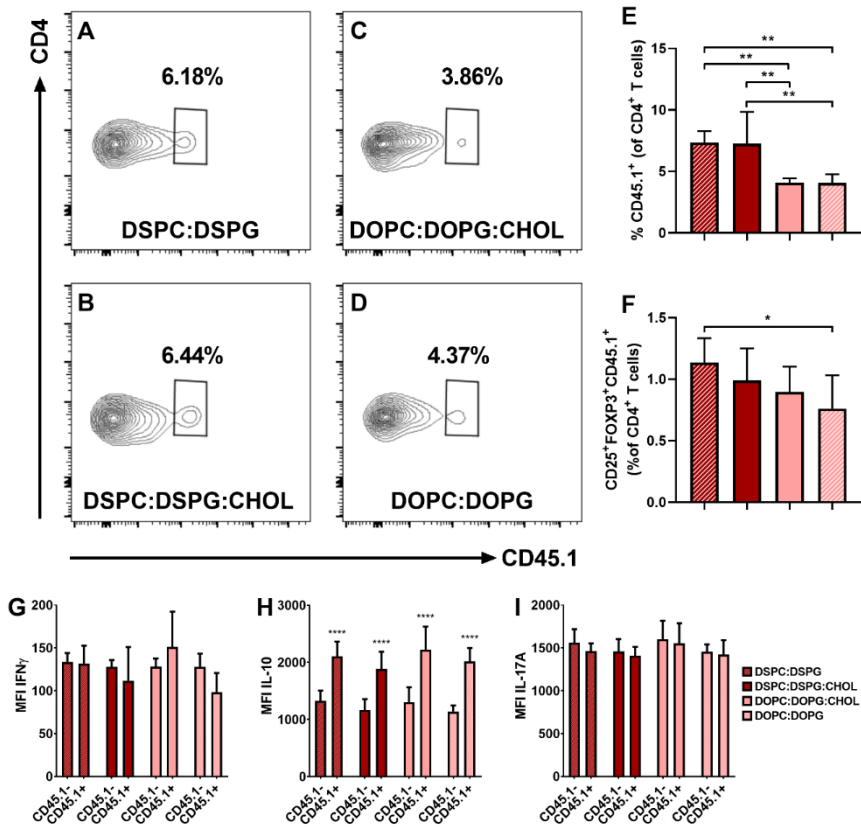


Figure 4. Expansion of OVA<sub>323</sub>-specific Tregs in spleens of mice 8 days after i.v. injection of OVA<sub>323</sub>-containing liposomes. Representative flow cytometry plots of OVA<sub>323</sub>-specific CD45.1<sup>+</sup>CD4<sup>+</sup> T cells in the spleen of a mouse injected with (A) DSPC:DSPG, (B) DSPC:DSPG:CHOL, (C) DOPC:DOPG:CHOL and (D) DOPC:DOPG liposomes containing OVA<sub>323</sub>. (E) Percentage of CD45.1<sup>+</sup> cells in the CD4<sup>+</sup> T cell population. (F) % of CD25<sup>+</sup>FOXP3<sup>+</sup>CD45.1<sup>+</sup> Tregs in the CD4<sup>+</sup> T cell population. Graphs show mean  $\pm$  SD, n = 8. \*p < 0.05, \*\*p < 0.01, compared to free OVA<sub>323</sub> determined by one-way ANOVA and Bonferroni's multiple comparisons test. Intracellular (G) IFN $\gamma$ , (H) IL-10, and (I) IL-17A staining in splenocytes restimulated with 10  $\mu$ g/mL OVA<sub>323</sub> peptide for 6 hours. \*\*\*\*p < 0.0001 comparing CD45.1<sup>+</sup>CD4<sup>+</sup> T cells to CD45.1<sup>+</sup>CD4<sup>+</sup> T cells. No significant differences found between liposomal formulations as measured by two way ANOVA with Bonferroni's post-test.

## Discussion

The induction of antigen-specific Tregs through vaccination is an attractive approach for the treatment of autoimmune diseases. We and others have previously shown that nanoparticles, such as liposomes, can be used to induce these Tregs<sup>10,13</sup>. Generally, approaches to optimize such nanoparticles are focused on studying the effect of particle size and surface charge, while another important parameter, rigidity, is often overlooked<sup>15</sup>. This parameter is usually approximated by the phase properties of the lipid bilayers by analytical techniques such as DSC and Laurdan anisotropy. Besides the fact that these techniques only provide information about the bilayer of liposomes and thereby exclude other influencing factors, such as size, lamellarity, antigen content, and formulation excipients, there are other issues associated with these techniques. For instance, many liposomal formulations contain CHOL in the lipid bilayer, which compromises the suitability of techniques such as DSC<sup>25</sup>, Fourier-transform infrared spectroscopy (FTIR)<sup>36</sup>, and Laurdan anisotropy<sup>37</sup>. Furthermore, compounds encapsulated in liposomes can also interfere with DSC<sup>38,39</sup> and FTIR measurements<sup>40</sup>. Other analytical techniques such as measuring the ability of particles to be extruded<sup>41,42</sup> are indirect measurements of rigidity. Importantly, all of the aforementioned techniques can only measure the average properties of a batch of particles. In contrast, AFM is an excellent technique to accurately measure the rigidity of individual particles and is not hindered by the presence of other compounds, such as CHOL and antigen. To further confirm this, studies should be performed to compare AFM to other techniques that measure liposomal rigidity.

We observed that CHOL reduces DSPC:DSPG liposome rigidity, and increases DOPC:DOPG liposome rigidity. The lipid bilayers of liposomes can generally be classified into three physical states with increasing rigidity: liquid disordered (bilayers composed of low- $T_m$  phospholipids), liquid ordered (bilayers composed of high- or low- $T_m$  phospholipids containing at least 20 mol % CHOL) and gel state (bilayers containing high- $T_m$  phospholipids). In the gel state, CHOL disrupts the tight packing of the lipids, while in the liquid disordered state, CHOL occupies space at the interfacial region near the membrane surface and replaces the hydrated  $\text{CH}_2$  groups. As the acyl chains become dehydrated and straighten out, the packing becomes tighter and rigidity is, therefore, increased<sup>43</sup>. While bilayer state is not the same as liposomal rigidity, it is most likely one of the most important parameters that influence the rigidity of the liposomes. This is also in line with results from Takechi-Haraya *et al.* who used AFM to study the effect of CHOL on liposome rigidity<sup>44</sup>.

From our study, it became clear that the introduction of lipid order mismatch significantly affects the rigidity of the liposomes. Mixing of lipids with different phase transitions in the absence of CHOL can lead to the formation of lipid



domains (e.g. rigid domains and fluid domains), which could destabilize the bilayer packing, and thereby the rigidity of the liposomes<sup>23</sup>. We observed a significant decrease in rigidity of liposomes in the presence of a small amount of lower- $T_m$  lipid (e.g. DSPC:DSPG:CHOL vs. DSPC:DPPG:CHOL, Table S3), which did not further decrease upon complete substitution (e.g. DSPC:DPPG:CHOL vs. DPPC:DPPG:CHOL). This suggests that the  $T_m$  values and the molar ratio of the constituent lipids are poor predictors of the rigidity of the liposomes (Figure S1). Physicochemical properties of liposomes other than bilayer composition can also affect their rigidity. For example, smaller liposomes, measured by AFM, are more rigid than larger liposomes<sup>45</sup>. This may be due to the different curvature of liposomes of different sizes, leading to more restricted molecular interactions between the lipids of smaller liposomes<sup>46</sup>. The charge of liposomes can also affect rigidity; neutral DOPC liposomes measured by AFM were shown to be more rigid than anionic DOPC:DOPG or cationic DOPC:DOTAP liposomes. This was hypothesized to be due to electrostatic repulsions causing structural destabilization of the lipid bilayer<sup>47</sup>. Due to technical limitations, the AFM measurements were performed at 25°C. Since temperature affects the phase state of the lipid bilayers, it also influences the rigidity of liposomes. However, the phase states of the used phospholipids are the same at 25°C and 37°C (Table S1), so the trends in YM at this physiologically more relevant temperature should be very similar to those observed at 25°C. Furthermore, a recent study found no difference in anionic liposome stiffness over the temperature range of 25-37°C<sup>48</sup>. Finally, antigen content may affect liposomal rigidity. In this study, we have generated liposomal formulations with similar size, antigen loading, and  $\zeta$ -potential to allow an *in vitro* and *in vivo* assessment primarily based on liposome rigidity.

The liposomes we measured had a range of YM from about 500 kPa to almost 4 MPa (Figure 1B). For comparison, the YM of most mammalian cells was measured to be between 0.02 and 400 kPa<sup>49</sup> and that of cortical bone was reported to be about 20 GPa<sup>50</sup>. Moreover, we have used our AFM method to measure other anionic particle type, PLGA nanoparticles (Z-average diameter of  $142.1 \pm 1.1$  nm, PDI of  $0.073 \pm 0.016$ ,  $\zeta$ -potential  $-49.7 \pm 4.2$  mV), which had a YM of  $14.4 \text{ MPa} \pm 1.8 \text{ MPa}$ . This illustrates that the range of rigidities of the liposomes is relatively small. This is especially true for the CHOL-containing liposomes, the rigidity of which ranged from about 800 kPa to 1500 kPa (Figure 1B). This was expected since their bilayers are all in the liquid disordered state. However, even such small differences in rigidity could be measured using our AFM method, and we could measure significant differences between formulations (Table S3), illustrating the strength of this technique.

We have reported the SD of YM values of all liposomes measured within a



batch. The SD of YM was relatively high for each liposomal formulation. The high SD was not due to a lack of precision of the AFM measurements, as repeated measurements of the same liposomes showed very low variation (the difference between two measurements of the same DSPC:DSPG:CHOL:OVA<sub>323</sub> liposomes was 2.8%, Table S4). Rather, it illustrates the variation in YM of the liposomes within a formulation, which is likely due to differences in size, lamellarity, and possibly antigen loading among different individual liposomes within the same batch. Variation in YM as measured in two different batches of DSPC:DSPG:CHOL:OVA<sub>323</sub> liposomes was also very low ( $1467 \pm 575$  kPa vs.  $1510 \pm 514$ , Figure S4).

Based on previous reports we expected that the rigidity of the liposomes would positively correlate with their uptake by APCs since it requires less energy for a cell membrane to wrap around rigid particles<sup>51</sup>. It is known that phospholipid saturation has a significant effect on their fate in biological systems. For instance, dimethyldioctadecylammonium:trehalose 6,6'-dibehenate (DDA:TDB) liposomes showed higher retention at the site of injection and uptake by APCs *in vivo* compared to more fluid (as measured by DSC) dimethyldioleoylammonium (DODA):TDB liposomes<sup>18</sup>. Furthermore, CHOL content negatively correlated with uptake by THP-1-derived macrophages<sup>52</sup>. In our study, almost all formulations show a positive trend between liposomal rigidity and APC association. However, DOPC:DOPG liposomes showed the highest association to BMDCs of all tested formulations (Figure 2A), which was not expected since these liposomes presented the lowest rigidity (Figure 1B). Their route of uptake could be different from that of the more rigid formulations. For instance, pure DOPC liposomes (YM of 45 kPa as measured by AFM) were hypothesized to fuse with cells<sup>53</sup>. The DOPC:DOPG liposomes showed high passive association (Figure 2B), and did not deliver their cargo to BMDCs (Figure 2C), explaining their inability to induce T cell responses (Figure 3C). There is evidence of an inverse relationship between liposomal rigidity and membrane permeability, as measured by calcein leakage<sup>37</sup>. So, it may be that the peptide had leaked out of the DOPC:DOPG and DOPC:DOPG:CHOL liposomes prior to BMDC association. This hypothesis is supported by our observation that a mixture of free OVA<sub>323</sub> and empty DOPC:DOPG or DOPC:DOPG:CHOL liposomes showed the same amount of OVA<sub>323</sub> association as encapsulated peptide (data not shown). Since we used fluorescently-labeled lipids and peptides, we cannot exclude the influence of the fluorophore itself on the measured association in BMDCs. However, since all formulations (aside from DOPC:DOPG liposomes) show almost no association of fluorophore when incubated at 4°C (Figure S2), the fluorophore itself likely has no effect on association.

We observed a clear correlation between the rigidity of the liposomes and the

Treg responses they elicited *in vitro* and *in vivo* (Figure 3D, Figure 4F). While others have shown a link between increased rigidity and MHC-II presentation<sup>19</sup>, and enhanced humoral and cellular responses<sup>54,55</sup>, we are the first to report the effects of rigidity on Treg responses. This may have implications for the design of delivery systems aimed to enhance antigen-specific Treg responses.

In conclusion, we showed that liposomal rigidity as measured by our optimized AFM method is an important parameter in eliciting antigen-specific Treg responses *in vitro* and *in vivo*. Our findings may contribute to a better understanding of the factors driving Treg responses. Moreover, this paper may contribute to a rational design of liposomal as well as other nanoparticulate vaccine formulations aiming to enhance antigen-specific Treg responses for the treatment of autoimmune diseases.

## References

- 1        Sakaguchi, S., Yamaguchi, T., Nomura, T. & Ono, M. Regulatory T cells and immune tolerance. *Cell* **133**, 775-787, doi:10.1016/j.cell.2008.05.009 (2008).
- 2        Mallat, Z., Ait-Oufella, H. & Tedgui, A. Regulatory T-cell immunity in atherosclerosis. *Trends Cardiovasc Med* **17**, 113-118, doi:10.1016/j.tcm.2007.03.001 (2007).
- 3        Keijzer, C., van der Zee, R., van Eden, W. & Broere, F. Treg inducing adjuvants for therapeutic vaccination against chronic inflammatory diseases. *Front Immunol* **4**, 245, doi:10.3389/fimmu.2013.00245 (2013).
- 4        Dominguez-Villar, M. & Hafler, D. A. Regulatory T cells in autoimmune disease. *Nat Immunol* **19**, 665-673, doi:10.1038/s41590-018-0120-4 (2018).
- 5        Faria, A. M. & Weiner, H. L. Oral tolerance: therapeutic implications for autoimmune diseases. *Clin Dev Immunol* **13**, 143-157, doi:10.1080/17402520600876804 (2006).
- 6        Kishimoto, T. K. & Maldonado, R. A. Nanoparticles for the Induction of Antigen-Specific Immunological Tolerance. *Front Immunol* **9**, 230, doi:10.3389/fimmu.2018.00230 (2018).
- 7        Macauley, M. S. *et al.* Antigenic liposomes displaying CD22 ligands induce antigen-specific B cell apoptosis. *J Clin Invest* **123**, 3074-3083, doi:10.1172/JCI69187 (2013).
- 8        Pang, L., Macauley, M. S., Arlian, B. M., Nycholat, C. M. & Paulson, J. C. Encapsulating an Immunosuppressant Enhances Tolerance Induction by Siglec-Engaging Tolerogenic Liposomes. *Chembiochem* **18**, 1226-1233, doi:10.1002/cbic.201600702 (2017).
- 9        Maldonado, R. A. *et al.* Polymeric synthetic nanoparticles for the induction of antigen-specific immunological tolerance. *Proc Natl Acad Sci U S A* **112**, E156-165, doi:10.1073/pnas.1408686111 (2015).
- 10       Rodriguez-Fernandez, S. *et al.* Phosphatidylserine-Liposomes Promote Tolerogenic Features on Dendritic Cells in Human Type 1 Diabetes by Apoptotic Mimicry. *Front Immunol* **9**, doi:10.3389/fimmu.2018.00253 (2018).
- 11       Watson, D. S., Endsley, A. N. & Huang, L. Design considerations for liposomal vaccines: influence of formulation parameters on antibody and cell-mediated immune responses to liposome associated antigens. *Vaccine* **30**, 2256-2272, doi:10.1016/j.vaccine.2012.01.070 (2012).
- 12       Hunter, Z. *et al.* A biodegradable nanoparticle platform for the induction of antigen-specific immune tolerance for treatment of autoimmune disease. *ACS Nano* **8**, 2148-2160, doi:10.1021/nn405033r (2014).
- 13       Benne, N. *et al.* Anionic 1,2-distearoyl-sn-glycero-3-phosphoglycerol (DSPG) liposomes induce antigen-specific regulatory T cells and prevent atherosclerosis in mice. *J Control Release* **291**, 135-146, doi:10.1016/j.jconrel.2018.10.028 (2018).
- 14       Bachmann, M. F. & Jennings, G. T. Vaccine delivery: a matter of size, geometry, kinetics and molecular patterns. *Nat Rev Immunol* **10**, 787-796, doi:10.1038/nri2868 (2010).
- 15       Benne, N., van Duijn, J., Kuiper, J., Jiskoot, W. & Slutter, B. Orchestrating immune responses: How size, shape and rigidity affect the immunogenicity of particulate vaccines. *J Control Release* **234**, 124-134, doi:10.1016/j.jconrel.2016.05.033 (2016).
- 16       Anselmo, A. C. & Mitragotri, S. Impact of particle elasticity on particle-based drug delivery systems. *Adv Drug Deliv Rev* **108**, 51-67, doi:10.1016/j.addr.2016.01.007 (2017).
- 17       Beningo, K. A. & Wang, Y. L. Fc-receptor-mediated phagocytosis is regulated by mechanical properties of the target. *J Cell Sci* **115**, 849-856 (2002).
- 18       Christensen, D. *et al.* A cationic vaccine adjuvant based on a saturated quaternary ammonium lipid have different in vivo distribution kinetics and display a distinct CD4 T cell-inducing capacity compared to its unsaturated analog. *J Control Release* **160**, 468-476, doi:10.1016/j.jconrel.2012.03.016 (2012).
- 19       Norling, K. *et al.* Gel Phase 1,2-Distearoyl-sn-glycero-3-phosphocholine-Based Liposomes Are Superior to Fluid Phase Liposomes at Augmenting Both Antigen Presentation on

- Major Histocompatibility Complex Class II and Costimulatory Molecule Display by Dendritic Cells in Vitro. *ACS Infect Dis*, doi:10.1021/acsinfecdis.9b00189 (2019).
- 20 Yasuda, T., Dancey, G. F. & Kinsky, S. C. Immunogenicity of liposomal model membranes in mice: dependence on phospholipid composition. *Proc Natl Acad Sci U S A* **74**, 1234-1236, doi:10.1073/pnas.74.3.1234 (1977).
- 21 Dancey, G. F., Yasuda, T. & Kinsky, S. C. Effect of liposomal model membrane composition on immunogenicity. *J Immunol* **120**, 1109-1113 (1978).
- 22 Bakouche, O. & Gerlier, D. Enhancement of immunogenicity of tumour virus antigen by liposomes: the effect of lipid composition. *Immunology* **58**, 507-513 (1986).
- 23 Mouritsen, O. G. & Jorgensen, K. Dynamical order and disorder in lipid bilayers. *Chem Phys Lipids* **73**, 3-25, doi:10.1016/0009-3084(94)90171-6 (1994).
- 24 Demetzos, C. Differential Scanning Calorimetry (DSC): a tool to study the thermal behavior of lipid bilayers and liposomal stability. *J Liposome Res* **18**, 159-173, doi:10.1080/08982100802310261 (2008).
- 25 Matsingou, C. & Demetzos, C. Calorimetric study on the induction of interdigitated phase in hydrated DPPC bilayers by bioactive labdanes and correlation to their liposome stability: The role of chemical structure. *Chem Phys Lipids* **145**, 45-62, doi:10.1016/j.chemphyslip.2006.10.004 (2007).
- 26 Spyratou, E., Mourelatou, E. A., Makropoulou, M. & Demetzos, C. Atomic force microscopy: a tool to study the structure, dynamics and stability of liposomal drug delivery systems. *Expert Opin Drug Deliv* **6**, 305-317, doi:10.1517/17425240902828312 (2009).
- 27 Varypataki, E. M., Benne, N., Bouwstra, J., Jiskoot, W. & Ossendorp, F. Efficient Eradication of Established Tumors in Mice with Cationic Liposome-Based Synthetic Long-Peptide Vaccines. *Cancer Immunol Res* **5**, 222-233, doi:10.1158/2326-6066.CIR-16-0283 (2017).
- 28 Filipe, V., Hawe, A. & Jiskoot, W. Critical evaluation of Nanoparticle Tracking Analysis (NTA) by NanoSight for the measurement of nanoparticles and protein aggregates. *Pharm Res* **27**, 796-810, doi:10.1007/s11095-010-0073-2 (2010).
- 29 Varypataki, E. M., van der Maaden, K., Bouwstra, J., Ossendorp, F. & Jiskoot, W. Cationic liposomes loaded with a synthetic long peptide and poly(I:C): a defined adjuvanted vaccine for induction of antigen-specific T cell cytotoxicity. *AAPS J* **17**, 216-226, doi:10.1208/s12248-014-9686-4 (2015).
- 30 van der Maaden, K., Sliedregt, K., Kros, A., Jiskoot, W. & Bouwstra, J. Fluorescent nanoparticle adhesion assay: a novel method for surface pKa determination of self-assembled monolayers on silicon surfaces. *Langmuir* **28**, 3403-3411, doi:10.1021/la203560k (2012).
- 31 Howarter, J. A. & Youngblood, J. P. Optimization of silica silanization by 3-aminopropyltriethoxysilane. *Langmuir* **22**, 11142-11147, doi:10.1021/la061240g (2006).
- 32 Duarte, A. A. *et al.* Adsorption kinetics of DPPG liposome layers: a quantitative analysis of surface roughness. *Microsc Microanal* **19**, 867-875, doi:10.1017/S1431927613001621 (2013).
- 33 Determining the elastic modulus of biological samples using atomic force microscopy. 1-9 (JPK Instruments AG Application Note).
- 34 Lin, D. C., Dimitriadis, E. K. & Horkay, F. Robust strategies for automated AFM force curve analysis--I. Non-adhesive indentation of soft, inhomogeneous materials. *J Biomech Eng* **129**, 430-440, doi:10.1115/1.2720924 (2007).
- 35 Liang, X., Mao, G. & Simon Ng, K. Y. Probing small unilamellar EggPC vesicles on mica surface by atomic force microscopy. *Colloids Surf B Biointerfaces* **34**, 41-51, doi:10.1016/j.colsurfb.2003.10.017 (2004).
- 36 Altunayar, C., Sahin, I. & Kazanci, N. A comparative study of the effects of cholesterol

- and desmosterol on zwitterionic DPPC model membranes. *Chem Phys Lipids* **188**, 37-45, doi:10.1016/j.chemphyslip.2015.03.006 (2015).
- 37 Takechi-Haraya, Y., Sakai-Kato, K. & Goda, Y. Membrane Rigidity Determined by Atomic Force Microscopy Is a Parameter of the Permeability of Liposomal Membranes to the Hydrophilic Compound Calcein. *AAPS PharmSciTech* **18**, 1887-1893, doi:10.1208/s12249-016-0624-x (2017).
- 38 Zhao, L., Feng, S. S., Kocherginsky, N. & Kostetski, I. DSC and EPR investigations on effects of cholesterol component on molecular interactions between paclitaxel and phospholipid within lipid bilayer membrane. *Int J Pharm* **338**, 258-266, doi:10.1016/j.ijpharm.2007.01.045 (2007).
- 39 Eloy, J. O. *et al.* Co-loaded paclitaxel/rapamycin liposomes: Development, characterization and in vitro and in vivo evaluation for breast cancer therapy. *Colloids Surf B Biointerfaces* **141**, 74-82, doi:10.1016/j.colsurfb.2016.01.032 (2016).
- 40 Toyran, N. & Severcan, F. Interaction between vitamin D2 and magnesium in liposomes: Differential scanning calorimetry and FTIR spectroscopy studies. *Journal of Molecular Structure* **839**, 19-27, doi:10.1016/j.molstruc.2006.11.005 (2007).
- 41 van den Bergh, B. A., Wertz, P. W., Junginger, H. E. & Bouwstra, J. A. Elasticity of vesicles assessed by electron spin resonance, electron microscopy and extrusion measurements. *Int J Pharm* **217**, 13-24, doi:10.1016/s0378-5173(01)00576-2 (2001).
- 42 Myerson, J. W. *et al.* Flexible Nanoparticles Reach Sterically Obscured Endothelial Targets Inaccessible to Rigid Nanoparticles. *Adv Mater* **30**, e1802373, doi:10.1002/adma.201802373 (2018).
- 43 Krause, M. R. & Regen, S. L. The structural role of cholesterol in cell membranes: from condensed bilayers to lipid rafts. *Acc Chem Res* **47**, 3512-3521, doi:10.1021/ar500260t (2014).
- 44 Takechi-Haraya, Y. *et al.* Atomic Force Microscopic Analysis of the Effect of Lipid Composition on Liposome Membrane Rigidity. *Langmuir* **32**, 6074-6082, doi:10.1021/acs.langmuir.6b00741 (2016).
- 45 Delorme, N. & Fery, A. Direct method to study membrane rigidity of small vesicles based on atomic force microscope force spectroscopy. *Phys Rev E Stat Nonlin Soft Matter Phys* **74**, 030901, doi:10.1103/PhysRevE.74.030901 (2006).
- 46 Nakano, K., Tozuka, Y., Yamamoto, H., Kawashima, Y. & Takeuchi, H. A novel method for measuring rigidity of submicron-size liposomes with atomic force microscopy. *Int J Pharm* **355**, 203-209, doi:10.1016/j.ijpharm.2007.12.018 (2008).
- 47 Takechi-Haraya, Y., Goda, Y. & Sakai-Kato, K. Atomic Force Microscopy Study on the Stiffness of Nanosized Liposomes Containing Charged Lipids. *Langmuir* **34**, 7805-7812, doi:10.1021/acs.langmuir.8b01121 (2018).
- 48 Takechi-Haraya, Y., Goda, Y., Izutsu, K. & Sakai-Kato, K. Improved Atomic Force Microscopy Stiffness Measurements of Nanoscale Liposomes by Cantilever Tip Shape Evaluation. *Analytical Chemistry* **91**, 10432-10440, doi:10.1021/acs.analchem.9b00250 (2019).
- 49 Kuznetsova, T. G., Starodubtseva, M. N., Yegorenkov, N. I., Chizhik, S. A. & Zhdanov, R. I. Atomic force microscopy probing of cell elasticity. *Micron* **38**, 824-833, doi:10.1016/j.micron.2007.06.011 (2007).
- 50 Rho, J. Y., Ashman, R. B. & Turner, C. H. Young's modulus of trabecular and cortical bone material: ultrasonic and microtensile measurements. *J Biomech* **26**, 111-119, doi:10.1016/0021-9290(93)90042-d (1993).
- 51 Yi, X., Shi, X. & Gao, H. Cellular uptake of elastic nanoparticles. *Phys Rev Lett* **107**, 098101, doi:10.1103/PhysRevLett.107.098101 (2011).
- 52 Kaur, R. *et al.* Effect of incorporating cholesterol into DDA:TDB liposomal adjuvants on bilayer properties, biodistribution, and immune responses. *Mol Pharm* **11**, 197-207, doi:10.1021/mp400372j (2014).

- 53 Guo, P. *et al.* Nanoparticle elasticity directs tumor uptake. *Nat Commun* **9**, 130, doi:10.1038/s41467-017-02588-9 (2018).
- 54 Garnier, F., Forquet, F., Bertolino, P. & Gerlier, D. Enhancement of in vivo and in vitro T cell response against measles virus haemagglutinin after its incorporation into liposomes: effect of the phospholipid composition. *Vaccine* **9**, 340-345, doi:10.1016/0264-410x(91)90061-a (1991).
- 55 Mazumdar, T., Anam, K. & Ali, N. Influence of phospholipid composition on the adjuvanticity and protective efficacy of liposome-encapsulated *Leishmania donovani* antigens. *J Parasitol* **91**, 269-274, doi:10.1645/GE-356R1 (2005).
- 56 Zhang, Y. P., Lewis, R. N. & McElhaney, R. N. Calorimetric and spectroscopic studies of the thermotropic phase behavior of the n-saturated 1,2-diacylphosphatidylglycerols. *Biophys J* **72**, 779-793, doi:10.1016/s0006-3495(97)78712-5 (1997).
- 57 Biltonen, R. L. & Lichtenberg, D. The Use of Differential Scanning Calorimetry as a Tool to Characterize Liposome Preparations. *Chemistry and Physics of Lipids* **64**, 129-142, doi:Doi 10.1016/0009-3084(93)90062-8 (1993).
- 58 Ulrich, A. S., Sami, M. & Watts, A. Hydration of DOPC bilayers by differential scanning calorimetry. *Biochim Biophys Acta* **1191**, 225-230, doi:10.1016/0005-2736(94)90253-4 (1994).
- 59 Smaal, E. B., Nicolay, K., Mandersloot, J. G., de Gier, J. & de Kruijff, B. 2H-NMR, 31P-NMR and DSC characterization of a novel lipid organization in calcium-dioleoylphosphatidate membranes. Implications for the mechanism of the phosphatidate calcium transmembrane shuttle. *Biochim Biophys Acta* **897**, 453-466, doi:10.1016/0005-2736(87)90442-1 (1987).

## Supplements

Table S1.  $T_m$  of phospholipids.

Lipid	Abbreviation	Structure	$T_m$ (°C)	Ref
Neutral				
1,2-distearoyl- <i>sn</i> -glycero-3-phosphocholine	DSPC	di-18:0 PC	55	<sup>56</sup>
1,2-dipalmitoyl- <i>sn</i> -glycero-3-phosphocholine	DPPC	di-16:0 PC	41	<sup>57</sup>
1,2-dioleoyl- <i>sn</i> -glycero-3-phosphocholine	DOPC	di-18:1 ( $\Delta 9$ -Cis) PC	-17	<sup>58</sup>
Anionic				
1,2-distearoyl- <i>sn</i> -glycero-3-phospho-(1'-rac-glycerol)	DSPG	di-18:0 PG	55	<sup>57</sup>
1,2-dipalmitoyl- <i>sn</i> -glycero-3-phospho-(1'-rac-glycerol)	DPPG	di-16:0 PG	41	<sup>57</sup>
1,2-dioleoyl- <i>sn</i> -glycero-3-phospho-(1'-rac-glycerol)	DOPG	di-18:1 ( $\Delta 9$ -Cis) PG	-18	<sup>59</sup>

Table S2. Rigidity, expressed as YM, of liposomes determined by AFM,  $n$  = number of liposomes measured

Lipid composition (molar ratio)	YM $\pm$ SD (kPa)	n
DSPC:DSPG (4:1)	3611 $\pm$ 1271	450
DSPC:DSPG:CHOL (4:1:2)	1498 $\pm$ 531	281
DSPC:DPPG:CHOL (4:1:2)	1208 $\pm$ 538	243
DPPC:DPPG:CHOL (4:1:2)	1195 $\pm$ 348	170
DSPC:DOPG:CHOL (4:1:2)	825 $\pm$ 307	31
DOPC:DOPG:CHOL (4:1:2)	911 $\pm$ 447	63
DOPC:DOPG (4:1)	494 $\pm$ 365	149

Table S3. Significant differences between liposomal rigidities as measured by One-way ANOVA and Bonferroni's post-test. \*\*\*\* $p$  < 0.0001, \*\*\* $p$  < 0.001, \*\* $p$  < 0.01. \* $p$  < 0.05.

DOPC:DOPG:CHOL vs. DSPC:DOPG:CHOL	ns
DOPC:DOPG:CHOL vs. DSPC:DSPG:CHOL	****
DOPC:DOPG:CHOL vs. DPPC:DPPG:CHOL	ns
DOPC:DOPG:CHOL vs. DSPC:DPPG:CHOL	ns
DOPC:DOPG:CHOL vs. DOPC:DOPG	*
DOPC:DOPG:CHOL vs. DSPC:DSPG	****
DSPC:DOPG:CHOL vs. DSPC:DSPG:CHOL	***
DSPC:DOPG:CHOL vs. DPPC:DPPG:CHOL	ns
DSPC:DOPG:CHOL vs. DSPC:DPPG:CHOL	ns
DSPC:DOPG:CHOL vs. DOPC:DOPG	ns
DSPC:DOPG:CHOL vs. DSPC:DSPG	****
DSPC:DSPG:CHOL vs. DPPC:DPPG:CHOL	**
DSPC:DSPG:CHOL vs. DSPC:DPPG:CHOL	**
DSPC:DSPG:CHOL vs. DOPC:DOPG	****
DSPC:DSPG:CHOL vs. DSPC:DSPG	****
DPPC:DPPG:CHOL vs. DSPC:DPPG:CHOL	ns
DPPC:DPPG:CHOL vs. DOPC:DOPG	****
DPPC:DPPG:CHOL vs. DSPC:DSPG	****
DSPC:DPPG:CHOL vs. DOPC:DOPG	****
DSPC:DPPG:CHOL vs. DSPC:DSPG	****
DOPC:DOPG vs. DSPC:DSPG	****

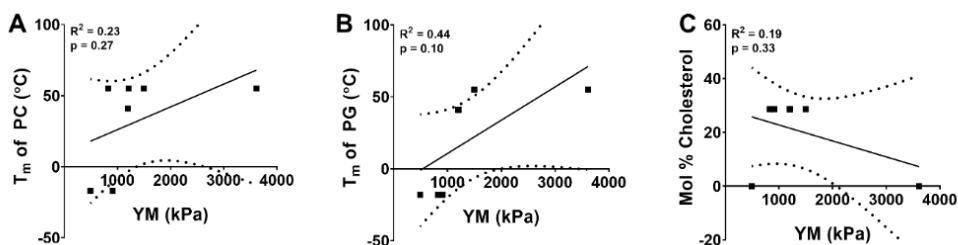


Figure S1. Linear correlations (95% CI) between YM and T<sub>m</sub> of PC or PG, CHOL content, liposome size, liposome ζ-potential and LE of OVA<sub>323</sub>. Correlations between (A) YM and T<sub>m</sub> of PC, (B) YM and T<sub>m</sub> of PG, (C) YM and mol % CHOL.

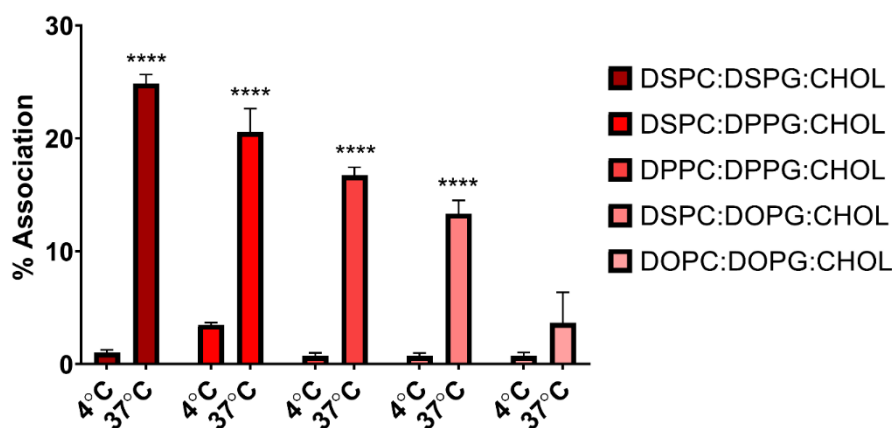


Figure S2. Liposomal association (uptake and/or adsorption) by BMDCs in vitro. OVA<sub>323</sub>-containing fluorescently labeled liposomes were incubated for 4 hours with BMDCs at 4°C and 37°C. Liposomes were subsequently washed away and cells were incubated overnight before being analyzed via flow cytometry. % Association indicates the percentage of live BMDCs that are positive for the fluorescent label in the liposomes. Graph shows mean ± SD, n = 3. \*\*\*\*p < 0.0001, comparing 4°C to 37°C determined by two-way ANOVA and Bonferroni's multiple comparisons test.



Table S4. DSPC:DSPG:CHOL:OVA<sub>323</sub> liposomes measured twice. Measurement 1 and 2 indicate repeated scans of the exact same liposomes.

Young's Modulus (kPa)	
Measurement 1	Measurement 2
1660.80	1651.40
1345.50	1643.60
2009.60	2393.20
1345.80	1731.60
957.60	1277.50
677.60	1229.10
857.90	784.50
1595.50	1394.40
636.00	792.30
1246.50	743.00
1842.50	1687.30
720.10	1128.00
1234.90	1886.80
1595.10	1229.20
1131.30	1038.60
1508.20	1324.50
1055.20	1406.50
1187.50	974.30
2258.40	1343.30
1226.00	1642.40
734.10	930.90
901.70	988.20
1385.20	1247.10
2038.90	1876.20
1854.40	1506.90
2111.80	2249.80
2949.30	2779.90
749.10	798.40
1253.40	1300.80
772.30	638.50
1607.90	2085.40
1626.90	1608.20
1604.00	1537.50
683.80	775.90
2214.00	2287.70
1562.20	1703.10
2994.10	3184.40
1706.60	1603.80
Average	
1443.20	1484.32

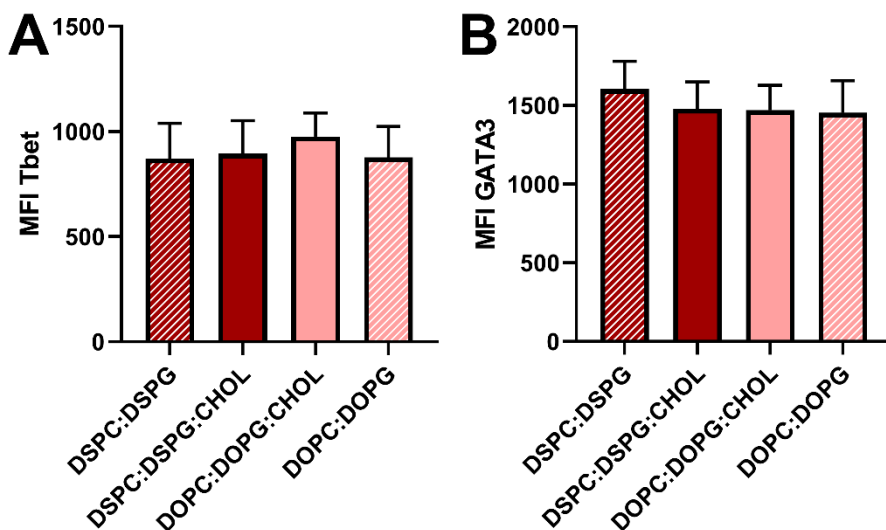


Figure S3. Th1 and Th2 responses in spleens of mice 8 days after i.v. injection of OVA<sub>323</sub>-containing liposomes. (A) MFI Tbet and (B) MFI GATA3 of CD45.1<sup>+</sup>CD4<sup>+</sup> T cells. Graphs show mean ± SD, n = 8. No significant differences between groups as analyzed by one-way ANOVA and Bonferroni's multiple comparisons test.

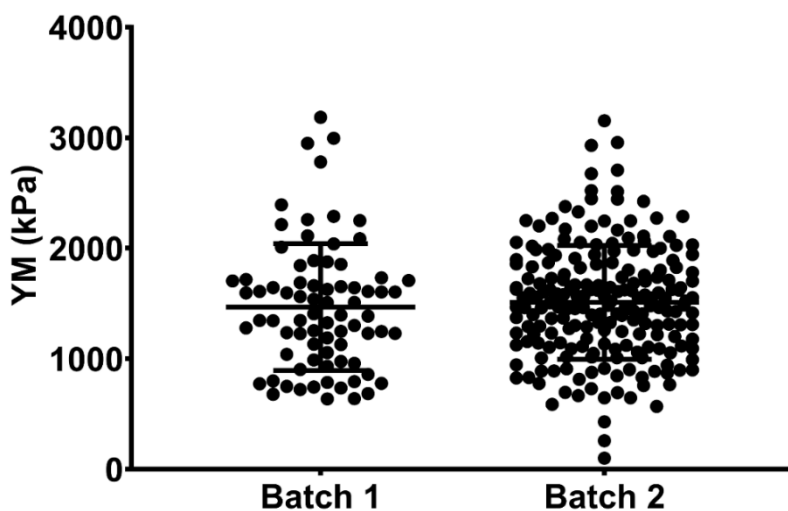


Figure S4. Comparison between two different batches of DSPC:DSPG:CHOL:OVA<sub>323</sub> liposomes. Each point represents a liposome measurement. Graph shows mean ± SD. No significant difference found between both batches with unpaired two-tailed t-test. N = 77-204.



# Chapter 4

## Antigen uptake after intradermal microinjection depends on antigen nature and formulation, but not on injection depth

RJT Lebout<sup>1#</sup>, P Schipper<sup>1#</sup>, TMM van Capel<sup>2</sup>, L Kong<sup>3,4</sup>, K van der Maaden<sup>5,6</sup>, A Kros<sup>3</sup>, W Jiskoot<sup>1</sup>, EC de Jong<sup>2\*</sup>, JA Bouwstra<sup>1\*</sup>

<sup>1</sup> Division of BioTherapeutics, Leiden Academic Centre for Drug Research, Leiden University, Leiden, the Netherlands

<sup>2</sup> Department of Experimental Immunology; Academic Medical Center; Amsterdam, the Netherlands

<sup>3</sup> Division of Supramolecular Chemistry, Leiden Institute of Chemistry, Leiden University, Leiden, the Netherlands

<sup>4</sup> Tongji School of Pharmacy, HuaZhong University of Science and Technology, Wuhan 430030, China

<sup>5</sup> Tumor Immunology Group, Department of Immunology, Leiden University Medical Center, Albinusdreef 2, 2333 ZA Leiden, The Netherlands

<sup>6</sup> TECO development GmbH, 53359 Rheinbach, Germany

# contributed equally

### \* Correspondence:

Joke Bouwstra: [bouwstra@lacdr.leidenuniv.nl](mailto:bouwstra@lacdr.leidenuniv.nl)

Esther de Jong: [e.c.dejong@amsterdamumc.nl](mailto:e.c.dejong@amsterdamumc.nl)

Frontiers of Allergy

April 2021

doi: 10.3389/falgy.2021.642788

## Abstract

The skin is an attractive alternative administration route for allergy vaccination, as the skin is rich in dendritic cells (DCs) and is easily accessible. In the skin multiple subsets of DCs with distinct roles reside at different depths. In this study antigen (= allergen for allergy) formulations were injected in *ex vivo* human skin in a depth-controlled manner by using a hollow microneedle injection system. Biopsies were harvested at the injection site, which were then cultured for 72 hours. Subsequently, the crawled-out cells were collected from the medium and analyzed with flow cytometry.

Intradermal administration of ovalbumin (OVA, model antigen) solution at various depths in the skin did not affect the migration and maturation of DCs. OVA was taken up efficiently by the DCs, and this was not affected by the injection depth. In contrast, Bet v 1, the major allergen in birch pollen allergy, was barely taken up by dermal DCs (dDCs). Antigens were more efficiently taken up by CD14<sup>+</sup> dDCs than CD1a<sup>+</sup> dDCs, which in turn were more efficient at taken up antigen than Langerhans cells. Subsequently, both OVA and Bet v 1 were formulated in cationic and anionic liposomes, which altered antigen uptake drastically following intradermal microinjection. While OVA uptake was reduced by formulation in liposomes, Bet v 1 uptake in dDCs was increased by encapsulation in both cationic and anionic liposomes. This highlights the potential use of liposomes as adjuvant in intradermal allergy vaccine delivery. In conclusion, we observed that antigen uptake after intradermal injection was not affected by injection depth, but varied between different antigens and formulation.

## Introduction

Allergen specific immunotherapy through vaccination is the only curative treatment for allergies. These allergy vaccines are traditionally administered subcutaneously (SCIT), but products for sublingual administration (SLIT) are available as well [1]. Both therapies are effective, but take 3-5 years to reach effectivity and require an intensive dosing regimen, which contributes to low therapy adherence. To improve therapy adherence, alternative administration sites and delivery methods are explored [2].

The skin is an interesting administration site for vaccination. It is easily accessible, has a large surface area and a high density of antigen presenting cells (APCs) resides in the skin which allows for a potent immune response [3-6]. Previous studies have shown that intradermal vaccination compared to conventional intramuscular or subcutaneous administration can result in equally effective or stronger immune responses, such as rabies [7-9] hepatitis B [10, 11], influenza [12, 13] and polio antigens [14, 15]. This illustrates that the intradermal route is an attractive alternative to the conventional vaccination routes.

The main challenge for vaccination via the skin is overcoming the physical barrier, the stratum corneum [3]. Several administration methods are available to deliver an antigen (= the allergen in case of allergy) into the skin. One of the most attractive approaches is the use of microneedles, as they are able to bypass the stratum corneum effectively and potentially without pain sensation [16, 17]. When the stratum corneum is surpassed, a large network of dendritic cells (DCs) is located in the viable epidermis and dermis. DCs are crucial cells for inducing both humoral and cellular immune responses [18-20].

Several phenotypically and functionally distinct subsets of DCs are known to reside in human skin: Langerhans cells (LCs) are located in the viable epidermis, while CD14<sup>+</sup>, CD1a<sup>+</sup> dermal DCs (dDCs) and classical DC type 1 cells (cDC1s) are located in the dermis [21]. cDC1s are identified by the expression of CD141 and XCR1. These cells are necessary for anti-tumor immunity. They represent a very small fraction of the total skin resident DCs [22].

LCs form a tight network with their dendrites close to the surface of the skin [23-25]. Human LCs are recognized by their expression of langerin and a very high expression of CD1a, but lack expression of CD14 on the cell surface. LCs are known to respond to viruses [26-29], but only weakly to bacteria [30-32], probably due to reduced expression of toll-like receptors (TLRs) 2, 4 and 5 [30]. Moreover, LCs play a role in skin homeostasis by maintaining a state of tolerance by inhibiting T-cells [33].

CD14<sup>+</sup> dDCs lack expression of langerin and CD1a, but do express CD14 on the cell surface. It has been suggested that this subset could be monocyte-derived macrophages rather than DCs [34]. CD14<sup>+</sup> dDCs are reported to preferentially polarize naïve CD4<sup>+</sup> T cells to develop into follicular helper T cells, which in turn induce naïve B cells to produce antibodies and to proliferate into plasma cells [27, 35, 36]. CD14<sup>+</sup> dDCs have shown poor ability to naïve CD8<sup>+</sup> T-cells [27].

CD1a<sup>+</sup> dDCs don't have langerin and CD14 expression, but do express CD1a on the cell surface. CD1a<sup>+</sup> dDCs are intermediately efficient in inducing humoral and cellular immune responses, in comparison to CD14<sup>+</sup> dDCs and LCs [27, 36-38]. Upon activation, LCs and dDCs will take up and process the antigen and subsequently migrate from the skin towards draining lymph nodes, where they present antigen fragments to B- and/or T-cells, initiating the adaptive immune response [23, 24, 39].

Some antigens are poorly taken up by APCs, which complicates the induction of an antigen-specific immune response. Antigen uptake can be increased by formulating antigens in nanoparticles such as liposomes [40-42]. Cationic particles are generally taken up more efficiently, as a result of electrostatic interactions with anionic cell surfaces [43, 44]. Particles smaller than 500 nm have been shown to be taken up more efficiently by DCs than larger counterparts [45, 46].

The influence of intradermal injection depth on the antigen uptake and subsequent immune response is difficult to examine and so far has not been established. In this study we have used a hollow microneedle based system which allows accurate injection of very small volumes (<1 µL) and controlled injection depth. We set out to obtain fundamental insight in the antigen fate after intradermal microinjection and how formulation into liposomal can alter antigen uptake as well as migration and maturation of LCs and dDCs in a model which directly translates to humans. We compared the uptake of ovalbumin and Bet v 1, the latter is the major allergen responsible for birch pollen allergy. We illustrated that antigen formulation in liposomes can increase uptake in dermal DCs approximately 10-fold.

## **Materials & Methods**

### **Materials**

OVA conjugated with Alexa Fluor® 488, Iscove's Modified Dulbecco's Medium (IMDM), Dil stain, Hank's balanced salt solution and anti-human CD11c-PE-Cy7 antibodies (catalogue number 25-0116-42), Alexa Fluor™ 488 NHS ester (succinimidyl ester) were purchased from Thermo Fisher Scientific (Bleiswijk, the Netherlands). Cholecalciferol (vitamin D3) and ethanol 96% (v/v) were

obtained from Sigma Aldrich (Zwijndrecht, the Netherlands). Sterile phosphate buffered saline (PBS) (163.9 mM Na<sup>+</sup>, 140.3 mM Cl<sup>-</sup>, 8.7 mM HPO<sub>4</sub><sup>2-</sup> and 1.8 mM H<sub>2</sub>PO<sub>4</sub><sup>-</sup>, pH 7.4) was ordered at B. Braun Melsungen (Oss, the Netherlands). Skin biopsy punches were purchased from Kai Europe (Solingen, Germany). BD Micro-Fine™ 30G 0.3 mL needle-syringes and anti-human CD1a-APC, CD86-PE and HLA-DR-PerCP antibodies (catalogue numbers 559775, 555665 and 347364, respectively) were obtained from Becton Dickinson (Breda, the Netherlands). Anti-human CD14-APC-Cy7 antibodies (catalogue number 301820) were ordered at Biolegend (Koblenz, Germany). HyClone™ fetal calf serum (FCS) was purchased from GE Healthcare Life Sciences (Eindhoven, the Netherlands). GM-CSF was obtained from Schering-Plough (Uden, the Netherlands). Costar® 48-well plates were ordered at Corning Life Sciences (Amsterdam, the Netherlands). Styrofoam was purchased from a local hardware store.

Recombinant Bet v 1 was purchased from the Department of Molecular Biology of the University of Salzburg (Salzburg, Austria). 1,2-dioleoyl-3-trimethylammonium-propane (DOTAP), 1,2-distearoyl-sn-glycero-3-phosphocholine (DSPC), 1,2-distearoyl-sn-glycero-3-phospho-(1'-rac-glycerol) (DSPG) and cholesterol were purchased from Avanti Lipids (Alabama, United States of America). Vivaspin columns (300.000 MWCO) were supplied by Sartorius (Goettingen, Germany).

#### Fluorescent labeling of antigen

Antigens were labeled according to the manufacturer's protocol [47]. In short: proteins were dissolved in 1 mL 100 mM carbonate buffer (pH 8.5) at a concentration of 4 mg per mL (Bet v 1, MW: 17.6 kDa) or 10 mg per mL (OVA, MW: 42.7kDa). NHS-ester of Alexa Fluor 488 (excitation 490 nm, emission 525 nm) was dissolved in anhydrous DMSO to a concentration of 20 mg/mL. 100 µL of the fluorescent dye solution was added to 1 mL protein solution. The mixture was slightly shaken (100 RPM) at room temperature for 1 hour in an Eppendorf shaker and subsequently stirred overnight at 4 °C. Free dye was removed from protein-bound dye by means of dialysis (2000 Da MWCO) against 10 mM phosphate buffer (pH 7.4). After conjugation, the yield and dye/protein ratio was determined according to the manufacturer's instructions. Protein yield was above 90% in all cases and dye/protein (molar) ratio was between 0.8 and 1.8 and similar for both proteins.

#### Preparation of human skin for intradermal (micro)injections

Abdominal or breast *ex vivo* human skin was obtained from local hospitals after cosmetic surgery. The procedure was according to the ethical principles of the Declaration of Helsinki. The skin was stored at 4 °C and used within 24 hours after surgery. The skin surface was cleaned by rinsing it with sterile PBS, 70% (v/v)



ethanol and sterile PBS again. The skin was slightly pre-stretched by pinning the skin on a flat piece of Styrofoam in an effort to simulate the stretch conditions of human skin *in vivo*. No difference between abdominal or breast-derived skin was observed, therefore all skin was pooled for analysis.

#### Dose-dependent DC activation and antigen uptake

For each experiment, sterile formulations of OVA and vitamin D3 were prepared. To determine the effect of the administered OVA dose on antigen uptake, migration and maturation of DCs, various doses of OVA in 10  $\mu$ L PBS were injected intradermally by using a conventional hypodermic needle-and-syringe (30G needle-syringes). As controls,  $1.25 \times 10^{-9}$  mole vitamin D3 in 10  $\mu$ L PBS (positive control) or 10  $\mu$ L PBS alone (negative control) were injected intradermally. Additionally, plain biopsies of untreated skin were included.

#### Depth-controlled intradermal microinjections

To perform injections at an accurate depth, intradermal microinjections were performed by using a digitally-controlled single hollow microneedle injection system (DC-shMN-iSystem). This system comprises a single hollow microneedle, which is fixed in an applicator, as explained in detail elsewhere [48, 49]. Accurate intradermal microinjections of very low volumes are feasible by controlling the microneedle applicator and syringe pump (NE-300, Prosense, Oosterhout, the Netherlands) *via* a microneedle applicator controller unit (uPRAX Microsolutions, Delft, The Netherlands) [50, 51]. Prior to use, the fluidics part of the DC-shMN-iSystem was sterilized by flushing it with 70% ethanol.

To maximize the accuracy of the microinjection depth, very low volumes were injected to avoid perfusion. Therefore, the microinjection volume was only 0.2  $\mu$ L and contained 0.1  $\mu$ g OVA in PBS. Intradermal microinjections were performed at a pre-selected depth of 50, 500 or 1000  $\mu$ m by using the DC-shMN-iSystem. As a control, 0.1  $\mu$ g OVA in 10  $\mu$ L PBS was injected intradermally with a conventional hypodermic needle-and-syringe (30G needle-syringes).

Liposomes were injected at 500  $\mu$ m depth in a similar way by using the DC-shMN-iSystem. For all formulations, 0.1  $\mu$ g of antigen was injected in a volume of 0.2  $\mu$ L. Consequently, the lipid dose varied between injections and formulations.

#### Culturing of human skin explants

Skin biopsies were harvested immediately after intradermal (micro)injection and were cultured as reported earlier [52, 53]. A full thickness skin biopsy of 6 mm in diameter was taken from the *ex vivo* human skin with the injection site centrally located. The subcutaneous fat was removed simultaneously. For each treatment, 12 biopsies were harvested. Each biopsy was floated with the epidermal side up

for 1 hour in 0.5 mL IMDM containing 1% FCS in a 48-well plate. Subsequently, the biopsies were transferred into 1 mL of IMDM containing 10% FCS and 100 ng/mL GM-CSF in a 48-well plate and were cultured with the epidermal side up at 37 °C and 5% CO<sub>2</sub> for 3 days. After removal of the biopsies, migrated cells were harvested and pooled for flow cytometric analysis.

### Preparation of antigen-containing liposomes

Liposomes were prepared according to a dehydration-rehydration method [54]. In short: 10 mg lipids were dissolved in chloroform and mixed in the desired ratios (Table 1) with a trace amount (0.2 mol%) of fluorescent lipid Dil (excitation 550 nm, emission 570 nm). The chloroform was removed in a rotary evaporator (150 mbar, 37 °C), yielding a lipid film. The lipid film was subsequently hydrated with (antigen-containing) phosphate buffered sucrose (PBS; 10 mM phosphate buffer and 280 mM sucrose, pH 7.4) at 37 °C. The lipid-antigen mixture was snap-frozen and lyophilized overnight. The resulting cake was hydrated at 37 °C with Milli-Q water in 3 steps: sequentially with 250 µL, 250 µL and 500 µL, resulting in a suspension containing 10 mg/ml lipids. After each addition, the mixture was briefly vortexed to create a smooth emulsion. The emulsion was homogenized by six-fold passage over a sequential stack of 400 and 200 nm polycarbonate filter by using an LIPEX extruder (Evonik, Canada). Antigen-loaded liposomes were further purified with centrifuge membrane concentrator (Vivaspin2, 300.000 MWCO, Sartorius), removing the non-associated antigen. All fractions were measured for their fluorescent content (antigen and lipids) in a Tecan Infinite M1000 plate reader (Männedorf, Switzerland) and encapsulation efficiency (EE) was determined as follows:

$$\frac{\text{fluorescence after purification}}{\text{fluorescence before purification}} * 100\%$$

Table 1. Liposome formulation composition.

Formulation name	Lipid 1	Lipid 2	Lipid 3	Molar lipid ratio
Cationic liposomes	DSPC	DOTAP	Cholesterol	2:1:1
Anionic liposomes	DSPC	DSPG	Cholesterol	2:1:1

### Analysis by flow cytometry

The percentage of specific subsets of total migrated HLA-DR<sup>+</sup> DCs, maturation and uptake of OVA by migrated LCs, CD1a<sup>+</sup> and CD14<sup>+</sup> dDCs were analyzed by using flow cytometry. All migrated cells were isolated and stained with fluorescently-labeled antibodies against CD11c, HLA-DR, CD1a and CD14. During flow cytometry analysis, migrated DCs were distinguished by their forward and sideward light scattering properties, in combination with high expression levels of HLA-DR and CD11c, after which LCs (defined as CD1a<sup>high</sup>), CD1a<sup>+</sup> and CD14<sup>+</sup> dDCs were discriminated from this population (Supplementary Figure 1). Antigen/lipid uptake by LCs, CD1a<sup>+</sup> and CD14<sup>+</sup> dDCs was quantified by the percentage of antigen- and/or lipid-containing cells within the LC, CD1a<sup>+</sup> and

CD14<sup>+</sup> dDC subpopulations. Additionally, maturation of LCs, CD1a<sup>+</sup> or CD14<sup>+</sup> dDCs was analyzed by measuring the mean fluorescence intensity (MFI) of the markers HLA-DR and CD86. Multicolor flow cytometry was performed on a FACS Canto II (Becton Dickinson) and FlowJo v10.3 (Tree Star, Ashland, OR, USA) was used for data analysis.

## Statistical analysis

Graphs were plotted with GraphPad Prism version 8. The data was statistically tested in GraphPad as well, as described in the caption of each figure. To compare antigen uptake between skin donors, uptake was normalized as follows:

$$\frac{\text{antigen uptake in formulation}}{\text{antigen uptake in PBS}} \times 100\%$$

Subsequently, outliers were removed by performing the ROUT outlier test with a 1% false discovery rate.

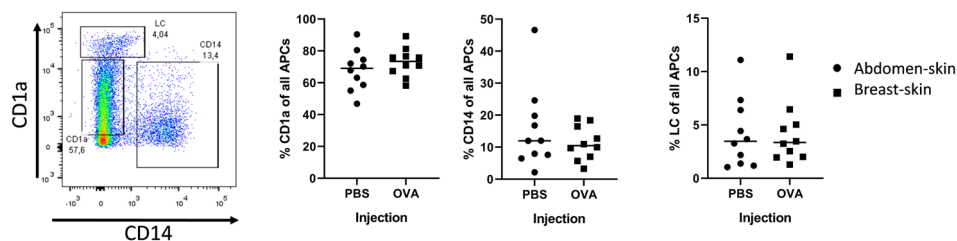
## Results

### Intradermal injections using a hypodermic needle and syringe

Currently intradermal injections are administered with a hypodermic needle and syringe-based system. To evaluate the delivery of antigen after intradermal injection, we have performed a series of experiments using conventional intradermal injections.

### Three distinct dendritic cell subsets migrated of *ex vivo* human skin

To determine what cells migrate from a skin explant, we injected model antigen OVA and PBS in *ex vivo* human skin and cultured skin biopsies for 72 hours. After intradermal injection three DC subsets had migrated out of the skin explant (Figure 1A) : LCs (CD14<sup>-</sup> and CD1a<sup>++</sup>), CD14<sup>+</sup> dDCs (CD1a<sup>-</sup> and CD14<sup>+</sup>), CD1a<sup>+</sup> dDCs (CD1a<sup>+</sup> and CD14<sup>-</sup>). The majority (ca. 70%) of DCs, as defined by HLA-DR and CD11c expression, were CD1a<sup>+</sup> dDCs (Figure 1B), 10% were CD14<sup>+</sup> (Figure 1C)

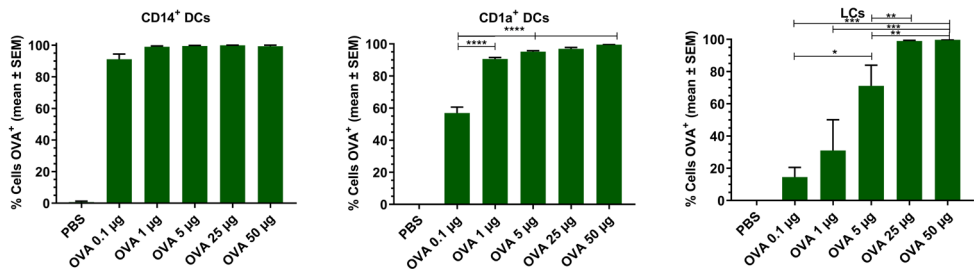


**Figure 1.** Detection of DCs after intradermal injection of 10  $\mu$ L with a hypodermic needle and syringe. The migrated DCs were collected from human *ex vivo* skin (circles = abdominal, squares = breast) explants after 72 hours of culturing. DCs were defined by expression of both HLA-DR and CD11c. A representative plot of the DCs shows the gating (A). In the DC population 3 subsets were identified: CD1a<sup>+</sup> dDCs (B), CD14<sup>+</sup> dDCs (C) and LCs (D) (n=10 independent experiments) showing each experiment and mean.

and 4% were LCs (Figure 1D). The percentage of each subset that migrated out of the explant was independent of the injected formulation (PBS vs OVA), but varied between the donors (Figure 1). Moreover, when skin was not injected at all, similar percentages of cells migrated from the skin explant (not shown). The total amount of cells that crawled out however, was consistently higher after injection of formulations that contained antigen than after PBS injection (data not shown).

### OVA uptake by skin-resident APCs is dose-dependent

To analyze the effect of the antigen dose on uptake by skin DCs, increasing doses of OVA were injected into the skin and migrated cells were analyzed. Antigen uptake by dDCs and LCs was evaluated after injecting various doses of OVA. Practically all CD14<sup>+</sup> dDCs had taken up detectable amounts of OVA, even when the low dose of 0.1 µg OVA was administered (Figure 2A). In contrast, approximately 60% of the CD1a<sup>+</sup> dDCs had taken up detectable OVA after 0.1 µg OVA was administered (Figure 2B). At higher doses, the majority (>95%) of CD1a<sup>+</sup> dDCs had taken up OVA. LCs showed a dose-dependent uptake of OVA in the investigated concentration range. Only after administration of the highest doses (50 or 25 µg) all LCs showed detectable amounts of OVA. 70% of LCs had taken up OVA after a 5 µg dose, with a dose-dependent decrease after administration of 1 µg and 0.1 µg OVA (Figure 2C).



**Figure 2.** Dose dependency of OVA uptake is DC subset specific. OVA uptake by LCs, CD1a<sup>+</sup> and CD14<sup>+</sup> dDCs was investigated by flow cytometry as function of the OVA dose after intradermal administration in abdominal skin by using a conventional hypodermic needle-and-syringe. OVA uptake was measured and displayed as percentage of cells that had taken up OVA within migrated CD14<sup>+</sup> dDCs (A), CD1a<sup>+</sup> dDCs (B) and LCs (C). The data represents mean  $\pm$  SEM ( $n \geq 3$  independent experiments) uptake was compared by one-way ANOVA with Tukey's multiple comparison test. \* =  $p < 0.05$ , \*\* =  $p < 0.01$ , \*\*\* =  $p < 0.001$ , \*\*\*\* =  $p < 0.0001$ .

### Depth-controlled microinjections via a hollow microneedle

Our previous results demonstrated that intradermal delivery of OVA results in uptake by dDCs and LCs. Because the different DC subsets reside at different depths in the skin, we hypothesized that OVA uptake may also depend on the depth of intradermal antigen application. To administer antigen at a specific

depth, conventional intradermal injection with needle and syringe cannot be used. Besides the difficulty to determine injection depth accurately, an injection volume of 10  $\mu\text{L}$  (equals 10  $\text{mm}^3$ ) is a too large volume for accurate injection in micrometer ranges. A digitally-controlled single hollow microneedle injection system allows for precise injections of 200 nL, enabling depth-controlled injections of a 50-fold smaller volume.

OVA uptake by skin-resident APCs is independent of injection depth

To study if injection depth affects the uptake of OVA in different subsets of DCs, OVA solution was injected at a depth of 50  $\mu\text{m}$  (viable epidermis), 500  $\mu\text{m}$  (superficial dermis) or 1000  $\mu\text{m}$  (deep dermis) with a hollow microneedle. This was compared to injections of 0.1  $\mu\text{g}$  OVA with a hypodermic needle, where the injection depth is not known and the injected volume is much bigger: 10  $\mu\text{L}$  instead of 0.2  $\mu\text{L}$ . Regardless of injection depth, 75% of all CD14<sup>+</sup> dDCs had taken up OVA after injection with hollow microneedles (Figure 3). Conventional intradermal injection resulted in a higher percentage of OVA positive (OVA<sup>+</sup>) cells. Uptake of OVA by CD1a<sup>+</sup> dDCs and LCs was slightly, albeit not significantly, lower at more shallow (50  $\mu\text{m}$ ) depth-controlled injections. Moreover, conventional injection resulted in slightly more OVA<sup>+</sup> cells in both subsets. Concomitantly, DC activation, as measured by CD86 and HLA-DR expression, was similar for all injection depths and conventional intradermal administration (Supplementary Figure 2). Altogether, injection depth did not influence antigen uptake or DC activation. Therefore, it was decided to perform all subsequent injections at only one depth: 500  $\mu\text{m}$ .

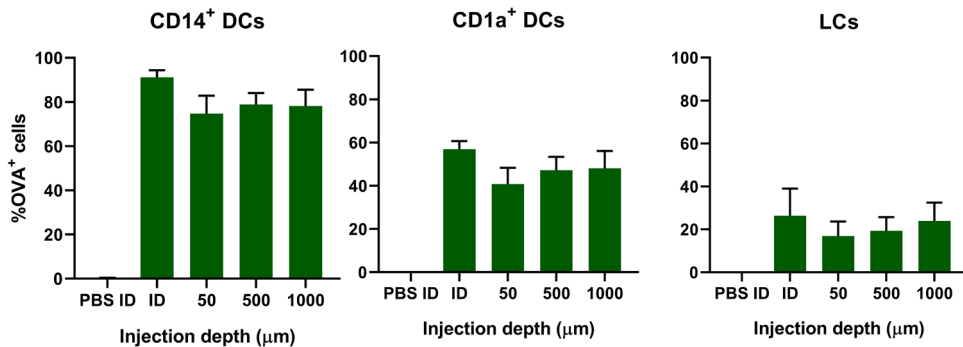


Figure 3. Uptake of OVA by skin-resident DCs is not dependent on injection depth. The uptake of OVA in CD14<sup>+</sup> dDCs, CD1a<sup>+</sup> dDCs or LCs as function of the depth in abdominal skin at which 0.1  $\mu\text{g}$  OVA was administered by using a single hollow microneedle or conventional hypodermic needle-and-syringe (ID). The data represents mean  $\pm$  SEM ( $n \geq 4$  independent experiments). No statistical differences were found between the different depths (one-way ANOVA).

### Bet v 1 is barely taken up by dermal APCs

To evaluate whether antigens with different properties are taken up in a similar fashion, we compared the uptake of model allergen OVA (42.7 kDa, pI 4.5) with the uptake of real allergen Bet v 1 (17.4 kD, pI 5.6) after administration of 0.2  $\mu$ L solution containing 0.1  $\mu$ g at 500  $\mu$ m depth. In contrast to OVA, Bet v 1 was barely taken up by any of the migrated dDCs and LCs (Figure 4). The mean fluorescence intensity (MFI) of the injected antigen in CD14<sup>+</sup> dDCs was slightly increased after microinjection of Bet v 1, but not in the other subsets (Supplementary Figure 3), while the MFI after OVA injection increased significantly. This illustrates that not all intradermally administered protein antigens, when free in solution, are taken up efficiently by APCs.

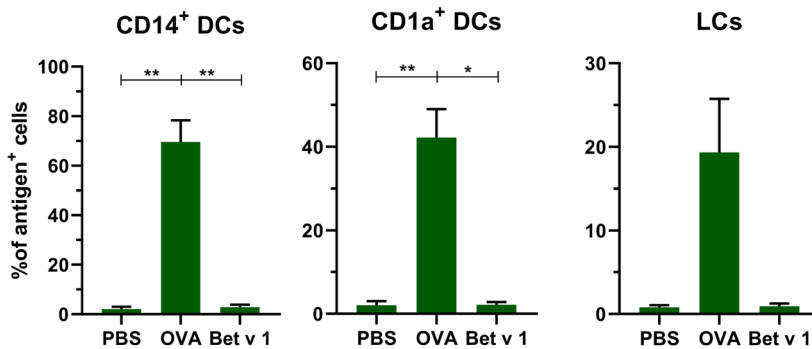


Figure 4. Not all antigens are taken up to the same extent by APCs. The uptake of fluorescent OVA or Bet v 1 in CD14<sup>+</sup> dDCs, CD1a<sup>+</sup> dDCs and LCs after microinjection at 500  $\mu$ m depth with 0.1  $\mu$ g of antigen in abdominal skin (mean  $\pm$  SEM;  $n \geq 6$  independent experiments). The percentage of cells that had taken up antigen was compared in a mixed-effects analysis with a Tukey's multiple comparison test. \* =  $p < 0.05$ , \*\* =  $p < 0.01$ .

### Both antigens were incorporated in fluorescently labeled cationic and anionic liposomes

Nanoparticles such as liposomes are generally considered to be efficiently taken up by APCs [55, 56]. Nanoparticle mediated uptake could overcome structural differences between antigens. Both OVA and Bet v 1 (size graph in supplementary Figure 4) were encapsulated in two types of liposomes: cationic and anionic liposomes (Table 2). Cationic liposomes with OVA encapsulated were larger than empty cationic liposomes, but the zeta potential was unchanged. Encapsulation of Bet v 1 in cationic liposomes did not affect the size, but decreased the zeta potential slightly. Anionic liposomes were slightly smaller after encapsulation of both antigens: 180 nm instead of 205 nm, while zeta potential remained negative. The encapsulation efficiency of OVA in cationic liposomes was higher (70%) than that of Bet v 1 (50%). Both OVA and Bet v 1 did not associate well with anionic liposomes (5% and 10%, respectively). The amount of antigen was

kept constant for intradermal injections, so the injected dose of lipids was higher for anionic liposomes than for cationic liposomes.

Table 2. Physicochemical properties of the liposomal formulations (mean values  $\pm$  SD,  $n = 3-5$ ).

Formulation	Z-ave (nm)	PDI	ZP (mV)	EE (%)
Cationic liposomes (DSPC:DOTAP:chol)	184.6 $\pm$ 5.6	0.102 $\pm$ 0.018	36.0 $\pm$ 14.5	-
Anionic liposomes (DSPC:DSPG:chol)	204.9 $\pm$ 13.6	0.128 $\pm$ 0.004	-44.4 $\pm$ 0.5	-
Cationic liposomes containing OVA	206.6 $\pm$ 25.1	0.140 $\pm$ 0.086	37.1 $\pm$ 3.9	70.9 $\pm$ 9.2
Anionic liposomes containing OVA	178.0 $\pm$ 12.1	0.035 $\pm$ 0.018	-38.8 $\pm$ 1.8	5.2 $\pm$ 0.7
Cationic liposomes containing Bet v 1	194.8 $\pm$ 14.9	0.129 $\pm$ 0.017	26.0 $\pm$ 7.4	49.4 $\pm$ 28.3
Anionic liposomes containing Bet v 1	180.6 $\pm$ 2.1	0.101 $\pm$ 0.023	-47.0 $\pm$ 18.8	10.6 $\pm$ 5.2

Abbreviations: Z-ave = hydrodynamic diameter, PDI = polydispersity index, ZP = zeta potential, EE = encapsulation efficiency, - = not applicable

Incorporation of Bet v 1, but not OVA, in liposomes increased uptake by dDCs

To evaluate the effect of liposome formulation on the uptake of OVA and Bet v 1, formulations were injected in *ex vivo* human skin with hollow microneedles at 500  $\mu$ m depth. After antigen encapsulation in liposomes an increase in uptake was observed for Bet v 1, but a decrease in uptake was observed for OVA (Figure

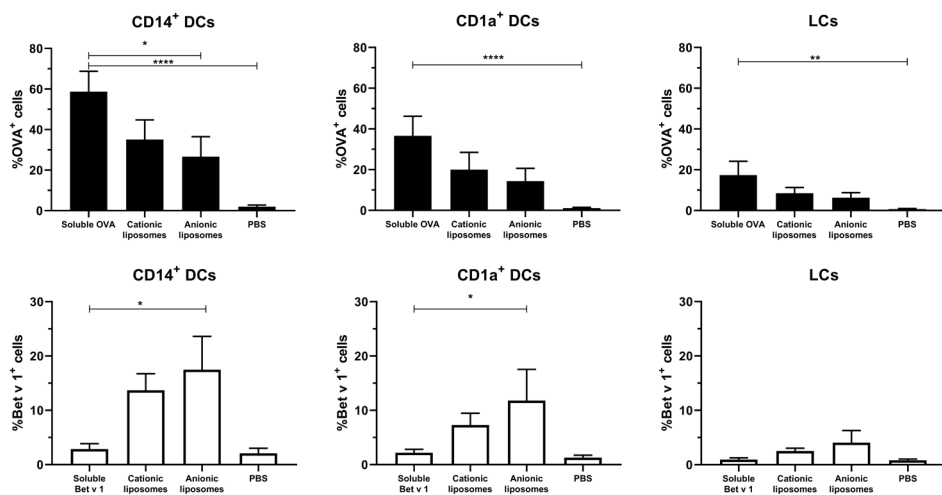


Figure 5. Effect of fluorescently labeled liposomes on antigen uptake. The uptake of fluorescent OVA (A-C) and Bet v 1 (D-F) in different dDCs or LCs was measured (mean  $\pm$  SEM;  $n \geq 6$  independent experiments). Antigens (0.1  $\mu$ g) were injected at 500  $\mu$ m depth in abdominal ( $n \geq 4$ ) or breast ( $n = 2$ ) skin explants. The percentage of dDCs that had taken up antigen was compared in a mixed-effects analysis and Dunnett post-test to compare uptake to free antigen. \* =  $p < 0.05$ , \*\* =  $p < 0.01$ , \*\*\* =  $p < 0.0001$ .

5). Encapsulation in cationic liposomes decreased OVA uptake in CD14<sup>+</sup> dDCs from 60% of all cells (for OVA solution) to 35%, whereas encapsulation of OVA in anionic liposomes decreased its uptake to 25% (Figure 5A). Similar trends were observed for CD1a<sup>+</sup> dDCs (Figure 5B) and LCs (Figure 5C).

For Bet v 1, an opposite effect was observed. Cationic liposomes increased the percentage of Bet v 1<sup>+</sup> CD14<sup>+</sup> dDCs to 14%, while anionic liposomes resulted in 17% antigen<sup>+</sup> CD14<sup>+</sup> dDCs (Figure 5D). Bet v 1<sup>+</sup> CD1a<sup>+</sup> dDCs percentage increased from 2% to 6% with cationic liposomes, and 12% with anionic liposomes (Figure 5E). A similar trend was observed in LCs, where the Bet v 1<sup>+</sup> % of cells was increased from 1% to 2.5% and 4%, respectively.

Antigen uptake of the same formulation varied substantially between skin donors. Therefore, to evaluate the effect of liposome formulation on antigen uptake, the uptake was normalized, i.e., uptake of free antigen was set as 100% uptake, and compared to uptake of antigen formulated in liposomes per donor (Figure 6). Cationic liposomes had little effect on OVA uptake: uptake in CD14<sup>+</sup> dDCs was reduced 0.8-fold, whereas uptake in CD1a<sup>+</sup> dDCs was unaffected and uptake in LCs was increased 1.4-fold (Figure 6). Anionic liposomes reduced uptake in CD14<sup>+</sup> dDCs and CD1a<sup>+</sup> dDCs by half, but increased uptake in LCs by 1.3-fold (Figure 6).

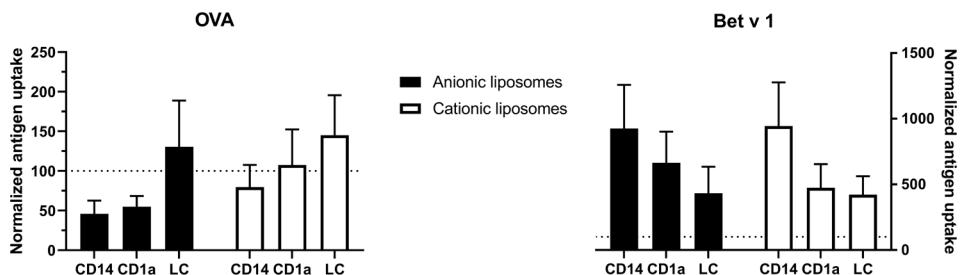


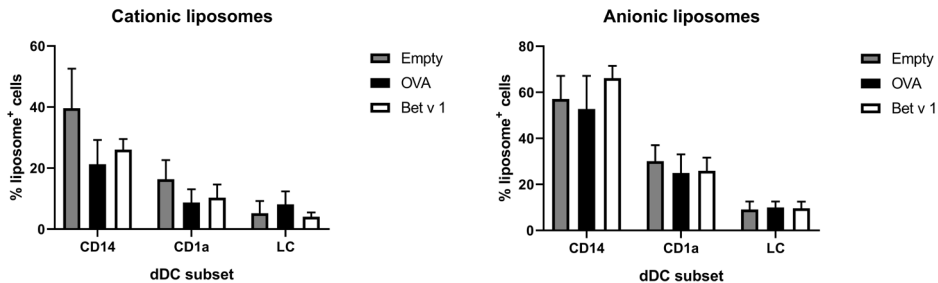
Figure 6. Normalized effect of fluorescently labeled liposomes on antigen uptake. The percentage of cells that had taken up free antigen, as displayed in figure 5, was set at 100% (dotted line in all graphs). Percentage of cells that had taken up antigen after formulation into liposomes was normalized to the uptake of free antigen. The normalized uptake of both OVA (left) and Bet v 1 (right) incorporated in cationic liposomes (white) and anionic liposomes (black) after administration at 500  $\mu$ m depth in abdominal ( $n \geq 4$ ) or breast ( $n = 2$ ) skin explants is shown (mean  $\pm$  SEM;  $n \geq 6$  independent experiments). Significant differences between dendritic cell subset and formulation were not found in a 2-way ANOVA for either antigen.

Cationic liposomes increased Bet v 1 uptake by CD14<sup>+</sup> dDCs over 9-fold, while increasing uptake in both CD1a<sup>+</sup> dDCs and LCs 4.5-fold (Figure 6). Anionic liposomes similarly increased Bet v 1 uptake in CD14<sup>+</sup> dDCs 9-fold, uptake in CD1a<sup>+</sup> dDCs 6.6-fold and uptake in LCs 4.3-fold (Figure 6). Uptake of Bet v 1 was increased drastically in especially CD14<sup>+</sup> and CD1a<sup>+</sup> dDCs by encapsulation



in liposomes. Contrarily, the uptake of OVA was reduced in these subsets after encapsulation in either cationic or anionic liposomes.

Anionic liposomes are taken up more efficiently than cationic liposomes. To determine whether the cells had also taken up liposomes, both liposome formulations contained a small amount of fluorescent lipid. Liposome uptake by the various subsets of DCs was measured. The loading of antigen did not affect the uptake of liposomes by the various subsets (Figure 7). Cationic liposomes were taken up less efficiently than anionic liposomes. Moreover, antigen formulated with cationic liposomes resulted in lower uptake of liposomes and antigen by the same cell than formulation in anionic liposomes (Supplementary Figure 5). Representative flow cytometry dot plots of each subset and each formulation are shown in supplementary figures 6 and 7.



**Figure 7.** Liposome uptake by skin resident APCs. The uptake of fluorescently labeled cationic liposomes (left) and anionic liposomes (right) in different skin APCs was measured (mean  $\pm$  SEM;  $n \geq 6$  independent experiments) after injection at 500  $\mu$ m depth in abdominal ( $n \geq 4$ ) or breast ( $n = 2$ ) skin explants. The percentage of dDCs or LCs that had taken up liposomes was compared in a 2-way ANOVA and showed no significant differences between OVA or Bet v 1 in each subset.

## Discussion

In this study we set out to obtain fundamental knowledge about the fate of antigen formulations after intradermal injections. This knowledge is important for rational development of formulations for intradermal administration. We evaluated migrated DCs after intradermal microinjections of two antigens, OVA and Bet v 1, in a human skin explant model. Both antigens were formulated in buffer and in 2 different liposome formulations. Injection depth did not affect antigen uptake, but we observed a significant difference in uptake between antigens. When formulated in buffer, Bet v 1 was barely taken up, whereas OVA was taken up very efficiently by APCs. By incorporating OVA, which was taken up efficiently on its own, lower percentages of APCs had taken up antigen encapsulated in liposomes. On the contrary, Bet v 1 (a relevant, but poorly internalized antigen) was delivered much more efficiently to the dDCs and LCs when encapsulated in liposomes upon injection.

Uptake of antigen upon conventional intradermal injection was dose-dependent. This illustrates the effect the antigen dose could have on the induced immunity. CD14<sup>+</sup> dDCs are poor at inducing CTLs, but induce a strong humoral response, while LCs are associated with strong CTL responses [27]. As these subsets reside at different depths of the skin, we performed injections at different depths to see if injection depth has any effect on uptake in different subsets.

Intradermal microinjections performed at 50, 500 or 1000  $\mu\text{m}$  did not show any significant difference in antigen fate, even though the different DC subsets reside in different parts of the skin. When compared to intradermal injection with a hypodermic needle, we saw less uptake after depth controlled microinjections. This may be as a result of injection accuracy: the DC-shMN-iSystem allows very precise injection volumes, whereas a conventional needle and syringe based system does not. Besides antigen uptake, DC activation was not affected by the injection depth either. This would also suggest that there will be no injection depth-dependent effect on the immune response. These findings are in corroboration with various vaccination studies in other species, even though skin composition and morphology differs between different species [57, 58]. Our results can explain why injection depth did not affect immune response in rats vaccinated with inactivated polio vaccine [48] and hairless guinea pigs vaccinated with OVA by others [59]. Moreover, a study on intradermal vaccination of human volunteers with rabies vaccine did not show an injection depth-dependent immune response either [60].

Unlike injection depth, the nature of the antigen had a huge impact on its uptake by DCs. The differences between OVA and Bet v 1 are numerous: OVA is glycosylated and phosphorylated [61], while Bet v 1 does not have such post-translational modifications, as it was produced in *E.coli*. OVA is 3 times heavier than Bet v 1 and has a lower isoelectric point, although both proteins are negatively charged at physiological pH. Especially the post-translational modifications can impact the uptake of a protein [62]: the mannose receptor has been shown to play a huge role in OVA uptake [63], while Bet v 1 uptake is reported to be caveolae-mediated [64].

OVA was taken up readily by the majority of CD14<sup>+</sup> dDCs. Bet v 1, however, was not taken up so easily: less than 5% of all dDCs and LCs had taken up Bet v 1. The difference in uptake between the two antigens was surprising, as a large number of publications have shown that both antigens are readily taken up in cell culture conditions by human monocytes [21, 36, 64-68]. This shows the limitations of cell culture experiments, where cells are continuously exposed to antigen. Thus, there is a translational gap between cell culture and injection in human skin. Our presented *ex vivo* human skin model is more representative for what would

happen after intradermal injection.

Two different liposomal formulations were prepared, both having sizes smaller than 500 nm, which has been reported to be ideal for uptake by DCs [45, 46]. Both formulations consisted for 50% of DSPC ( $T_m \sim 55^\circ\text{C}$ ) and contained 25% cholesterol. The only difference between the liposome formulations is the charged lipid, which allows for a direct comparison of surface charge effect. DOTAP-containing liposomes were cationic, and had a higher encapsulation efficiency with OVA and bet v 1 than anionic DSPG-containing liposomes. This is most likely related to electrostatic interactions, as both proteins have a negative charge at physiological pH. However, part of the antigens may be associated on the surface of liposomes rather than be encapsulated in the liposome core. This could result in quick desorption after injection, which we indeed seemed to observe: for cationic liposomes there were more OVA<sup>+</sup> than liposome<sup>+</sup> cells, which would otherwise not be possible. Free OVA was taken up in more cells (%-wise) than when encapsulated in liposomes, while the uptake of Bet v 1 was increased drastically when encapsulated in liposomes compared to free Bet v 1. This difference can probably be attributed to the uptake of soluble antigen. Encapsulated OVA uptake depends on the uptake of liposomes, which was not as effective as that of soluble OVA.

Formulation of antigens (= allergen in case of allergy) in liposomes could also contribute to more efficient allergen specific immunotherapy. By encapsulating Bet v 1 in the core, it is not available on the surface and cannot bind circulating antibodies and thereby reduce adverse events [2]. For this purpose anionic liposomes would be the preferential choice, as there seems to be more antigen dissociation from cationic liposomes. Moreover, by increasing the antigen uptake the effectivity can potentially be increased. The increased effectivity could lead to a reduction of therapy duration [1, 2, 69].

Intradermal vaccination has been reported to induce a stronger CD8<sup>+</sup> T-cell immune responses compared to conventional subcutaneous or intramuscular injections [70, 71]. Most nanoparticle-based approaches use cationic delivery systems, because cationic formulations are taken up to a higher extent than anionic ones *in vitro* [57], and we have seen the same with the formulations we have used (data not shown). Those studies however describe *in vitro* situations, where the extracellular matrix and presence of other cell types (e.g. keratinocytes) is not taken into consideration, which has been shown to reduce delivery of cargo from cationic nanoparticles before [72]. We demonstrated that anionic liposomes resulted in more efficient delivery of Bet v 1 to APCs than cationic liposomes in intact human skin. There does not seem to be a targeting effect to any of the subsets. The same uptake pattern (CD14<sup>+</sup> dDCs > CD1a<sup>+</sup> dDCs

> LCs) is observed with liposomes as for OVA in buffer.

Unexpectedly, anionic liposomes resulted in higher Bet v 1 uptake than cationic liposomes, which have been used successfully in a multitude of intradermal vaccine delivery studies [73-76]. We should however realize that, as antigen dose was kept constant, more liposomes were injected for anionic liposomes than cationic liposomes. Uptake by skin DCs is only the first step in the induction of antigen-specific immunity. The activation state, antigen processing and subsequent T-cell stimulation has not been investigated. Cationic liposomes typically induce an inflammatory Th1 and CD8<sup>+</sup> T-cell based immune response, which is desired for cancer immunotherapy. Contrarily, anionic liposomes are reported to induce regulatory responses, which could be beneficial for the treatment of allergy or auto-immune diseases [44, 55, 77-81]. So, both cationic and anionic liposomes are interesting adjuvant candidates that can increase the uptake of antigens which are not efficiently taken up by themselves.

## **Conclusion**

Intradermal injection depth of antigens in *ex vivo* human skin does not affect antigen uptake by migrated dDCs and LCs. However, a large difference in effect occurs based on the kind of antigen and the kind of formulation applied. OVA was readily taken up by dDCs and LCs in contrast to Bet v 1, a relevant antigen in allergy. After incorporation in cationic and especially anionic liposomes, Bet v 1 was taken up by more dDCs and LCs. We conclude that both antigen nature and formulation, but not injection depth determine the degree to which antigens are taken up by skin resident APCs. Moreover, we have shown that uptake of poorly internalized antigens can be significantly improved by encapsulating them in liposomes in an *ex vivo* human skin model.

## **Funding**

This work was supported by the Nederlandse Organisatie voor Wetenschappelijk Onderzoek (TKI-NCI, grant 731.014.207 and the Dutch Technology Foundation, grant 11259). Koen van der Maaden is the recipient of a H2020-MSCA-Intra European Fellowship-2018 (Grant Number 832455-Need2immune).

## References

1. Pfaar, O., I. Agache, F. de Blay, S. Bonini, A.M. Chaker, S.R. Durham, et al., *Perspectives in allergen immunotherapy: 2019 and beyond*. Allergy, 2019. **74 Suppl 108**: p. 3-25.
2. Klimek, L., R. Brehler, E. Hamelmann, M. Kopp, J. Ring, R. Treudler, et al., *Development of subcutaneous allergen immunotherapy (part 2): preventive aspects and innovations*. Allergo Journal International, 2019. **28**(4): p. 107-119.
3. Nicolas, J.F. and B. Guy, *Intradermal, epidermal and transcutaneous vaccination: from immunology to clinical practice*. Expert Rev Vaccines, 2008. **7**(8): p. 1201-1214.
4. Bonnotte, B., M. Gough, V. Phan, A. Ahmed, H. Chong, F. Martin, et al., *Intradermal injection, as opposed to subcutaneous injection, enhances immunogenicity and suppresses tumorigenicity of tumor cells*. Cancer Res, 2003. **63**(9): p. 2145-2149.
5. Belshe, R.B., F.K. Newman, J. Cannon, C. Duane, J. Treanor, C. Van Hoecke, et al., *Serum antibody responses after intradermal vaccination against influenza*. N Engl J Med, 2004. **351**(22): p. 2286-2294.
6. Kaushik, S., A.H. Hord, D.D. Denson, D.V. McAllister, S. Smitra, M.G. Allen, et al., *Lack of pain associated with microfabricated microneedles*. Anesth Analg, 2001. **92**(2): p. 502-504.
7. Warrell, M.J., K.G. Nicholson, D.A. Warrell, P. Suntharasamai, P. Chanthavanich, C. Viravan, et al., *Economical multiple-site intradermal immunisation with human diploid-cell-strain vaccine is effective for post-exposure rabies prophylaxis*. Lancet, 1985. **1**(8437): p. 1059-1062.
8. Quiambao, B.P., E.M. Dimaano, C. Ambas, R. Davis, A. Banzhoff and C. Malerczyk, *Reducing the cost of post-exposure rabies prophylaxis: efficacy of 0.1 ml PCEC rabies vaccine administered intradermally using the Thai Red Cross post-exposure regimen in patients severely exposed to laboratory-confirmed rabid animals*. Vaccine, 2005. **23**(14): p. 1709-1714.
9. Ambrozaitis, A., A. Laiskonis, L. Balciuniene, A. Banzhoff and C. Malerczyk, *Rabies post-exposure prophylaxis vaccination with purified chick embryo cell vaccine (PCECV) and purified Vero cell rabies vaccine (PVRV) in a four-site intradermal schedule (4-0-2-0-1-1): an immunogenic, cost-effective and practical regimen*. Vaccine, 2006. **24**(19): p. 4116-4121.
10. Propst, T., A. Propst, K. Lhotta, W. Vogel and P. Konig, *Reinforced intradermal hepatitis B vaccination in hemodialysis patients is superior in antibody response to intramuscular or subcutaneous vaccination*. Am J Kidney Dis, 1998. **32**(6): p. 1041-1045.
11. Micozkadioglu, H., A. Zumrutdal, D. Torun, S. Sezer, F.N. Ozdemir and M. Haberal, *Low dose intradermal vaccination is superior to high dose intramuscular vaccination for hepatitis B in unresponsive hemodialysis patients*. Ren Fail, 2007. **29**(3): p. 285-288.
12. Arakane, R., R. Annaka, A. Takahama, K. Ishida, M. Yoshiike, T. Nakayama, et al., *Superior immunogenicity profile of the new intradermal influenza vaccine compared to the standard subcutaneous vaccine in subjects 65 years and older: A randomized controlled phase III study*. Vaccine, 2015. **33**(48): p. 6650-6658.
13. Holland, D., R. Booy, F. De Looze, P. Eizenberg, J. McDonald, J. Karrasch, et al., *Intradermal influenza vaccine administered using a new microinjection system produces superior immunogenicity in elderly adults: a randomized controlled trial*. J Infect Dis, 2008. **198**(5): p. 650-658.
14. Cadorna-Carlos, J., E. Vidor and M.C. Bonnet, *Randomized controlled study of*

- fractional doses of inactivated poliovirus vaccine administered intradermally with a needle in the Philippines.* Int J Infect Dis, 2012. **16**(2): p. 110-116.
15. Troy, S.B., D. Kouivaskaia, J. Siik, E. Kochba, H. Beydoun, O. Mirochnitchenko, et al., *Comparison of the Immunogenicity of Various Booster Doses of Inactivated Polio Vaccine Delivered Intradermally Versus Intramuscularly to HIV-Infected Adults.* J Infect Dis, 2015. **211**(12): p. 1969-1976.
  16. Bal, S.M., Z. Ding, E. van Riet, W. Jiskoot and J.A. Bouwstra, *Advances in transcutaneous vaccine delivery: do all ways lead to Rome?* J Control Release, 2010. **148**(3): p. 266-282.
  17. van der Maaden, K., W. Jiskoot and J. Bouwstra, *Microneedle technologies for (trans) dermal drug and vaccine delivery.* J Control Release, 2012. **161**(2): p. 645-655.
  18. Banchereau, J. and R.M. Steinman, *Dendritic cells and the control of immunity.* Nature, 1998. **392**(6673): p. 245-52.
  19. Kapsenberg, M.L., *Dendritic-cell control of pathogen-driven T-cell polarization.* Nat Rev Immunol, 2003. **3**(12): p. 984-993.
  20. Mellman, I. and R.M. Steinman, *Dendritic cells: specialized and regulated antigen processing machines.* Cell, 2001. **106**(3): p. 255-268.
  21. Bond, E., W.C. Adams, A. Smed-Sørensen, K.J. Sandgren, L. Perbeck, A. Hofmann, et al., *Techniques for time-efficient isolation of human skin dendritic cell subsets and assessment of their antigen uptake capacity.* J Immunol Methods, 2009. **348**(1-2): p. 42-56.
  22. Noubade, R., S. Majri-Morrison and K.V. Tarbell, *Beyond cDC1: Emerging Roles of DC Crosstalk in Cancer Immunity.* Frontiers in Immunology, 2019. **10**: p. 1014.
  23. Levin, C., H. Perrin and B. Combadiere, *Tailored immunity by skin antigen-presenting cells.* Hum Vaccin Immunother, 2015. **11**(1): p. 27-36.
  24. Teunissen, M.B., M. Haniffa and M.P. Collin, *Insight into the immunobiology of human skin and functional specialization of skin dendritic cell subsets to innovate intradermal vaccination design.* Curr Top Microbiol Immunol, 2012. **351**: p. 25-76.
  25. Rowden, G., M.G. Lewis and A.K. Sullivan, *la antigen expression on human epidermal Langerhans cells.* Nature, 1977. **268**(5617): p. 247-248.
  26. Ratzinger, G., J. Baggers, M.A. de Cos, J. Yuan, T. Dao, J.L. Reagan, et al., *Mature human Langerhans cells derived from CD34+ hematopoietic progenitors stimulate greater cytolytic T lymphocyte activity in the absence of bioactive IL-12p70, by either single peptide presentation or cross-priming, than do dermal-interstitial or monocyte-derived dendritic cells.* J Immunol, 2004. **173**(4): p. 2780-2791.
  27. Klechevsky, E., R. Morita, M. Liu, Y. Cao, S. Coquery, L. Thompson-Snipes, et al., *Functional specializations of human epidermal Langerhans cells and CD14+ dermal dendritic cells.* Immunity, 2008. **29**(3): p. 497-510.
  28. Klechevsky, E., M. Liu, R. Morita, R. Banchereau, L. Thompson-Snipes, A.K. Palucka, et al., *Understanding human myeloid dendritic cell subsets for the rational design of novel vaccines.* Hum Immunol, 2009. **70**(5): p. 281-288.
  29. van der Aar, A.M., R. de Groot, M. Sanchez-Hernandez, E.W. Taanman, R.A. van Lier, M.B. Teunissen, et al., *Cutting edge: virus selectively primes human langerhans cells for CD70 expression promoting CD8+ T cell responses.* J Immunol, 2011. **187**(7): p. 3488-3492.
  30. van der Aar, A.M., R.M. Sylva-Steenland, J.D. Bos, M.L. Kapsenberg, E.C. de Jong and M.B. Teunissen, *Loss of TLR2, TLR4, and TLR5 on Langerhans cells abolishes bacterial recognition.* J Immunol, 2007. **178**(4): p. 1986-1990.

31. Takeuchi, J., E. Watari, E. Shinya, Y. Norose, M. Matsumoto, T. Seya, et al., *Down-regulation of Toll-like receptor expression in monocyte-derived Langerhans cell-like cells: implications of low-responsiveness to bacterial components in the epidermal Langerhans cells*. Biochem Biophys Res Commun, 2003. **306**(3): p. 674-679.
32. Flacher, V., M. Bouschbacher, E. Verronese, C. Massacrier, V. Sisrak, O. Berthier-Vergnes, et al., *Human Langerhans cells express a specific TLR profile and differentially respond to viruses and Gram-positive bacteria*. J Immunol, 2006. **177**(11): p. 7959-7967.
33. Steinman, R.M., D. Hawiger and M.C. Nussenzweig, *Tolerogenic Dendritic Cells*. Annual Review of Immunology, 2003. **21**(1): p. 685-711.
34. McGovern, N., A. Schlitzer, M. Gunawan, L. Jardine, A. Shin, E. Poyner, et al., *Human dermal CD14(+) cells are a transient population of monocyte-derived macrophages*. Immunity, 2014. **41**(3): p. 465-477.
35. Caux, C., C. Massacrier, B. Vanbervliet, B. Dubois, I. Durand, M. Cella, et al., *CD34+ hematopoietic progenitors from human cord blood differentiate along two independent dendritic cell pathways in response to granulocyte-macrophage colony-stimulating factor plus tumor necrosis factor alpha: II. Functional analysis*. Blood, 1997. **90**(4): p. 1458-1470.
36. Fehres, C.M., S.C. Bruijns, B.N. Sotthwes, H. Kalay, L. Schaffer, S.R. Head, et al., *Phenotypic and Functional Properties of Human Steady State CD14+ and CD1a+ Antigen Presenting Cells and Epidermal Langerhans Cells*. PLoS One, 2015. **10**(11).
37. Morelli, A.E., J.P. Rubin, G. Erdos, O.A. Tkacheva, A.R. Mathers, A.F. Zahorchak, et al., *CD4+ T cell responses elicited by different subsets of human skin migratory dendritic cells*. J Immunol, 2005. **175**(12): p. 7905-7915.
38. Zaba, L.C., J. Fuentes-Duculan, R.M. Steinman, J.G. Krueger and M.A. Lowes, *Normal human dermis contains distinct populations of CD11c+BDCA-1+ dendritic cells and CD163+FXIIIa+ macrophages*. J Clin Invest, 2007. **117**(9): p. 2517-2525.
39. Worbs, T., S.I. Hammerschmidt and R. Forster, *Dendritic cell migration in health and disease*. Nat Rev Immunol, 2017. **17**(1): p. 30-48.
40. Hansen, S. and C.-M. Lehr, *Nanoparticles for transcutaneous vaccination*. Microbial Biotechnology, 2012. **5**(2): p. 156-167.
41. Benne, N., J. van Duijn, J. Kuiper, W. Jiskoot and B. Slütter, *Orchestrating immune responses: How size, shape and rigidity affect the immunogenicity of particulate vaccines*. Journal of Controlled Release, 2016. **234**: p. 124-134.
42. Zolnik, B.S., Á. González-Fernández, N. Sadrieh and M.A. Dobrovolskaia, *Minireview: Nanoparticles and the Immune System*. Endocrinology, 2010. **151**(2): p. 458-465.
43. Kang, J.H., W.Y. Jang and Y.T. Ko, *The Effect of Surface Charges on the Cellular Uptake of Liposomes Investigated by Live Cell Imaging*. Pharm Res, 2017. **34**(4): p. 704-717.
44. Nakanishi, T., J. Kunisawa, A. Hayashi, Y. Tsutsumi, K. Kubo, S. Nakagawa, et al., *Positively charged liposome functions as an efficient immunoadjuvant in inducing cell-mediated immune response to soluble proteins*. J Control Release, 1999. **61**(1-2): p. 233-240.
45. Tran, K.K. and H. Shen, *The role of phagosomal pH on the size-dependent efficiency of cross-presentation by dendritic cells*. Biomaterials, 2009. **30**(7): p. 1356-1362.
46. Foged, C., B. Brodin, S. Frokjaer and A. Sundblad, *Particle size and surface charge affect particle uptake by human dendritic cells in an in vitro model*. International Journal of Pharmaceutics, 2005. **298**(2): p. 315-322.
47. *Amine-Reactive Probes*. 2013, Molecular Probes.



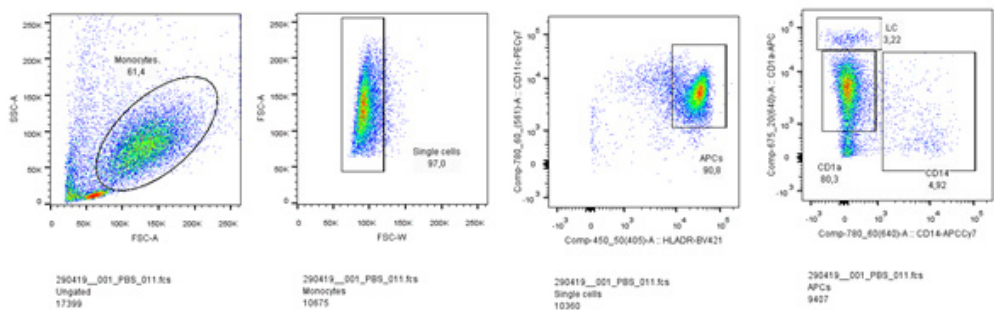
48. Schipper, P., K. van der Maaden, S. Romeijn, C. Oomens, G. Kersten, W. Jiskoot, et al., *Determination of Depth-Dependent Intradermal Immunogenicity of Adjuvanted Inactivated Polio Vaccine Delivered by Microinjections via Hollow Microneedles*. Pharmaceutical Research, 2016. **33**(9): p. 2269-2279.
49. van der Maaden, K., S. Trietsch, H. Kraan, E. Varypataki, S. Romeijn, R. Zwier, et al., *Novel Hollow Microneedle Technology for Depth-Controlled Microinjection-Mediated Dermal Vaccination: A Study with Polio Vaccine in Rats*. Pharmaceutical research, 2014. **31**: p. 1846–1854.
50. van der Maaden, K., J. Heuts, M. Camps, M. Pontier, A. Terwisscha van Scheltinga, W. Jiskoot, et al., *Hollow microneedle-mediated micro-injections of a liposomal HPV E743-63 synthetic long peptide vaccine for efficient induction of cytotoxic and T-helper responses*. J Control Release, 2018. **269**: p. 347-354.
51. Schipper, P., K. van der Maaden, V. Groeneveld, M. Ruigrok, S. Romeijn, S. Uleman, et al., *Diphtheria toxoid and N-trimethyl chitosan layer-by-layer coated pH-sensitive microneedles induce potent immune responses upon dermal vaccination in mice*. Journal of Controlled Release, 2017. **262**: p. 28-36.
52. Bakdash, G., L.P. Schneider, T.M. van Capel, M.L. Kapsenberg, M.B. Teunissen and E.C. de Jong, *Intradermal application of vitamin D3 increases migration of CD14+ dermal dendritic cells and promotes the development of Foxp3+ regulatory T cells*. Hum Vaccin Immunother, 2013. **9**(2): p. 250-258.
53. Schneider, L.P., A.J. Schoonderwoerd, M. Moutaftsi, R.F. Howard, S.G. Reed, E.C. de Jong, et al., *Intradermally administered TLR4 agonist GLA-SE enhances the capacity of human skin DCs to activate T cells and promotes emigration of Langerhans cells*. Vaccine, 2012. **30**(28): p. 4216-4224.
54. Varypataki, E.M., K. van der Maaden, J. Bouwstra, F. Ossendorp and W. Jiskoot, *Cationic liposomes loaded with a synthetic long peptide and poly(I:C): a defined adjuvanted vaccine for induction of antigen-specific T cell cytotoxicity*. The AAPS journal, 2014. **17**(1): p. 216-226.
55. Benne, N., J. van Duijn, F. Lozano Vigario, R.J.T. Lebourg, P. van Veelen, J. Kuiper, et al., *Anionic 1,2-distearoyl-sn-glycero-3-phosphoglycerol (DSPG) liposomes induce antigen-specific regulatory T cells and prevent atherosclerosis in mice*. J Control Release, 2018. **291**: p. 135-146.
56. Foged, C., C. Arigita, A. Sundblad, W. Jiskoot, G. Storm and S. Frokjaer, *Interaction of dendritic cells with antigen-containing liposomes: effect of bilayer composition*. Vaccine, 2004. **22**(15): p. 1903-1913.
57. Wei, J.C.J., G.A. Edwards, D.J. Martin, H. Huang, M.L. Crichton and M.A.F. Kendall, *Allometric scaling of skin thickness, elasticity, viscoelasticity to mass for micro-medical device translation: from mice, rats, rabbits, pigs to humans*. Scientific Reports, 2017. **7**(1).
58. Hirschberg, H.J.H.B., E. van Riet, D. Oosterhoff, J.A. Bouwstra and G.F.A. Kersten, *Animal models for cutaneous vaccine delivery*. European Journal of Pharmaceutical Sciences, 2015. **71**: p. 112-122.
59. Widera, G., J. Johnson, L. Kim, L. Libiran, K. Nyam, P.E. Daddona, et al., *Effect of delivery parameters on immunization to ovalbumin following intracutaneous administration by a coated microneedle array patch system*. Vaccine, 2006. **24**(10): p. 1653-1664.
60. Laurent, P.E., H. Bourhy, M. Fantino, P. Alchas and J.A. Mikszta, *Safety and efficacy of novel dermal and epidermal microneedle delivery systems for rabies vaccination*



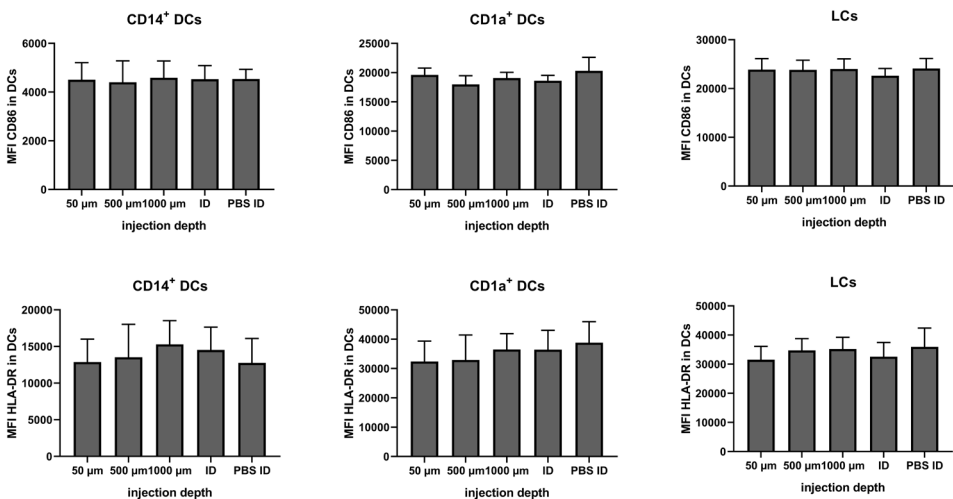
- in healthy adults*. Vaccine, 2010. **28**(36): p. 5850-5856.
61. Huntington, J.A. and P.E. Stein, *Structure and properties of ovalbumin*. Journal of Chromatography B: Biomedical Sciences and Applications, 2001. **756**(1): p. 189-198.
  62. Gordon, S., *Pattern Recognition Receptors: Doubling Up for the Innate Immune Response*. Cell, 2002. **111**(7): p. 927-930.
  63. Burgdorf, S., V. Lukacs-Kornek and C. Kurts, *The Mannose Receptor Mediates Uptake of Soluble but Not of Cell-Associated Antigen for Cross-Presentation*. The Journal of Immunology, 2006. **176**(11): p. 6770-6776.
  64. Smole, U., C. Radauer, N. Lenggler, M. Svoboda, N. Rigby, M. Bublin, et al., *The major birch pollen allergen Bet v 1 induces different responses in dendritic cells of birch pollen allergic and healthy individuals*. PLoS One, 2015. **10**(1).
  65. Roulias, A., U. Pichler, M. Hauser, M. Himly, H. Hofer, P. Lackner, et al., *Differences in the intrinsic immunogenicity and allergenicity of Bet v 1 and related food allergens revealed by site-directed mutagenesis*. Allergy, 2013. **69**(2): p. 208-215.
  66. Pichler, U., C. Asam, R. Weiss, A. Isakovic, M. Hauser, P. Briza, et al., *The Fold Variant BM4 Is Beneficial in a Therapeutic Bet v 1 Mouse Model*. BioMed Research International, 2013. **2013**: p. 1-5.
  67. Wallner, M., M. Hauser, M. Himly, N. Zaborsky, S. Mutschlechner, A. Harrer, et al., *Reshaping the Bet v 1 fold modulates TH polarization*. Journal of Allergy and Clinical Immunology, 2011. **127**(6): p. 1571-1578.
  68. Smole, U., N. Balazs, K. Hoffmann-Sommergruber, C. Radauer, C. Hafner, M. Wallner, et al., *Differential T-cell responses and allergen uptake after exposure of dendritic cells to the birch pollen allergens Bet v 1.0101, Bet v 1.0401 and Bet v 1.1001*. Immunobiology, 2010. **215**(11): p. 903-909.
  69. Gunawardana, N.C. and S.R. Durham, *New approaches to allergen immunotherapy*. Annals of Allergy, Asthma & Immunology, 2018: p. 293-305.
  70. Varypataki, E.M., N. Benne, J. Bouwstra, W. Jiskoot and F. Ossendorp, *Efficient Eradication of Established Tumors in Mice with Cationic Liposome-Based Synthetic Long-Peptide Vaccines*. Cancer Immunol Res, 2017. **5**(3): p. 222-233.
  71. Combadière, B., A. Vogt, B. Mahé, D. Costagliola, S. Hadam, O. Bonduelle, et al., *Preferential amplification of CD8 effector-T cells after transcutaneous application of an inactivated influenza vaccine: a randomized phase I trial*. PLoS One, 2010. **5**(5): p. e10818.
  72. van den Berg, J.H., K. Oosterhuis, W.E. Hennink, G. Storm, L.J. van der Aa, J.F.J. Engbersen, et al., *Shielding the cationic charge of nanoparticle-formulated dermal DNA vaccines is essential for antigen expression and immunogenicity*. Journal of Controlled Release, 2010. **141**(2): p. 234-240.
  73. van der Maaden, K., J. Heuts, M. Camps, M. Pontier, A. Terwisscha van Scheltinga, W. Jiskoot, et al., *Hollow microneedle-mediated micro-injections of a liposomal HPV E743–63 synthetic long peptide vaccine for efficient induction of cytotoxic and T-helper responses*. Journal of Controlled Release, 2018. **269**: p. 347-354.
  74. Du, G., M. Leone, S. Romeijn, G. Kersten, W. Jiskoot and J.A. Bouwstra, *Immunogenicity of diphtheria toxoid and poly(I:C) loaded cationic liposomes after hollow microneedle-mediated intradermal injection in mice*. International Journal of Pharmaceutics, 2018. **547**(1): p. 250-257.
  75. Du, G., R.M. Hathout, M. Nasr, M.R. Nejadnik, J. Tu, R.I. Koning, et al., *Intradermal vaccination with hollow microneedles: A comparative study of various protein antigen and adjuvant encapsulated nanoparticles*. Journal of Controlled Release,

2017. **266**: p. 109-118.
76. Varypataki, E.M., K. van der Maaden, J. Bouwstra, F. Ossendorp and W. Jiskoot, *Cationic Liposomes Loaded with a Synthetic Long Peptide and Poly(I:C): a Defined Adjuvanted Vaccine for Induction of Antigen-Specific T Cell Cytotoxicity*. The AAPS Journal, 2015. **17**(1): p. 216-226.
  77. Heuts, J., E.M. Varypataki, K. van der Maaden, S. Romeijn, J.W. Drijfhout, A.T. van Scheltinga, et al., *Cationic Liposomes: A Flexible Vaccine Delivery System for Physicochemically Diverse Antigenic Peptides*. Pharmaceutical Research, 2018. **35**(11).
  78. Christensen, D., K.S. Korsholm, I. Rosenkrands, T. Lindenstrøm, P. Andersen and E.M. Agger, *Cationic liposomes as vaccine adjuvants*. Expert Review of Vaccines, 2007. **6**(5): p. 785-796.
  79. Hamborg, M., F. Rose, L. Jorgensen, K. Bjorklund, H.B. Pedersen, D. Christensen, et al., *Elucidating the mechanisms of protein antigen adsorption to the CAF/NAF liposomal vaccine adjuvant systems: Effect of charge, fluidity and antigen-to-lipid ratio*. Biochimica et Biophysica Acta (BBA) - Biomembranes, 2014. **1838**(8): p. 2001-2010.
  80. Henriksen-Lacey, M., D. Christensen, V.W. Bramwell, T. Lindenstrom, E.M. Agger, P. Andersen, et al., *Liposomal cationic charge and antigen adsorption are important properties for the efficient deposition of antigen at the injection site and ability of the vaccine to induce a CMI response*. J Control Release, 2010. **145**(2): p. 102-108.
  81. Pujol-Autonell, I., A. Serracant-Prat, M. Cano-Sarabia, R.M. Ampudia, S. Rodriguez-Fernandez, A. Sanchez, et al., *Use of Autoantigen-Loaded Phosphatidylserine-Liposomes to Arrest Autoimmunity in Type 1 Diabetes*. PLOS ONE, 2015. **10**(6).

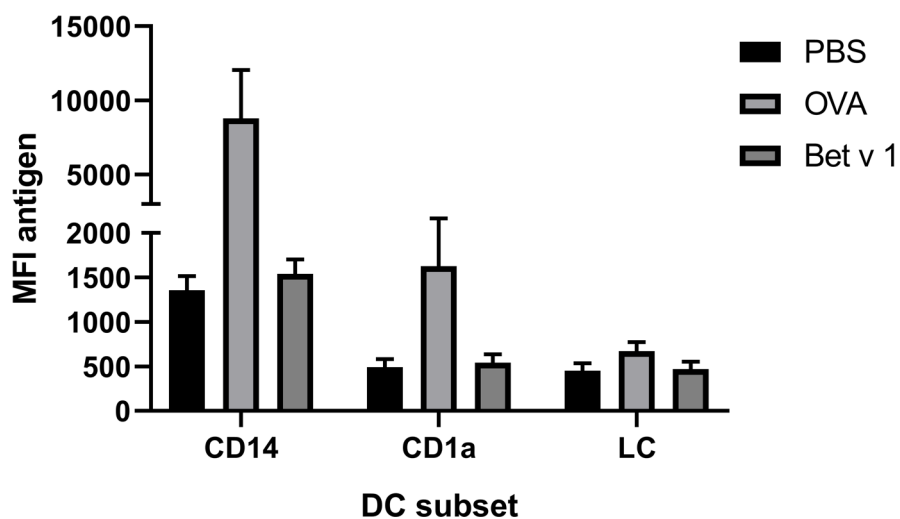
# Supplementary information



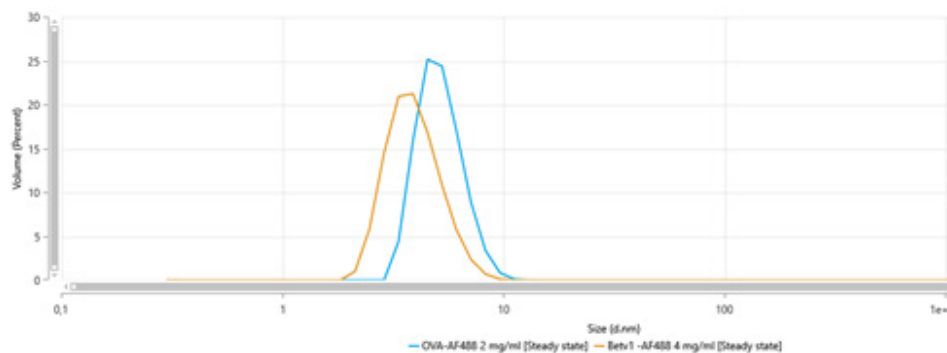
Supplementary Figure 1. Gating strategy for flow cytometry analysis to distinguish the different dermal dendritic cells and LCs. Langerhans cells (LCs), CD1a<sup>+</sup> dDCs and CD14<sup>+</sup> dDCs are distinct populations.



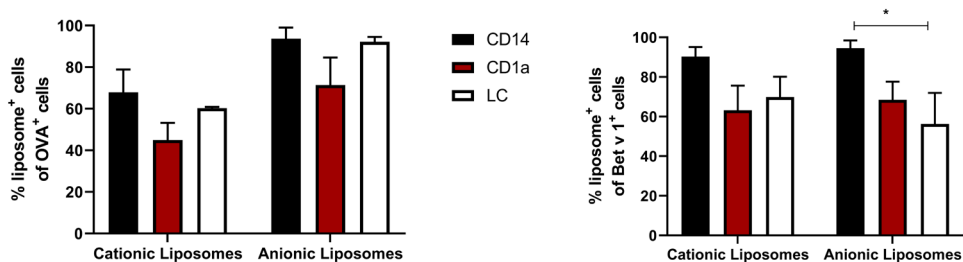
Supplementary Figure 2. Injection depth dependent DC activation. 0.1 µg OVA was injected at different depths in ex vivo human skin explants and compared to conventional intradermal injection. Activation markers CD86 (upper plots) and HLA-DR (lower plots) on different dDC subsets were measured (mean ± SEM (n = 3)).



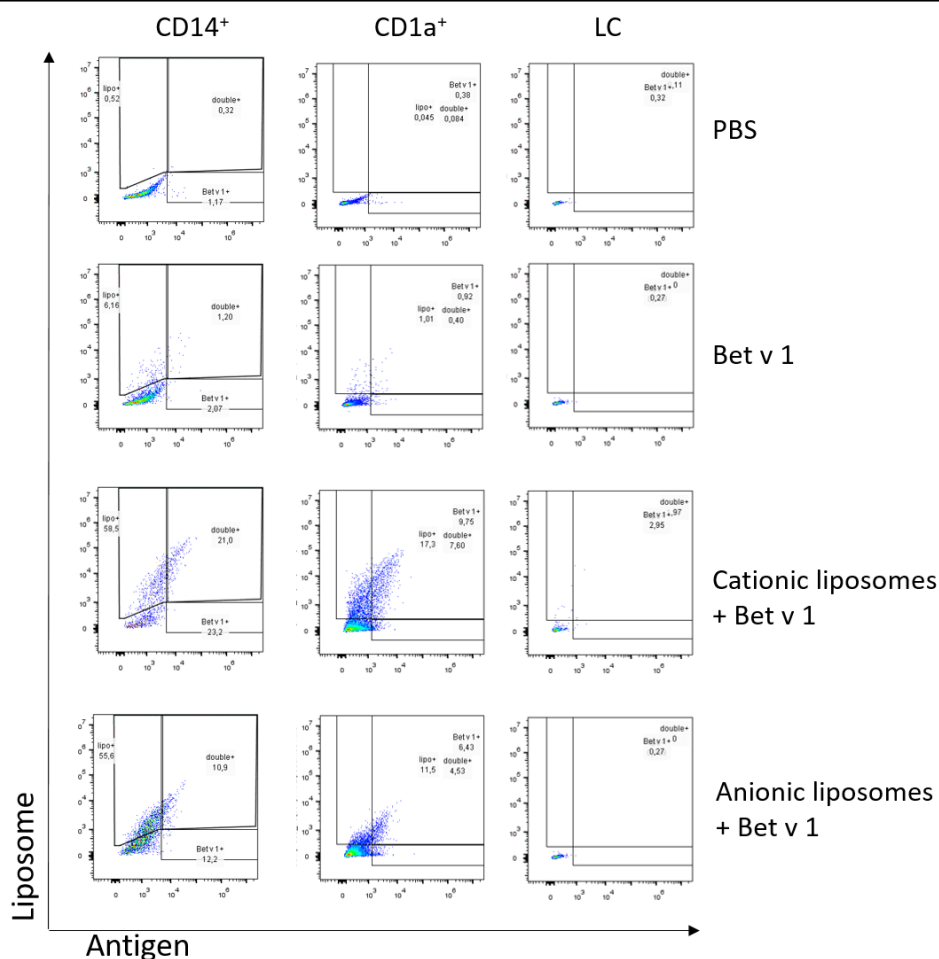
Supplementary Figure 3. Antigen uptake by DC subsets. Mean fluorescence intensity of the antigen-label in CD14 dDCs, CD1a dDCs and LCs.



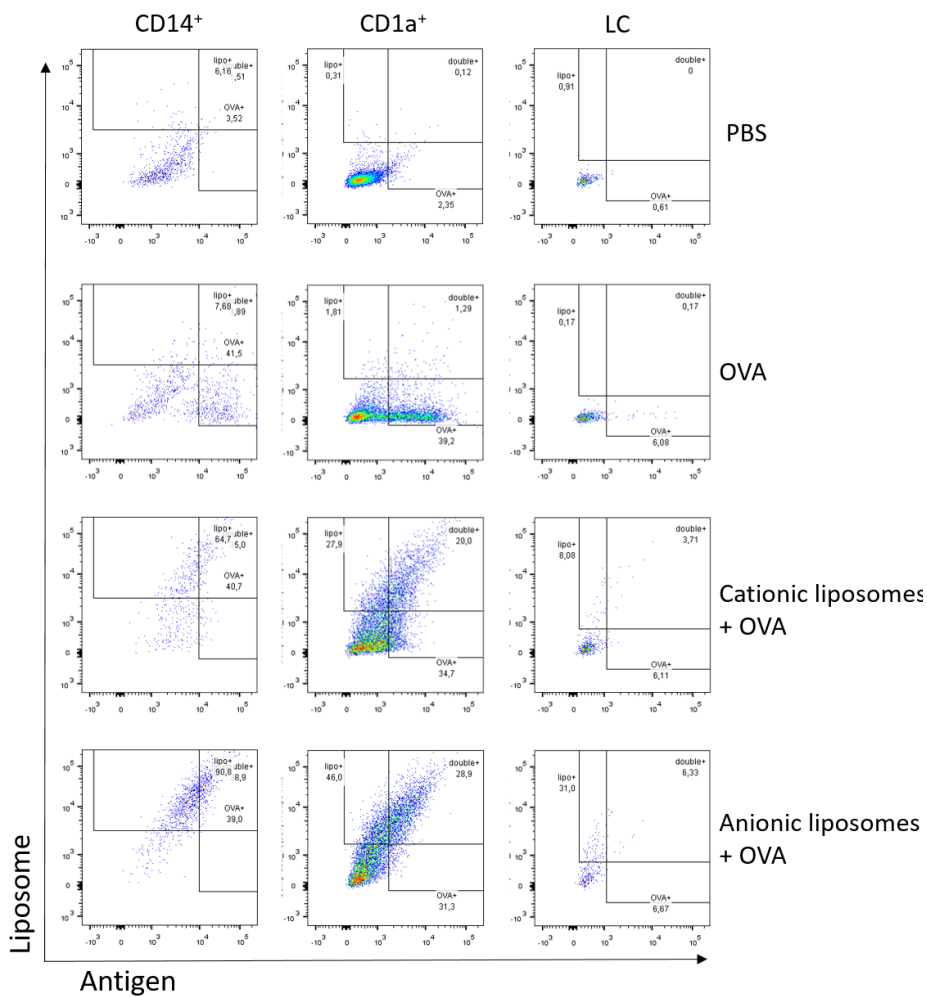
Supplementary Figure 4. Size distribution by volume of OVA-AF488 (blue) and Bet v 1-AF488 (orange) as measured by DLS.



Supplementary Figure 5. Co-uptake of antigen and liposomes. Liposome uptake by dDCs that had also taken up antigen after injection at 500  $\mu$ m depth in ex vivo human skin explants of OVA-containing formulations (left) and Bet v 1-containing formulations (right) 1 (mean  $\pm$  SEM;  $n \geq 4$ ). The difference between antigens was compared with a 2-way ANOVA. \* =  $p < 0.05$ .



Supplementary Figure 6. Representative flow cytometry plots of uptake of liposomes and Bet v 1 in different APC subsets after injection at 500  $\mu$ m depth in ex vivo skin explants.



Supplementary Figure 7. Representative flow cytometry plots of uptake of liposomes and OVA in different APC subsets after injection at 500  $\mu$ m depth in ex vivo skin explants.



## Chapter 5

# High-affinity antigen association to cationic liposomes via coiled coil-forming peptides induces a strong antigen-specific CD4<sup>+</sup> T-cell response

R.J.T. Leboux<sup>1</sup>, N. Benne<sup>1\*</sup>, W.L. van Os<sup>2</sup>, J. Bussmann<sup>1</sup>, A. Kros<sup>2</sup>, W. Jiskoot<sup>1</sup>, B.A. Slütter<sup>1#</sup>

<sup>1</sup> Division of BioTherapeutics, Leiden Academic Centre for Drug Research, Leiden University, Leiden, the Netherlands

<sup>2</sup> Div. of Supramolecular & Biomaterials Chemistry, Leiden Institute of Chemistry, Leiden University, Leiden, the Netherlands

\* Current address: Dep. Infectious Diseases and Immunology, Veterinary Science, Utrecht University, Utrecht, the Netherlands

# **Correspondence:** b.a.slutter@lacdr.leidenuniv.nl



## Abstract

Liposomes are widely investigated as vaccine delivery systems, but antigen loading efficiency can be low. Moreover, adsorbed antigen may rapidly desorb under physiological conditions. Encapsulation of antigens overcomes the latter problem but results in significant antigen loss during preparation and purification of the liposomes. Here, we propose an alternative attachment method, based on a complementary heterodimeric coiled coil peptide pair pepK and pepE.

PepK was conjugated to cholesterol (yielding CPK) and pepE was covalently linked to model antigen OVA323 (yielding pepE-OVA323). CPK was incorporated in the lipid bilayer of cationic liposomes (180 nm in size). Antigen was associated more efficiently to functionalized liposomes (Kd 166 nM) than to cationic liposomes (Kd not detectable). *In vivo* co-localization of antigen and liposomes was strongly increased upon CPK-functionalization (35% -> 80%). CPK-functionalized liposomes induced 5-fold stronger CD4<sup>+</sup> T-cell proliferation than non-functionalized liposomes *in vitro*. Both formulations were able to induce strong CD4<sup>+</sup> T-cell expansion in mice, but more IFN- $\gamma$  and IL-10 production was observed after immunization with functionalized liposomes.

In conclusion, antigen association via coiled coil peptide pair increased co-localization of antigen and liposomes, increased CD4<sup>+</sup> T-cell proliferation *in vitro* and induced a stronger CD4<sup>+</sup> T-cell response *in vivo*.

## Introduction

The latest generation of vaccines moves away from whole pathogens and instead uses pathogen-derived proteins or peptides (i.e., subunits) as antigen. Subunit based vaccines are safer than whole pathogen-based vaccines but require adjuvants because these antigens alone are poorly immunogenic. Liposomes, vesicles composed of a phospholipid bilayer, are a widely investigated adjuvant because of their versatility and proven success [1-4]. The lipid composition directs the physico-chemical properties of the liposomes, such as size, zeta potential, membrane fluidity and rigidity [1, 3]. These properties greatly influence their behavior upon injection and the immune response they may induce [3, 5-8]. Cationic liposomes have been used extensively as vaccine adjuvants. They are known to induce strong T-cell expansion and pro-inflammatory T helper (Th) 1-skewed immune response [9-14].

For a maximum adjuvant effect, the adjuvant and antigen need to be taken up by the same antigen presenting cell. This is most efficiently achieved when the antigen and the adjuvant are physically or chemically associated [15, 16]. Antigens can be associated with liposomes in various ways. For instance, hydrophilic molecules can be encapsulated in the aqueous core, whereas lipophilic molecules can be incorporated in the lipid bilayer. Although encapsulation usually ensures sustained co-localization, the encapsulation of an antigen in liposomes can be a challenging and costly process. Very few examples have shown 100% encapsulation efficiency, which oftentimes means that a large amount (up to 99%) of a valuable antigen is lost during liposome preparation and purification [10, 17-19]. Moreover, the encapsulation process has to be optimized for each new antigen, and might require a change of composition of the liposomes, thereby potentially sacrificing adjuvant potential [19, 20]. A more straightforward method is association of antigens on the outside of the liposome, which could be achieved by simple mixing of the antigen with preformed liposomes. Administration of antigens adsorbed to liposomes, via electrostatic interaction, has been shown to enhance the induced immune response compared to administration of plain antigen [12, 21]. However, the degree of association may vary between antigens and formulations [22-25]. Moreover, after administration of liposomes with electrostatically adsorbed antigen, the antigen may rapidly diffuse away from the liposomes because of competition between the antigen and extracellular biomolecules. Another disadvantage of electrostatic adsorption of antigens is that it requires an opposite charges on the liposome and antigen [26]. This complicates the development of a general vaccine adjuvant that can be used for a diverse range of antigens.

Here we provide an attractive alternative method of antigen association to functionalized liposomes based on designer coiled coil (CC) motifs. In this method,

complementary peptides interact resulting in the formation of noncovalent intermolecular helices [27, 28]. The formation of these helices is based on a complementary peptide pair, peptide E (pepE) and peptide K (pepK), which form a parallel heterodimer CC [27-29]. The pepE-pepK peptide pair has been shown to remain intact under physiological conditions. Moreover, liposomes functionalized with pepK have shown to be able to target cells functionalized with pepE *in vitro* and *in vivo* [30-34]. We investigated the possibility to use this CC forming peptide pair as an attachment platform for association of antigens to liposomes. We hypothesized that the binding affinity of these CC-forming peptides results in a higher association efficiency of the antigen and a more stable association *in vivo* as compared to electrostatic interaction. Here we report that indeed the association of antigen (pepE-OVA323) with pepK-functionalized liposomes remained intact under physiological conditions. Moreover, we show this way of association significantly enhanced the immunogenicity of the antigen, resulting in a stronger CD4<sup>+</sup> T-cell activation.

## Material and Methods

### Chemicals

Cholesterol (Chol), 1,2-distearoyl-sn-glycero-3-phosphocoline (DSPC) and 1,2-dioleoyl-3-trimethylammonium-propane (DOTAP) were purchased from Avanti Lipids (AL, USA). OVA323-339 and granulocyte-macrophage colony-stimulating factor (GM-CSF) were supplied by Bio-Connect (Huissen, Netherlands), 1,1'-Diocetadecyl-3,3',3'-Tetramethylindodicarbocyanine, 4-Chlorobenzenesulfonate (DiD), phorbol 12-myristate 13-acetate (PMA), ionomycin, Brefeldin A, Penicillin-Streptomycin (PenStrep), GlutaMAX<sup>™</sup> were supplied by Thermo Fisher (Bleiswijk, Netherlands). Iscove's Modified Dulbecco's Medium (IMDM) and Roswell Park Memorial Institute 1640 (RPMI) were supplied by Lonza (Basel, Switzerland). Fetal Calf Serum (FCS) was purchased from PAA Laboratories (Ontario, Canada). Dimethylformamide (DMF), piperidine, acetic anhydride, pyridine, trifluoroacetic acid (TFA) and acetonitrile (ACN) were purchased from Biosolve (Valkenswaard, Netherlands). N,N-diisopropylethylamine (DIPEA), and Ethyl cyanohydroxyiminoacetate (Oxyma) were obtained from Carl Roth (Karlsruhe, Germany). Dichloromethane (DCM) and diethyl ether were supplied by Honeywell (Landsmeer, Netherlands). Tentagel HL-RAM was obtained from Rapp Polymere (Tübingen, Germany). All amino acids were supplied by NovaBioChem (Darmstadt, Germany). Fmoc-NH-PEG<sub>4</sub>-COOH was purchased from Iris Biotech GmbH (Marktredwitz, Germany). All fluorescent antibodies for flow cytometry were purchased from eBioscience (MA, USA) and are displayed in supplementary table 1. CD4 and CD8 T-cell enrichment kit was purchased from Miltenyi (Leiden, Netherlands). All other chemicals were purchased from Sigma Aldrich (Zwijndrecht, Netherlands).

## Mouse experiments

C57Bl/6, OT-I and OT-II transgenic mice on a C57Bl/6 background were purchased from Jackson Laboratory (CA, USA), bred in-house under standard laboratory conditions, and provided with food and water *ad libitum*. All animal work was performed in compliance with the Dutch government guidelines and the Directive 2010/63/EU of the European Parliament. Experiments were approved by the Ethics Committee for Animal Experiments of Leiden University.

## Peptide synthesis

Peptides were synthesized on a microwave-assisted, automated peptide synthesizer (Liberty Blue). An overview of all the synthesized compounds can be found in Supplementary table 2. Synthesis was performed at a 0.1 mmol scale on the solid-phase Tentagel HL-RAM resin with a loading of 0.39 mmol/g. Fmoc-deprotection was achieved with 20% piperidine in DMF at 90 °C for 60 s. Amide coupling was achieved using 5 equiv. of Fmoc-protected amino acid with 5 equiv. of DIC as activator and 5 equiv. of Oxyma as the activator base heated at 95 °C for 240 s. Upon completion of synthesis, peptides were acetylated with an excess of acetic anhydride and pyridine in DMF. Cholesterol-coupled pepK (CPK) was synthesized as described elsewhere [35]. In short, resin-bound peptides were PEGylated with 2.5 equiv. of Fmoc-NH-PEG<sub>4</sub>-COOH in the presence of 5 equiv. of DIPEA and 2.5 equiv. of HATU for 4 hours at room temperature. Subsequently, the protecting Fmoc was removed with 20% piperidine in DMF and the reactive amine was coupled to 1.05 equiv. amino-cholestene hemisuccinate in the presence of 5 equiv. DIPEA and 2.5 equiv. HATU for 4 hours at room temperature, before cleavage from the resin was performed by using a mixture of TFA:TIPS:water, 95:2.5:2.5. The peptide was precipitated in ice-cold diethyl ether; the precipitate was subsequently collected by centrifugation and dissolved in a water and ACN mixture. The ACN was removed using a rotary evaporator and water was removed by lyophilization, resulting in crude peptide as an off-white powder.

All peptides and conjugates were purified by reversed-phase HPLC (RP-HPLC) on a Kinetic Evo C18 column with a Shimadzu system comprising two LC-8A pumps and an SPD-10AVP UV-Vis detector. Peptides were purified using a gradient of 20-80% B, (where B is ACN containing 1% TFA, and A is water with 1% TFA) over 20 minutes with a flow rate of 12 mL/min. The collected fractions were analyzed on a LC-MS system (Thermo Scientific TSQ quantum access MAX mass detector connected to a Ultimate 3000 liquid chromatography system fitted with a 50 × 4.6 mm Phenomenex Gemini 3 µm C18 column) and those deemed to be pure were pooled. Organic solvent was removed under reduced pressure (150 mbar) before lyophilization to obtain a dry purified peptide powder.

AlexaFluor488-labeled pepE-OVA323 was synthesized starting from pepE-OVA323 with an additional glycine and cysteine at the C-terminus. The peptide

was incubated with 1.1 equiv. AlexaFluor 488 C<sub>5</sub> maleimide (Thermo Fisher, Netherlands) in 100 mM HEPES buffer (pH 7.4) in the dark at room temperature. After 2 hours, free dye was removed by dialysis under constant stirring in a 2k MWCO Slide-A-Lyzer™ (Thermo Fisher, Netherlands) at 4 degrees to Milli-Q (18,2 MOhm/cm) overnight. Finally, the pure peptide was obtained by centrifugation at 1,000 x g for 30 minutes.

### Liposome preparation and characterization

Liposomes were prepared by the dehydration-rehydration method as described elsewhere [17]. In brief: 15 µmol total lipids with or without CPK were dissolved in 1:2 methanol:chloroform in the desired ratio (2:1:1 DSPC:DOTAP:cholesterol molar ratio with 1 mol% CPK). In case of fluorescent liposomes, 0.1 mol% of total lipid DiD was added in this step. Subsequently, the organic solvent was evaporated at 150 mbar and 50 °C in a rotary evaporator, yielding a lipid film. This film was hydrated in the presence of glass beads with a 10 mM HEPES, 280 mM sucrose, pH 7.4 (H/S buffer), with antigen in the case of encapsulation, frozen in liquid nitrogen and lyophilized overnight. The resulting lipid cake was rehydrated with Milli-Q to a final volume of 1 mL (resulting in a 15 mM lipid suspension) and homogenized with a LIPEX extruder (Evonik, Canada) by repeated passage over stacked filters of 400 nm and 200 nm (Nuclepore Track-Etch membrane from Whatman, Netherlands).

Hydrodynamic diameter and polydispersity were measured by dynamic light scattering (DLS) using a Zetasizer Nano ZS (Malvern Instruments Ltd., Worcestershire, UK). The zeta potential was measured using laser Doppler electrophoresis on the same machine with a zeta dip cell (Malvern Instruments Ltd.). Each sample was diluted 100-fold in 10 mM HEPES buffer (pH 7.4) before measurement.

### Isothermal titration calorimetry

Isothermal titration calorimetry (ITC) was performed with a MicroCal PEAQ-ITC Automated machine (Malvern Instruments Ltd., Worcestershire, UK). Free pepK or liposomes containing CPK (300 µl, 50 µM pepK or CPK in H/S buffer) were used in the receptor compartment. 3 µl of pepE, pepE-OVA323 or pepE-OVA257 (500 µM) was added every 180 seconds.

For data analysis, the first injection was removed from the raw data. Subsequently a One-sided fitting was performed, which was optimized by 100 iterations until the values for binding constant, stoichiometry and dH did not change anymore.

### Far-UV circular dichroism spectroscopy

Far-UV circular dichroism (CD) measurements were performed on a Jasco J815 CD spectrometer equipped with a Jasco PTC 123 Peltier temperature controller

in a 1 mm quartz cuvette. Far-UV CD spectra between 190–260 nm were also collected at T = 25°C. The molar ellipticity  $[\theta]$  was calculated from the measured ellipticity  $\theta$ , the path length  $l$  in centimeter, the molar monomer concentration  $cM$ , and the number of amino acids per peptide  $N$  as:

$$[\theta] = \frac{100 \cdot \theta}{l \cdot ((cM1 \cdot N1) + (cM2 \cdot N2))} \quad (\text{Equation 1})$$

as described elsewhere [36].

### Association efficiency

To determine the association efficiency of pepE-OVA323 to liposomes, liposomes with and without CPK (800 µg lipids/mL) were incubated with antigen (30 µg/mL) for 30 minutes. Subsequently, unbound antigen was separated from liposomes with a centrifuge membrane concentrator (Vivaspin2, 300.000 MWCO, Sartorius) by spinning down for 10 minutes at 500 x g. The unbound fraction (flow through) was measured by RP-UPLC (Waters ACQUITY UPLC, Waters, MA, USA).

Liposomes with and without CPK (800 µg lipids/mL) were mixed with pepE-OVA257 (30 µg/mL) and dialyzed in a Float-A-Lyzer® G2 (Spectrum labs, CA, United States) of 1 mL and MWCO of 100 kD for 5 days against 10 mM HEPES buffer pH 7.4. Remaining antigen in the dialysis membrane was measured by RP-UPLC (Waters ACQUITY UPLC, Waters, MA, USA).

### Ex vivo T-cell stimulation

Bone marrow-derived dendritic cells (BMDCs) were prepared as described elsewhere [37]. In short, bone marrow was isolated from murine tibia and femurs of C57BL/6 mice. Bone marrow cells were stimulated for 10 days with 20 ng/mL GM-CSF in complete IMDM (cIMDM, IMDM supplemented with 100 U/mL PenStrep, 2 mM glutaMAX and 8% FCS). After 10 days, the BMDCs (50,000 cells per well) were exposed to the different formulations for 4 hours. Subsequently the BMDCs were washed twice with cIMDM and incubated with either 100,000 CD4<sup>+</sup> T-cells derived from OT-II mice or 100,000 CD8<sup>+</sup> T-cells derived from OT-I mice, which were purified according to manufacturer's protocol [38], for 72 hours in complete RPMI (cRPMI, supplemented with 100 U/mL PenStrep, 2 mM glutaMAX, 50 µM β-mercaptoethanol and 10% FCS). After 72 hours, the cell suspension was harvested and prepared for flow cytometry.

### Flow cytometry measurements and analysis

For flow cytometry measurements, the cell suspension was washed with FACS buffer (PBS with 1% FCS and 2 mM EDTA). Subsequently, the suspension was stained for 30 minutes in the dark at 4 °C with FACS buffer containing fluorescent antibodies against the surface markers of interest (an overview of the used antibodies is found in Supplementary table 1). After the staining, the

cells were washed with PBS and measured in the flow cytometer (CytoFLEX S, BeckmanCoulter, CA, US). For intracellular markers, the cells were subsequently fixed and stained according to manufacturer's protocol with the Transcription Factor Staining Buffer Set (eBioscience, catalogue number 00-5523-00) for transcription factors, or the Intracellular Fixation & Permeabilization Buffer Set (eBioscience, catalogue number 88-8824-00). Before measurement, the cells were resuspended in PBS. All flow cytometry data were analyzed using FlowJo vX.

### Peptide uptake in BMDCs

BMDCs were prepared as described above and 50,000 BMDCs per well were plated in a flat bottomed 96 wells plate. Subsequently, different liposome formulations containing DiD (ex/em wavelength: 644/665 nm) were added to the culture medium of these BMDCs. After 4 hours, cell medium was refreshed twice to remove any unbound formulation. Subsequently, cells were prepared for flow cytometry.

### Biodistribution studies in zebrafish embryos

Zebrafish (*Danio rerio*, strain AB/TL or Tg(kdrl:RFP-CAAX)s916 [39]) were maintained and handled according to the guidelines from the Zebrafish Model Organism Database (<http://zfin.org>) and in compliance with the directives of the local animal welfare committee of Leiden University. Fertilization was performed by natural spawning at the beginning of the light period, and eggs were raised at 28.5 °C in egg water (60 g/mL Instant Ocean sea salts). Prior to injection, zebrafish embryos were embedded and anesthetized in 0.4% agarose containing 0.01% tricaine. Liposomal formulations (containing 5 mM lipids and/or 200 µg/ml pepE-OVA323-AF488) were injected with 1 nL volume in the duct of Cuvier, at 2.5 days post fertilization (dpf) as described previously [40]. For each treatment, two independently formulated liposome preparations were imaged using confocal microscopy. Embryos were randomly picked from a dish of 10-20 successfully injected embryos (exclusion criteria were: no backward translocation of erythrocytes after injection and/or damage to the yolk ball).

Confocal z-stacks were captured on a Leica TCS SPE confocal microscope, using a 10× air objective (HCX PL FLUOTAR) or a 40× water-immersion objective (HCX APO L). For whole-embryo views, 3–5 overlapping z-stacks were captured to cover the complete embryo. Laser intensity, gain, and offset settings were identical between stacks and sessions. Images were processed using the Fiji distribution of ImageJ [41, 42]. The greyscale threshold for both liposomal and peptide signal was determined and set identical for an entire experiment. All pixels with intensity above the threshold were set at a maximum value of 255, whereas negative pixels were set at 0. Subsequently, the “3D-multi coloc” plugin



of 3d Image suite was used to determine co-localization [43].

#### **Adoptive transfer and vaccination study**

C57Bl/6 mice (10-15 week-old females) were randomized into groups. On day 0, all mice received 500,000 CD4<sup>+</sup> T-cells, that were purified from sex-matched OT-II transgenic mice with a CD4<sup>+</sup> T-cell enrichment kit (Miltenyi, Netherlands) according to manufacturer's protocol [38], via the tail vein. On day 1, mice were immunized subcutaneously with a single injection of formulation in a total volume of 200  $\mu$ l in H/S buffer. Seven days after immunization, mice were sacrificed and blood, spleen and axillary and brachial lymph nodes (LNs) were removed. Organs were processed and measured by flow cytometry.

Splenocytes (10<sup>6</sup> per well) of each mouse were stimulated in cRPMI for 1 hour with either medium, pepE-OVA323, or PMA and ionomycin, after which brefeldin A was added and the cells were incubated for another 5 hours and subsequently prepared for flow cytometry.

#### **Statistical analysis**

Data was processed and analyzed in GraphPad v8 (Prism) for Windows. Statistical analysis was performed with the same program and the method of analysis is indicated in the figure legends.

### **Results**

#### **Peptide and liposome characterization**

The MHC-II (I-A<sup>b</sup>) restricted epitope of ovalbumin (OVA323-339, ISQAVHAAHAEINEAGR) was synthesized at the C-terminus of pepE resulting in the pepE-OVA323 conjugate. The same was done for the MHC-I (H2-K<sup>b</sup>) restricted epitope (OVA257-264, SIINFEKL), resulting in pepE-OVA257. All peptides were of >95% purity according to RP-HPLC (Supplementary figures 1-4). Subsequently, positively charged (DOTAP-containing) liposomes were prepared with and without CPK to assess the effect of its incorporation on the physico-chemical properties of liposomes composed of DOTAP, DSPC and cholesterol. The size (179 vs 177 nm for liposomes without and with CPK respectively), polydispersity index (PDI, 0.073 vs 0.071 for liposomes without and with CPK respectively) and zeta potential (between 48 vs 45 mV for liposomes without and with CPK respectively) of liposomes were unaffected by the addition of 1 mol% CPK (Table 1).



*Table 1. Overview of the particle size (z-average), polydispersity index (PDI) and zeta potential of non-functionalized liposomes (DOTAP:DSPC:cholesterol) and CPK-functionalized liposomes before and after mixing with pepE-OVA323 or pepE-OVA257. Moreover, the dissociation constant (Kd) as measured by ITC is shown. \* = significantly different than the liposomes without antigen. # = beyond detection limit. Values represent average values  $\pm$  SD ( $n \geq 2$ ). N.a. = not applicable.*

Liposome formulation	Z-average (nm)	PDI	Zeta potential (mV)	Kd (nM)	Association efficiency (%)
Non-functionalized liposomes	179.3 $\pm$ 13.8	0.073 $\pm$ 0.039	48.1 $\pm$ 3.3	n.a.	n.a.
CPK-functionalized liposomes	176.7 $\pm$ 14.4	0.071 $\pm$ 0.047	44.9 $\pm$ 6.2	n.a.	n.a.
Non-functionalized liposomes + pepE-OVA323	188.6 $\pm$ 6.6	0.116 $\pm$ 0.028 *	35.0 $\pm$ 5.2 *	> 10 <sup>5</sup> #	78.1 $\pm$ 4.0
CPK-functionalized liposomes + pepE-OVA323	185.8 $\pm$ 4.2	0.080 $\pm$ 0.014	28.6 $\pm$ 7.0 *	166 $\pm$ 68	>95% #
Non-functionalized liposomes + pepE-OVA257	182.5 $\pm$ 2.3	0.092 $\pm$ 0.004	45.0 $\pm$ 2.4	> 10 <sup>5</sup> #	1.69 $\pm$ 2.4
CPK-functionalized liposomes + pepE-OVA257	184.6 $\pm$ 2.5	0.089 $\pm$ 0.004	38.8 $\pm$ 1.3 *	392 $\pm$ 264	47.5 $\pm$ 7.1

To confirm the presence of CPK in the functionalized liposomes, and the ability of CPK to interact with pepE-conjugates, we performed far-UV CD spectroscopy and ITC, respectively. Far-UV CD spectra showed minima at 222 and 208 nm in CPK-functionalized liposomes which indicates presence of  $\alpha$ -helices. Upon mixing with pepE, the peak at 208 nm and overall signal increased, pointing to interaction and the formation of a CC structure (Supplementary figure 5). ITC was used to determine the binding energy and dissociation constant (Kd) between peptide and liposome. No binding energy was measured in non-functionalized liposomes (Figure 1), whereas the binding energy of pepE and pepE-conjugates titrated into a suspension of CPK-functionalized liposomes decreased slowly during the first 6 injections after which a plateau was reached (Figure 1). Kd values were determined for both pepE-conjugates onto CPK-functionalized liposomes and all were in the order of 10<sup>-7</sup> M, but could not be measured with non-functionalized liposomes. Moreover, antigen was mixed with both formulations and unbound antigen was removed by centrifugal filtration or dialysis to measure association efficiency. We observed an association efficiency of 78% after mixing pepE-OVA323 with non-functionalized liposomes, which substantially increased after mixing with functionalized liposomes (Table 1), where the unbound antigen concentration was below the limit of detection. Thus, CC interaction provided a simple and highly efficient method to associate antigen to liposomes, which appeared stronger than adsorption to non-functionalized liposomes.

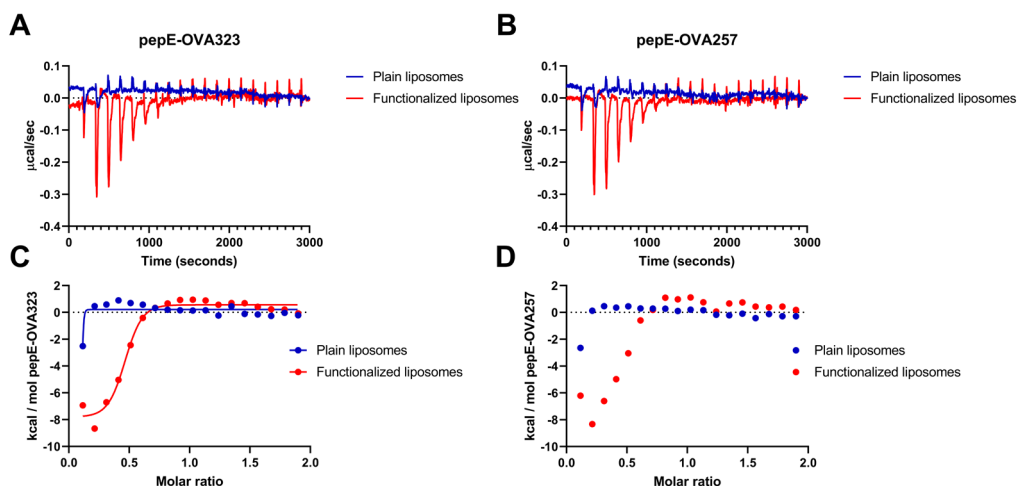
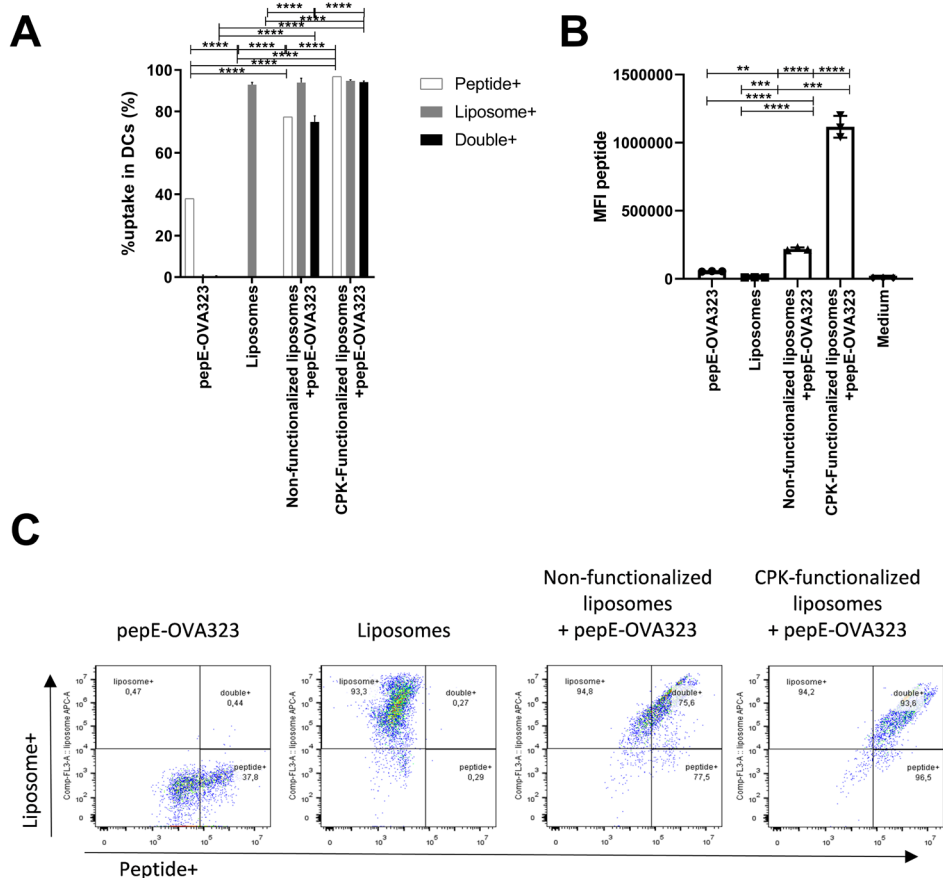


Figure 1. Antigen binding to liposomes. Buffer corrected heat plots of isothermal titration calorimetry measurements in which non-functionalized and functionalized liposomes were titrated with pepE-OVA323 (A) and pepE-OVA257 (B). The calculated energy per mol of pepE-OVA323 (C) or pepE-OVA257 (D) was used to derive the dissociation constant  $K_d$  (B).

## Peptide uptake in BMDCs

We assessed whether the increased affinity provided by CC-mediated association would result in an increased antigen and liposome uptake by BMDCs. Fluorescently labeled pepE-OVA323 and the DiD-labeled fluorescent liposomes were used to facilitate cell uptake studies using flow cytometry. The incorporation of a small amount of fluorescent dye resulted in a slightly smaller size (160 vs 180 nm) of the liposomes (Supplementary Figure 6), but . BMDCs were incubated for 4 hours with fluorescent formulations containing pepE-OVA323. Over 90% of all BMDCs had taken up liposomes, irrespective of CPK-functionalization or presence of antigen (Figure 2). However, dendritic cells had taken up antigen in presence of CPK-functionalized liposomes. Uptake of peptides in the absence of liposomes was limited (39%). Association with non-functionalized liposomes increased the uptake from 40% to 75%, but was this increased to >99% after association to CPK-functionalized liposomes (Figure 2A). The fluorescent signal in cells (Mean Fluorescence Intensity, MFI) after exposure to pepE-OVA323 was significantly increased with functionalized liposomes (20-fold), compared to a 4-fold increase by association to non-functionalized liposomes (Figure 2B), which indicates more uptake of pepE-OVA323 per cell. These data show that under physiological conditions (including serum), the strong association of antigen to CPK functionalized liposomes via coiled coil formation results in an improved uptake of the antigen.

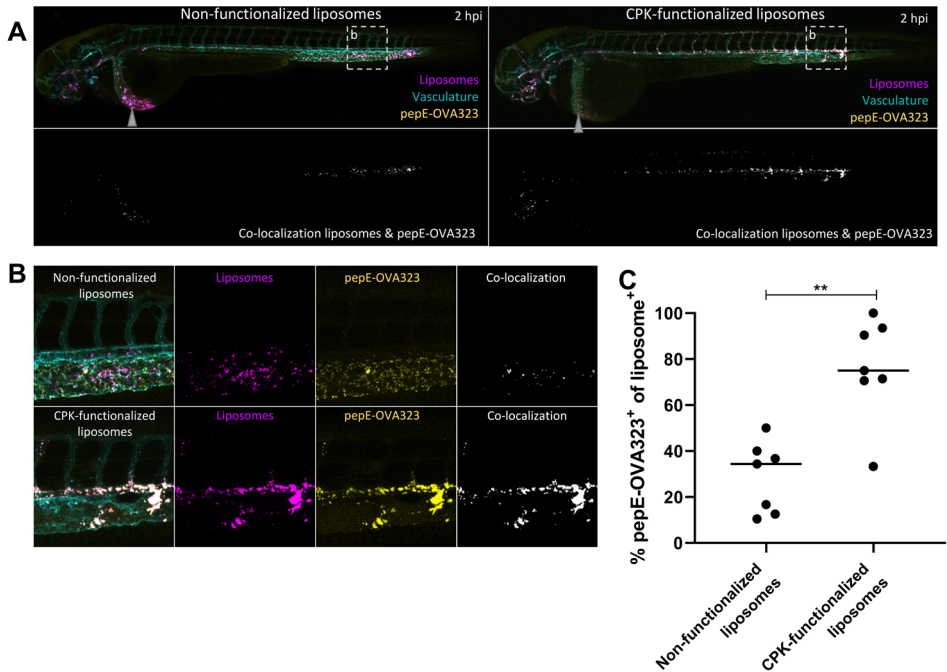


**Figure 2.** Uptake of pepE-OVA323 and liposomes in MHCII<sup>+</sup>CD11c<sup>+</sup> BMDCs. BMDCs were incubated in cIMDM for 4 hours with different formulations containing fluorescent liposomes and fluorescent pepE-OVA323. Subsequently, the BMDCs were analyzed by flow cytometry for peptide and liposome uptake. C shows representative FACS plots of BMDC population for each formulation. A Two-way ANOVA with a Tukey's multiple comparison test to was performed to determine statistically significant differences in antigen and liposome uptake. MFI was compared with a One-way ANOVA and Tukey's multiple comparison test. \*\* =  $p < 0.01$ , \*\*\* =  $p < 0.001$ , \*\*\*\* =  $p < 0.0001$ .

### *In vivo* distribution in zebrafish embryos

The *in vitro* studies revealed that CPK-functionalized liposomes increased antigen and liposome co-localization compared to non-functionalized liposomes. To evaluate how these *in vitro* findings translate to *in vivo* administration in complex tissue, we investigated the biodistribution of pepE-OVA323 and cationic liposomes after intravenous injection in zebrafish embryos. Free peptide, free liposomes, non-functionalized and CPK-functionalized liposomes incubated with pepE-OVA323 were injected in zebrafish embryos. Confocal fluorescence

microscopy was used to assess the biodistribution of both liposomes and peptides after injection. Co-localization throughout the embryo was observed after injection of functionalized liposomes with pepE-OVA323, and was especially prominent in the caudal vein (Figure 3A, B). In contrast, for cationic liposomes with pepE-OVA323, co-localization was only observed in the caudal aspect of the tail and at the injection site for non-functionalized liposomes with pepE-OVA323 (Figure 3A). Non-functionalized liposomes that were associated with pepE-OVA323 displayed similar distribution to the individual components alone (Supplementary figure 7). This difference of pepE-OVA323 distribution after association with functionalized liposomes and non-functionalized liposomes was more profound when zoomed in on the tail vein (Figure 3B). We observed 75% of the functionalized liposome signal co-localized with pepE-OVA323, in contrast to pepE-OVA323 associated to non-functionalized liposomes (34%) (Figure 3C). In 3D representation, the co-localization can be observed at the subcellular level



**Figure 3.** Liposome and antigen distribution in zebrafish embryos. Representative images of zebrafish embryos 2 hours post injection (hpi) of pepE-OVA323 adsorbed to non-functionalized liposomes and CPK-functionalized liposomes. Gray arrows indicate the site of injection. Images were taken by confocal microscopy at 10x magnification (A) and 40x magnification (B), compressed and processed by ImageJ. PepE-OVA323 (yellow), liposomes (magenta) and the vascular system (cyan; *kdr1:mCherry*) of the zebrafish are shown in the upper image; co-localization of pepE-OVA323 and liposomes (i.e., the pixels in which the signals of fluorescence were above the background signal) is white in the lower image of whole fish (A). The percentage of all pixels that had liposome signal which also had pepE-OVA323 signal (C) was compared with a Mann Whitney test, \*\* =  $p < 0.01$ .

as well (Supplementary video 1 and 2). Thus, pepE-OVA323 remained strongly associated with functionalized liposomes *in vivo*, but only in part associated with non-functionalized liposomes.

### Ex vivo T-cell stimulation and proliferation

Next, we investigated whether the strong association and co-localization of antigen and liposome results in improved immunogenicity. We pulsed BMDCs with plain pepE-OVA323 or pepE-OVA323 adsorbed to liposomes with and without CPK for 4 hours, after which CD4<sup>+</sup> T-cells derived from OT-II transgenic mice were co-cultured with these BMDCs. We observed that BMDCs pulsed with soluble pepE-OVA323 successfully induced concentration-dependent T-cell proliferation (Figure 4A). Compared to plain peptide, BMDCs pulsed with pepE-OVA323 associated with non-functionalized liposomes resulted in an approximately 5-fold lower EC50. The same antigen associated to CPK-functionalized liposomes, however, showed an 18-fold lower EC50 than soluble peptide.

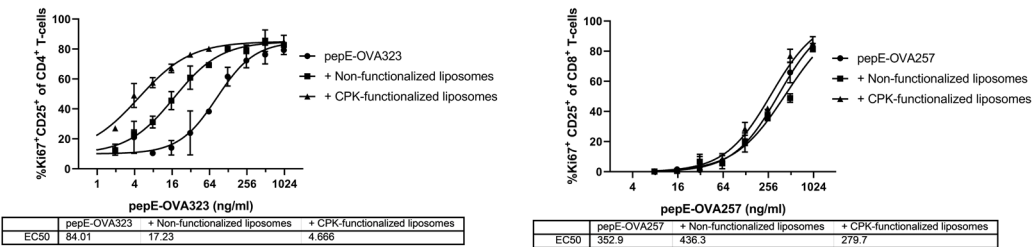


Figure 4. *In vitro* T-cell proliferation. A) CD8<sup>+</sup> T-cell proliferation induced by BMDCs pulsed with pepE-OVA257 in different formulations. B) CD4<sup>+</sup> T-cell proliferation induced BMDCs pulsed with pepE-OVA323 in different formulations. EC50 values were calculated based on a non-linear dose-response model fit with variable slope (four parameters) in which top and bottom were shared between all groups. Graph shows average of 3 points for each concentration and is a representative of 3 separate experiments.

A similar experiment was performed with pepE-OVA257, an MHC-I restricted epitope of ovalbumin and CD8<sup>+</sup> T-cells derived from OT-I transgenic mice. There we also found a concentration-dependent T-cell proliferation profile. Interestingly, in contrast to the CD4<sup>+</sup> T-cell proliferation, there were no differences in proliferation induced by plain peptide, or antigen associated with either liposome formulation (Figure 4B).

### In vivo immune response in mice

As both non-functionalized and CPK-functionalized liposomes increased the CD4<sup>+</sup> T-cell responses *in vitro*, we vaccinated mice that had received an adoptive transfer of ovalbumin-specific CD4<sup>+</sup> T-cells derived from OT-II mice to compare

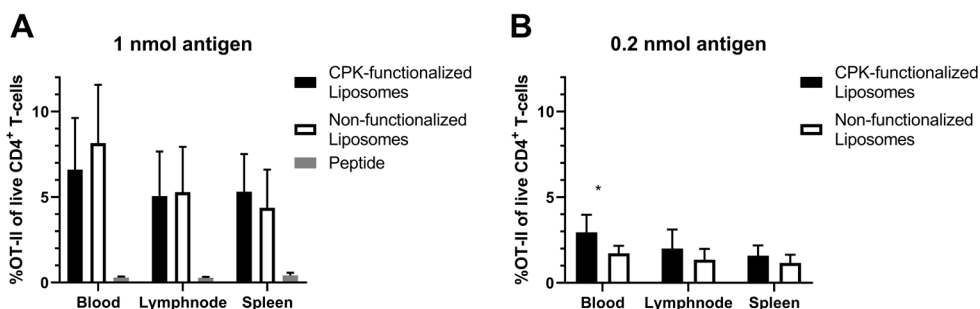


Figure 5. OT-II T-cell expansion after vaccination. OT-II CD4<sup>+</sup> T-cell expansion *in vivo* induced by vaccination with 1 nmol antigen (A, mean  $\pm$  SD,  $n = 8$  for liposomes,  $n = 4$  for peptide) and 0.2 nmol antigen (B, mean  $\pm$  SD,  $n = 7$ ) as measured by flow cytometry. Effect of the formulation in each organ was compared by multiple student's *t* tests. \* =  $p < 0.05$

the effect of non-functionalized and CPK-functionalized liposomes on the *in vivo* immunogenicity. One day after the adoptive transfer, mice received pepE-OVA323 in buffer or associated to either non-functionalized or CPK-functionalized liposomes. The expansion of the transferred CD4<sup>+</sup> T-cells was successfully induced by both liposome formulations (Figure 5A & B), whereas few OT-II cells were present in mice that were vaccinated with peptide alone. Two different doses were used for vaccination. There were no differences in T-cell expansion in the high dose, but in the low dose treatment we observed increased expansion in the group which received the antigen with functionalized liposomes (Figure 5B).

The majority of the OT-II cells that were found in all organs were positive for the transcription factor T-bet. Few OT-II cells expressed Gata3, ROR $\gamma$ t or FoxP3 (Supplementary figure 8), suggesting a Th1 profile. Indeed, upon *ex vivo* stimulation with PMA and ionomycin, IFN- $\gamma$  was the most abundantly expressed cytokine (Figure 6A) while almost no IL-4 or IL-17 was expressed (Supplementary figure 9). We observed a significant increase in IFN- $\gamma$  production after immunization with CPK-functionalized liposomes compared to non-functionalized liposomes. Interestingly, the expanded cells also produced IL-10 (Fig 6B) despite the absence of FoxP3 expression. The IL-10 production was significantly higher in mice that received functionalized liposomes. Further inspection of these cytokine-producing T-cells revealed an increase of double-producing OT-II cells after vaccination with functionalized liposomes (Figure 6C, D).

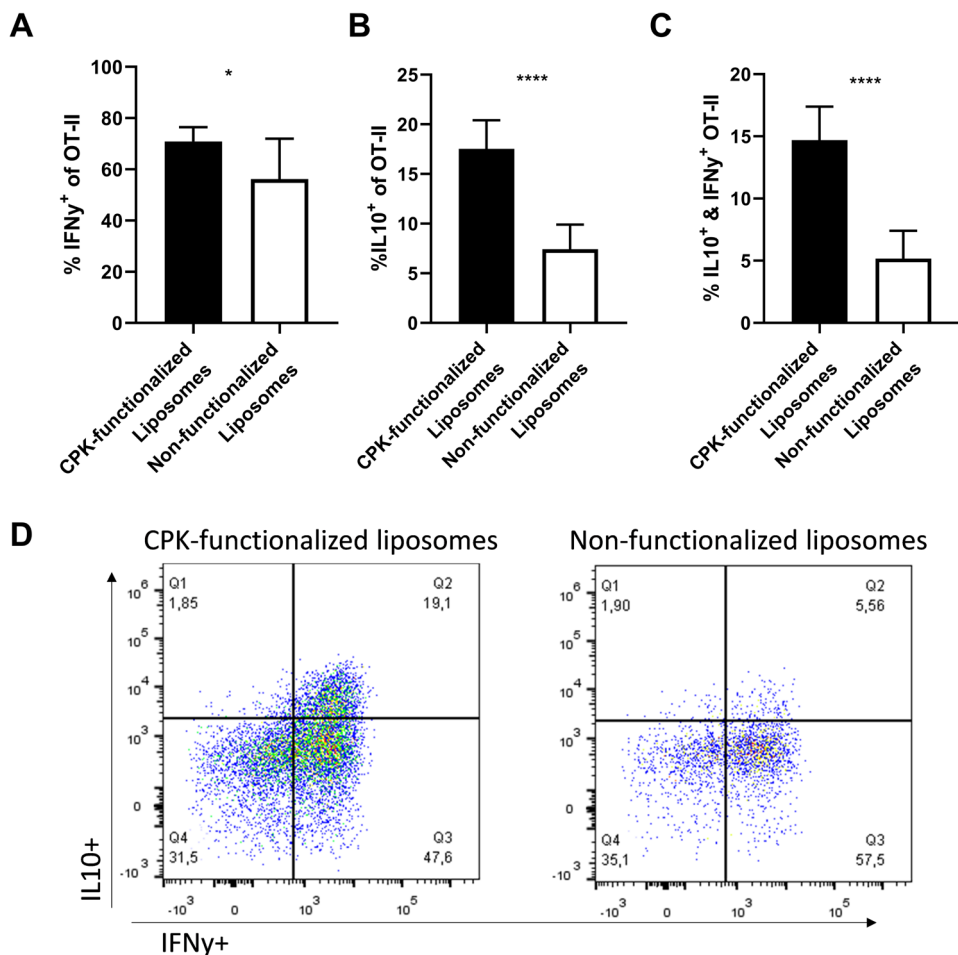


Figure 6. Cytokine production by expanded OT-II T-cells after ex vivo stimulation. OT-II cells that produced IFN- $\gamma$  (A), IL-10 (B), and both IL-10 and IFN- $\gamma$  (C) after stimulation for 6 hours with PMA and ionomycin from the spleen after vaccination with 1 nmol antigen associated with either CPK-functionalized or non-functionalized liposomes (mean  $\pm$  SD,  $n \geq 6$ ). A representative FACS plot of OT-II cells for each formulation is shown in D. Mice where less than 200 OT-II cells were detected, were excluded from the analysis. Outliers were detected with Grubb's outliers test and groups were compared with an unpaired student's t test. \* =  $p < 0.05$ , \*\*\*\* =  $p < 0.0001$ .

## Discussion

In this study, we demonstrated a novel antigen association method to liposomes based on a complementary peptide pair that forms a CC upon interaction. PepK was coupled to cholesterol to yield CPK, which was encapsulated in the lipid bilayer, whereas pepE was synthesized with two different antigenic epitopes. The interaction between pepE and pepK was already known to be stable under physiological conditions [33, 44] and we now demonstrate its use as a method of antigen association. We established that incorporation of CPK in the liposomal



bilayers did not affect the size, polydispersity or zeta potential of liposomes composed of DSPC, DOTAP and cholesterol.

The binding affinity between pepK and pepE is in line with expected values reported before [45]. We observed Kds around  $10^{-7}$  M when mixing both soluble peptides. This did not change when CPK-functionalized liposomes were used instead of soluble peptide or pepE-antigen was used instead of pepE. Moreover, we observed an increase in ellipticity in the CD spectrum, which strongly suggests that the association indeed occurs via the formation of a CC [36, 46]. By simple mixing of the antigen and liposomes, high efficiency adsorption was achieved. This adsorption is very stable and resulted in high co-localization of antigen and liposome both *in vitro* and *in vivo*.

We showed in both BMDCs and zebrafish embryos that peptides associated to non-functionalized liposomes, but not to functionalized liposomes, can rapidly dissociate from the liposomes. While we saw a degree of co-localization of antigen with non-functionalized liposomes, this was significantly increased when antigen was associated with functionalized liposomes. PepE-OVA323 was taken up by BMDCs and showed accumulation in zebrafish endothelial cells even without liposomes. This is constant with the net anionic charge of this peptide, which leads to rapid clearance by scavenger endothelial cells which are similar to liver sinusoidal endothelial cells in mammals [40]. CC association, as demonstrated, results in prolonged co-localization and therefore potentially increases exposure to antigen-coated liposomes and could result in more antigen presentation and TCR stimulation.

This prolonged TCR stimulation is in line with our *in vitro* observations, where we confirmed the adjuvant effect of cationic liposomes [1, 5]. Antigen association with non-functionalized liposomes resulted in a stronger T-cell proliferation, reducing the EC50 approximately 5-fold. Stronger antigen association to CPK-functionalized liposomes resulted in an 18-fold EC50 reduction compared to plain antigen in CD4<sup>+</sup>, but not in CD8<sup>+</sup> T-cells. For CD8<sup>+</sup> T-cells more proliferation was observed at higher pepE-OVA257 concentrations. The proliferation however was barely affected by the addition of either non-functionalized or functionalized liposomes to the formulation. This suggests that the T-cell proliferation is only induced by unbound antigen, but not liposome-associated antigen. Possibly the antigens associated to these liposomes are less capable of endosomal escape and therefore do not enter the cytosol after uptake by BMDCs. MHC-II restricted epitopes are loaded into MHC-II molecules in the late endosome, and therefore not affected by the absence of endosomal escape [47-50]. MHC-I restricted epitopes however require this escape to be efficiently cross-presented to MHC-I molecules in the ER [47, 50-52]. The potential lack of endosomal escape would be



surprising, as cationic liposomes are often used to induce CD8<sup>+</sup> T-cell responses *in vitro* and *in vivo* [17-19], and are even found to promote cross presentation [22, 53, 54]. Apparently, this is not the case for the liposomes we have investigated. Strong T-cell expansion of transferred OT-II derived CD4<sup>+</sup> T-cells was observed 1 week after vaccination with antigen associated to both non-functionalized and functionalized liposomes. When the vaccination was performed with 1 nmol of antigen, we found that approximately 5-6% of all CD4<sup>+</sup> T-cells were expanded OT-II cells, which is in line with previous work [10]. Both liposomes directed the induced immune response towards a Th1 phenotype, as most of our OT-II cells expressed T-bet, which is in agreement with previous findings [9, 10, 21, 26]. Hardly any cells were expressing transcription factors associated with Th2 (Gata3), Th17 (RORγT) or Treg (FoxP3) phenotypes. This was confirmed by the cytokine production upon *ex vivo* stimulation of spleen-derived lymphocytes. Approximately 55% of all OT-II cells in the spleen were producing IFN-γ, a typical Th1 cytokine, in mice which received antigen associated with non-functionalized liposomes. In mice that received functionalized liposomes significantly more OT-II cells produced IFN-γ, suggesting a stronger immune response.

A striking difference was the production of IL-10 after immunization. In mice that received non-functionalized liposomes, approximately 7% of all OT-II cells produced IL-10, but in mice that were vaccinated with CPK-functionalized liposomes, over 15% produced IL-10. Practically all of these IL-10-producing cells were also producing IFN-γ. The double-producing CD4<sup>+</sup> T-cells were previously observed in parasitic infections and have proven critical for host-survival. They are considered to dampen the ongoing immune response more effectively than ordinary regulatory T-cells [55-58]. They could be an interesting phenotype to induce in the treatment of auto-immune diseases and allergy, as both IFN-γ and IL-10 have an inhibitory effect on the Th2 immune response [56, 59, 60]. It is thought that this subset of IL-10- and IFN-γ-producing Th1 cells is the result of continuous antigen presentation and T-cell receptor (TCR) overstimulation [55, 58, 61-64]. This suggests that immunization with antigen associated to CPK-functionalized liposomes resulted in more stimulation of the TCRs by antigen presenting cells than antigen associated to non-functionalized liposomes, which could be explained by the enhanced affinity of pepE-OVA323 to functionalized liposomes.

In conclusion, we have demonstrated the use of CC-forming peptides as an antigen-attachment tool for peptide-based antigens. The antigens have a high affinity for the liposomes and have a high association efficiency. Moreover, the association remains intact *in vitro* and *in vivo* and could be used for peptide-based MHC-II restricted epitopes. The induced immune response by DCs pulsed with CC-adsorbed antigen to liposomes was much higher than for electrostatically

adsorbed antigen. Moreover, *in vivo* we observed a strong increase in IL-10- and IFN- $\gamma$ -producing antigen-specific CD4<sup>+</sup> T-cells, which suggests a stronger TCR stimulation after CC-mediated association of antigen.

### **Funding**

This work was supported by the Nederlandse Organisatie voor Wetenschappelijk Onderzoek (TKI-NCI, grant 731.014.207).

### **Acknowledgements**

We thank J. van Strien, A. Boyle, N. Crone, J. van Duijn, F. Lozano, S. Romeijn, K. Hajmohammadebrahimtehrani and A.I. Kotsogianni Teftsoglou for technical assistance.

### **Declaration of Interest**

None.

## References

1. Christensen, D., et al., *Cationic liposomes as vaccine adjuvants*. Expert Review of Vaccines, 2007. **6**(5): p. 785-796.
2. Varypataki, E.M., et al., *Cationic liposomes loaded with a synthetic long peptide and poly(I:C): a defined adjuvanted vaccine for induction of antigen-specific T cell cytotoxicity*. The AAPS journal, 2014. **17**(1): p. 216-226.
3. Schwendener, R.A., *Liposomes as vaccine delivery systems: a review of the recent advances*. Therapeutic Advances in Vaccines, 2014. **2**(6): p. 159-182.
4. Joshi, M.D., et al., *Targeting tumor antigens to dendritic cells using particulate carriers*. J Control Release, 2012. **161**(1): p. 25-37.
5. Benne, N., et al., *Orchestrating immune responses: How size, shape and rigidity affect the immunogenicity of particulate vaccines*. Journal of Controlled Release, 2016. **234**: p. 124-134.
6. Badiiee, A., et al., *The role of liposome size on the type of immune response induced in BALB/c mice against leishmaniasis: rgp63 as a model antigen*. Experimental Parasitology, 2012. **132**(4): p. 403-409.
7. Watson, D.S., A.N. Endsley, and L. Huang, *Design considerations for liposomal vaccines: Influence of formulation parameters on antibody and cell-mediated immune responses to liposome associated antigens*. Vaccine, 2012. **30**(13): p. 2256-2272.
8. Bachmann, M.F. and G.T. Jennings, *Vaccine delivery: a matter of size, geometry, kinetics and molecular patterns*. Nature Reviews Immunology, 2010. **10**: p. 787-796.
9. Hussain, M.J., et al., *Th1 immune responses can be modulated by varying dimethyldioctadecylammonium and distearoyl-sn-glycero-3-phosphocholine content in liposomal adjuvants*. J Pharm Pharmacol, 2014. **66**(3): p. 358-66.
10. Benne, N., et al., *Anionic 1,2-distearoyl-sn-glycero-3-phosphoglycerol (DSPG) liposomes induce antigen-specific regulatory T cells and prevent atherosclerosis in mice*. J Control Release, 2018. **291**: p. 135-146.
11. Bal, S.M., et al., *Co-encapsulation of antigen and Toll-like receptor ligand in cationic liposomes affects the quality of the immune response in mice after intradermal vaccination*. Vaccine, 2011. **29**(5): p. 1045-1052.
12. Du, G., et al., *Immunogenicity of diphtheria toxoid and poly(I:C) loaded cationic liposomes after hollow microneedle-mediated intradermal injection in mice*. Int J Pharm, 2018. **547**(1-2): p. 250-257.
13. Henriksen-Lacey, M., et al., *Liposomal vaccine delivery systems*. Expert Opinion on Drug Delivery, 2011. **8**(4): p. 505-519.
14. Perrie, Y., et al., *A case-study investigating the physicochemical characteristics that dictate the function of a liposomal adjuvant*. Human Vaccines & Immunotherapeutics, 2013. **9**(6): p. 1374-1381.
15. Slütter, B., et al., *Antigen-Adjuvant Nanoconjugates for Nasal Vaccination: An Improvement over the Use of Nanoparticles?* Molecular Pharmaceutics, 2010. **7**(6): p. 2207-2215.
16. Slütter, B., et al., *Conjugation of ovalbumin to trimethyl chitosan improves immunogenicity of the antigen*. Journal of Controlled Release, 2010. **143**(2): p. 207-214.
17. Varypataki, E.M., et al., *Cationic Liposomes Loaded with a Synthetic Long Peptide and Poly(I:C): a Defined Adjuvanted Vaccine for Induction of Antigen-Specific T Cell Cytotoxicity*. The AAPS Journal, 2015. **17**(1): p. 216-226.

18. Varypataki, E.M., et al., *Cationic DOTAP-based liposomes: a vaccine formulation platform for synthetic long peptides with widely different physicochemical properties*, in *Leiden Academic Center for Drug Research*. 2016, Leiden University: Leiden.
19. Heuts, J., et al., *Cationic Liposomes: A Flexible Vaccine Delivery System for Physicochemically Diverse Antigenic Peptides*. *Pharmaceutical Research*, 2018. **35**(11).
20. Colletier, J.-P., et al., *Protein encapsulation in liposomes: efficiency depends on interactions between protein and phospholipid bilayer*. *BMC Biotechnology*, 2002. **2**(1): p. 2-9.
21. Henriksen-Lacey, M., et al., *Liposomes based on dimethyldioctadecylammonium promote a depot effect and enhance immunogenicity of soluble antigen*. *J Control Release*, 2010. **142**(2): p. 180-186.
22. Schmidt, S.T., et al., *The administration route is decisive for the ability of the vaccine adjuvant CAF09 to induce antigen-specific CD8+ T-cell responses: The immunological consequences of the biodistribution profile*. *Journal of Controlled Release*, 2016. **239**: p. 107-117.
23. Kaur, R., et al., *Effect of Incorporating Cholesterol into DDA:TDB Liposomal Adjuvants on Bilayer Properties, Biodistribution, and Immune Responses*. *Molecular Pharmaceutics*, 2014. **11**(1): p. 197-207.
24. Henriksen-Lacey, M., et al., *Comparison of the Depot Effect and Immunogenicity of Liposomes Based on Dimethyldioctadecylammonium (DDA), 3β-[N-(N',N'-Dimethylaminoethane)carbonyl] Cholesterol (DC-Chol), and 1,2-Dioleoyl-3-trimethylammonium Propane (DOTAP): Prolonged Liposome Retention Mediates Stronger Th1 Responses*. *Molecular Pharmaceutics*, 2011. **8**(1): p. 153-161.
25. Henriksen-Lacey, M., et al., *Liposomal cationic charge and antigen adsorption are important properties for the efficient deposition of antigen at the injection site and ability of the vaccine to induce a CMI response*. *J Control Release*, 2010. **145**(2): p. 102-108.
26. Hamborg, M., et al., *Elucidating the mechanisms of protein antigen adsorption to the CAF/NAF liposomal vaccine adjuvant systems: Effect of charge, fluidity and antigen-to-lipid ratio*. *Biochimica et Biophysica Acta (BBA) - Biomembranes*, 2014. **1838**(8): p. 2001-2010.
27. Robson Marsden, H. and A. Kros, *Self-assembly of coiled coils in synthetic biology: inspiration and progress*. *Angew Chem Int Ed Engl*, 2010. **49**(17): p. 2988-3005.
28. Versluis, F., H.R. Marsden, and A. Kros, *Power struggles in peptide-amphiphile nanostructures*. *Chemical Society Reviews*, 2010. **39**(9): p. 3434-3444.
29. Beesley, J.L. and D.N. Woolfson, *The de novo design of α-helical peptides for supramolecular self-assembly*. *Current Opinion in Biotechnology*, 2019. **58**: p. 175-182.
30. Kong, L., et al., *Light-Triggered Cancer Cell Specific Targeting and Liposomal Drug Delivery in a Zebrafish Xenograft Model*. *Advanced Healthcare Materials*, 2020. **9**(6): p. 1901489.
31. Kong, L., et al., *Temporal Control of Membrane Fusion through Photolabile PEGylation of Liposome Membranes*. *Angewandte Chemie International Edition*, 2016. **55**(4): p. 1396-1400.
32. Yang, J., et al., *Application of Coiled Coil Peptides in Liposomal Anticancer Drug Delivery Using a Zebrafish Xenograft Model*. *ACS Nano*, 2016. **10**(8): p. 7428-35.

33. Oude Blenke, E.E., et al., *Coiled coil interactions for the targeting of liposomes for nucleic acid delivery*. *Nanoscale*, 2016. **8**(16): p. 8955-8965.
34. Yang, J., et al., *Drug Delivery via Cell Membrane Fusion Using Lipopeptide Modified Liposomes*. *ACS Central Science*, 2016. **2**(9): p. 621-630.
35. Versluis, F., et al., *In Situ Modification of Plain Liposomes with Lipidated Coiled Coil Forming Peptides Induces Membrane Fusion*. *Journal of the American Chemical Society*, 2013. **135**(21): p. 8057-8062.
36. Crone, S.N., et al., *Peptide-Mediated Liposome Fusion: The Effect of Anchor Positioning*. *International Journal of Molecular Sciences*, 2018. **19**(1).
37. Wang, W., et al., *Culture and Identification of Mouse Bone Marrow-Derived Dendritic Cells and Their Capability to Induce T Lymphocyte Proliferation*. *Medical science monitor : international medical journal of experimental and clinical research*, 2016. **22**: p. 244-250.
38. Miltenyi, *CD4+ T Cell Isolation Kit\_mouse\_#130-104-454*. 2016.
39. Hogan, B.M., et al., *cclbe1 is required for embryonic lymphangiogenesis and venous sprouting*. *Nature Genetics*, 2009. **41**: p. 396-398.
40. Campbell, F., et al., *Directing Nanoparticle Biodistribution through Evasion and Exploitation of Stab2-Dependent Nanoparticle Uptake*. *ACS Nano*, 2018. **12**(3): p. 2138-2150.
41. Schindelin, J., et al., *Fiji: an open-source platform for biological-image analysis*. *Nature Methods*, 2012. **9**: p. 676-682.
42. Schneider, C.A., W.S. Rasband, and K.W. Eliceiri, *NIH Image to ImageJ: 25 years of image analysis*. *Nature Methods*, 2012. **9**: p. 671-675.
43. Ollion, J., et al., *TANGO: a generic tool for high-throughput 3D image analysis for studying nuclear organization*. *Bioinformatics*, 2013. **29**(14): p. 1840-1841.
44. Poulcharidis, D., et al., *A flow cytometry assay to quantify intercellular exchange of membrane components*. *Chemical Science*, 2017. **8**(8): p. 5585-5590.
45. Litowski, J.R. and R.S. Hodges, *Designing Heterodimeric Two-stranded  $\alpha$ -Helical Coiled-coils: effects of hydrophobicity and  $\alpha$ -helical propensity on protein folding, stability and specificity* *Journal of Biological Chemistry*, 2002. **277**(40): p. 37272-37279.
46. Rabe, M., H.R. Zope, and A. Kros, *Interplay between Lipid Interaction and Homocooling of Membrane-Tethered Coiled-Coil Peptides*. *Langmuir*, 2015. **31**(36): p. 9953-9964.
47. Neefjes, J., et al., *Towards a systems understanding of MHC class I and MHC class II antigen presentation*. *Nature Reviews Immunology*, 2011. **11**: p. 823-836.
48. van den Hoorn, T., et al., *Routes to manipulate MHC class II antigen presentation*. *Current Opinion in Immunology*, 2011. **23**(1): p. 88-95.
49. Delamarre, L., H. Holcombe, and I. Mellman, *Presentation of Exogenous Antigens on Major Histocompatibility Complex (MHC) Class I and MHC Class II Molecules Is Differentially Regulated during Dendritic Cell Maturation*. *The Journal of Experimental Medicine*, 2003. **198**(1): p. 111-122.
50. Guermonprez, P., et al., *Antigen Presentation and T Cell Stimulation by Dendritic Cells*. *Annual Review of Immunology*, 2002. **20**(1): p. 621-667.
51. Banchereau, J. and R.M. Steinman, *Dendritic cells and the control of immunity*. *Nature*, 1998. **392**: p. 245-252.
52. Burgdorf, S., et al., *Distinct Pathways of Antigen Uptake and Intracellular Routing in CD4 and CD8 T Cell Activation*. *Science*, 2007. **316**(5824): p. 612-616.

53. Gao, J., et al., *Cationic liposomes promote antigen cross-presentation in dendritic cells by alkalizing the lysosomal pH and limiting the degradation of antigens*. International journal of nanomedicine, 2017. **12**: p. 1251-1264.
54. Joffre, O.P., et al., *Cross-presentation by dendritic cells*. Nature Reviews Immunology, 2012. **12**: p. 557-569.
55. Villegas-Mendez, A., et al., *Parasite-Specific CD4+ IFN-gamma+ IL-10+ T Cells Distribute within Both Lymphoid and Nonlymphoid Compartments and Are Controlled Systemically by Interleukin-27 and ICOS during Blood-Stage Malaria Infection*. Infect Immun, 2016. **84**(1): p. 34-46.
56. Ng, T.H., et al., *Regulation of adaptive immunity; the role of interleukin-10*. Front Immunol, 2013. **4**.
57. Sun, J., et al., *Effector T cells control lung inflammation during acute influenza virus infection by producing IL-10*. Nat Med, 2009. **15**(3): p. 277-84.
58. Jankovic, D., et al., *Conventional T-bet(+)Foxp3(-) Th1 cells are the major source of host-protective regulatory IL-10 during intracellular protozoan infection*. J Exp Med, 2007. **204**(2): p. 273-283.
59. Akdis, M. and C.A. Akdis, *Mechanisms of allergen-specific immunotherapy*. Journal of Allergy and Clinical Immunology, 2007. **119**(4): p. 780-789.
60. Larche, M., C.A. Akdis, and R. Valenta, *Immunological mechanisms of allergen-specific immunotherapy*. Nat Rev Immunol, 2006. **6**(10): p. 761-771.
61. Gabrysova, L., et al., *c-Maf controls immune responses by regulating disease-specific gene networks and repressing IL-2 in CD4(+) T cells*. Nat Immunol, 2018. **19**(5): p. 497-507.
62. Villegas-Mendez, A., et al., *Long-Lived CD4+IFN-gamma+ T Cells rather than Short-Lived CD4+IFN-gamma+IL-10+ T Cells Initiate Rapid IL-10 Production To Suppress Anamnestic T Cell Responses during Secondary Malaria Infection*. J Immunol, 2016. **197**(8): p. 3152-3164.
63. Jankovic, D., D.G. Kugler, and A. Sher, *IL-10 production by CD4+ effector T cells: a mechanism for self-regulation*. Mucosal Immunol, 2010. **3**(3): p. 239-246.
64. O'Garra, A. and P. Vieira, *TH1 cells control themselves by producing interleukin-10*. Nature Reviews Immunology, 2007. **7**(6): p. 425-428.

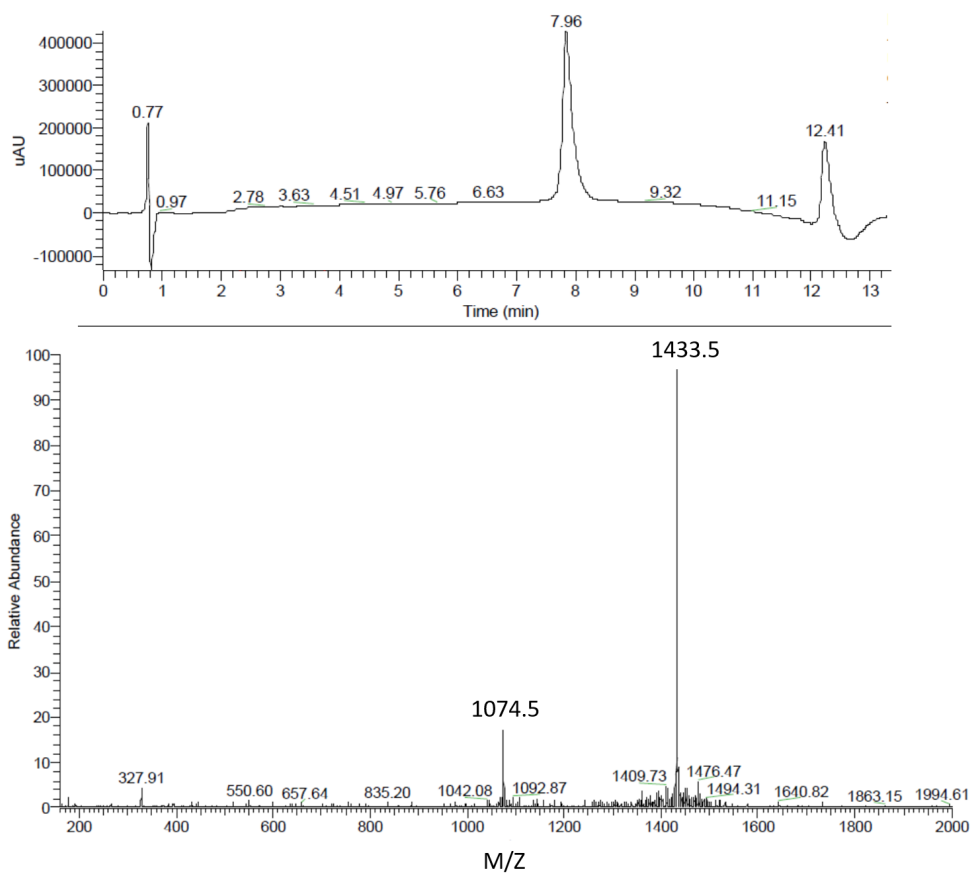
## Supplements

*Supplementary table 1 Overview of all fluorescent antibodies used for flow cytometry. All antibodies were purchased from eBioscience.*

Antibody Target	Fluorescent label
CD25	PE
CD4	APC
CD4	PE
CD4	V500
CD45.1	eFluor 450
CD8	eFluor 450
Fixable Viability Dye	eFluor 780
FOXP3	APC
FOXP3	eFluor 450
Gata3	PE
IFN- $\gamma$	BV650
IL-10	PE
IL-17	FITC
IL-4	APC
Ki-67	FITC
ROR $\gamma$ T	BV650
T-bet	PE-cy7
Thy1.2	PE
Thy1.2	PE-cy7
Thy1.2	PerCP

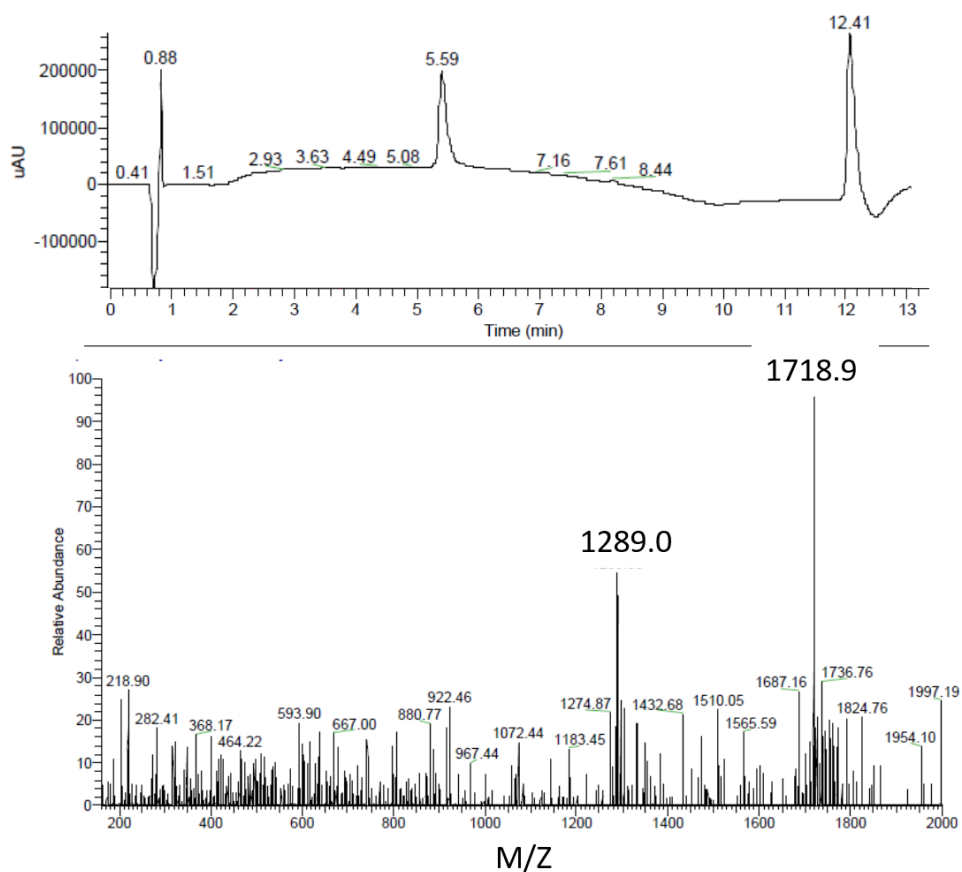
*Supplementary table 2. Overview of all peptides that were synthesized. All names that are used throughout the manuscript with the sequence, calculated theoretical molecular weight (MW) and expected mass per charge (m/z) values for different positive charges (2, 3 and 4 protons added) which will be measured in mass spectrometry.*

Name	Sequence	MW (Da)	2+ m/z	3+ m/z	4+ m/z
CPK	cholesterol – (PEG)4 – KIAALKEKIAALKEKIAALKEKIAALKE	3747.2	1874.6	1250.1	937.8
pepE-OVA323	YGEIAALEKEIAALEKEIAALEKISQAVHAAHAEINEAGR	4299.3	2150.7	1434.1	1075.8
pepE-OVA257	YGEIAALEKEIAALEKEIAALEKSIINFEKL	3489.0	1745.5	1164.0	873.3
pepE-OVA323-AF488	GC-AF488	5160.9	2581.5	1721.3	1291.2

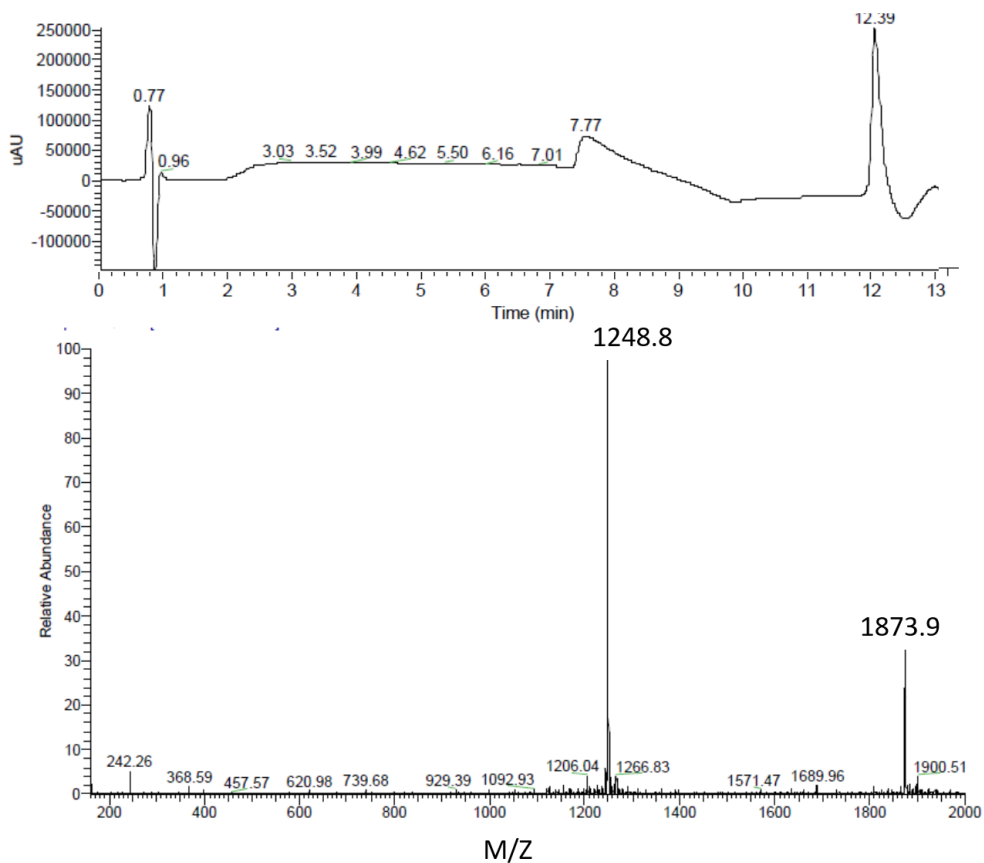


Supplementary Figure 1. LC (top) chromatogram and MS (bottom) spectrum of LC peak at 7.96 minute of pepE-OVA323. The sequence of acetylated pepE-OVA323 is Ac-YGEIAALEKEIAALEKEIAA LEKISQAVHAAHAEINEAGR, which has a molecular mass of 4299.3. the expected m/z values are: 1434.1 and 1075.8 for 3+ and 4+, respectively.

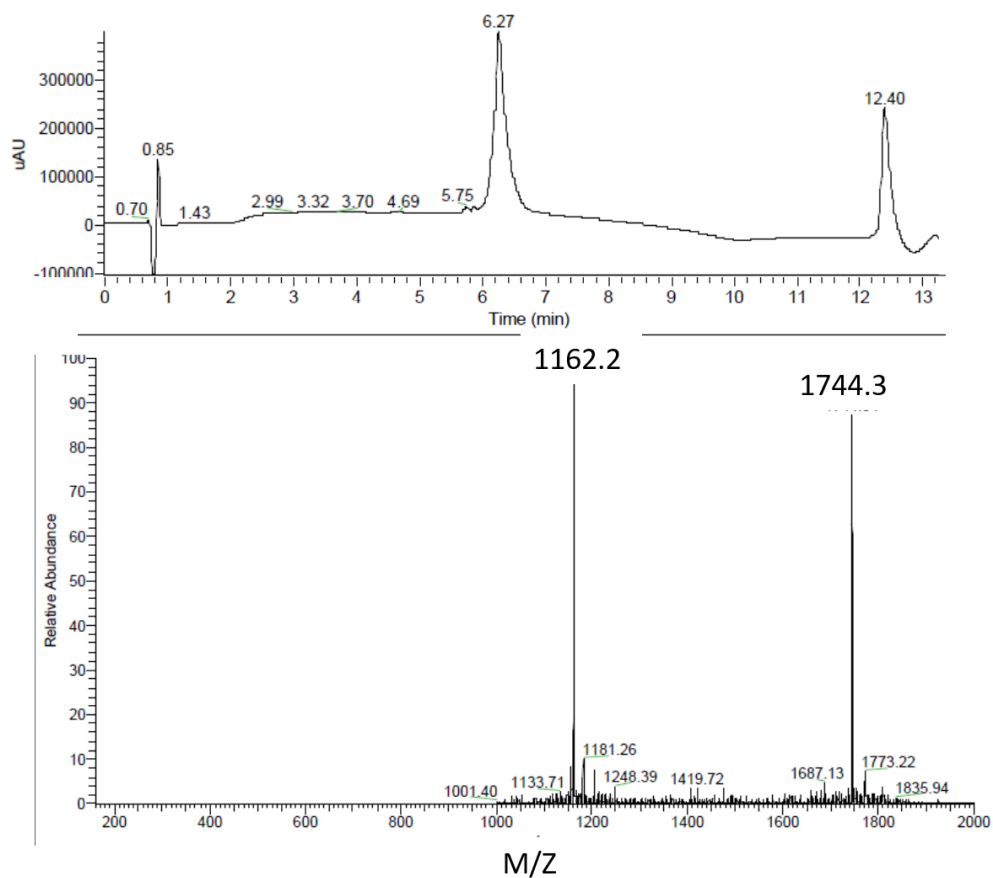




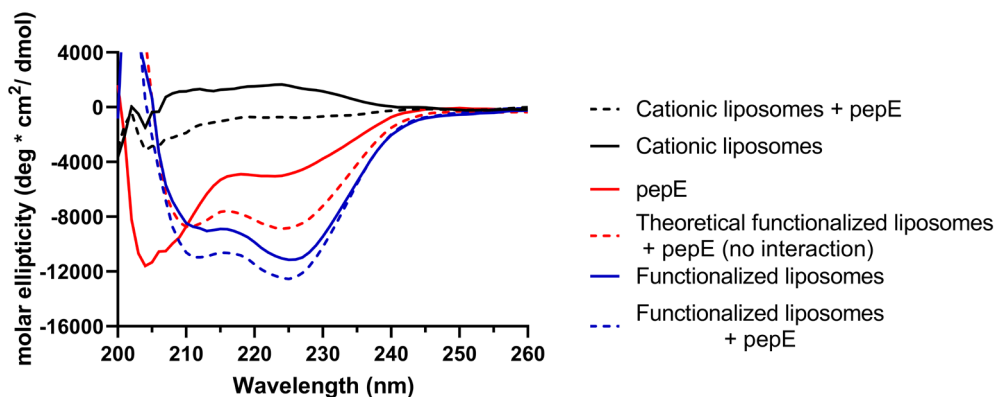
Supplementary Figure 2. LC (top) chromatogram and MS (bottom) spectrum of peak at 5.59 min of acetylated pepE-OVA323-AF488. The sequence of pepE-OVA323-AF488 is Ac-YGEIAALEKEIAALEKEIAALEKISQAVHAAHAEINEAGRGC-AF488, which has a molecular mass of 5160.9. the expected m/z values are: 1721.3 and 1291.2 for 3+ and 4+, respectively.



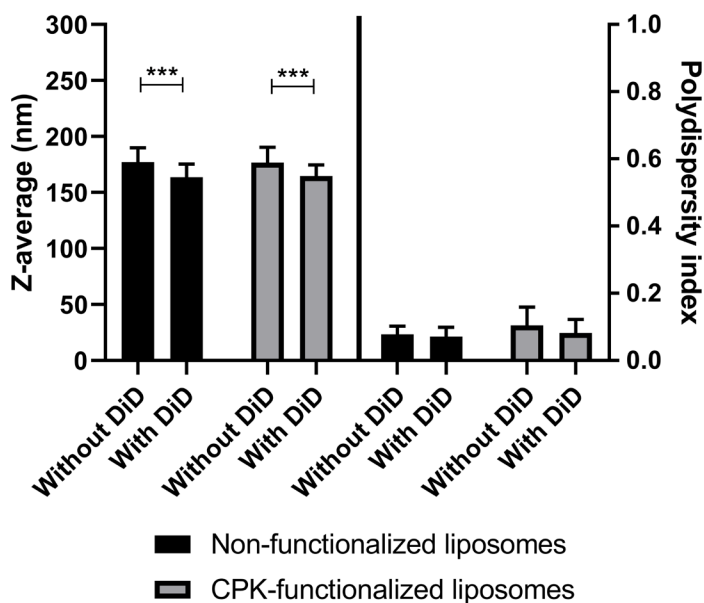
Supplementary Figure 3. LC (top) chromatogram and MS (bottom) spectrum of peak at 7.77 minute of CPK. The sequence of CPK is cholesterol-PEG4-KIAALKEKIAALKEKIAALKEKIAALKE, which has a molecular mass of 3747.2. The expected  $m/z$  values are: 1874.6 and 1250.1 for 2+ and 3+, respectively.



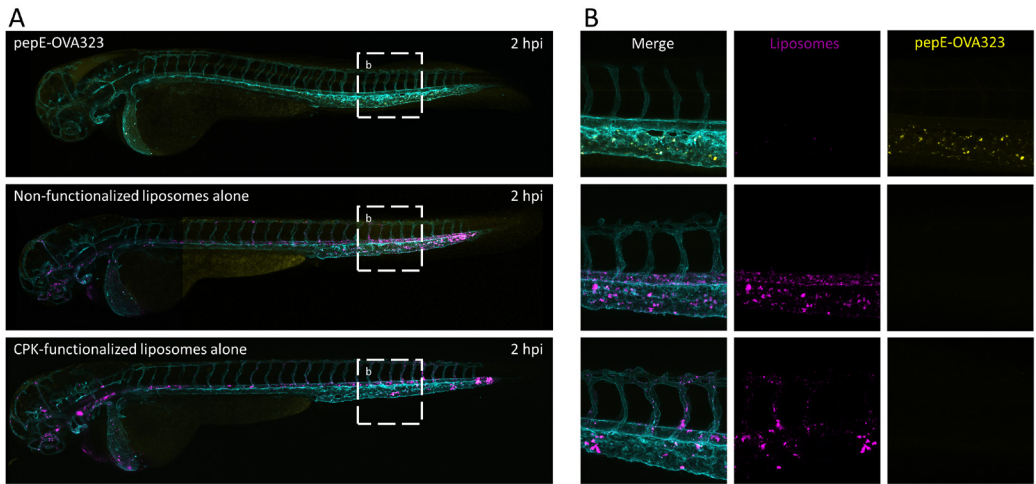
Supplementary Figure 4. LC (top) chromatogram and MS (bottom) spectrum of peak at 6.27 min of acetylated pepE-OVA257. The sequence of pepE-OVA257 is Ac-YGEIAALEKEIAALEKEIAALEKSIIN FEKL, which has a molecular mass of 3489.0. the expected  $m/z$  values are: 1745.5 and 1164.0 for 2+ and 3+, respectively.



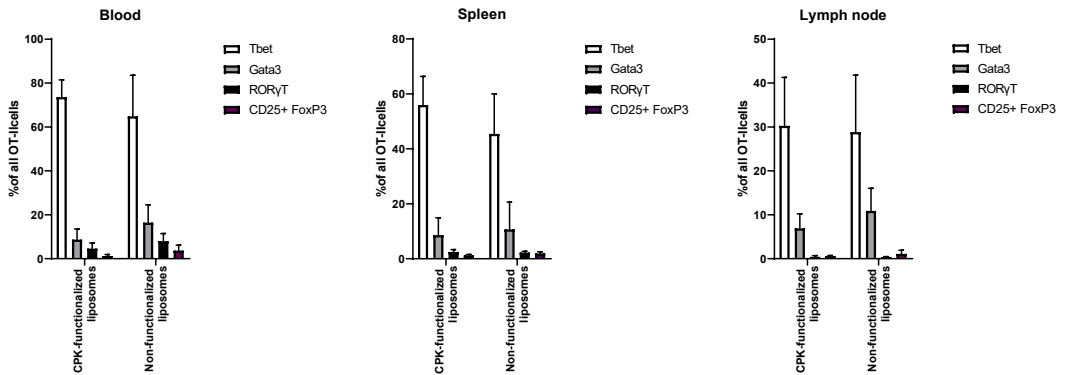
Supplementary Figure 5. Far-UV circular dichroism spectrum of pepE and liposomes with and without CPK. Plain (black) and functionalized liposomes (blue) with (dashed lines) and without pepE (connected lines). The spectrum of pepE (red, connected line) and the theoretical spectrum of pepE and functionalized liposomes if there is no interaction (red, dashed). Non-functionalized liposomes, for calculation purpose, were considered to have the same molar amount of CPK as functionalized liposomes. All lines were smoothened (7 neighbors).



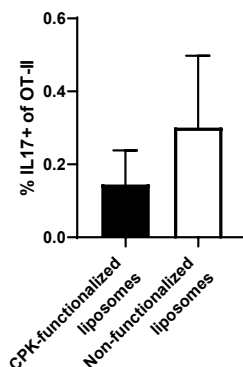
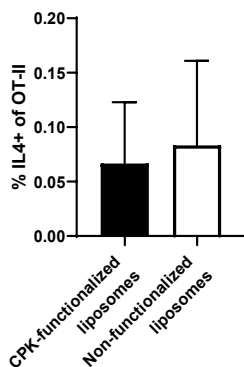
Supplementary Figure 6. Effect of fluorophore DiD on liposome size and polydispersity index. Measured hydrodynamic diameter (Z-average) of liposomes with or without fluorophore (mean  $\pm$  SD,  $n \geq 9$ , of at least 3 separate formulations). Groups were compared in a two-way ANOVA with a Sidak's multiple comparison post-test. \*\* =  $p < 0.01$



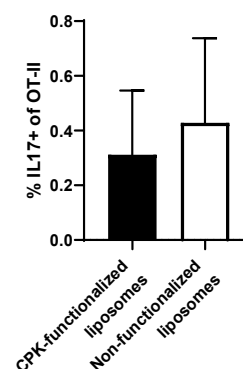
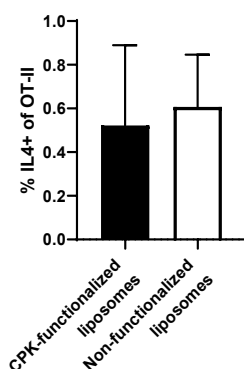
Supplementary Figure 7. Distribution of pepE-OVA323, non-functionalized liposomes and CPK-functionalized liposomes in zebrafish embryo 2 hour post injection. Gray arrows indicate the injection site. The vasculature (cyan), peptide (yellow) and liposomes (magenta) were visualized in a confocal microscope at 10x magnification (A) and 40x magnification (B).



Supplementary Figure 8. Percentage of cell that expressed Tbet, Gata3, RORγT or CD25 and Foxp3 of OT-II cells measured by flow cytometry found in blood, spleen and lymph node after vaccination with 1 nmol antigen with either non-functionalized or CPK-functionalized liposomes (mean  $\pm$  SD,  $n = 8$ ). Only mice where more than 100 OT-II cells were found, were considered for this analysis, so negative controls are not shown.



**Spleen**



**Lymph node**

Supplementary Figure 9. Ex vivo cytokine production. Lymphocytes of mice vaccinated with pepE-OVA323 and non-functionalized or CPK-functionalized liposomes were stimulated for 6 hour with PMA and ionomycin of which 5 with Brefeldin A. The percentage of OT-II cells that produced IL-4 and IL-17 was measured by flow cytometry (mean  $\pm$  SD).



<https://youtu.be/EEJNRSuJ1PY>

Supplementary video 1. 3D projection of zebrafish embryo tail vasculature (cyan) 2 hours after injection of cationic liposomes (magenta) with pepE-OVA323 (yellow).



<https://youtu.be/rki5ATyZgOM>

Supplementary video 2. 3D projection of zebrafish embryo tail vasculature (cyan) 2 hours after injection of functionalized liposomes (magenta) with pepE-OVA323 (yellow).



## Chapter 6

# Bet v 1 attached to cationic liposomes through coiled coil-forming peptides induces stronger antibody responses than aluminum-adsorbed Bet v 1

R.J.T. Leboux<sup>a\*</sup>, H.J.M. Warmenhoven<sup>b,c\*</sup>, A. Bethanis<sup>d</sup>, J. van Strien<sup>e</sup>, A. Logiantara<sup>b</sup>, J.W.P.M. van Schijndel<sup>c</sup>, L. Aglas<sup>d</sup>, L. van Rijt<sup>b</sup>, B. Slütter<sup>a</sup>, A. Kros<sup>e</sup>, W. Jiskoot<sup>a</sup>, R. van Ree<sup>b,f,@</sup>

<sup>a</sup> Division of BioTherapeutics, Leiden Academic Centre for Drug Research, Leiden University, Leiden, The Netherlands

<sup>b</sup> Department of Experimental Immunology, Amsterdam University Medical Centers, location AMC, Amsterdam, The Netherlands

<sup>c</sup> HAL Allergy BV, J.H. Oortweg, Leiden, The Netherlands

<sup>d</sup> Department of Biosciences, University of Salzburg, Salzburg, Austria

<sup>e</sup> Department of Supramolecular & Biomaterials Chemistry, Leiden Institute of Chemistry, Leiden University, Leiden, the Netherlands

<sup>f</sup> Department of Otorhinolaryngology, Amsterdam University Medical Centers, location AMC, , Amsterdam, The Netherlands

\*Both authors contributed equally to this work.

# **Correspondence:** R. van Ree [r.vanree@amsterdamumc.nl](mailto:r.vanree@amsterdamumc.nl)



## **Abstract**

**Background:** Although aluminum hydroxide (alum) has long been used as safe vaccine adjuvant, there is growing concern about its toxicity after chronic exposure via allergen specific immunotherapy (SCIT). Replacing alum with safer alternatives is currently being investigated.

**Objective:** The aim of this study was to evaluate Bet v 1 bearing cationic liposomes as an alternative vaccine delivery system/adjuvant to replace alum in SCIT.

**Methods:** Cationic liposomes were functionalized with one peptide of a coiled coil (CC) forming peptide pair. The resulting liposomes were characterized with dynamic light scattering and laser Doppler electrophoresis. IgE binding and cross-linking were studied by ImmunoCAP and rat basophil leukemia cell assays. The immune responses of naïve mice immunized with Bet v 1 bearing liposomes or alum adsorbed Bet v 1 were compared.

**Results:** Bet v 1 bearing cationic liposomes were 200 nm in size and had a positive zeta potential. The coiled coil attachment between the liposomes and Bet v 1 resulted in approximately 15-fold less allergenic potential than free Bet v 1 and was crucial to induce high Bet v 1-specific IgG1 and IgG2a levels, which were several orders of magnitude higher than alum-adsorbed Bet v 1 immunized mice. This strong humoral response was accompanied by relatively high IL-10 cytokine levels.

**Conclusion:** The hypoallergenic character and strong humoral immune response of cationic liposomes bearing Bet v 1 via coiled coil attachment are advantageous properties for SCIT adjuvants. Therefore, these liposomes are a promising replacement for alum in SCIT.

## Introduction

Subcutaneous allergy immunotherapy (SCIT) has been used to treat allergies for more than 100 years [1]. The treatment commonly consists of monthly subcutaneous injections of allergen extracts for 3 to 5 years to achieve optimal therapeutic effect. Therapy adherence is relatively low because of this long duration and the allergic side-effects that can occur [2]. Often, aluminum hydroxide (alum) is used as adjuvant for SCIT. Although alum has been reported to skew towards T helper (Th) 2 immune responses [3], during SCIT it has been shown to result in a more mixed Th1/Treg cytokine response in combination with production of interleukin (IL)-10 by regulatory T- and B-cells [4, 5]. Most importantly, these regulatory B-cells then also produce the required protective allergen-specific immunoglobulin (Ig) G<sub>4</sub> antibodies. In mouse models, the protective effect of SCIT has been associated with the production of allergen-specific IgG1 and particularly IgG2a antibodies and of IL-10 [6, 7].

Alum has a long history of safe use in vaccines for infectious diseases but also in SCIT [3]. Nevertheless, there is growing concern with respect to the long-term exposure to alum during SCIT, particularly in a pediatric setting [8]. Therefore, good alternatives to ultimately replace alum as adjuvant for SCIT are needed. Besides directing the immune response, alum also serves as a depot for adsorption of allergens, shielding them from IgE antibodies and reducing the risk of allergic side-effects [9]. In recent years, different types of nanoparticles have drawn attention to serve as effective vaccine delivery systems [7, 10, 11]. Liposomes are one of the most promising nanoparticles that could replace alum [12, 13].

Liposomes consist of one or more lipid bilayers with an aqueous core and are a versatile delivery system and adjuvant for vaccines [13, 14]. Antigens can be adsorbed to the lipid bilayer [15], incorporated in the lipid bilayer [16], or encapsulated in the aqueous core of the vesicle [17, 18]. Recently, we described a novel antigen attachment method which is based on the interaction between two complementary  $\alpha$ -helical peptides that form a coiled coil (CC) structure [19]. Immunization of mice with antigen attached to cationic liposomes via this CC formation resulted in strong CD4<sup>+</sup> T-cell proliferation and production of both interferon gamma (IFN- $\gamma$ ) and IL-10. These cytokines are a signature of a Th1 and a regulatory T-cell response, respectively, both of which are reported to be required for effective SCIT [7, 20-22].

The goal of this study was to design a novel, alum free SCIT candidate vaccine using Bet v 1, the major allergen in birch pollen allergy, and liposomes. We produced a fusion protein between Bet v 1 and one of the two CC forming peptides, peptide E (pepE-Bet v 1) and attached this to cationic liposomes

bearing the complimentary CC forming peptide, peptide K (pepK). The resulting liposomes were characterized and compared to alum-adsorbed Bet v 1 with regard to physicochemical and immunological properties.

## Material & Methods

### Chemicals and reagents

Cholesterol, 1,2-distearoyl-sn-glycero-3-phosphocoline (DSPC), 1,2-dioleoyl-3-trimethylammonium-propane (DOTAP) were purchased from Avanti Lipids. Recombinant protein Bet v 1 (isoform Bet v 1.0101) was produced by the Department of Molecular Biology of the University of Salzburg (Salzburg, Austria) [23]. Dimethylformamide (DMF), piperidine, acetic anhydride, pyridine, trifluoroacetic acid (TFA) and acetonitrile (ACN) were purchased from Biosolve (Valkenswaard, Netherlands). N,N-diisopropylethylamine (DIPEA), and ethyl cyanohydroxyiminoacetate (Oxyma) were obtained from Carl Roth (Karlsruhe, Germany). Dichloromethane (DCM) and diethyl ether were supplied by Honeywell (Landsmeer, Netherlands). Tentagel HL-RAM was obtained from Rapp Polymere (Tübingen, Germany). All amino acids were supplied by NovaBioChem (Darmstadt, Germany). Fmoc-NH-PEG<sub>4</sub>-COOH was purchased from Iris Biotech GmbH (Marktredwitz, Germany). Pierce BCA assay and Imject<sup>®</sup> Alum were purchased from Thermo Fisher Scientific (Rockford, Ill., USA). Isopropyl β-D-1-thiogalactopyranoside was obtained from Invitrogen (Carlsbad, CA., USA). Fetal calf serum (FCS) was supplied by Thermo Fisher Scientific. Sucrose, HEPES, HATU, Triisopropylsilane (TIPS), sodium azide, Tyrode's salts, BSA, lysozyme, sodium bicarbonate, 4-methyl umbelliferyl-N-acetyl-beta-D-glucosaminide, Triton X-100 and 3-(4,5-dimethylthiazol-2-yl)-2,5-diphenyltetrazolium bromide (MTT) were obtained from Sigma-Aldrich. Disodium hydrogen phosphate and sodium dihydrogen phosphate were purchased from Merck (Darmstadt, Germany). Ampicillin was obtained from Roche (Basel, Switzerland).

### Mice

Six to eight weeks old female BALB/c mice were purchased from ENVIGO (The Netherlands). The animals were housed under specific pathogen-free conditions at the animal facility of the Amsterdam University Medical Centers, location AMC. All experiments were performed in compliance with the Dutch government guidelines and the Directive 2010/63/EU of the European Parliament and were approved by the Animal Ethics Committee of the AMC.

### Peptide synthesis

Peptides (pepK: CG-KIAALKEKIAALKEKIAALKE, and K4: KIAALKEKIAALKEKIAALKEKIAALKE) were synthesized by standard Fmoc chemistry using solid-phase peptide synthesis with an automated microwave peptide synthesizer (CEM liberty blue).

Cholesterol-PEG-K4 (CPK) was prepared as described elsewhere [10]. In short: Fmoc-NH-PEG<sub>4</sub>-COOH was coupled to resin-bound K4 in the presence of DIPEA (5 eq.) and HATU (2.5 eq.) for 2.5 hours. Fmoc was removed with 20% piperidine in DMF before the reactive amine was coupled to 1.05 equivalents amino-cholestene hemisuccinate in the presence of DIPEA (5 eq.) and HATU (2.5 eq.) for 4 hours at room temperature. The peptide was cleaved from the resin with a mixture of TFA:TIPS:water (95:2.5:2.5 v/v/v), precipitated in ice-cold diethyl ether and collected via centrifugation.

Crude peptides were purified using a Shimadzu RP-HPLC system comprising two LC-8A pumps and a SPD-10AVP UV-Vis detector equipped with a Kinetic Evo C18 column. A gradient of 20-80% B, (where B is ACN containing 1% v/v TFA, and A is water with 1% v/v TFA) with a flow rate of 12 mL/min was used. Collected fractions were measured on a LC-MS system (Thermo Scientific TSQ quantum access MAX mass detector connected to a Ultimate 3000 liquid chromatography system fitted with a 50 × 4.6 mm Phenomenex Gemini 3 μm C18 column). The resulting chromatogram and spectrum are shown in Supplementary Figure 1. ACN was removed by rotary evaporation (150 mbar, 50 °C) before lyophilization, leaving dry purified peptide powder which was stored at -20 °C until use.

#### Design, expression and purification of pepE-Bet v 1.

A detailed description of the manufacturing of pepE-Bet v1 can be found in the supplementary Materials and Methods. In short, the pepE-Bet v 1 gene was produced by GenScript (Piscataway, NJ, USA) and used to transfect *E. coli* BL21 (DE3) cells. Ampicillin resistant clones were grown in a 5 L stirred tank coupled to a BIOSTAT® controller (Sartorius Stedim Biotech) for protein production. Harvested cells were pelleted by centrifugation and frozen for storage. The protein was isolated from the frozen cell pellets by disrupting the cells using sonication. Cellular debris was removed by centrifugation. The supernatant was filtered through 0.2 μm before affinity purification using cross-linked agarose beads functionalized with PepK, the complementary peptide of the pepE/K self-assembling peptide pair. The affinity purification matrix was equilibrated with buffer, loaded with filtered supernatant and washed to remove unbound proteins. Bound pepE-Bet v 1 was eluted by lowering the pH to 2.5 to unfold the pepE/pepK coiled coil. Elution fractions were collected and directly neutralized with 1 mol/L TrisHCl, pH 9. Flow through, wash and elution fractions were analyzed with SDS PAGE. Elution fractions containing pepE-Bet v 1 were pooled and loaded onto a Superdex 75 pg column (GE Healthcare) for polishing. Fractions containing the pure protein were pooled and stored at -20°C until further use.

#### Preparation of liposomes

Liposomes were prepared by the dehydration-rehydration method as described

elsewhere [15]. In short: lipids (DSPC, DOTAP and cholesterol in a 2:1:1 molar ratio, optionally including 1 mol% CPK) were mixed in the desired ratio. Subsequently, the organic solvent was evaporated in a rotary evaporator, leaving a lipid film. This film was hydrated in the presence of glass beads with a 10 mmol/L HEPES, 280 mmol/L sucrose buffer and lyophilized overnight. The resulting lipid cake was rehydrated with filtered Milli-Q® water to a final volume of 2 mL and homogenized using a LIPEX extruder (Evonik, Canada) over a stacked 400 nm & 200 nm Nuclepore Track-Etch membrane (Whatman, Netherlands). Throughout this manuscript 3 different liposome formulations were used:

1. Cationic liposomes with pepE-Bet v 1 adsorbed (pepE-Bet v 1 liposomes)
2. CPK-functionalized liposomes with Bet v 1 adsorbed (Bet v 1 CPK-liposomes)
3. CPK-functionalized liposomes with pepE-Bet v 1 adsorbed (pepE-Bet v 1 CC-liposomes)

Each of these formulations was prepared by adding 50 µg of either Bet v 1 or pepE-Bet v 1 (as was determined by BCA) to a liposome suspension (1 mg lipids) with a final volume of 1 mL. This mixture was incubated for at least 15 minutes.

#### Liposome characterization.

Hydrodynamic diameter ( $Z_{ave}$ ) and polydispersity (PDI) were measured by dynamic light scattering (DLS) using a Zetasizer Nano Zs (Malvern Instruments Ltd., Worcestershire, UK). The zeta potential was measured using laser Doppler electrophoresis (IDe) on the same machine with a Zeta Dip Cell (Malvern Instruments Ltd.). Each sample was diluted 100 fold in 10 mmol/L HEPES buffer (pH 7.4, 0.2 µm filtered) before measurement.

#### ImmunoCAP IgE inhibition

IgE binding to pepE-Bet v 1 CC-liposomes was determined by ImmunoCap IgE inhibition assay using rBet v 1 ImmunoCAPs (T215). The liposomes and control samples were serially diluted (10-fold dilutions) in 10 mmol/L HEPES, 280 mmol/L sucrose, pH 7.4 and pre-incubated 1:1 (v/v) at room temperature with a serum pool. The pool was composed of 36 birch pollen allergic patient sera, 1:1 (v/v) mixed and was pre-diluted to approximately 14 kU/mL before mixing with sample. Bet v 1, pepE-Bet v 1 and serum without sample were used as controls.

#### Rat basophil leukemia (RBL) assay

To assess the allergenicity of pepE-Bet v 1-CC-liposomes, their ability to induce mediator release from effector cells was compared to that of soluble wild type rBet v 1.0101 (hereafter designated Bet v 1) [16] and pepE-Bet v 1. To that end, rat basophil leukemia cells (RBL-2H3), transfected with the human high-affinity IgE receptor (FcεRI) [17], were sensitized with serum of Bet v 1 sensitized birch pollen

allergic patients, and a  $\beta$ -hexosaminidase mediator release assay was performed as previously described [16]. In short,  $2 \times 10^5$  transfected RBL-2H3 cells/well were seeded in flat-bottom 96-well, Nunclon Delta-treated microplates (Thermo Fisher Scientific, Waltham, MA, USA) and passively sensitized overnight with sera derived from birch pollen allergic patients ( $n=8$ ). To neutralize the complement system, the sera were incubated with P3X63Ag8.653 cells ((ATCC CRL-1580™), Manassas, VA, USA) prior to the sensitization step. For  $\beta$ -hexosaminidase release, the cells were stimulated with the samples in eight 15-fold dilution steps ranging from 10  $\mu\text{g/mL}$  to 0.06  $\mu\text{g/mL}$  Bet v 1 concentration. Samples were diluted in Tyrode's buffer containing 9.5 g/L Tyrode's salts, 0.1% (w/v) BSA, 0.5 g/L sodium bicarbonate. The cells were stimulated with the samples for one hour at 37 °C, 7%  $\text{CO}_2$  before the cell supernatant was incubated with the  $\beta$ -hexosaminidase substrate, 4-methyl umbelliferyl-N-acetyl-beta-D-glucosaminide, diluted in 0.1 M citric acid (pH 4.5) for another hour at 37 °C and then quenched with 0.2 M of glycine buffer (pH 10.7). The fluorescence was measured with an Infinite 200Pro spectrophotometer (Tecan, Switzerland) at an excitation and emission wavelength of 360 nm and 465 nm, respectively. The data are presented as percentage of cell release normalized to the maximal enzyme release caused by cell lysis (10% Triton X-100, Sigma-Aldrich, Inc.), which was firstly corrected for spontaneous release (no serum sensitization). Cell viability was confirmed by performing a MTT assay.

### Animal study

Mice were immunized subcutaneously on day 0, 7 and 14 with pepE-Bet v 1-CC-liposomes or alum-adsorbed Bet v 1 (1 mg alum per dose) containing 10  $\mu\text{g}$  Bet v 1. Control groups received buffer (10 mmol/L HEPES, 280 mmol/L sucrose, pH 7.4), pepE-Bet v 1 liposomes or Bet v 1 CPK-liposomes. Serum for antibody detection was collected on days -1, 6, 13 and 20. On day 27, 28 and 29 the animals received an intranasal challenge under 3% (v/v) isoflurane anesthesia with 100  $\mu\text{g/mL}$  birch pollen extract (BPE) in PBS to induce lung inflammation. On day 31, the mice were sacrificed and blood and lung draining lymph nodes were collected to analyze Bet v 1 specific levels of IgG1, IgG2a and IgE in serum and determine the production of cytokines (IL-4, IL-5, IL-13, IL-10 and IFN- $\gamma$ ) after stimulation of lymphocytes in the lymph nodes with Bet v 1.

### Determination of Bet v 1 specific antibodies

Serum was analyzed for the level of Bet v 1-specific IgG1 and IgG2a by ELISA (IgG1: Opteia, BD, San Diego, CA, USA, IgG2a: eBioscience) as previously described [6]. In short, Maxisorp plates were coated overnight with Bet v 1. After blocking with FCS (10%), serum samples were incubated for 2 hours and followed by an HRP-conjugated anti IgG1 or IgG2a detection step, according to the manufacturer's instructions. Serum samples were diluted 10,000-fold, unless stated otherwise.

*Ex vivo* re-stimulation of lung draining lymph node cells.

Lung draining lymph node cell suspensions were plated in a 96-well round bottom plate at a density of  $2 \times 10^5$  cells per well in RPMI supplemented with gentamicin, 10% FCS and  $\beta$ -mercaptoethanol. The cells were re-stimulated for 4 days with 10  $\mu\text{g/mL}$  Bet v 1. Expression levels of cytokines (IL-4, IL-5, IL-10, IL-13, IFN- $\gamma$  and IL-17A) were determined in the supernatant by ELISA (eBioscience).

## Statistics

Data was processed and statistically analyzed in GraphPad v8 (Prism) for Windows. The statistical method is indicated in the figure legends.

## Results

All liposomes were cationic and approximately 200 nm in size.

To determine the size and charge, all formulations were characterized by DLS and laser Doppler electrophoresis. All liposome formulations had a hydrodynamic diameter of approximately 200 nm and a positive zeta potential. The pepE-Bet v 1 CC-liposomes were slightly larger than the other formulations. The zeta potential was lower after coiled-coil mediated antigen adsorption. In contrast to liposomes, alum-adsorbed Bet v 1 showed a slightly negative zeta potential and the Z-average diameter was larger than 1000 nm (Table 1).

*Table 1. Overview of all formulations and their physicochemical characteristics (mean values  $\pm$  SD,  $n = 3-5$ ). All formulations contained the same buffer composed of 10 mmol/L HEPES, 280 mmol/L sucrose, pH 7.4.*

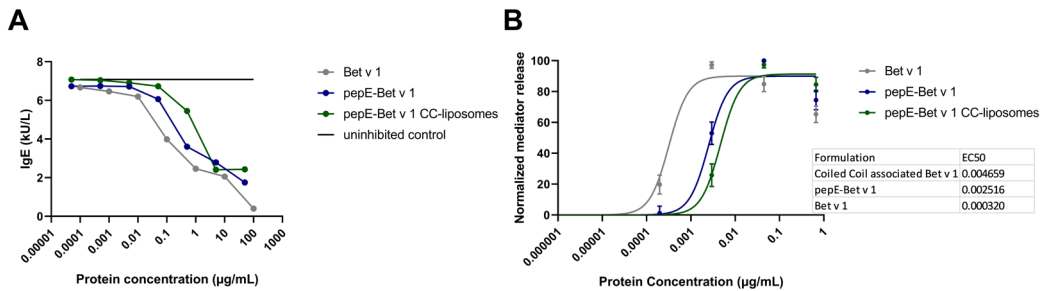
Formulation	Protein/carrier ratio (w/w)	Z-average diameter (nm)	PDI	Zeta potential (mV)
Liposomes (non-functionalized)	n.a.	$179.3 \pm 13.8$	$0.073 \pm 0.039$	$48.1 \pm 3.3$
CPK-liposomes	n.a.	$176.7 \pm 14.4$	$0.071 \pm 0.047$	$44.9 \pm 6.2$
pepE-Bet v 1 CC-liposomes	1/10	$207.2 \pm 10.7$	$0.159 \pm 0.064$	$29.4 \pm 4.2$
Bet v 1 CPK-liposomes	1/10	$189.3 \pm 17.6$	$0.165 \pm 0.029$	$40.0 \pm 1.7$
pepE-Bet v 1 liposomes	1/10	$176.8 \pm 16.4$	$0.145 \pm 0.043$	$38.1 \pm 3.9$
Alum-adsorbed Bet v 1	1/100	$1245.1 \pm 131.9$	$0.318 \pm 0.036$	$-6.3 \pm 1.0$

PepE-Bet v 1 CC-liposomes are hypoallergenic compared to Bet v 1.

Next, we characterized the IgE binding capacity of pepE-Bet v 1 CC-liposomes by testing its potential to inhibit IgE binding to rBet v 1 caps. Compared to Bet v 1, the IgE inhibition curves of pepE-Bet v 1 and pepE-Bet v 1 CC-liposomes revealed a higher inhibitor concentrations which indicated reduced IgE binding capacity (Figure 1A). Subsequently, we tested the IgE cross-linking capacity of pepE-Bet v 1 CC-liposomes by RBL mediator release assay. Testing a broad concentration



range yielded typical bell-shaped mediator release curves [24]. Based on the ascending part of the bell shaped curve, pepE-Bet v 1 appeared hypoallergenic compared to Bet v 1. PepE-Bet v 1 CC-liposomes induced approximately 15-fold less mediator release than recombinant Bet v 1 (Figure 1B). This was observed in all individual donors. Moreover, except for 1 donor, pepE-Bet v 1 CC-liposomes were more hypoallergenic than pepE-Bet v 1 (Supplementary Figure 3).



**Figure 1.** ImmunoCAP IgE inhibition assay and rat basophil lymphocyte assay. (A) The amount of IgE binding to serially diluted Bet v 1, pepE-Bet v 1 and Bet v 1 CC-liposomes was determined by immunoCAP. (B) Basophils loaded with IgE from serum of Bet v 1-sensitized subjects were exposed to a titration of different allergen formulations. Mediator release was measured and normalized based on positive and negative controls. Each data point is the mean of 8 experiments. A non-linear regression (variable slope, 4 parameters) fit was used to extract the EC50.

Cationic liposomes with coiled-coil associated Bet v 1 triggered strong antibody responses in naïve mice.

To evaluate the immune response induced by pepE-Bet v 1 CC-liposomes, naïve mice were immunized 3 times at weekly intervals followed by intranasal birch pollen extract challenge. Bet v 1-specific antibody levels were measured before each injection and at the end of the experiment. Mice that received pepE-Bet v 1 CC-liposomes had 77 fold higher IgG1 and 220 fold higher IgG2a levels (Figure 2A and B, respectively) than alum-adsorbed Bet v 1 at the endpoint. The IgE levels in all the liposome receiving groups were higher than the Bet v 1 + alum group but this was not significant (Figure 2C, 2F). In fact, the IgG1/IgE and IgG2a/IgE ratios in the pepE-Bet v 1 CC-liposomes group was much more favorable compared to the alum-adsorbed Bet v 1 (11.2 vs. 1.72 and 3.78 vs. 0.25 respectively).

To evaluate whether the CC formation was crucial for the strong humoral response, Bet v 1 CC-liposomes were compared to pepE-Bet v 1 liposomes (non-functionalized liposomes) and Bet v 1 CPK liposomes (non-functionalized Bet v 1). IgG1 and IgG2a induction was already observed 6 days after the second injection of the pepE-Bet v 1 CC-liposomes, but not after injection of the other liposome groups (Figure 3A and B, respectively). At the endpoint, all liposome formulations induced stronger antibody responses than allergen alone, but significantly more IgG1 and IgG2a was detected in mice immunized with pepE-



Bet v 1 CC-liposomes (Figure 2D and E), while the level of IgE was similar (Figure 2F). A serial dilution of pooled serum confirmed that pepE-Bet v 1 CC-liposomes induced the strongest immune response (Supplementary Figure 4). This also revealed that pepE-Bet v 1 induced a higher level of IgG1 than alum-adsorbed Bet v 1. Moreover, Bet v 1 attached to liposomes without CC induced a stronger humoral response than alum-adsorbed Bet v 1 or antigen without adjuvant.

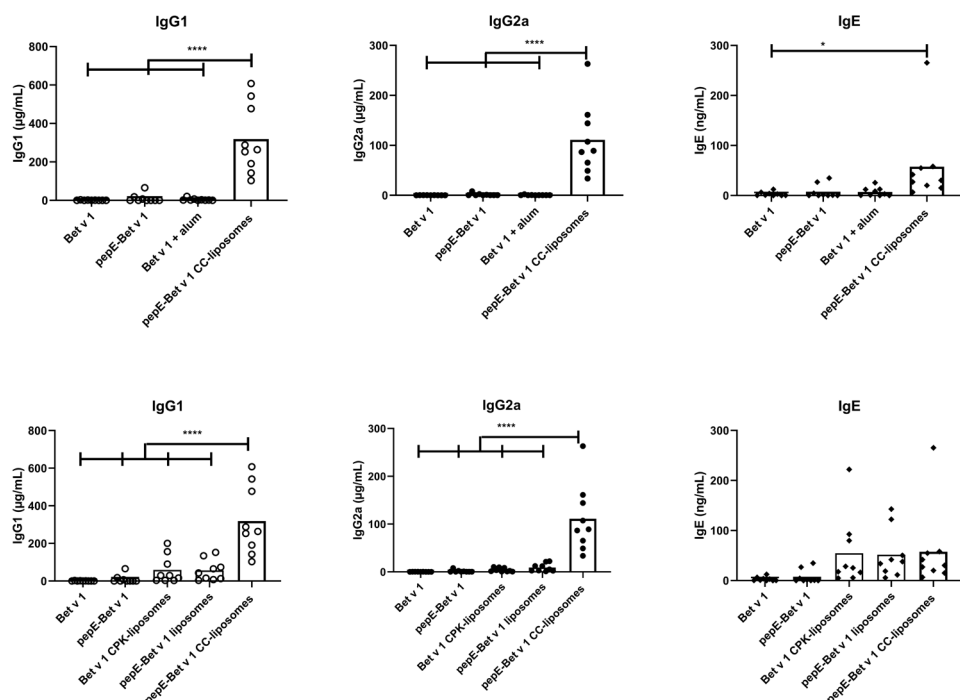


Figure 2. Serum levels of Bet v 1-specific IgG1 (A, D), IgG2a (B, E) and IgE (C, F). Mice ( $n=9$ ) were immunized with various formulations on day 0, 7 and 14 and received 3 intranasal challenges with birch pollen extract for 3 consecutive days prior to the sacrifice. Group means were compared with a one-way ANOVA and subsequent Tukey's multiple comparison test (\* =  $p < 0.05$ , \*\*\*\* =  $p < 0.0001$ ).

PepE-Bet v 1 CC-liposomes induced a strong, regulatory skewed immune response.

To evaluate the cellular immune response, cells were isolated from lung-draining lymph nodes and stimulated with Bet v 1. Mice immunized with alum-adsorbed Bet v 1 showed induction of Th2 related cytokines IL-4, IL-5, IL-13, T regulatory (Treg) associated IL-10, Th1 associated IFN- $\gamma$  and Th17 associated IL-17a. Immunization with pepE-Bet v 1 CC-liposomes, however, resulted in significantly higher IL-4, IL-5, IL-13 and IL-10 production compared to the other groups (Supplementary Figure 5). Remarkably, when ratios of different cytokines were calculated pepE-Bet v 1 CC-liposomes had a significantly higher IL-10/IL-4

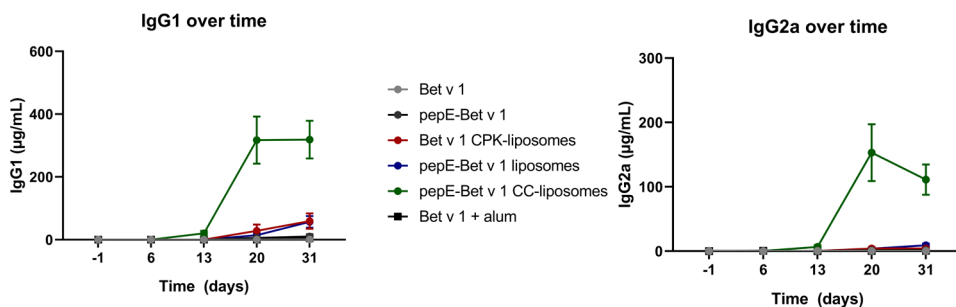


Figure 3. Bet v 1-specific levels (mean  $\pm$  SEM) of IgG1 (A) and IgG2a (B) over time. Mice ( $n=9$ ) were immunized with various formulations on day 0, 7 and 14 and received 3 intranasal challenges with birch pollen extract for 3 consecutive days prior to the sacrifice.

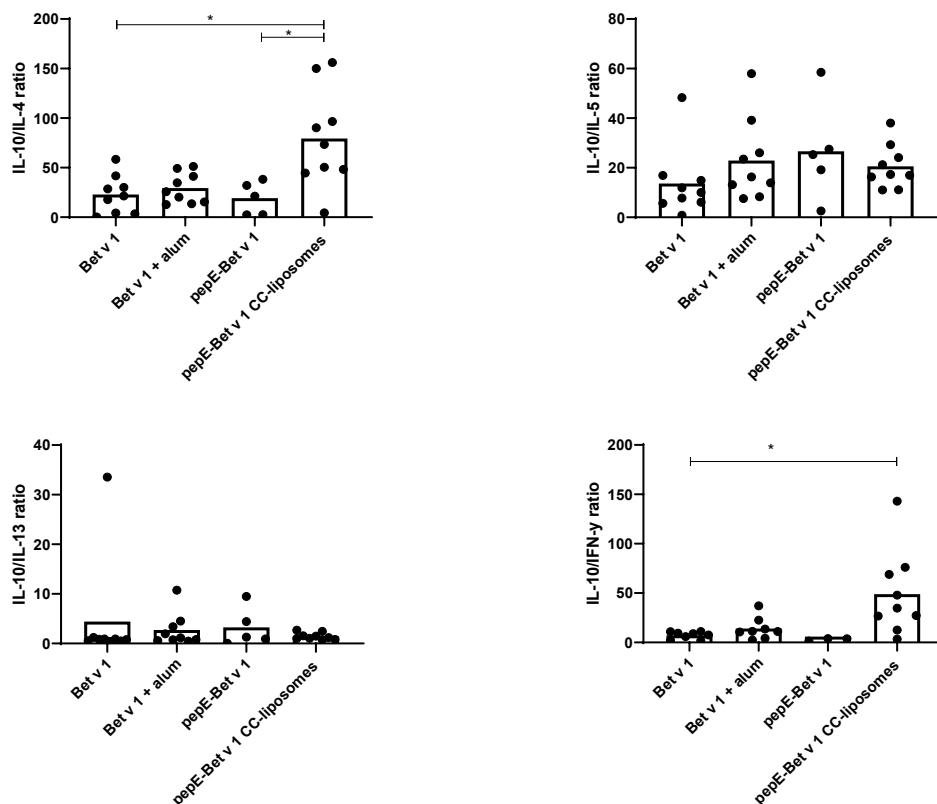


Figure 4. Ratios between cytokines that were detected in supernatants of lung draining lymph node cells after *ex vivo* stimulation with Bet v 1 as measured by ELISA. Mice were immunized with various formulations on day 0, 7 and 14 and received 3 intranasal challenges with birch pollen extract for 3 consecutive days prior to the sacrifice. Bars represent the mean ratio ( $n=6-9$ ). Group means were compared with a Kruskal Wallis test and Dunn's multiple comparison test. \* =  $p < 0.05$ .

ratio, which indicates a more regulatory skewed response compared to Bet v 1 or alum-adsorbed Bet v 1 (Figure 4).

## Discussion

Previously we described the functionalization of cationic liposomes with a CC-forming peptide, which enhanced the immune response to model antigen OVA323 [19]. In the current study, the CC functionalized cationic liposomes were used to design a new birch pollen SCIT vaccine. In our vaccine design, Bet v 1 was attached to the functionalized liposome surface via peptide E fused to the N-terminus of Bet v 1 which already appeared to interfere with IgE binding. More importantly, the reduced IgE cross-linking capacity of pepE-Bet v 1 CC-liposomes compared to pepE-Bet v 1 indicates a hypoallergenic phenomenon that has also been reported by others. For example, despite being recognized by IgE, intact Fel d 1 displayed on the surface of VLPs failed to cross-link IgE on mast cells [25, 26]. Similarly, trimeric Der p 2 displayed on engineered bioparticles also showed reduced IgE cross-linking potential although the effect of trimerization on IgE cross-linking/binding capacity was not reported [27]. How this hypoallergenic effect is established is not completely clear. Allergens packed on the particle surface could sterically hide IgE epitopes from IgE binding, thereby preventing efficient IgE cross-linking and downstream induced mediator release [27]. Moreover, compared to allergens in buffer, particulate allergy vaccines might be taken up more efficiently by DCs or macrophages before they enable IgE cross-linking on the surface of basophils or mast cells which could also reduce the risk of IgE mediated side effects. Alternatively, combined with a lower diffusion coefficient, the effective free allergen concentration of allergen bearing nanoparticles is strongly reduced which provides another physical explanation for the reduced IgE cross-linking capacity [26]. Nevertheless, more studies are needed to elucidate how allergen bearing nanoparticles show reduced IgE cross-linking capacity compared to free allergen.

Subcutaneously administered alum-adsorbed Bet v 1 induced low antibody levels which is in line with previous observations [28]. In contrast, all tested liposomes in this study were more potent antibody inducers compared to alum-adsorbed Bet v 1. More importantly, the humoral response was strongest when Bet v 1 was associated to cationic liposomes via CC rather than electrostatic adsorption. This might be explained by a relatively stable, multivalent display of Bet v 1 on the liposome surface after CC formation. A repetitive antigenic surface organization has been associated with efficient B-cell receptor cross-linking and subsequent antibody production [29]. This highlights and confirms the potency of cationic liposomes [14, 17] and the added advantage of CC attachment to induce strong antibody responses.

Together with the hypoallergenic character, the strong humoral response of pepE-Bet v 1 CC-liposomes could be advantageous in SCIT. In humans, allergic symptom relief after SCIT is correlated to increased levels of allergen specific IgG<sub>4</sub> and allergen specific IL-10 production [5, 30, 31]. It is hypothesized that IgG<sub>4</sub> blocks IgE binding to allergens which reduces IgE mediated clinical symptoms. In mice, both IgG1 and IgG2a have been associated with relief of clinical symptoms [6, 25]. pepE-Bet v 1 CC-liposomes induced both antibody isotypes strongly which could reduce treatment frequency and duration to achieve early onset and long lasting therapeutic effect.

The strong induction of Th1 associated IgG2a, is in line with the previously observed induction of Th1 CD4<sup>+</sup> T-cells [19]. These cells were found to produce high levels of IFN- $\gamma$  and IL-10 [19]. Both cytokines are beneficial for SCIT: IFN- $\gamma$  is able to suppress Th2 related IL-4 and Treg related IL-10 is able to suppress both IFN- $\gamma$  and IL-4. In fact, the ratio of IL-10/IL-4 ratio was the highest after immunization with pepE-Bet v 1 CC-liposomes. This indicates a more regulatory skewed immune response which could aid the suppression of the ongoing Th2 based, pro-inflammatory immune response in allergic subjects during SCIT. However, these murine results should be confirmed with human derived immune cell studies. For instance, T-cell polarization studies using human monocyte-derived dendritic cells isolated from peripheral blood mononuclear cells co-cultured with T-cells could shed more light on the T-cell subset differentiation pattern of pepE-Bet v 1 CC-liposomes.

In summary, we have developed a nanoparticle based delivery system using functionalized, cationic liposomes bearing Bet v 1 via CC formation. The hypoallergenic character, strong humoral as well as regulatory skewed T-cell responses induced by this formulation are advantageous properties for a novel, safe and highly efficacious SCIT vaccines. As such, our functionalized cationic liposomes could present a promising replacement of alum.

## **Funding**

This work was supported by the Nederlandse Organisatie voor Wetenschappelijk Onderzoek (TKI-NCI, grant 731.014.207). The work has also been supported by the Austrian Science Funds (Projects P32189) and by the University of Salzburg priority program "Allergy-Cancer-BioNano Research Centre.

## **Acknowledgements**

We acknowledge prof F. Ferreira for the opportunity to perform the RBL assays in her lab.

## References

1. Finegold, I., et al., *Immunotherapy throughout the decades: from Noon to now*. Annals of Allergy, Asthma & Immunology, 2010. **105**(5): p. 328-336.
2. Allam, J.P., et al., *Comparison of allergy immunotherapy medication persistence with a sublingual immunotherapy tablet versus subcutaneous immunotherapy in Germany*. J Allergy Clin Immunol, 2018. **141**(5): p. 1898-1901.
3. He, P., Y. Zou, and Z. Hu, *Advances in aluminum hydroxide-based adjuvant research and its mechanism*. Hum Vaccin Immunother, 2015. **11**(2): p. 477-88.
4. Klimek, L., et al., *Evolution of subcutaneous allergen immunotherapy (part 1): from first developments to mechanism-driven therapy concepts*. Allergo Journal International, 2019: p. 78–95.
5. Shamji, M.H. and S.R. Durham, *Mechanisms of allergen immunotherapy for inhaled allergens and predictive biomarkers*. J Allergy Clin Immunol, 2017. **140**(6): p. 1485-1498.
6. van Rijt, L.S., et al., *Birch Pollen Immunotherapy in Mice: Inhibition of Th2 Inflammation Is Not Sufficient to Decrease Airway Hyper-Reactivity*. International Archives of Allergy and Immunology, 2014. **165**(2): p. 128-139.
7. Pfaar, O., et al., *Perspectives in allergen immunotherapy: 2019 and beyond*. Allergy, 2019. **74 Suppl 108**: p. 3-25.
8. Alvaro-Lozano, M., et al., *EAACI Allergen Immunotherapy User's Guide*. Pediatric allergy and immunology : official publication of the European Society of Pediatric Allergy and Immunology, 2020. **31 Suppl 25**(Suppl 25): p. 1-101.
9. van der Kleij, H.P.M., et al., *Chemically modified peanut extract shows increased safety while maintaining immunogenicity*. Allergy, 2019. **74**(5): p. 986-995.
10. Patil, S.U. and W.G. Shreffler, *Novel vaccines: Technology and development*. J Allergy Clin Immunol, 2019. **143**(3): p. 844-851.
11. Gunawardana, N.C. and S.R. Durham, *New approaches to allergen immunotherapy*. Annals of Allergy, Asthma & Immunology, 2018: p. 293-305.
12. Perrie, Y., et al., *Designing liposomal adjuvants for the next generation of vaccines*. Adv Drug Deliv Rev, 2016. **99**(Pt A): p. 85-96.
13. Schwendener, R.A., *Liposomes as vaccine delivery systems: a review of the recent advances*. Therapeutic Advances in Vaccines, 2014. **2**(6): p. 159-182.
14. Christensen, D., et al., *Cationic liposomes as vaccine adjuvants*. Expert Review of Vaccines, 2007. **6**(5): p. 785-796.
15. Watson, D.S., A.N. Endsley, and L. Huang, *Design considerations for liposomal vaccines: Influence of formulation parameters on antibody and cell-mediated immune responses to liposome associated antigens*. Vaccine, 2012. **30**(13): p. 2256-2272.
16. Hanson, M.C., et al., *Liposomal vaccines incorporating molecular adjuvants and intrastructural T-cell help promote the immunogenicity of HIV membrane-proximal external region peptides*. Vaccine, 2015. **33**(7): p. 861-868.
17. Heuts, J., et al., *Cationic Liposomes: A Flexible Vaccine Delivery System for Physicochemically Diverse Antigenic Peptides*. Pharmaceutical Research, 2018. **35**(11).
18. Colletier, J.-P., et al., *Protein encapsulation in liposomes: efficiency depends on interactions between protein and phospholipid bilayer*. BMC Biotechnology, 2002. **2**(1): p. 2-9.
19. Lebourg, R.J.T., et al., *High-affinity antigen association to cationic liposomes via*

- coiled coil-forming peptides induces a strong antigen-specific CD4+ T-cell response.* European Journal of Pharmaceutics and Biopharmaceutics, 2020.
20. Akdis, M., *Immune tolerance in allergy.* Current Opinion in Immunology, 2009. **21**(6): p. 700-707.
  21. Akdis, M. and C.A. Akdis, *Mechanisms of allergen-specific immunotherapy.* Journal of Allergy and Clinical Immunology, 2007. **119**(4): p. 780-789.
  22. Larche, M., C.A. Akdis, and R. Valenta, *Immunological mechanisms of allergen-specific immunotherapy.* Nat Rev Immunol, 2006. **6**(10): p. 761-771.
  23. Himly, M., et al., *Standardization of allergen products: 1. Detailed characterization of GMP-produced recombinant Bet v 1.0101 as biological reference preparation.* Allergy, 2009. **64**(7): p. 1038-1045.
  24. Hemmings, O., et al., *Basophil Activation Test: Old and New Applications in Allergy.* Current Allergy and Asthma Reports, 2018. **18**(12): p. 77.
  25. Schmitz, N., et al., *Displaying Fel d1 on virus-like particles prevents reactogenicity despite greatly enhanced immunogenicity: a novel therapy for cat allergy.* J Exp Med, 2009. **206**(9): p. 1941-55.
  26. Engeroff, P., et al., *Allergens displayed on virus-like particles are highly immunogenic but fail to activate human mast cells.* Allergy, 2018. **73**(2): p. 341-349.
  27. Gomord, V., et al., *Design, production and immunomodulatory potency of a novel allergen bioparticle.* PLoS One, 2020. **15**(12): p. e0242867.
  28. Wallner, M., et al., *Reshaping the Bet v 1 fold modulates T(H) polarization.* J Allergy Clin Immunol, 2011. **127**(6): p. 1571-8 e9.
  29. Bachmann, M.F. and G.T. Jennings, *Vaccine delivery: a matter of size, geometry, kinetics and molecular patterns.* Nat Rev Immunol, 2010. **10**(11): p. 787-796.
  30. Akdis, M. and C.A. Akdis, *Mechanisms of allergen-specific immunotherapy: Multiple suppressor factors at work in immune tolerance to allergens.* Journal of Allergy and Clinical Immunology, 2014. **133**(3): p. 621-631.
  31. Geroldinger-Simic, M., et al., *Birch pollen-related food allergy: clinical aspects and the role of allergen-specific IgE and IgG4 antibodies.* J Allergy Clin Immunol, 2011. **127**(3): p. 616-622.
  32. Biotechnology, P., *Instructions : SulfoLink® Coupling Resin.* 2011, Thermo Fisher Scientific: <http://www.thermoscientific.com/pierce>. p. 5.

## Supplementary information

### Supplementary Material and Methods

Design, expression and purification of pepE-Bet v 1.

The gene of pepE-Bet v 1 was optimized for expression in *E. coli* and ligated into the p19b expression vector by GenScript (Piscataway, NJ, USA):

ATGTATGGAGAAATCGCAGCCCTTGAAAAAGAGATTGCCGCCTTAGAAAAAGAAATTGCCGCACT  
GGAAAAGGGTGTTCATTACGAACTGAGACCACCTCTGTTATCCAGCAGCTCGACTGTTCA  
AGGCCTTTATCCTTGATGGCGATAATCTCTTTCCAAAGGTTGCACCCCAAGCCATTAGCAGTTTGA  
AAACATTGAAGGAAATGGAGGGCCTGGAACCATTAAGAAGATCAGCTTTCCCGAAGGCTTCCCTT  
TCAAGTACGTGAAGGACAGAGTTGATGAGGTGGACCACACAACTTCAAATACAATTACAGCGTG  
ATCGAGGGCGGTCCCATAGGCGACACATTGGAGAAGATCTCCAACGAGATAAAGATAGTGGCAA  
CCCCTGATGGAGGATCCATCTTGAAGATCAGCAACAAGTACCACACCAAGGTGACCATGAGGT  
GAAGGCAGAGCAGGTTAAGGCAAGTAAAGAAATGGGCGAGACACTTTTGAGGGCCGTTGAGAGC  
TACCTCTTGGCACACTCCGATGCCTACAATAA.

The underscored base pairs denote the DNA sequence coding for EIAALEKEIAALEKEIAALEK, the pepE amino acid sequence.

The pepE-Bet v 1 fusion protein was expressed in competent *E. coli* BL21 (DE3) cells (Novagen, USA) by transfecting the cells with 5 ng DNA followed by heat shock treatment at 42 °C. Subsequently, the transformed cells were grown on antibiotic selective LB plates containing ampicillin (50 µg/mL). Protein expression was induced in 5 mL Difco™ Terrific Broth (BD, Europe) cultures with 1 mmol/L IPTG at OD<sub>600</sub> nm 0.6 for 3 hours at 37°C. The highest producing clones were used for protein production by inoculating 4 L TB medium in a 5 L stirred tank coupled to a BIOSTAT® controller (Sartorius Stedim Biotech). Protein production was induced for 3 hours with 1 mmol/L IPTG when the cells reached an OD<sub>600</sub> nm of 0.6. Finally, the cells were pelleted by centrifugation at 4600 rpm and stored at -20 °C until further use.

Frozen cell pellets were thawed on ice and re-suspended in ice cold lysis buffer (100 mmol/L sodium phosphate, 100 µg/mL lysozyme, pH 7.0) for 1 hour. The cells were disrupted by sonicating at 15 µm amplitude at 5 x 30 second bursts with 30 second intervals. Cellular debris was spun down at 20,000 g and 8°C for 20 minutes. The supernatant was collected. Bacterial DNA was precipitated with 0.4% (v/v) polyethyleneimine and spun down again at 12,000 g and 8 °C for 20 minutes. The supernatant was filtered through 0.2 µm before loading onto the affinity column.

An affinity purification column was prepared by coupling PepK (CGKIAALKEKIAALKEKIAALKE) to a supporting matrix. PepK was synthesized

as described in the main article. The peptide was coupled to 6% cross-linked agarose beads functionalized with iodoacetyl groups (Sulfolink, Thermo Scientific) according to the manufacturer's instructions [32].

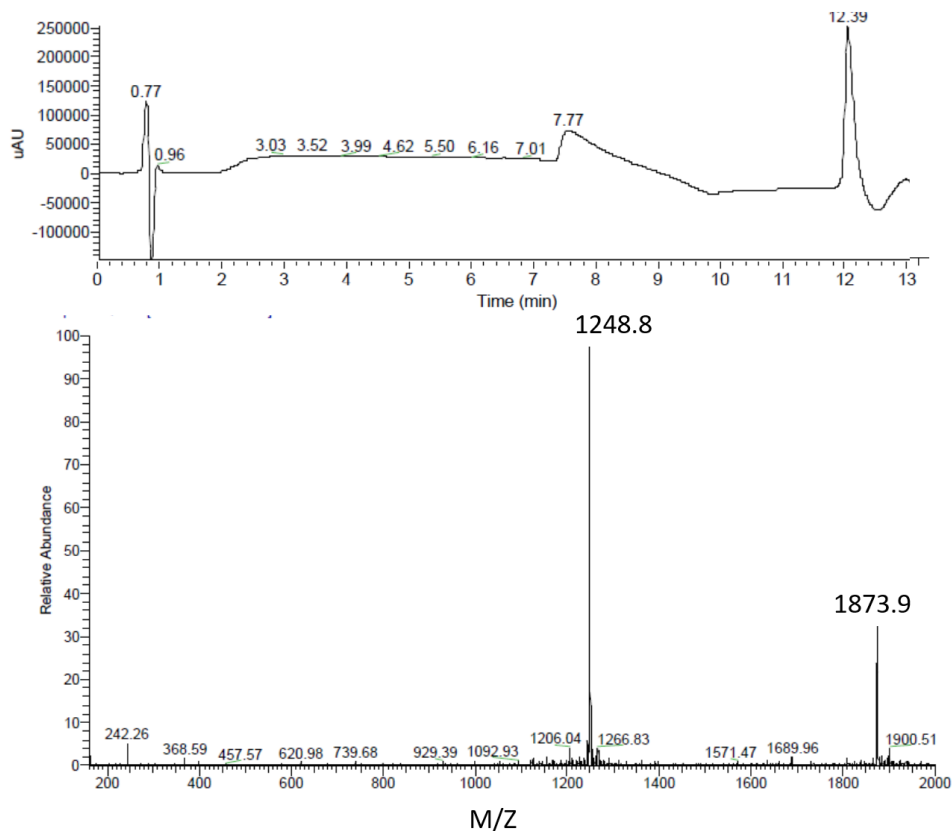
[32]. The affinity matrix was equilibrated with 5 column volumes (CV) 100 mmol/L sodium phosphate, 500 mmol/L sodium chloride, pH 7.0. Filtered supernatant was loaded onto the column and unbound proteins were washed out with 10 CV equilibration buffer. Bound pepE-Bet v 1 was eluted by lowering the pH with 5 CV of 100 mmol/L glycine HCl, pH 2.5 to unfold the pepE/pepK coiled coil. Elution fractions were collected and directly neutralized with (1:4, v/v) 1 mol/L TrisHCl, pH 9. Flow through, wash and elution fractions were analyzed with SDS PAGE (supplementary figure 2A and 2B). Elution fractions containing pepE-Bet v 1 were pooled and concentrated before gel filtration. The concentrate was loaded at 1 mL/minute onto a Superdex 75 pg column (GE Healthcare) equilibrated with 10 mmol/L HEPES, 280 mmol/L sucrose, pH 7.4 as a final step. Fractions containing the pure protein were pooled and stored at -20°C until further use.

#### SDS-PAGE

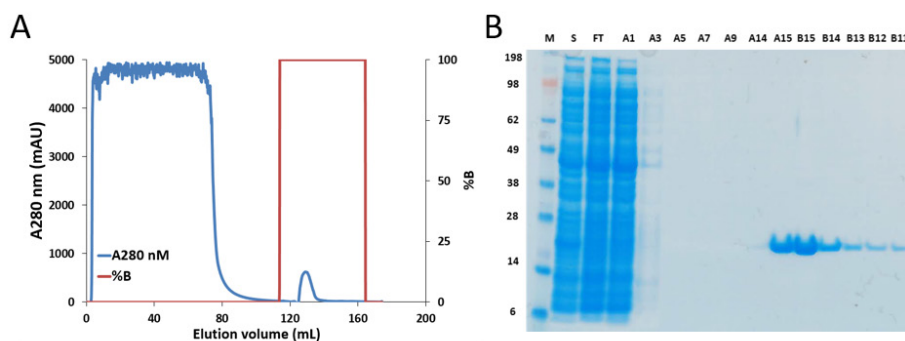
Purification fractions were analyzed with sodium dodecyl sulfate polyacrylamide gel electrophoresis (SDS-PAGE) using 4-12% Bis-Tris gels (GE Healthcare) according to manufacturer's instructions. Gels were stained with PageBlue Coomassie and de-stained overnight in water.



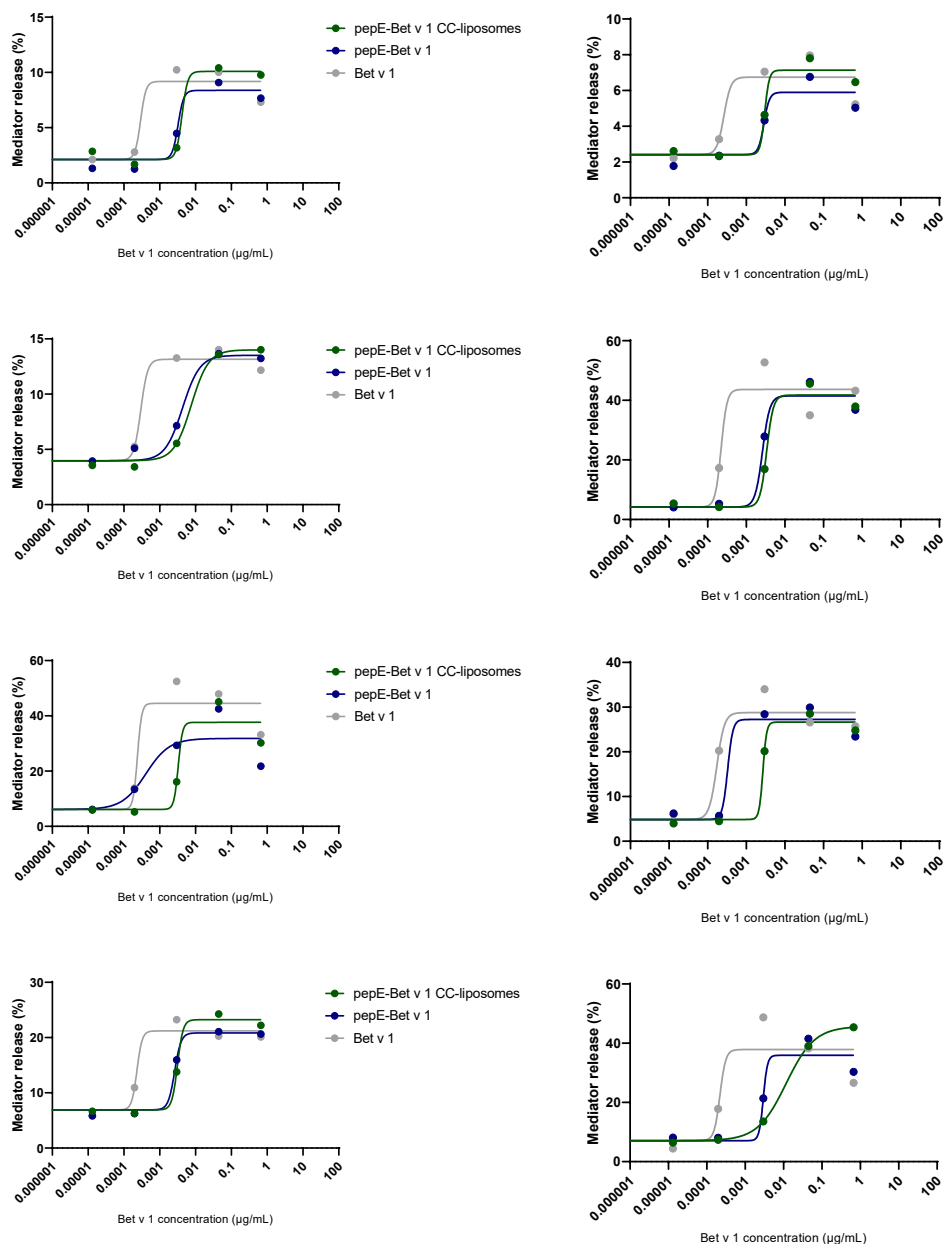
## Supplementary figures



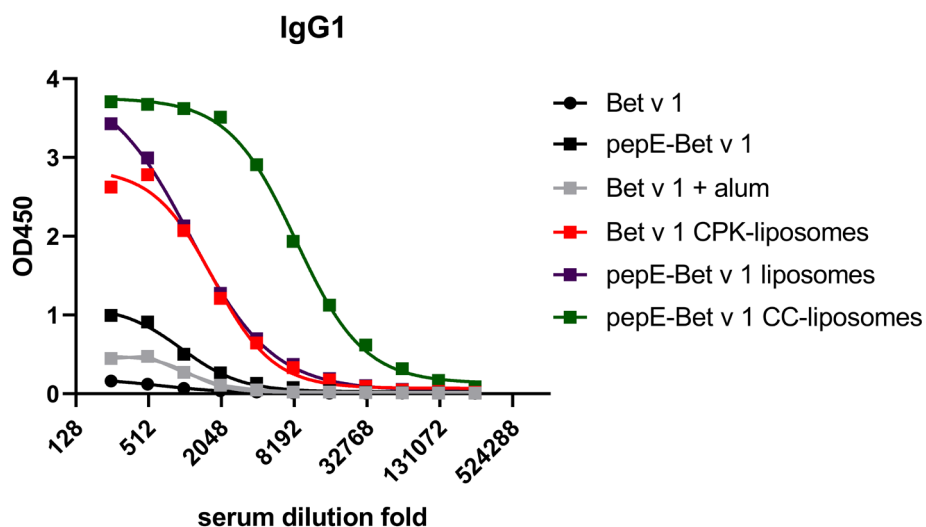
Supplementary Figure 1. LC (top) chromatogram and MS (bottom) spectrum of the CPK peak eluting at 7.77 minutes. The sequence of CPK is cholesterol-PEG4-KIAALKEKIAALKEKIAALKEKIAALKE, which has a theoretical molecular mass of 3747.2. The expected  $m/z$  values are: 1874.6 and 1250.1 for 2+ and 3+, respectively.



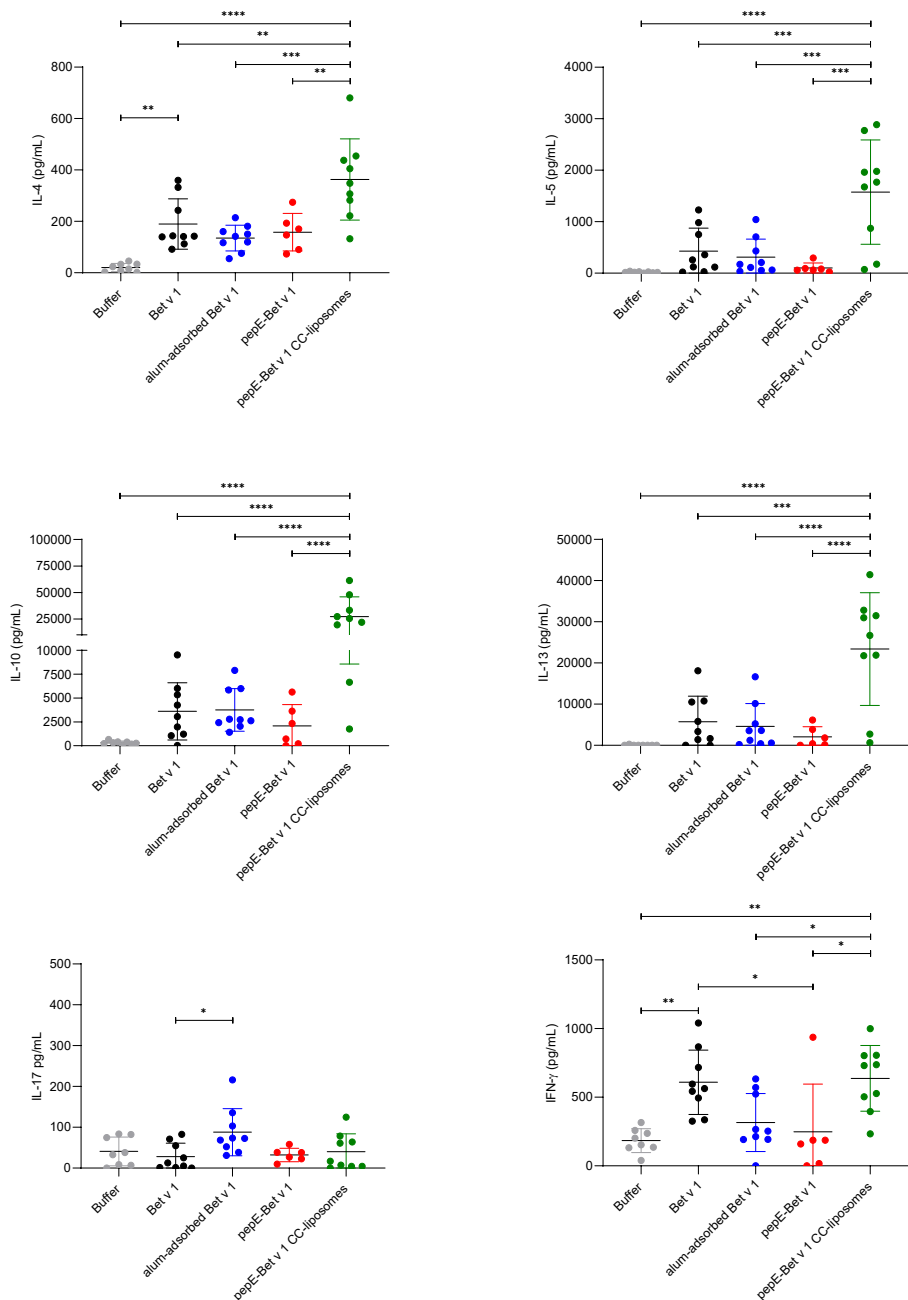
Supplementary Figure 2. Affinity purification and analysis of pepE-Bet v 1. A) elution from pepK-affinity column shows one peak, in which only a protein with the correct molecular weight is found on SDS-PAGE (B).



*Supplementary Figure 3. Results of rat basophil leukemia assay. Basophils were loaded with IgE from serum of Bet v 1-sensitized subjects and subsequently exposed to 15-fold dilutions of different allergen formulations. Mediator release was measured and normalized based on positive and negative controls. A non-linear regression (variable slope, 4 parameters) fit was used to extract the EC50. Each graph represents the mediator release response of one patient. This data is summarized in Figure 1.*



*Supplementary Figure 4. Detection of Bet v 1-specific IgG1 in a 10-fold serial dilution of pooled serum samples of mice that were immunized with various formulations on day 0, 7 and 14 and received 3 intranasal challenges with birch pollen extract for 3 consecutive days prior to the sacrifice.*



Supplementary Figure 5. Cytokine production in supernatants of lung draining lymph node cells after ex vivo stimulation with Bet v 1. Bars represent the mean cytokine concentration and data points represent the signals for each individual mouse (n=6-9). Group means were compared with a one-way ANOVA and subsequent Tukey's multiple comparison test. \* =  $p < 0.05$ , \*\* =  $p < 0.01$ , \*\*\* =  $p < 0.001$ .



## **Chapter 7**

### **Summary, discussion, conclusion**

In this thesis, we set out to explore the use of liposomes as adjuvants in subcutaneous allergen specific immunotherapy (SCIT). We evaluated different methods for associating a recombinant birch pollen allergen, Bet v 1, with liposomes. This led us to develop a new association method, based on the strong interaction of two complementary peptides, which resulted in a formulation that is able to induce a strong immune response upon subcutaneous administration in mice.

To evaluate how different antigen association methods affect physico-chemical properties and immune response of cationic liposomes, Bet v 1 was associated with cationic liposomes in various ways in **chapter 2**. Bet v 1 was adsorbed onto the lipid bilayer surface, encapsulated in the aqueous core of the liposomes, or both adsorbed and encapsulated. With increasing amount of Bet v 1, the size and polydispersity of the liposomes increased slightly for the adsorption method, but not for the encapsulation method or the combination. Above a protein/lipid ratio of 0.15 (w/w), aggregation was observed for both the association method and the combination method. For both methods, the association efficiency decreased with increased amounts of Bet v 1. Balb/c mice immunized with Bet v 1 either adsorbed to or encapsulated in cationic liposomes produced more antigen-specific IgG1 than Bet v 1 adsorbed to colloidal aluminum hydroxide. A combination of encapsulation and adsorption resulted in an even stronger IgG1 response as well as more cytokine (IL-4, IL-5, IL-10 and IL-13) production in lung draining lymph nodes. None of the formulations induced measurable antigen-specific IgG2a levels. While Bet v 1 in combination with cationic liposomes induced a stronger response than colloidal aluminum hydroxide-adjuvanted Bet v 1, these results reflect a Th2 skewed immune response. For allergen specific immunotherapy a Th1 or Treg type is more desirable, the latter has reportedly been induced by using anionic liposomes. Therefore in **chapter 3**, anionic liposomes were used. The effect of liposome rigidity on antigen-specific T-cell responses was evaluated. The rigidity of nanoparticles, such as liposomes, is an often overlooked property, for which no standard measurement method is available. Atomic force microscopy (AFM) was used to measure the rigidity of anionic liposomes containing OVA323, a MHC-II restricted epitope. A series of liposome formulations was prepared, in which surface charge, surface chemistry (*i.e.*, phospholipid head group), antigen content and particle size as measured by dynamic light scattering (DLS) were kept the same, in order to focus on the effect liposome rigidity. The incorporation of cholesterol in the lipid bilayer increased the rigidity of fluid-state liposomes and decreased that of gel-state liposomes. With the exception of liposomes consisting solely of dioleoylphosphatidyl phospholipids, all formulations showed a direct correlation between formulation rigidity and uptake by antigen presenting cells (APCs). Moreover, a significant correlation was observed between rigidity of liposomes and the regulatory

T-cell responses that were induced *in vitro* and *in vivo*, i.e., the more rigid the liposomes, the stronger the responses. An adjuvant that induces a stronger regulatory T-cell response is in potential a better adjuvant for immunotherapy. In **chapter 4**, the behavior after intradermal injection of both cationic and anionic liposomes was compared. Ovalbumin (OVA) and Bet v 1 were encapsulated in both types of liposomes, after which the uptake by skin resident dendritic cells of these formulations after intradermal injection in *ex vivo* human skin was assessed in a DC crawl-out model. There was a major difference in uptake between antigens: OVA was taken up very efficiently by skin resident dendritic cells, while Bet v 1 uptake was minimal. Encapsulation of Bet v 1 in liposomes, both anionic and cationic, increased its uptake drastically (>10-fold), whereas OVA uptake was decreased by encapsulation. While antigen uptake did not vary significantly between cationic or anionic liposomes, uptake of anionic liposomes was more efficient as compared to cationic ones. This was an unexpected finding, as it is generally accepted that cationic liposomes are taken up more efficiently by dendritic cells.

As observed in the previous chapters, in general the encapsulation of (usually precious) antigen is not efficiently achieved. For cationic liposomes, 60-80% of Bet v 1 was lost during preparation and purification and this process was even less efficient for anionic liposomes. Therefore, in **Chapter 5** a new association method was developed and evaluated with model antigens and Bet v 1. Antigen association to liposomal membranes was based on the interaction of two complementary alpha-helical peptides, pepE and pepK, to form a heterodimeric coiled coil (CC) complex. For this, pepK was conjugated to cholesterol, resulting in CPK, and incorporated in the lipid bilayer of cationic liposomes, while the antigenic peptides OVA323 (= pepE-OVA323, MHCII restricted epitope) and OVA257 (= pepE-OVA257, MHC-I restricted epitope) were extended at the N-terminus with pepE. Antigen affinity for liposomes via CC-formation was very high ( $K_d \approx 100\text{-}400\text{ nM}$  range), as compared to traditional association methods based on electrostatic interactions ( $K_d > 10^5\text{ nM}$ ). Moreover, CC-associated antigens remained associated with the liposomes after insertion in serum-containing culture medium or after intravenous injection in zebrafish larvae, whereas the electrostatically adsorbed antigens were mostly dissociated from the liposomes under these conditions. PepE-OVA323 associated to CPK-functionalized liposomes resulted in a 4-fold stronger CD4<sup>+</sup> T-cell proliferation *in vitro* as compared to non-functionalized liposomes. Surprisingly this was not the case for pepE-OVA257 and CD8<sup>+</sup> T-cells, which showed a dose-dependent CD8<sup>+</sup> T-cell proliferation regardless of the formulation (free antigen, non-functionalized liposomes, CPK-functionalized liposomes). Finally, antigen associated via CC formation resulted in stronger CD4<sup>+</sup> T-cell responses after subcutaneous immunization in mice. PepE-OVA323 associated with either non-



functionalized liposomes or CPK-functionalized liposomes induced a Th1-skewed immune response, as illustrated by the expression of T-bet by CD4<sup>+</sup> T-cells and the production of IFN- $\gamma$ . Coiled coil associated antigen induced more antigen specific IFN- $\gamma$  and IL-10 production by CD4<sup>+</sup> T-cells, indicating both Th1 and Treg properties of these CD4<sup>+</sup> T-cells and therefore a promising immune response for immunotherapy against allergens.

Based on these findings, in **chapter 6** a genetic fusion antigen of pepE and Bet v 1 (= pepE-Bet v 1) was produced in *E. coli* to further study the effect of CC-based antigen binding to cationic liposomes. A rat basophil leukemia assay revealed that CC-associated Bet v 1 to liposomes was approximately 10-fold less allergenic than wild type Bet v 1, in terms of mediator release in IgE-loaded basophils. Alum adsorbed Bet v 1 was compared to cationic liposomes with Bet v 1 adsorbed in various ways. CC adsorbed pepE-Bet v 1 induced a strong antigen specific IgG1 and IgG2a response after 3 immunizations, which was significantly higher than the responses induced by alum adsorbed Bet v 1 or the antigens without adjuvant. Moreover, neither cationic liposomes with Bet v 1 adsorbed nor non-functionalized liposomes with pepE-Bet v 1 induced as strong responses as CC adsorbed pepE-Bet v 1. These results clearly show that CC-mediated Bet v 1 association with cationic liposomes is an effective way to elicit a strong antigen-specific immune response *in vivo*.

## General discussion

While allergen specific immunotherapy already exists for over 100 years, the formulations for SCIT have not substantially changed in decades [1-3]. Typically, an allergen extract is mixed with an adjuvant and administered subcutaneously, requiring up to 54 injections over the course of 3-5 years before the therapy is completed [4-6]. The most commonly used adjuvant is colloidal aluminum hydroxide, while microcrystalline tyrosine, monophosphoryl lipid A (MPLA) and calcium phosphate are also available. Aluminum hydroxide initially boosts the ongoing Th2 skewed immune response, before inducing tolerance [7-9]. Despite SCIT being effective, there is room for improvement.

This can be achieved by strategies leading to 1) reduction of the number of injections, 2) reduction of the time period before symptom relief occurs and 3) fewer side effects. Therefore, safer formulations with increased immunogenicity are urgently needed and various innovations are studied in this thesis: recombinant proteins to replace allergen extracts, new administration routes and new adjuvants to replace colloidal aluminum hydroxide [2, 5]. Rather than using a birch pollen extract, recombinant Bet v 1 and pepE-Bet v 1 were used. In chapter 4 we explored a model for intradermal administration and evaluated the uptake of antigen by antigen presenting cells (APCs). And finally, the major

thread throughout this thesis was the use of liposomes as adjuvant for SCIT.

### Liposomes as adjuvant for SCIT

Currently the most used adjuvant for SCIT is colloidal aluminum hydroxide. It has high adsorption capacity and upon injection forms a depot from which the antigen is slowly released. The former means it can be used for a large variety of antigens while the latter leads to prolonged antigen exposure [1]. Moreover, aluminum hydroxide has been used for decades and is considered safe.

The desired immune response for SCIT is one that induces antigen-specific IgG4 and IL-10, which is associated with a tolerogenic response (characterized by regulatory T- and B-cells) towards the allergen. It is argued that induction of a Th1-type immune response could also be beneficial [4, 5]. Aluminum hydroxide however has been shown to enhance allergy-associated IgE prior to the induction of IgG4 in patients receiving SCIT [10, 11]. If the phase of SCIT where levels of allergy-associated biomarkers (*e.g.*, IgE) are increased, can be avoided, the therapy may become more efficient.

Liposomes can replace role of aluminum hydroxide as adjuvant for SCIT. They are a versatile adjuvant that consists of (phospho)lipids with proven clinical safety [12]. The composition can be altered, which will alter the properties and consequently the behavior after administration [13]. Cationic liposomes can form a depot after injection, can adsorb a wide variety of antigens (in particular those that are negatively charged), and are considered to be taken up most efficiently and induce a Th1-skewed immune response [14-17]. Anionic liposomes have shown, in mice, to be able to induce a specific tolerogenic response to encapsulated antigens [18, 19]. Moreover, in chapter 4, we have shown that encapsulation of antigens in liposomes of either charge can increase the antigen uptake by dendritic cells after injection in human skin. The lipid composition and consequential charge will likely determine the type of immune response that is induced by liposomes. Both cationic and anionic liposomes could be able to improve SCIT as adjuvant.

To ensure that liposomes and antigen are taken up by the same antigen presenting cell (APC), antigens can be encapsulated in the core of liposomes. This process is both inefficient and expensive. Encapsulation efficiency is typically <50%, as shown in this thesis (Chapter 2-4) and the literature [20-24]. Moreover, for oppositely charged antigen it is difficult to distinguish between surface adsorbed antigen and encapsulated antigen. The difference between encapsulated and surface adsorbed antigen could have consequences for the induced immune response, adverse events and the stability of the liposomal formulation. For the induction of a strong humoral response, intact antigen is

required. If intact antigen is freely diffusing, it could bind to IgE molecules on mast cells or basophils, resulting in an allergic reaction [25-27].

An ideal liposomal adjuvant for SCIT should have the following characteristics 1) high antigen association, 2) intact antigen is available on the surface to induce a strong humoral response, 3) no antigen is released from the adjuvant to potentially induce adverse events and 4) be applicable to a range of antigens. On top of the above-listed characteristics, a SCIT formulation should foremost also be stable and induce a strong immune response, which comprises the production of antigen-specific IL-10 and high-affinity neutralizing antibodies (IgG4 in humans).

#### Antigen association to liposomes via coiled coil-forming peptides

The newly developed association method using CC-forming peptides (chapter 5 and 6) leads to antigen-containing liposomes matching the desired characteristics mentioned in the previous paragraph. High antigen association efficiency for several tested antigens (pepE-OVA323, pepE-OVA257 and pepE-Bet v 1) was obtained, which remained intact in the presence of serum or in circulation in live zebrafish larvae. Moreover, in chapter 6 we showed that in mice that CC-associated liposomal Bet v 1 induced a superior immune response compared to otherwise associated Bet v 1. In addition to the strong immunogenicity of the formulation, it was also hypo-allergenic in a rat basophil leukemia assay, which is a good indication of an improved safety profile.

A liposome formulation based on CC-forming peptides for antigen association will likely offer enhanced stability compared to encapsulated antigen, because the antigen and the liposomes can be stored separately and mixed prior to administration. This stability could be further increased by improving the formulation buffer, which currently only consists of an aqueous solution of sucrose and HEPES. Liposomes and antigen can be mixed shortly before injection, with high association efficiency. Charged, small liposomes are generally very stable at 2-8°C, as electrostatic repulsion avoids aggregation, while Brownian motion prevents the suspension from collapsing. This stability based on repulsion could be compromised when antigen and liposomes have opposite charges.

In summary, allergen association to liposomes via CC formation shows great promise as allergy vaccine carrier platform. The formulation could be further optimized. For an approach based on cationic liposomes, the induced immune response could be enhanced by incorporation of immunomodulatory molecules in the liposome, such as MPLA or dimethyldioctadecylammonium (DDA). These may skew towards a Th-1 biased response [28, 29]. Owing to their amphiphilic nature, incorporation in lipid bilayers without compromising liposome stability

is feasible.

Anionic liposome-based vaccines on the other hand require more formulation optimization as CPK incorporation into anionic liposomes resulted in almost instantaneous aggregation. Thus, the CC-forming peptides should probably be reversed: pepE (anionic) should be linked to cholesterol, while pepK (cationic) should be coupled with the antigen. Moreover, anionic liposomes for SCIT could benefit from incorporation of molecules such as vitamin D, to induce a stronger tolerogenic response [30].

Another interesting possibility that could be explored is the association of multiple antigens via CC formation. This could induce tolerance to multiple allergens (and consequently multiple allergies) with only one formulation. Finally, other applications than allergy could be explored, such as rheumatoid arthritis which is also associated with CD4<sup>+</sup> T-cell responses. The ability to associate antigens in a highly efficient and reproducible manner could result in a platform technology. This would improve the development of new formulations, which would require only minimal optimization for new antigens.

### **Concluding remarks**

While aluminum has been used successfully as adjuvant to treat allergies, SCIT could probably be improved drastically by improving the formulation. In this thesis we investigated liposomes as adjuvant for SCIT. We studied several methods of antigen association with cationic and anionic liposomes, and the effect thereof on the loading efficiency and immunogenicity of the antigen. We have developed a novel association method based on a complementary peptide pair. This association method reduced antigen loss during formulation and resulted in superior immune responses compared to colloidal aluminum hydroxide-adsorbed antigen and otherwise associated antigen. The overall results provide a solid basis for further improvements with respect to the design of these liposomes, which potentially may replace colloidal aluminum hydroxide as adjuvant in SCIT.

## References

1. Klimek, L., et al., *Evolution of subcutaneous allergen immunotherapy (part 1): from first developments to mechanism-driven therapy concepts*. Allergo Journal International, 2019: p. 78–95.
2. Klimek, L., et al., *Development of subcutaneous allergen immunotherapy (part 2): preventive aspects and innovations*. Allergo Journal International, 2019. **28**(4): p. 107-119.
3. Gunawardana, N.C. and S.R. Durham, *New approaches to allergen immunotherapy*. Annals of Allergy, Asthma & Immunology, 2018: p. 293-305.
4. Jensen-Jarolim, E., et al., *State-of-the-art in marketed adjuvants and formulations in Allergen Immunotherapy: a position paper of the European Academy of Allergy and Clinical Immunology (EAACI)*. Allergy, 2019: p. 746-760.
5. Pfaar, O., et al., *Perspectives in allergen immunotherapy: 2019 and beyond*. Allergy, 2019. **74 Suppl 108**: p. 3-25.
6. Mahler, V., et al., *Understanding differences in allergen immunotherapy products and practices in North America and Europe*. Journal of Allergy and Clinical Immunology, 2019. **143**(3): p. 813-828.
7. Zubeldia, J.M., et al., *Adjuvants in allergen-specific immunotherapy: modulating and enhancing the immune response*. J Investig Allergol Clin Immunol, 2018: p. 103-111.
8. Heydenreich, B., et al., *Adjuvant effects of aluminium hydroxide-adsorbed allergens and allergoids - differences in vivo and in vitro*. Clin Exp Immunol, 2014. **176**(3): p. 310-319.
9. Moingeon, P., *Adjuvants for allergy vaccines*. Human Vaccines & Immunotherapeutics, 2012. **8**(10): p. 1492-1498.
10. Exley, C., *Aluminium adjuvants and adverse events in sub-cutaneous allergy immunotherapy*. Allergy, asthma, and clinical immunology : official journal of the Canadian Society of Allergy and Clinical Immunology, 2014. **10**(1): p. 4-4.
11. Akdis, M. and C.A. Akdis, *Mechanisms of allergen-specific immunotherapy: Multiple suppressor factors at work in immune tolerance to allergens*. Journal of Allergy and Clinical Immunology, 2014. **133**(3): p. 621-631.
12. He, W., et al., *Nanocarrier-Mediated Cytosolic Delivery of Biopharmaceuticals*. Advanced Functional Materials, 2020. **30**(37): p. 1910566.
13. Schwendener, R.A., *Liposomes as vaccine delivery systems: a review of the recent advances*. Therapeutic Advances in Vaccines, 2014. **2**(6): p. 159-182.
14. Hussain, M.J., et al., *Th1 immune responses can be modulated by varying dimethyldioctadecylammonium and distearoyl-sn-glycero-3-phosphocholine content in liposomal adjuvants*. J Pharm Pharmacol, 2014. **66**(3): p. 358-366.
15. Hamborg, M., et al., *Protein Antigen Adsorption to the DDA/TDB Liposomal Adjuvant: Effect on Protein Structure, Stability, and Liposome Physicochemical Characteristics*. Pharmaceutical Research, 2013. **30**(1): p. 140-155.
16. Korsholm, K.S., P.L. Andersen, and D. Christensen, *Cationic liposomal vaccine adjuvants in animal challenge models: overview and current clinical status*. Expert Review of Vaccines, 2012. **11**(5): p. 561-577.

17. Henriksen-Lacey, M., et al., *Liposomal cationic charge and antigen adsorption are important properties for the efficient deposition of antigen at the injection site and ability of the vaccine to induce a CMI response*. J Control Release, 2010. **145**(2): p. 102-108.
18. Benne, N., et al., *Atomic force microscopy measurements of anionic liposomes reveal the effect of liposomal rigidity on antigen-specific regulatory T cell responses*. Journal of Controlled Release, 2020. **318**: p. 246-255.
19. Benne, N., et al., *Anionic 1,2-distearoyl-sn-glycero-3-phosphoglycerol (DSPG) liposomes induce antigen-specific regulatory T cells and prevent atherosclerosis in mice*. J Control Release, 2018. **291**: p. 135-146.
20. Heuts, J., et al., *Cationic Liposomes: A Flexible Vaccine Delivery System for Physicochemically Diverse Antigenic Peptides*. Pharmaceutical Research, 2018. **35**(11).
21. Du, G., et al., *Intradermal vaccination with hollow microneedles: A comparative study of various protein antigen and adjuvant encapsulated nanoparticles*. Journal of Controlled Release, 2017. **266**: p. 109-118.
22. Liu, L., et al., *Immune responses to vaccines delivered by encapsulation into and/or adsorption onto cationic lipid-PLGA hybrid nanoparticles*. Journal of Controlled Release, 2016. **225**: p. 230-239.
23. Bal, S.M., et al., *Co-encapsulation of antigen and Toll-like receptor ligand in cationic liposomes affects the quality of the immune response in mice after intradermal vaccination*. Vaccine, 2011. **29**(5): p. 1045-1052.
24. Carstens, M.G., et al., *Effect of vesicle size on tissue localization and immunogenicity of liposomal DNA vaccines*. Vaccine, 2011. **29**(29): p. 4761-4770.
25. Platts-Mills, T.A., *The allergy epidemics: 1870-2010*. J Allergy Clin Immunol, 2015. **136**(1): p. 3-13.
26. Allahyari, M., et al., *In-vitro and in-vivo comparison of rSAG1-loaded PLGA prepared by encapsulation and adsorption methods as an efficient vaccine against Toxoplasma gondii*. Journal of Drug Delivery Science and Technology, 2020. **55**.
27. Thérien, H.-M., D. Lair, and E. Shahum, *Liposomal vaccine: influence of antigen association on the kinetics of the humoral response*. Vaccine, 1990. **8**(6): p. 558-562.
28. Schülke, S., et al., *MPLA shows attenuated pro-inflammatory properties and diminished capacity to activate mast cells in comparison with LPS*. Allergy, 2015. **70**(10): p. 1259-1268.
29. Henriksen-Lacey, M., et al., *Liposomes based on dimethyldioctadecylammonium promote a depot effect and enhance immunogenicity of soluble antigen*. J Control Release, 2010. **142**(2): p. 180-186.
30. Jeffery, L.E., et al., *1,25-Dihydroxyvitamin D and IL-2 Combine to Inhibit T Cell Production of Inflammatory Cytokines and Promote Development of Regulatory T Cells Expressing CTLA-4 and FoxP3*. The Journal of Immunology, 2009. **183**(9): p. 5458-5467.



## Chapter 8

### Nederlandse samenvatting



In dit proefschrift is de mogelijke toepassing van liposomen als hulpstof in subcutane immunotherapie tegen berkenpollen allergie bestudeerd. Dit is gedaan door het dominante allergeen in berken pollenallergie, Bet v 1, op verschillende manieren aan liposomen te adsorberen. Uiteindelijk heeft dit geleid tot het ontwikkelen van een nieuwe methode om eiwitten of peptiden aan liposomen te binden. Deze methode is gebaseerd op de specifieke interactie tussen twee peptiden, die een dubbele helix vormen. Conjugatie van Bet v 1 aan liposomen zorgde na subcutane toediening voor een sterkere immuunreactie in muizen in vergelijking van Bet v 1 gebonden aan liposomen via standaardmethoden.

In **hoofdstuk 2** wordt beschreven hoe het beladen van positief geladen liposomen met eiwitten de fysisch-chemische eigenschappen en stabiliteit van de deeltjes beïnvloedt. Bovendien wordt de opgewekte immuunrespons van de verschillende methoden vergeleken. Bet v 1 werd aan de buitenkant van de liposomen geadsorbeerd, aan de binnenkant verpakt (ingebouwd), en een combinatie van de twee werd bekeken. De deeltjesgrootte en de spreiding van de deeltjesgrootte namen toe, bij een hogere dosis Bet v 1 aan de buitenkant, maar dit gebeurde niet als Bet v 1 aan de binnenkant zat, of bij een combinatie van de twee. In alle gevallen werd boven een eiwit/lipide ratio van 0.15 (gewicht/gewicht) aggregatie van de liposomen waargenomen. Het adsorberen van Bet v 1 aan de buitenkant, en ingebouwd in liposomen, werd minder efficiënt bij een toenemende dosis van Bet v 1.

Muizen die geïmmuniseerd werden met de verschillende liposoom-formuleringen produceerde meer Bet v 1-specifieke antistoffen dan muizen die geïmmuniseerd werden met colloïdaal aluminium hydroxide, de hulpstof die gebruikt wordt in immunotherapie tegen berkenpollen allergie. De combinatie van Bet v 1 ingebouwd in de liposomen en geadsorbeerd aan het liposoomoppervlak wekte de meeste antistoffen op. De antistoffen die werden opgewekt, waren IgG1, maar niet IgG2a. IgG1 wordt geassocieerd met een helper T-cellen van type (Th)-2-gemedieerde immuunreactie, terwijl voor allergie-specifieke immunotherapie een gemengde Th-1 en regulatoire T-cel (Treg) reactie gewenst is. Deze laatste wordt beter opgewerkt door negatief geladen liposomen. Vandaar dat in **hoofdstuk 3 en 4** negatief geladen liposomen gebruikt werden.

Eerst werd het effect van lipide-bilaag stijfheid bestudeerd. Er is echter geen standaardmethode beschikbaar om eenvoudig de stijfheid van de lipide-bilaag te meten. In deze studie werd atoomkrachtmicroscopie (AFM) gebruikt om de stijfheid van een reeks negatief geladen liposomen met verschillende samenstelling te meten. Deze verschillende liposomen hadden een vergelijkbare deeltjesgrootte, oppervlaktechemie en belading van peptide. Het enige verschil was de verzadiging van de fosfolipiden en/of de toevoeging van cholesterol.

Dit lipide verhoogt de stijfheid van vloeibare membranen, maar verlaagt juist de stijfheid van gel-achtige membranen. Van de reeks liposomen die gemaakt was, werd de stijfheid gemeten, maar ook de opname door dendritische cellen (DCs) en de mate van Treg activatie in muizen en celkweek. Dit toonde aan dat liposomen met hogere stijfheid beter worden opgenomen door DCs en meer Treg activatie veroorzaakten. Hulpstoffen die meer Treg activatie opwekken, zullen waarschijnlijk beter zijn voor immunotherapie.

In **hoofdstuk 4** werd het verschil in opname door DCs tussen twee eiwitten (ovalbumine en Bet v 1) met en zonder liposomen (positief of negatief geladen) na injectie in humane huid vergeleken. Hiervoor werd de opname door dendritische cellen uit de huid bestudeerd in een *ex vivo* huid model. Grote verschillen in opname werden waargenomen tussen de verschillende eiwitten. Ovalbumine werd heel goed opgenomen door alle verschillende dendritische cellen, in tegenstelling tot Bet v 1. Door de eiwitten in te bouwen in liposomen werd de opname van Bet v 1 drastisch verhoogd ( $>10\times$ ), echter de opname van ovalbumine nam af. Dit effect was zowel bij positief als negatief geladen liposomen te zien. Bovendien werden negatief geladen liposomen beter opgenomen dan positief geladen liposomen. Dit was onverwacht, omdat juist wordt aangenomen dat positief geladen deeltjes beter worden opgenomen door dendritische cellen.

In de eerdere hoofdstukken van dit proefschrift is al gebleken dat het inbouwen van antigenen in liposomen vaak geen efficiënt proces is. Voor positief geladen liposomen ging 60-80% van het Bet v 1 verloren tijdens de zuivering. Voor negatief geladen liposomen was dit verlies nog groter. Om dit probleem op te lossen, werd in **hoofdstuk 5** een nieuwe methode beschreven om antigenen met liposomen te associëren. Deze methode is eerst met een model antigeen (peptide) gekarakteriseerd, en vervolgens in **hoofdstuk 6** met Bet v 1 beschreven. Het antigeen wordt aan liposomen geadsorbeerd door gebruik te maken van complexvorming tussen 2 complementaire peptiden. Deze peptiden vormen een zogenaamd coiled-coil motief. Eén van deze peptiden (peptide K) werd geconjugéerd aan cholesterol resulterend in een peptide-amfifiel (CPK) welke verankerd werd in het membraan van positief geladen liposomen. Het complementaire peptide (peptide E) werd geconjugéerd aan twee verschillende antigenen "OVA323" en "OVA257" resulterend in respectievelijk pepE-OVA323 en pepE-OVA257. De affiniteit van de nieuwe pepE-varianten met CPK-liposomen was hoog ( $K_d \approx 100-400$  nM) in vergelijking met adsorptie door elektrostatische interacties ( $K_d > 10^5$  nM). Bovendien bleven antigenen die via coiled coils aan liposomen waren gebonden bij elkaar in celkweek medium en na injectie in zebravislarven, in tegenstelling tot antigenen die zonder coiled coils aan liposomen waren gebonden. Ook zorgden coiled coil-gebonden antigenen aan

liposomen voor een 4 keer zo hoge activatie van CD4<sup>+</sup> T-cellen *in vitro*. Bovendien werd in muizen die geïmmuniseerd werden met coiled coil-geïmmobiliseerd antigeen meer interferon gamma (IFN- $\gamma$ ) en interleukine (IL) 10 geproduceerd door CD4<sup>+</sup> T-cellen dan muizen die antigeen via elektrostatische interacties aan liposomen geplakt waren. Deze combinatie van IFN- $\gamma$  en IL-10, die kenmerkend zijn voor respectievelijk een Th1 en Treg-gestuurde immuunreactie, is bij uitstek interessant om allergieën te bestrijden.

In **hoofdstuk 6** werd in *E. coli* een fusie-eiwit geproduceerd van pepE met Bet v 1, om Bet v 1 ook via coiled coils aan positief geladen liposomen te binden. Deze liposomen waren een factor 10 minder allergeen dan vrij Bet v 1. Dit is belangrijk om bijwerkingen van het preparaat te voorkomen. Daarnaast werden muizen geïmmuniseerd met positief geladen liposomen met Bet v 1 aangeplakt via elektrostatische interacties of coiled coil. Dit werd vergeleken met de huidige therapie voor berken pollenallergie, namelijk aluminium hydroxide geadsorbeerd Bet v 1. Muizen geïmmuniseerd met coiled coil gebonden Bet v 1 produceerde de meeste IgG1 en IgG2a. Dit was significant hoger dan Bet v 1 gebonden aan liposomen via elektrostatische interacties, welke meer antilichamen produceerde dan de muizen die met aluminium geïmmuniseerd werden. Deze resultaten laten duidelijk zien dat het binden van een antigeen aan liposomen via coiled coil interacties een sterke immuunreactie kan opwekken.

In dit proefschrift is aangetoond dat zowel positief als negatief geladen liposomen gebruikt kunnen worden als verpakking van eiwit-antigenen. Bovendien hebben we een nieuwe methode ontwikkeld om antigenen aan liposomen te plakken. Deze methode is getest met verschillende antigenen (peptiden en eiwit) en bleek voor allemaal goed te werken. Bovendien zorgde deze methode voor een sterkere binding dan via conventionele binding (via elektrostatische interacties). Antigenen die via deze manier aan positief geladen liposomen gebonden waren, zorgden ook voor een sterkere immuunreactie dan antigeen dat via elektrostatische interacties geplakt was. Bovendien is de immuunrespons die opgewekt werd, een gemengde response van Th1 en Treg, interessant voor de toekomstige behandeling van allergieën via immunotherapie.





# Chapter 9

## Curriculum Vitae

Romain was born on April 13th, 1990 in Utrecht and raised in Houten. After graduating from secondary school, he started studying Bio-Pharmaceutical Sciences at the University of Leiden in 2008. During the bachelor of this study he discovered the world of drug delivery technology, which he has not left since. The final bachelor's internship under daily supervision of Koen van der Maaden, with a one-year break, turned into a master's internship in the field of microneedles. He subsequently conducted research studying liposomes as a vaccine adjuvant at the Staten Serum Institute in Denmark under supervision of Dennis Christensen. He graduated in December 2014.

Before starting his PhD studies, he developed the course "Farmaceutische Technologie" for the then-new fast-track to pharmacy. During his PhD he contributed to this course several times as a (guest) lecturer. His PhD project titled "Supramolecular peptide amphiphile nanoparticles as a novel allergy vaccine platform" under supervision of Wim Jiskoot, Alexander Kros and Bram Slütter started in the summer of 2015. During his PhD trajectory, several posters were presented on FIGON DMD conferences, Biopharmacy days, ULLA summerschool Helsinki and GPEN Singapore 2018. In December 2020 Romain started at Janssen Vaccines as senior associate scientist in the department of Formulation Science and Technology.

## List of publications

K. van der Maaden, H. Yu, K. Sliedregt, R. Zwier, R. Leboux, M. Oguri, A. Kros, W. Jiskoot and J. Bouwstra, Nanolayered chemical modification of silicon surfaces with ionizable surface groups for pH-triggered protein adsorption and release: application to microneedles. *Journal of Materials Chemistry B*, 2013, 1(35): p. 4466-4477. (DOI:10.1039/C3TB20786B)

N. Benne, J. van Duijn, F. Lozano Vigario, R.J.T. Leboux, P. van Veelen, J. Kuiper, W. Jiskoot, B. Slütter, Anionic 1,2-distearoyl-sn-glycero-3-phosphoglycerol (DSPG) liposomes induce antigen-specific regulatory T cells and prevent atherosclerosis in mice. *Journal of Controlled Release*, 2018, p. 135-146. (<https://doi.org/10.1016/j.jconrel.2018.10.028>)

D. Christensen, L. Hansen Boellehuus, R. Leboux, W. Jiskoot, J.P. Christensen, P. Andersen, J. Dietrich, A Liposome Based Adjuvant Containing Two Delivery Systems with the Ability to Induce Mucosal Immunoglobulin A Following a Parenteral Immunization. *ACS Nano*, 2019, p1116-1126. (DOI:10.1021/acsnano.8b05209)

N. Benne, R.J.T. Leboux, M. Glandrup, J. van Duijn, F. Lozano Vigario, M. Aaby Neustrup, S. Romeijn, F. Galli, J. Kuiper, W. Jiskoot, B. Slütter, Atomic force microscopy measurements of anionic liposomes reveal the effect of liposomal rigidity on antigen-specific regulatory T cell responses. *Journal of Controlled Release*, 2019, p. 246-255. (<https://doi.org/10.1016/j.jconrel.2019.12.003>)

J. van Duijn, N. Benne, R.J.T. Leboux, M. van Ooijen, N. Kruit, A. Foks, W. Jiskoot, I. Bot, J. Kuiper, B. Slütter, Tc17 CD8+ T-cells accumulate in murine atherosclerotic lesions and modulate local inflammatory responses. *Cardiovascular Research*, 2020, cvaa286, (<https://doi.org/10.1093/cvr/cvaa286>)

R.J.T. Leboux, N. Benne, W.A. van Os, J. Bussmann, A. Kros, W. Jiskoot, B.A. Slütter, High-affinity antigen association to cationic liposomes via coiled coil-forming peptides induces a strong antigen-specific CD4+ immune response. *European Journal of Pharmaceutics and Biopharmaceutics*, 2020, 158, p96-105. (<https://doi.org/10.1016/j.ejpb.2020.11.005>)

R.J.T. Leboux, P. Schipper, T.M.M. van Capel, L. Kong, K. van der Maaden, A. Kros, W. Jiskoot, E.C. de Jong, J. Bouwstra, Not injection depth, but antigen and formulation determine antigen uptake after intradermal injection. *Frontiers in Allergy*, 2021, 2 (<https://doi.org/10.3389/falgy.2021.642788>)



